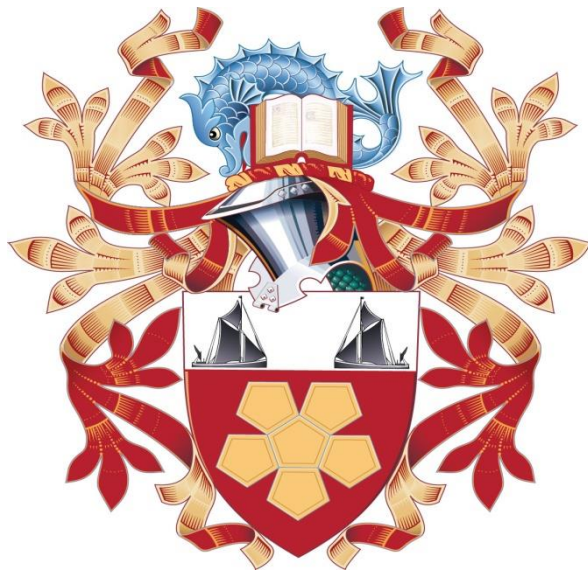


# STUDY OF FLUID FLOW ASSURANCE IN HYDROCARBON PRODUCTION – INVESTIGATION WAX MECHANISMS



**Muhammad Ali Theyab**

A thesis submitted in partial fulfilment of requirement of London  
South Bank University for degree of Doctorate of Philosophy

This Research programme was carried out in the collaboration with  
Ministry of Higher Education and Scientific Research of IRAQ

School of Engineering, Chemical Engineering  
London South Bank University  
103 Borough Road  
London SE1 0AA

March 2017

© Copyright Ministry of Higher Education and Scientific Research of IRAQ & Muhammad Ali  
Theyab, March, 2017. All rights reserved.

Experimental Studies on the Fluid Flow Assurance in Hydrocarbon Production

APPROVED BY:

---

Dr Pedro Diaz  
First Supervisor  
Senior Lecturer in Chemical & Petroleum  
Engineering, Head of Chemical and  
Petroleum Engineering Division  
School of Engineering  
London South Bank University

---

Dr John Orrin  
Second Supervisor  
Visiting Fellow in Chemical & Petroleum  
Engineering  
School of Engineering  
London South Bank University

## **Abstract**

The current work is a study of wax deposition, a phenomenon that is one of the main flow assurance problems faced by the oil industry, affecting numerous oil companies around the world. Wax deposition can result in the restriction of crude oil flow in the pipeline, creating pressure abnormalities and causing an artificial blockage that can lead to reduced or interrupted production. Wax can precipitate as a solid phase on the pipe wall when its temperature drops below the wax appearance temperature (WAT).

The aim of this research is to study in a lab rig the influence of some of the factors that control and affect the wax deposition process, such as pipe wall temperature (inlet coolant temperature), flow rate, pressure drop, oil temperature, shear stress, recirculation time of crude oil and viscosity. It aims to study the chemical and mechanical methods of inhibiting wax deposition in pipelines. The work also aims to simulate the multiphase flow process in the rig for this study.

A new experimental flow loop system was built in the lab to study the variation of wax deposition under single-phase transport through a pipe. A series of experiments were carried out for varying inlet coolant temperatures, flow rates and run times, while the pressure drop was monitored to evaluate the effect of chemical inhibitors and to evaluate the effect of spiral flow on wax deposition. Multiphase flow numerical simulations were undertaken using OLGA software in order to study the effect of the factors that control the wax deposition. Use of mixtures of inhibitors was evaluated, considering their effects on the rheological behaviour of the crude oil.

The experimental results show that there is a direct relation between the deposition time, pressure drop and wax deposit thickness, which is also highly dependent on the temperature. The wax deposit increases as the inlet coolant temperature decreases, even if the oil temperature exceeds the WAT, resulting in a larger pressure drop. The wax inhibition percentage was the highest using a combination of spiral flow with the inhibitor polyacrylate polymer (C16-C22) due to the synergy effect of high shear stress and the effect of an inhibitor that interferes with wax crystal growth. Three different mixtures of inhibitors were prepared in this work depending to the inhibitors that provide the greatest reduction in wax deposition; the mixtures of inhibitors presented a high reduction in crude oil viscosity, even at lower temperatures, due to interfere with wax molecules and prevent the growth processes.

The findings of the numerical simulation, using a simulator to reproduce the experimental results by tuning analogical properties (assumptions), show agreement with the experimental results. This study presents the spiral flow and the combination of spiral flow with the inhibitor polyacrylate polymer (C16-C22) as efficient mitigation methods to prevent or reduce wax deposition in hydrocarbon pipelines.

## **Declaration**

I declare that the thesis has been composed by myself. The thesis is submitted for examination in consideration of the award of a higher degree of Doctor of Philosophy in Chemical, Process and Energy Engineering is my personal effort and that the work has not been submitted for any other degree or professional qualification. Furthermore, I took reasonable care to ensure that the work is original, and, to the best of his knowledge, does not breach copyright law, and has not been taken from other sources except where such work has been cited and acknowledged within the text.

## **To My Family...**

For believing in me from the start and keeping me smiling until the end.

## **Acknowledgments**

First of all, I would like to thank Allah for giving me such wonderful every loving parent for their good wishes and prayers. I am grateful to them for supporting me in all fields of life and helping me in achieving set goal. I am thanks to God Almighty to bless me with a wonderful partner, my wife. Who supported me throughout my educational journey and along the way bearing my three beautiful children Abdullah, Marwan, and Rania.

I would like to express my sincere gratitude to my supervisor Dr. Pedro Diaz for the continuous support for my PhD study. He had been continuously been Motivating, encouraging me to strive more with his immense knowledge. His guidance helped me in all the time of research and writing of this thesis.

My sincere thanks to my uncle Prof. Abid Theyab Al-Ajeeli for his encouragement and supporting. My thanks to all of my father in law Prof. Yousif Yeheya, my siblings, my uncles, my mother in law, my brothers in law Mohammed and Osamah Yousif for their support during my study.

I would like to thank the Iraqi Ministry of Higher Education and Scientific Research for the financial support to make this PhD possible.

I would like to present this simple and humble work as a gift to my country Iraq and all my family members.

# Contents

Abstract .....	i
Declaration .....	ii
Acknowledgments .....	iv
List of Tables .....	ix
List of Figures .....	x
List of Nomenclature .....	xiii
Chapter 1: Introduction .....	1
1.1 Chapter One Overview .....	1
1.2 Motivation of Study .....	1
1.3 Background of Wax Deposition.....	3
1.4 Wax Deposition Problem Identification .....	3
1.5 Aims and Objectives.....	8
1.6 Thesis Structure .....	9
1.7 Publications .....	10
Chapter 2: Literature Review .....	11
2.1 Chapter Two Overview .....	11
2.2 Fluid Flow Assurance Issues .....	11
2.2.1 Hydrates.....	11
2.2.2 Asphaltenes .....	12
2.2.3 Slugging .....	13
2.2.4 Naphthenates.....	14
2.2.5 Scales .....	15
2.2.6 Corrosion.....	16
2.2.7 Erosion.....	17
2.2.8 Emulsions.....	18
2.3 Wax Deposition .....	19
2.4 Wax Crystallisation .....	20
2.5 Wax Deposition Mechanisms .....	21
2.5.1 Molecular Diffusion.....	22
Step 1: Precipitation of dissolved wax molecules.....	23
Step 2: Formation of radial concentration gradient of dissolved waxy components.....	24
Step 3: Deposition of waxy components on the surface of an existing deposit	24
Step 4: Internal diffusion and precipitation of waxy components in the deposit	25
2.5.2 Shear Dispersion.....	26
2.5.3 Brownian Diffusion.....	27
2.5.4 Gravity Settling.....	28

2.6	Factors Affecting the Wax Deposition Process.....	29
2.6.1	Temperature Differential and Cooling Rate.....	29
2.6.2	Crude Oil Composition .....	30
2.6.3	Experimental Time (Lab Rigs) .....	31
2.6.4	Flow Rate .....	31
2.6.5	Pressure.....	32
2.6.6	Pipe Surface Properties.....	32
2.6.7	Lab Experiment Investigation Rigs .....	33
2.7	Wax Mitigation Methods .....	35
2.7.1	Chemical Inhibitors.....	36
2.7.2	The Spiral Flow .....	37
2.8	Wax Deposition Simulation.....	40
2.8.1	Wax Deposition Models Contained in OLGA .....	41
	□ RRR Model.....	41
	□ Matzain Model .....	43
	□ Heat Analogy Model .....	45
2.9	Original Contribution to Knowledge .....	45
Chapter 3: Experimental Methodology .....		49
3.1	Chapter Three Overview.....	49
3.2	Crude Oil under Study .....	49
3.2.1	Specific Gravity and API.....	49
3.2.2	Rheological Behaviour.....	49
3.2.3	Wax Content.....	51
3.2.4	SARA Analysis .....	51
3.3	Study of the Effect of the Inhibitors on Crude Oil Rheology .....	52
3.4	Wax Deposition Experimental Rig Design .....	53
3.4.1	Test Section .....	54
3.4.2	Copper Pipe Jacket .....	54
3.4.3	Pump.....	55
3.4.4	Crude Oil Reservoir .....	55
3.4.5	Hot Bath Water.....	55
3.4.6	Churchill Conair Chiller .....	55
3.4.7	Manometer Pressure Gauge .....	55
3.4.8	Thermocouples.....	56
3.4.9	Condenser.....	56
3.4.10	Pico-Meter .....	56
3.5	Study of the Effect of the Spiral Flow on Wax Deposition .....	57



3.6	Process of Experiments.....	58
3.7	Methods for Estimate Wax Thickness.....	61
3.7.1	Direct Method (Pigging Method) .....	61
3.7.2	Pressure Drop Method .....	61
3.7.3	Heat Transfer Method.....	62
3.7.4	Liquid Displacement-level Detection Technique (LD-LD).....	63
3.8	Average Wax Thickness Measurement .....	63
3.9	Benchmarking of the Rig of this Study.....	64
3.10	Uncertainty, Standard Deviation (SD), and Reproducibility of Experimental Data	66
3.11	OLGA Wax Module.....	67
1.	Input – input boundary and initial conditions, fluid data and pipe and process data. ....	68
2.	Output – define variables to be reported in the output file.....	68
3.	Process – calculations of variables along the pipeline. ....	69
3.11.1	Crude Oil Properties used in PIPEsim to Create PVT File .....	69
3.11.2	Methodology of Wax Deposition Simulation.....	70
3.11.3	Methodology of Tuning OLGA Parameters for Improved Predictions	71
Chapter 4:	Results and Discussion: Rheological Evaluation – Inhibitor Effects .....	73
4.1	Chapter Four Overview .....	73
4.2	Characterisation of Crude Oil .....	73
4.3	Effect of Inhibitors on Crude Oil Rheology .....	73
4.3.1	Effect of Inhibitors on Viscosity .....	74
4.3.2	Effect of Inhibitors on Pour Point .....	77
4.3.3	Effect of Inhibitors on Wax Appearance Temperature.....	79
4.3.4	Study of the Effect of Inhibitor Mixtures on Oil Rheology .....	81
4.4	Effect of Shear Rate on Oil Viscosity at Different Concentrations of Inhibitor .....	83
Chapter 5:	Results and Discussion: Wax Formation .....	85
5.1	Chapter Five Overview .....	85
5.2	Wax Deposition Process.....	85
5.2.1	Effect of Mitigation Methods on Wax Deposition.....	88
5.2.2	Effect of Shear Rate on Wax Appearance Temperature .....	89
5.2.3	Effect of Shear Rate and Shear Stress on Crude Oil Viscosity .....	91
5.2.4	Measuring Wax Thickness Using Different Methods.....	92
5.2.5	Effect of Inlet Coolant Temperature .....	94
5.2.6	Effect of Wax Deposition Recirculation Time .....	95
5.2.7	Effect of Flow Rate on Wax Deposit Volume .....	96

5.2.8	Effect of Inhibitor Poly Acrylate Polymer on Wax Deposition .....	97
5.2.9	Effect of Spiral Flow on Wax Deposition .....	100
5.2.10	Effect of Spiral Flow on Wax Deposition at Different Inlet Coolant Temperatures .....	102
5.2.11	Effect of Spiral Flow on Crude Oil Temperature.....	103
5.2.12	Comparison of the Best Mitigation Methods.....	104
5.2.13	Analysis of Spiral Flow Mechanism .....	105
5.3	Comparison between Real Field Data and Laboratory Data .....	112
5.4	Economical Evaluation of Research .....	113
Chapter 6: Multiphase Flow Simulation.....		116
6.1	Chapter Six Overview.....	116
6.2	Distribution of the Single Carbon Number and the n-Paraffin in Crude Oil 116	
6.3	Comparison between the Wax Simulation Models.....	117
6.4	Results and Discussion of the Wax Simulation .....	118
6.4.1	The Base Case of Wax Deposition Simulation.....	118
6.4.2	Tuning of OLGA Parameters for Improved Predictions .....	120
6.4.3	Comparison of Wax Simulations with Experimental Data.....	126
6.4.4	Wax Mitigation Methods .....	128
Chapter 7: Conclusions and Future Work .....		131
7.1	Conclusions .....	131
7.2	Recommendations for Future Work.....	132
References .....		133
Appendix A: Published Papers .....		146

## List of Tables

Table 1: The chemistry of wax inhibitors used during this study. ....	53
Table 2: Experiments carried out at a flow rate of 2.7 L/min., different inlet coolant temperatures, different recirculation times and different methods. ....	60
Table 3: Experiments carried out at a flow rate of 4.8 L/min., different inlet coolant temperatures, different experimental times and different methods. ....	60
Table 4: Characterisation of crude oil for this study and Jha et al.'s (2014) study. ....	69
Table 5: Carbon number distribution in the crude oil (Jha et al., 2014). ....	70
Table 6: Distribution of normal + non-normal paraffin in wax of crude oil (Jha et al., 2014). ....	70
Table 7: Crude oil characteristics. ....	73
Table 8: Wax deposit volume at inlet coolant temperature 14°C. ....	86
Table 9: Wax deposit volume in different experiment sets, at inlet coolant temperature 24°C. ....	87
Table 10: Wax deposit volume at inlet coolant temperature 33°C. ....	88
Table 11: Estimating wax thickness ( $\delta w$ ) using the different methods at flow rate 2.7 L/min. ....	93
Table 12: Measuring wax thickness ( $\delta w$ ) using different techniques at flow rate 4.8 L/min. ....	94
Table 13: Estimated shear stress and wax thickness at different pressure drops and different inlet coolant temperature at flow rate 2.7 L/min with and without the spiral flow. ....	110
Table 14: Estimated shear stress and wax thickness at different pressure drops and different inlet coolant temperature at flow rate 4.8 L/min with and without the spiral flow. ....	110
Table 15: Estimated shear stress and wax thickness at different pressure drops and different inlet coolant temperature at flow rate 6 L/min with and without the spiral flow. ....	111
Table 16: Comparison between the real field data of Ekofisk-Teesside pipeline and the data of the experimental rig pipeline of this study. ....	112
Table 17: Illustrate the electricity consumed and the total cost of each experiment. ....	115
Table 18: Weight percentage of carbon number distributed in the crude oil used in the simulation with the new weight percentage after removing 10, 20 and 30% from C6 and distributing that percentage of each case to the rest of the carbon numbers. ....	125

## List of Figures

Figure 1: Wax deposition plug in the wellbore on platform C in the North Sea (Akpabio, 2013). .....	4
Figure 2: Hydrate plug formed in a subsea hydrocarbon pipeline (Irmann-Jacobsen, 2013; Heriot-Watt University, 2014).....	12
Figure 3: Polar compounds of asphaltenes (Alberta Innovates Technology Futures, 2016). .....	13
Figure 4: Slug formation in the riser of the hydrocarbon pipeline (modified from Johal, 2012). .....	14
Figure 5: An example of a naphthenic acid structure (Johal, 2012). .....	15
Figure 6: Formation of scale in the pipe (McLay, 2015). .....	16
Figure 7: Corrosion formation in the pipe (Southwest Gas, 2016).....	17
Figure 8: The effects of sand erosion at a pipe bend (Johal, 2012). .....	18
Figure 9: Photomicrograph of a water-in-oil emulsion (PetroWiki, 2015).....	19
Figure 10: Wax deposition process in the hydrocarbon pipeline (Lee, 2008; Al-Yaari, 2011).....	20
Figure 11: Polarised picture of wax crystals (Siljberg, 2012).....	21
Figure 12: Illustration of how wax molecules diffuse to form the wax deposit layer (modified from Siljberg, 2012). .....	23
Figure 13: Schematic of molecular diffusion as the wax deposition mechanism (Huang et al., 2015).....	24
Figure 14: Long wax particle located in shear flow (modified from Siljberg, 2012). .....	26
Figure 15: A Bohlin Gemini II Rheometer used to measure WAT (LSBU). ...	50
Figure 16: Variation of viscosity of Arunachal crude oil with temperature, indicating the WAT and pour point using the rheometer.....	50
Figure 17: (a) Filtration equipment used to separate asphaltene, and (b) chromatographic column used to separate saturate, aromatic and resin during this study.....	52
Figure 18: Schematic of wax deposition test flow loop in this study. ....	57
Figure 19: Apparatus of wax deposition in the lab for this study. ....	57
Figure 20: Illustration of the twisted aluminium plate inside the test section pipe to create spiral flow. ....	58
Figure 21: Average wax thickness inside the flow loop pipe for this study....	64
Figure 22: Steps of the OLGA simulation process (OLGA 7, SPT Group). ...	68
Figure 23: Schematic flow line diagram in the OLGA software for this study. ....	71
Figure 24: The rheological behaviour of the crude oil with the chemical inhibitors at a concentration of 1000 and 2000ppm and different range of temperatures, and shear rate 120 1/s.....	74
Figure 25: The effect of inhibitors mixture Mix01 and its components on crude oil viscosity at 4°C, at 500ppm, 1000ppm and 2000ppm. ...	76
Figure 26: The effect of inhibitors mixture Mix02 and its components on crude oil viscosity at 4°C, at 500ppm, 1000ppm and 2000ppm. ...	76

Figure 27: The effect of inhibitors mixture Mix03 and its components on crude oil viscosity at 4°C and a concentration of 500ppm and 1000ppm.....	77
Figure 28: The effect of inhibitors mixture Mix01 and its components on pour point temperature at 500ppm, 1000ppm and 2000ppm.....	78
Figure 29: The effect of inhibitors mixture Mix02 and its components on pour point temperature at 500ppm, 1000ppm and 2000ppm.....	78
Figure 30: The effect of inhibitors mixture Mix03 and its components on pour point temperature at a concentration of 1000ppm. ....	79
Figure 31: The effect of inhibitors mixture Mix01 and its components on WAT at 500ppm, 1000ppm and 2000ppm. ....	80
Figure 32: The effect of inhibitors mixture Mix02 and its components on WAT at 500ppm, 1000ppm and 2000ppm. ....	81
Figure 33: The effect of inhibitors mixture Mix03 and its components on WAT at 500ppm and 1000ppm. ....	81
Figure 34: The effect of the inhibitors, Mix01 and Mix02 at 1000ppm and 2000ppm, and Mix03 at 1000ppm, on crude oil rheology (WAT, pour point and viscosity) at different temperatures.....	82
Figure 35: The effect of shear rate on crude oil viscosity at concentration 500, 1000, and 2000ppm of the mixtures of inhibitors Mix01, Mix02, and Mix03. ....	84
Figure 36: The effects of mitigation methods on wax deposition volume at flow rate 2.7 L/min and experimental time 2 hours.....	89
Figure 37: Viscosity profile of the oil sample at different shear rates and temperatures; shows the WAT around 39°C measured in this study. ....	90
Figure 38: Effect of the shear rate on the viscosity at the same temperature. ....	91
Figure 39: Shear stress and shear rate at different temperatures. ....	92
Figure 40: The effect of inlet coolant temperature on wax thickness at different flow rates, (a) 2.7 L/min, (b) 4.8 L/min, and different techniques. ....	95
Figure 41: The effect of the experimental time on wax deposited volume at flow rate 2.7 L/min and an inlet coolant temperature of 14°C. ....	96
Figure 42: The effect of flow rate on wax deposition volume at inlet coolant temperature 14°C. ....	97
Figure 43: The effect of inhibitor W802 on wax thickness at 2.7 and 4.8 L/min, at inlet temperature 14°C. ....	98
Figure 44: SEM micrographs showing the structure of wax before (a) and after (b) adding the inhibitor W802. ....	99
Figure 45: Wax deposition inside the pipe (a) without inhibitor and (b) with W802 inhibitor. ....	100
Figure 46: Mechanisms of wax deposition inside the pipes for this study, with laminar flow (left: modified from Siljberg, 2012) and spiral flow (right: in this study).....	101

Figure 47: The effects of spiral flow on wax thickness at an inlet coolant temperature of 14°C. ....	102
Figure 48: The effect of the spiral flow on wax thickness at different inlet coolant temperatures at flow rate 2.7 L/min.....	103
Figure 49: The impact of the spiral flow on the crude oil temperature. ....	104
Figure 50: The effects of the inhibitor W802, spiral flow, and bending the spiral flow with the inhibitor on wax thickness at the same experimental conditions. ....	105
Figure 51: Forces affects on the element of fluid flow in a pipe. ....	106
Figure 52: Forces affects on the element of fluid in a pipe with the effect of spiral flow.....	107
Figure 53: The effect of shear stress with spiral flow (S) and non-spiral flow (NS) on wax deposit thickness at different pressures and different inlet coolant temperatures. ....	111
Figure 54: Distribution of the single carbon number (SCN) in the crude oil and the n-Paraffin using PIPEsim.....	116
Figure 55: Phase envelope of the crude oil used for wax simulations using PIPEsim. ....	117
Figure 56: Comparison of the three models in the OLGA software: RRR, Matzain and Heat Analogy.....	118
Figure 57: Simulation output of wax deposition profile along the test section pipe of the experimental rig for this study, at a flow rate of 2.7 L/min.....	119
Figure 58: Simulation output of wax deposition profile along the test section pipe of the experimental rig for this study, at a flow rate of 4.8 L/min.....	120
Figure 59: The effect of wax porosity on predicted wax thickness at flow rate 2.7 L/min and an inlet coolant temperature of 14°C. ....	122
Figure 60: The effect of changes in wax porosity in OLGA simulation on predicted wax thickness at flow rate 4.8 L/min and an inlet coolant temperature of 14°C. ....	122
Figure 61: The effect on the predicted wax thickness of changing crude oil components, using OLGA at a flow rate of 2.7 L/min and an inlet coolant temperature of 14°C. ....	124
Figure 62: The effect of simulation time on the wax thickness at 2.7 L/min, an inlet coolant temperature of 14°C and a wax porosity of 0.6. ....	126
Figure 63: Comparison between the experimental results and the simulation results at flow rate 2.7 L/min. ....	127
Figure 64: Comparison between the experimental results and the simulation results at a flow rate of 4.8 L/min.....	128
Figure 65: Simulating the effect of the inhibitor on wax thickness using OLGA and comparing this with the experimental results with and without the inhibitor.....	129
Figure 66: The effect of the insulation layer thickness on the wax formation at a flow rate of 2.7 L/min and coolant temperature of 14°C. ....	130

Figure 67: The effect of the insulation layer thickness on the wax formation at a flow rate of 4.8 L/min and coolant temperature of 14°C. ....130

## List of Nomenclature

$\Delta P$ : Pressure drop (Pa).  
 $d$ : Diameter (m).  
 $L$ : Length (m).  
 $r$ : Pipeline radius (m).  
 $T$ : Temperature ( $^{\circ}\text{C}$ ).  
 $\rho$ : Fluid density ( $\text{kg}/\text{m}^3$ ).  
 $\rho_{\text{deposit}}$ : Deposit density ( $\text{kg}/\text{m}^3$ ).  
 $\rho_{\text{wax}}$ : Wax density ( $\text{kg}/\text{m}^3$ ).  
 $\delta$ : Wax thickness (m).  
 $\mu$ : Viscosity (Pa s).  
 $Q$ : The volumetric flow rate.  
 $T_f$ : The bulk fluid temperature in the pipe.  
 $T_o$ : The outside pipe wall temperature.  
 $q_o$ : The heat flux through the outside pipe wall.  
 $h_w$ : The film heat transfer coefficient ( $\text{W}/\text{m}^2 \text{K}$ ).  
 $k_p$ : The thermal conductivities of the pipe wall ( $\text{W}/\text{mK}$ ).  
 $k_w$ : The thermal conductivities of deposited wax ( $\text{W}/\text{mK}$ ).  
 $\Delta T_f$ : The oil temperature drop.  
 $C_p$ : The specific heat of the waxy oil.  
 $d_1$ : Diameter of the clean pipe (m)  
 $d_2$ : Diameter of the pipe with wax (m).  
 $V_{\text{wax}}$ : Wax volume ( $\text{m}^3$ ).  
 $dM_w/dt$ : The rate of wax deposited ( $\text{kg}/\text{s}$ ).  
 $\rho_w$ : The density of the solid wax ( $\text{kg}/\text{m}^3$ ).  
 $D_w$ : The diffusion coefficient of the wax in the oil phase ( $\text{m}^2/\text{s}$ ).  
 $A_w$  is the area of wax deposition ( $\text{m}^2$ ).  
 $dC/dr$ : The wax concentration gradient ( $1/\text{m}$ ).  
 $dC/dT$ : The solubility coefficient of the wax crystal in the oil phase ( $1/^{\circ}\text{C}$ ).  
 $dT/dr$ : The radial temperature gradient of the wall ( $^{\circ}\text{C}/\text{m}$ ).  
 $T_a$ : The absolute temperature (K).  
 $M$ : The molecular weight of the oil solvent (g/mol).  
 $V$ : The wax molar volume (cc/g.mole).  
 $\mu$ : Dynamic viscosity (cP).  
 $\xi$ : The effective molecular weight of the solvent with respect to molecular diffusion.  
 $T_a$ : Absolute temperature ( $^{\circ}\text{C}$ ).  
 $V^{0.6}$ : Proportional to the absolute temperature  $T_a$ .

$\gamma$  : Oil shear rate at the pipe wall (1/s).  
 $d_w$  : Wax particle diameter (m).  
 $\phi_w$  : The wax volume fraction out of the solution at the wall.  
 $D_s$  : The shear dispersion coefficient (m<sup>2</sup>/s).  
 $M_B$  : The mass of deposited wax due to Brownian diffusion (kg).  
 $\frac{dC}{dr}$  : The concentration gradient over the pipe radial coordinates (1/m).  
 $A_w$  : The area of wax deposition (m<sup>2</sup>).  
 $D_B$  : The Brownian diffusion coefficient (m<sup>2</sup>/s).  
 $R$  : The gas constant (J/(mol.K)).  
 $T_a$  : The absolute temperature (K).  
 $\mu$  : The oil viscosity (Ns/m<sup>2</sup>).  
 $a$  : The Brownian particle diameter (m).  
 $N$  : Avogadro's number (1/mol).  
 $U$  : The settling velocity (m/s).  
 $a$  : The particle diameter (m).  
 $n$  : The power-law index.  
 $g$  : The acceleration due to gravity (m/s<sup>2</sup>).  
 $K_p$  : The power-law consistency index.  
 $\tau$  : Shear stress (N/m<sup>2</sup>).  
 $Vol_{wax}^{diff}$  : The volume rate of wax deposition  
 $i$  : Wax forming composition.  
 $N_w$  : is the number of wax component.  
 $D_i$  : The diffusion coefficient (m<sup>2</sup> /s).  
 $\Delta C$  : The concentration difference between the bulk phase and the wax phase.  
 $S_f$  : The fraction of wetted perimeter by wax.  
 $K$  : The shear deposition constant.  
 $\Phi_w$  : The volume fraction of deposited wax in the bulk fluid (porosity).  
 $A$  : The surface area available for deposition (m<sup>2</sup>).  
 $l_{wax}$  : The total volume rate of deposited wax.  
 $\frac{d\delta}{dt}$  : The change in wax thickness deposited on the wall layers with time (m/s).  
 $\Pi_1$  : The empirical relation for the rate enhancement due to oil trapped in wax layer.  
 $\Pi_2$  : The empirical relation for the rate reduction due to shear stripping.  
 $d\delta$  : The change in wax thickness deposited on the wall layers with time (m/s).  
 $D_w$  : The diffusion coefficient.  
 $C_w$  : The concentration of wax in solution (weight %).



$C_L$  : The porosity effect coefficient.

$N_{Re}$  : Reynolds number.

$N_{SR}^{C_3}$  : The flow regime dependent Reynolds number.

$v$  : Oil velocity (m/s).

$k_L$  : Thermal conductivity of the oil (W/mK).

$h_{wall}$  : Inner wall heat transfer coefficient (W/m<sup>2</sup> K).

$T_b$  : Bulk fluid temperature (K).

$T_{wall}$  : The inner wall surface temperature (K).

$\rho_{water}$  : Water density (kg/m<sup>3</sup>).

$F_1$  : Inlet force to the pipe (N)

$F_2$  : Outlet force from the pipe (N).

$A_x$  : The cross-section area of the pipe (m<sup>2</sup>).

$F_3$  : Shear stress force on the pipe (N)

$\tau$  : Shear stress (Pa).

$u$  : The fluid flow velocity (m/s).

$A_{Xpipe}$  : The cross-section area of the pipe (m<sup>2</sup>).

$A_{Xplate}$  : The cross section area of the twisted plate (m<sup>2</sup>).

PT: Pressure in OLGA software (Pa).

TM: Fluid Temperature OLGA software (°C).

DXWX: thickness of wax layer deposited at wall (mm).

MWXDIS: mass of wax dissolved in oil (kg/m<sup>3</sup>).

# **Chapter 1: Introduction**

## **1.1 Chapter One Overview**

In this chapter brief outline is provided explaining the motivation of this study which includes arising the challenges of growing wax deposition in the hydrocarbon pipelines by increasing production in the cold environment due to increasing demand for energy. Mitigation methods are used to address this problem, such as chemical, mechanical and thermal methods, but despite the available inhibition methods, many oil companies currently suffer from wax deposition problems and are still looking for a good solution to solve this issue.

This study presents chemical and mechanical methods and a combination of chemical and mechanical methods as a solution to this problem. The understanding of the wax deposition problem is outlined and aims and objectives of this study are presented, along with a goal to be met at the end of the work. This chapter presents a brief outline of the structure of different chapters of this thesis.

## **1.2 Motivation of Study**

The world demand for energy has led oil companies to expand their operations in cold environments such as the offshore deepwater and onshore for more reservoirs. During hydrocarbon production in the cold environment, these oil companies are challenged with the problem of wax deposition from the crude oil building up on the pipe wall.

Crude oil is a complex mixture of saturates (paraffins/waxes), aromatics, naphthenes, asphaltenes and resins. Among these components, high molecular weight paraffin (wax) is typically responsible for the problems during production and transportation in the hydrocarbon pipeline systems.

Wax accumulation in the crude oil pipelines depends on the temperature change between the crude oil and the pipe wall. Two conditions must be met for wax deposition to occur in a pipe. These conditions are included, the oil temperature near the pipe wall must be lower than the wax appearance temperature, and the pipe wall temperature must be lower than the oil temperature (Singh et.al, 2000).

At the reservoirs, the temperatures range between (70-150 °C) and pressures range between (50-100MPa), therefore, wax molecules are dissolved in the crude oil. However, as the crude oil flows through a subsea pipeline resting on the ocean floor at a temperature of 4°C, or through onshore pipelines in the cold environment, the temperature of oil eventually decreases below its wax appearance temperature because of the heat losses to the surroundings (Lee, 2008).

The solubility of wax decreases drastically as the temperature decreases and wax molecules start to precipitate out of the crude oil. Because of the high

demand for energy, oil production in deep sea areas and cold environment onshore has increased significantly.

The exploration and production technologies in deep sea areas have made deep water drilling economically feasible and the oil industry has drilled subsea oil wells as far as 160 miles away from the shore. As oil wells are developed further offshore, wax problems will become more severe and extensive due to the increased transportation lines on the cold ocean floor (Nguyen, 2004; Lee, 2008).

Global offshore oil production (including lease condensate and hydrocarbon gas liquids) from deepwater projects reached 9.3 million barrels per day in 2015. Deepwater production, or production in water of depths greater than 125 meters, has increased 25% from nearly 7 million b/d a decade ago. Shallow water has been relatively less expensive and less technically challenging for operators to explore and drill, but changing economics and the exhaustion of some shallow offshore resources has helped to push producers to deepwater or, in some areas, ultra-deepwater (at depths of 1,500 meters or more) resources. The share of offshore production from shallow water in 2015 was 64%, the lowest on record (Matthew, 2016).

This research is motivated by interesting challenges arising from the growing size of wax deposition in the hydrocarbon pipelines by increasing production in the cold environment. Therefore, the author came up and designed this research, and designed and structure the new rig from a crash in the lab of this study aiming to reduce or prevent wax deposition and to study the influence of some of the factors that control and affect the wax deposition process, such as pipe wall temperature (inlet coolant temperature), flow rate, pressure drop, oil temperature, shear stress, recirculation time of crude oil and viscosity.

Also, the motivation behind this research is to evaluate the performance of the chemical inhibitors such as polyacrylate polymer (C16-C22), spiral flow, and the combination of the chemical inhibitor with the spiral flow on wax deposition. Where, the high cost of using the conventional mitigation methods and the high cost of using the chemical inhibitors at the present time to mitigate wax deposition in the hydrocarbon pipelines motivated the author to look for different techniques to reduce or prevent wax deposition.

The different techniques include using the chemical inhibitors and a combination of chemical inhibitors to increase its efficiency to reduce wax deposition. Also, Raise interest in the possibility of increasing the shear rate to prevent wax deposition, using spiral flow as a way to increase the shear rate in the flow to reduce wax deposition by mixing the wax crystals with the crude oil and prevent it to deposit on the pipe wall. Moreover, undertake a systematic study of inhibition of wax deposition using the effects of combination spiral flow with a chemical inhibitor to increase the effect of the mitigation process.

It is desired through the outcome of this research to expand the literature on the role wax inhibitor play in reducing wax deposition in terms of the amount of wax volume deposited and the effects it has on the hydrocarbons.

Consequently, a fundamental understanding of wax deposition phenomena and a comprehensive wax deposition model based on this fundamental understanding is strongly necessitated in order to overcome the challenges in production and transportation of pipelines in the cold environment.

### **1.3 Background of Wax Deposition**

As early as 1928, wax deposition was reported as an issue that led to many difficult problems in the production, transportation and storage of crude oil (Huang et al., 2015). In 1969, control of wax deposition in U.S. domestic production annually cost \$4.5-\$5 million. The problem of onshore wax deposition could be addressed by relatively simple methods, including the optimisation of the operating conditions (pipeline size, pressure, etc.), because of easy access and management of these resources. Heating of the onshore pipeline or mechanical removal of the wax deposit was used occasionally, but was generally not as prohibitive (Huang et al., 2015).

During the late twentieth century, as the problem of wax deposition became increasingly challenging, as the production of petroleum fluids shifted from onshore resources toward offshore reservoirs around the world (Huang et al., 2015). In the offshore Lasmø field in the UK, wax deposition was so severe and frequent that the entire field was abandoned at a cost of over \$100 million (Singh et al., 2000, Al-Yaari, 2011).

The severity of the wax problem needs evaluated in the design of every subsea and onshore development across the world, including the Gulf of Mexico, the North Slope, the North Sea, North Africa, Northeast Asia, Southern Asia and South America (Huang et al., 2015); about the onshore including oil fields in North America, South America, Asia, Africa and Europe to estimate the cost of suitable remediation methods for wax deposition in the subsea pipeline and to avoid blockage.

### **1.4 Wax Deposition Problem Identification**

Wax deposition is, a common problem, a critical operational challenge and one of the main flow assurance problems in the oil industry around the world including the offshore and onshore oil fields. Wax deposition occurs when paraffin components in crude oil (alkanes with carbon numbers greater than 20) precipitate and deposit on the cold pipeline wall when the inner wall temperature falls below the wax appearance temperature (Singh et al., 2000).

The formation of wax in the pipe during the fluid production from the bottom hole of the well to the surface can restrict the flow of crude oil, creating pressure abnormalities and causing an artificial blockage, as shown in figure 1, leading to the reduction or even cessation of production (Burke and Kashou, 1995; Bern et al., 1981; Trina and Johansen, 2015; Botne, 2012;

Kjøraas, 2012; Siljoberg, 2012; Tordal, 2006). Wax deposition also leads to formation damage near the wellbore, reduction in permeability, changes in the reservoir fluid composition and fluid rheology due to phase separation as wax solid precipitates (Zhu et al., 2008).

Wax precipitation is impacted by several factors, such as: crude oil composition (Singh et al., 1991), flow rate, temperature gradient (Salam et al., 2014), pipe wall temperature (inlet coolant temperature), crude oil temperature, shear stress, recirculate time of oil in the rig (production time in the field) and oil viscosity (Adeyanju and Oyekunle, 2013; Valinejad and Solaimany, 2013).



Figure 1: Wax deposition plug in the wellbore on platform C in the North Sea (Akpabio, 2013).

Wax deposition in crude oil production systems can be reduced or prevented by a chemical, mechanical, or thermal remediation method or by a combination of some of them (Woo et al., 1984; Al-Yaari, 2011). If preventive methods for wax deposition (e.g. insulation of pipeline, injection of wax inhibitor, or combination of both) are not successful, a wax gel layer grows rapidly in thickness and impedes the flow of oil due to the flow restriction (Singh et al., 2000; Lee, 2008). Those mitigation methods become increasingly significant as the oil industry continues to expand deepwater operations to greater depths and distances in cold environments, which poses a great challenge to the industry (Bott and Gudmunsson, 1977, Zhu et al., 2008; White, 2008; Aiyejina et al., 2011; Huang et al., 2015).

One of the most commonly used corrective methods used in the fields is pigging. In pigging, a pig (a solid object with the diameter smaller than the inner diameter of the pipe) passes through the pipeline to scrape off the wax deposit. However, the pigging method cannot efficiently be utilized without a proper wax deposition prediction. For example, pigs at times get stuck inside

the pipeline in the presence of thick hard deposits making the situation worse, which occurred in a Gulf of Mexico pipeline. In the worst cases, production must be stopped in order to replace the plugged portion of the line, which is estimated to cost approximately \$40,000,000 per incident (Huang et al., 2015).

Another notable remediation technique is to use a fused chemical reaction with controlled heat emission to remove the wax deposit. However, in order to successfully use this technique, it is critical to know the thickness profile and the wax fraction of the deposit as a function of axial location and time. If this technique were to be used based on inaccurate information on the location of wax deposit and its wax fraction, there could be unwanted local high temperature in the pipeline due to the failure of re-dissolving wax deposit.

Successful management of wax deposition will become more important in the future because new explorations and productions are being made farther offshore. The wax deposition management cost to the petroleum production industry is enormous and will increase both in terms of capital costs (e.g. preventive methods) and operating costs (e.g. corrective methods) (Lee, 2008; Al-Yaari, 2011).

Recently, three technologies are used for mitigating wax deposition in the offshore and onshore oil fields around the world, namely, wax inhibitors (chemical inhibitors), thermal management, and pigging. Most of the oil companies are using the wax inhibitors, as a main mitigation method to reduce wax, combined with pigging or thermal insulation. Below, are some case studies of wax deposition in the offshore and onshore oil fields pipelines around the world.

For example, In India offshore field to the west of India. The oil is transported through a 30-inch, 203-km pipeline from the offshore platform to a terminal on land. This crude oil has high wax content and a 30°C pour point. Given that the average seabed temperature is 22°C, pour point depressant (PPD) is injected. Specifically, 300 ppm/350 ppm of PPD is injected to achieve a pour point of 21°C/18°C and therefore maintain the flow of the oil. The subsea pipelines are regularly pigged. The cost of PPD injection alone is US\$15 million/year. Whereas the use of PPD has maintained the oil flow, an on-going increase in the pipeline pressure has been observed over time. This indicates the presence of wax deposits in the subsea pipeline. According to a technical survey, approximately 20,000 m<sup>3</sup> of wax has already been deposited in the pipeline (which has a volume of 90,226 m<sup>3</sup>). A combination of PPD and dispersant was being considered to mitigate the wax deposition and therefore reduce the frequency of pigging (Kang et al, 2014).

Another case study, the Gannet oil field is located approximately 180 km east of Aberdeen in United Kingdom in a depth of about 90 m. The Gannet field is located 16 km northeast of the Gannet Alpha platform. Risers 31 and

32 carry oil from Gannet. The wax appearance temperature of this oil is approximately 35.5°C. Wax deposition in the subsea pipeline of Gannet was estimated to be around 21 m<sup>3</sup> of wax had built up over a length of 8 km. An appropriate solvent was selected and injected at a rate of 0.6 m<sup>3</sup>/min. After solvent injection, an additional 480 m<sup>3</sup>/day of oil could be recovered. Also, the pigging method was used frequently with the inhibitors to remove wax deposition in Gannet oil field (Craddock et al., 2007; Kang et al, 2014).

The Power Play oil field is located in 706 m of water in Garden Banks block 28, Gulf of Mexico, and began production in 2008. It is a subsea tieback to a host facility with a subsea flow loop to enable oil circulation and pigging. The subsea architecture consists of two 10 km 4.5 × 7" (pipe in pipe) PIP pipeline pigging loop systems with insulated steel catenary risers. The wax appearance temperature of the oil is 41.1°C, and the pour point ranges between -5°C and 19°C. Given that the WAT is high, wax deposition is possible. To mitigate this risk, a PIP system was applied to minimize heat loss from the oil. As observed in the northern and southern subsea pipelines during oil production, a simultaneous increase in the flowing bottomhole pressure and a drop in the oil production rate pointed to the possibility of partial plugging as a result of wax deposition in the pipeline. To mitigate this plugging, xylene solvent was injected into the pipelines at a rate of between 0.04 and 0.32 m<sup>3</sup>/min. This, combined with an increase in the pressure, was not able to remediate the wax deposition. Rather, the operation opted to switch the production zone from the lower zone to the higher zone to increase the flow rate. This increased the flow temperature to above the WAT and successfully mitigated wax deposition (Goodman and Joshi, 2013).

On another hand, Russian oil production is almost exclusively onshore and suffering from the problem of wax deposition such as padovskoe oil field, Mukhanovskoe oilfield, Petrukhovskoe oil field and Urmanskoe oil field. Technological methods such as pigging and thermal insulation have been used combined with the chemical inhibitors to reach the highest efficiency to control the wax deposition in the pipelines. The chemical inhibitors that have been used to reduce wax deposition are includes surfactant (nanylphenol, synthanol), aromatic solvents (benzene, xylene, toluene), and aliphatic alcohol (butano, pentanol, hexanol) (Struchkov et al, 2017).

The wax deposition problem can occur even in the high temperature areas. For example, Kirkuk – Ceyhan crude oil pipeline between Iraq and Turkey is an example for the onshore pipelines that have wax deposition in winter season of the year. The average lowest temperature is about 2°C in winter between north of Iraq and Turkey, therefore, it's enough to form and deposit wax inside the pipeline. The 40-inch pipeline is 1049 km long, of which 986-km pass through Turkish territory, and it had a capacity of 700,000 b/d. It was observed that wax mole fraction starts to rise around 300 km from inlet with a value of 0.193 and reaches 0.2225 at the end of the pipeline. The pigging method and the aromatic solvents used to mitigate wax deposition in the pipeline (Kok and Saracoglu, 2000).

Many oil companies prefer chemical additives in analysing the economics of waxy crude oil production in cold environments, considering this the best solution to reduce wax deposition in pipelines due to chemical additives does not need to stop production for cleaning the pipe but it considers as an online mitigation method (Huang et al., 2015). Some researchers are stating that even though many wax inhibitors have been developed, there is currently no universal type of inhibitor that can be used for all kinds of crude oil due to the varying properties of crude oils (Ridzuan et al., 2014; Kang et al., 2014; Adeyanju and Oyekunle, 2014; Halim et al., 2011). This is an investigation to understand the wax deposition problem, because of the universal inhibitor may solve the wax deposition problem and create more problems such as (corrosion) due to varying properties of crude oils and the different climate.

A universal solution would be a both convenient and cost effective response to the current demand. Presently, most of the companies have their personalised technique to tackle the wax deposition. This is not very practical as oil viscosity changes depending on the geology and geographical location. If spiral flow technique is adopted universally in the correct way, it will help to reduce the amount of investment as well as man power to achieve better results.

Researchers have used various different types of chemical inhibitors, such as polyethylene, copolymer esters, ethylene/vinyl acetate copolymers (Kang et al., 2014; Jafari Ansaroudi et al., 2013; Halim et al., 2011), olefin/ester copolymers, ester/vinyl acetate copolymers, polymethacrylates (Wu et al., 2012; Al-Sabagh et al., 2009; Han et al., 2009; Duffy and Rodger, 2002;), alkyl phenol resins, toluene and xylene (Kang et al., 2014; Jennings and Newberry, 2008; Jang et al., 2007), studying their effects on wax appearance temperature, wax content, pour point, and crude oil viscosity using analytical methods, to evaluate the suitable inhibitor for the waxy crude oil that provides the desired results in preventing wax deposition.

A small number of researchers have used an experimental flow loop to study and determine dynamically the efficiency of wax inhibitors on wax deposition inside the pipe, such as some of them are Ridzuan et al. (2014), Adeyanju and Oyekunle (2014), and Hoffmann and Amundsen (2013).

The difference between the analytical methods and the experimental flow loop systems is the experimental conditions used in the flow loop deposition test affected the performance of paraffin inhibitors, indicating that temperature gradients (i.e., oil temperature and inlet coolant temperature) must be optimized to achieve the highest reduction in wax deposition. While, the experimental conditions in the analytical methods can be controlled, such as pressure, temperature, and shear rate, providing accurate results in the analytical of wax inhibition (Perez et al., 2015).



Ridzuan et al. (2014) investigated the effect of chemical inhibitors such as poly(ethylene-co-vinyl acetate) (EVA) and poly(maleic anhydride-alt-1-octadecene) (MA) on wax deposition, using cold finger apparatus. The wax inhibition percentage of their study was 23.1% using EVA and 7.5% using MA at a coolant temperature of 25°C. Adeyanju and Oyekunle (2014) investigated the effect of groups of acrylate ester copolymers of varying alkyl side chains as wax inhibitors during the flow of crude oil in the flow loop. Wax inhibition percentages of 25-55% were obtained at high coolant temperatures above 20°C at a concentration of 5000ppm of the inhibitor. Hoffmann and Amundsen (2013) found that about 60%-90% of wax thickness was reduced by applying different concentrations (125, 250 and 500ppm) of the commercial inhibitor, and using silicon as an insulation material during experimental work investigation.

In the previous studies, even though many different types of chemical inhibitors have been used at different concentration, at different inlet coolant temperatures, there is still wax deposit on the pipe wall due to the researchers missed investigate the effect of combining the chemical inhibitors on wax deposition.

A small number of researches mentioned using the spiral flow and studied its effects in different areas (Xie, 2013; Betül and Tulin, 2007; Li et al., 2011; Zhang et al., 2005; Zhang et al., 2002; Zhang et al., 2001; Liu et al., 2012), however, there is no research mentioning the use of spiral flow to reduce or mitigate wax deposition.

Therefore, according to the previous studies, it can be concluded that there is a need to:

- Undertake a systematic study of inhibition of wax deposition using chemicals and combinations of chemicals.
- Raise interest in the possibility of increasing the shear rate to prevent wax deposition, using spiral flow as a way to increase shear rate in the flow.
- Undertake a systematic study of inhibition of wax deposition using the effects of combination spiral flow with a chemical inhibitor.

A multiphase flow simulation is implemented during this work using OLGA software in order to study the effect of the factors that control the wax deposition process and to easily study the behaviour of the system.

## **1.5 Aims and Objectives**

The main aim of this research is to experimentally study the wax deposition process and investigate the effect of the chemical and mechanical methods to reduce or prevent wax deposition, modelling this process using a multiphase flow simulator. The main objectives of this study are:

- To design and construct a new flow loop system in the lab of London South Bank University from scratch depending on the previous research papers to study the wax deposition process under single phase transport through a pipe.
- To carry out experiments in the lab rig to study the effect of factors on wax deposition, such as inlet coolant temperature, flow rate, pressure drop, shear stress, recycling crude oil and experimental time, to contribute to the understanding of the wax deposition process.
- To evaluate the chemical inhibitor effects on the rheological behaviour of the crude oil.
- To study and examine the chemical inhibitor effects on wax deposition in the lab rig.
- To study and examine spiral flow effects on wax deposition in the lab rig.
- To use OLGA software to simulate the multiphase flow in the rig pipe for this study.

## **1.6 Thesis Structure**

Chapter one presents the introduction and outlines the research project's objectives in the study of the wax deposition problem.

Chapter two reviews the literature associated with the wax deposition problem. The proposed mechanisms of wax deposition and the factors that affect and control the wax deposition process are reviewed. The relevant wax mitigation methods are also reviewed, such as the chemical inhibitors. The spiral flow in different study areas has been reviewed and used as a new wax mitigation method in this study. Gaps in knowledge and rationale for this work are discussed.

Chapter three reviews the details of the flow loop system designed and used in this work to study the wax deposition process and present the set-up used to study the rheological behaviour of crude oil and the impact of chemical inhibitors. It also presents the design to study the spiral flow as a waxing mitigation method.

Chapter four discusses the results of using the effect of the chemical inhibitors on crude oil rheology, such as alkylated phenol in heavy aromatic naphtha, polyacrylate based polymer (C16-C22), copolymer and acrylated monomers, copolymer dissolved in solvent naphtha and ethylvinyl acetate. The synergy of using mixtures of these chemicals is also discussed.

Chapter five discusses the results of the experiments and to investigate the effect of the chemical inhibitor and spiral flow on wax deposit thickness. A discussion of the effect of factors, such as inlet coolant temperature, flow rate, pressure drop, oil temperature, and experimental time, on wax thickness is presented.

Chapter six describes the underlining wax models implemented using the multiphase flow simulator OLGA, in order to reproduce experimental results of this study by tuning analogies properties.

Chapter seven presents the conclusions of the research and recommendations for future work.

## 1.7 Publications

1. Theyab, M.A., Diaz, P. (2017) Experimental Study on the Effect of Polyacrylate Polymer (C16-C22) on Wax Deposition. *International Journal of Chemical Engineering and Applications* 8 (1): 16-21. doi: 10.18178/ijcea.2017.8.1.624.
2. Theyab, M.A., Diaz, P. (2017) An Experimental and Simulation Study of Wax Deposition in Hydrocarbon Pipeline. *Global Journal of Engineering Science and Researches* 4(7): 27-40. doi: 10.5281/zenodo.821334.
3. Theyab, M.A., Diaz, P. (2016) Experimental Study of Wax Deposition in Pipeline – Effect of Inhibitor and Spiral Flow. *International Journal of Smart Grid and Clean Energy* 5 (3): 174-181. doi: 10.12720/sgce.5.3.174-181.
4. Theyab MA, Diaz P (2016) Experimental Study on the Effect of Inhibitors on Wax Deposition. *Journal of Petroleum and Environmental Biotechnology* 7 (6): 310. doi: 10.4172/2157-7463.1000310.
5. Theyab, M.A., Diaz, P. (2016) Experimental Study on the Effect of Spiral Flow on Wax Deposition Thickness, *One petro*, presented at SPE Russian Petroleum Technology Conference and Exhibition, Moscow, Russia, 24-26 October. SPE 181954-MS. <https://doi.org/10.2118/181954-MS> (*published in English and Russian languages*).
6. Theyab, M.A., Diaz, P. (2016) Experimental Study on the Effect of Spiral Flow on Wax Deposition Volume, *One petro*, presented at Abu Dhabi International Petroleum Exhibition and Conference, Abu Dhabi, UAE, 7-10 November. SPE-182936-MS. doi:10.2118/182936-MS.

## **Chapter 2: Literature Review**

### **2.1 Chapter Two Overview**

This chapter outlines the way in which waxing is one of the fluid flow assurance issues associated with multiphase transport in oil fields. It provides an overview of research that has been done in the area of the wax deposition process in offshore pipelines. The chapter also presents an evaluation of both experimental and simulation work conducted in the past on the wax precipitation process in the pipeline. Some of the main proposed mechanisms for wax deposition are presented, along with a discussion of the factors that affect and control the wax deposition process. Wax mitigation methods are studied, such as the chemical inhibitors and spiral flow. Gaps in knowledge and a rationale for this work are reviewed.

### **2.2 Fluid Flow Assurance Issues**

Flow assurance is defined as the process of ensuring the successful and economical flow of hydrocarbon stream transport from the reservoir to the point of sale (Irmann-Jacobsen, 2013). In recent years, flow assurance has been considered the most critical task in deep-water energy production due to long distances, high pressures and low temperatures (Tarek Ahmed, 2007; Johal, 2012) that cause financial losses based on production interruption and damage in pipeline or surface facilities due to solid deposits.

Flow assurance is applied to the petroleum flow path during all stages of production, including system selection, detailed design, surveillance, troubleshooting operation problems, increased recovery in late life, etc. (Tarek Ahmed, 2007; Irmann-Jacobsen, 2013).

The major flow assurance issues that need to be considered for the production of multiphase flow through pipelines and risers in offshore or onshore oil and gas field developments are waxing, hydrates, asphaltenes, slugging, naphthenates, scales, corrosion, erosion and emulsions. Waxing is the main issue in this research, so it will be considered in more detail below.

#### **2.2.1 Hydrates**

Hydrates are crystalline materials similar to ice in structure and form; at high-pressure and low-temperature conditions when light hydrocarbons (e.g. methane, ethane, propane, isobutane and inorganic molecules such as CO<sub>2</sub> and H<sub>2</sub>S) meet with water, crystalline molecular complexes form that cause blockages in gas flowlines, as shown in figure 2.



Figure 2: Hydrate plug formed in a subsea hydrocarbon pipeline (Irmann-Jacobsen, 2013; Heriot-Watt University, 2014).

The most effective solutions to resolve this issue involve the use of the chemical inhibitors such as monoethylene glycol (MEG) or methanol, pipeline insulation, depressurisation, direct electrical heating, or the cold flow method (Johal, 2012; Larsen et al., 2003).

### **2.2.2 Asphaltenes**

Asphaltenes are polar compounds, as shown in figure 3, which present in the heaviest fractions of the crude oil and are defined by their solubility characteristics. They are precipitated if diluted by normal alkane, such as n-heptane, and soluble in aromatic solvents such as toluene. It is known that during production asphaltenes can precipitate as a result of a large change in pressure, temperature and fluid composition. Asphaltene precipitation is more likely to occur in an under-saturated, light reservoir fluid than a heavy hydrocarbon system.

Various problems result due to asphaltene precipitation, including a decline in the production rate and other operational problems, such as higher viscosity and water-oil emulsion, etc. In the industry, there is a consensus that the prevention principle is the best way to solve the problems caused by solids deposition (Johal, 2012; Joshi et al., 2003).



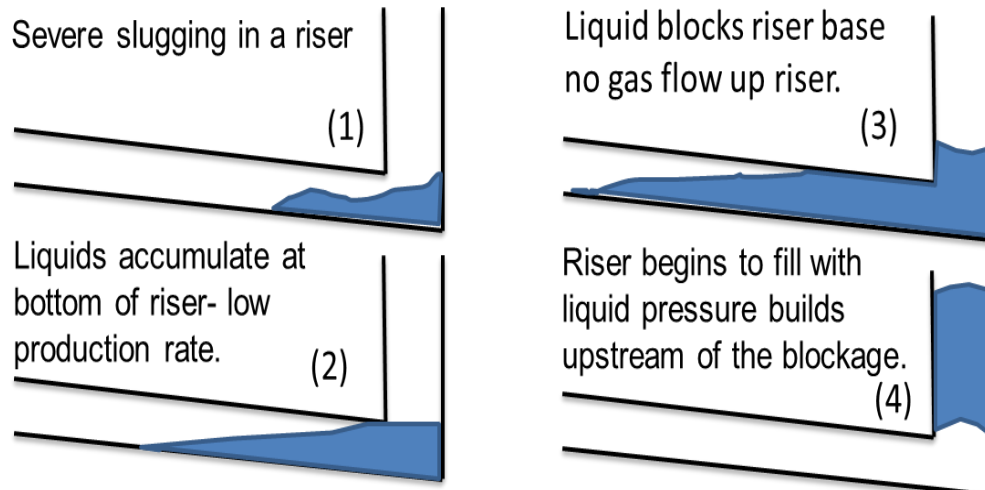
Figure 3: Polar compounds of asphaltenes (Alberta Innovates Technology Futures, 2016).

### **2.2.3 Slugging**

Slug flow is one of the flow patterns occurring in multiphase pipelines. It is characterised by a series of liquid plugs (slugs) separated by relatively large gas pockets, as shown in figure 4. Slugging in production pipelines and risers has been a major operational issue due to the creation of instability in production flow as a result of pressure fluctuation, thereby causing considerable and unnecessary loss in production and revenue (Guo et al., 2005).

Severe slugging is a phenomenon occurring in two-phase flow through a downward inclined flow line followed by a vertical riser at low gas flow rates. In this phenomenon, the liquid accumulations in the riser and curvature section of the flow line blocking the passage of gas in the lowest point of the system. As a result, the gas front penetrates the liquid blockage intermittently, causing extremely large slugs, severe fluctuations, and flooding of downstream equipment (Barreto et al, 2017).

There are several techniques that can be used to mitigate production slugging, such as the riser base gas-lift system, complex detection and control systems, use of large slug catchers, and intelligent slug mitigation systems (Guo et al.,2005; Johal, 2012, Malekzadeh, 2012; Barreto et al, 2017).



Upstream pressure > hydrostatic head in riser. Slug of liquid accelerates up riser. Gas surge follows liquid slug.

Figure 4: Slug formation in the riser of the hydrocarbon pipeline (modified from Johal, 2012).

#### 2.2.4 Naphthenates

Over the past two decades, many operators have faced the complex deposition problem of naphthenate along with other higher organic and inorganic scale. Such deposits can hinder oil production in two possible ways, formation of hard and sticky deposit, and creation of sludgy foam contributing to forming tough emulsion. Naphthenates can cause serious oilfield issues, such as the potential shutdown of the offshore facilities due to naphthenate deposits, or the formation of tough micr-emulsion contribute to a decline in oil quality and production rate (Mohamed et al, 2016).

Naphthenates are formed from the salts of naphthenic acids when they precipitate as acidic fractions resulting from the processing of petroleum products. A naphthenate is composed of a heavy mixture of organic acids such as cycloalkyl carboxylic acids, see figure 5 (Johal, 2012). The formation of naphthenate salts is an emerging problem and occurs in the production of crudes with significant amount of naphthenic acids and produced water with significant amounts of alkali or alkali earth metals (Junior et al., 2013).

In general, all kinds of naphthenates can cause production losses in oil fields. Naphthenates can also have a major effect on separation efficiency of the host processing facilities, especially calcium and sodium types, which the most are commonly found naphthenates in oil fields (Johal, 2012; Junior et al., 2013).



Figure 5: An example of a naphthenic acid structure (Johal, 2012).

### 2.2.5 Scales

Scales can develop in the transportation system as a result of water forming deposits, as a crystalline growth of insoluble salt or oxides held within the water component. Scale compounds will precipitate out of water when their individual solubility in water is exceeded as a result of incompatibility, and this will reduce the transport capacity of flowlines and potentially cause plugging, as shown in figure 6. The formation of scale deposits depends on temperature, the concentration of scale forming species, pH, water quality and hydrodynamic conditions. Scale inhibition mechanism is based on the prevention of nucleation and salt crystal growth in the solution (Abdel-Aal et al., 2015).

There are different types of scale inhibitors for preventing different kinds of inorganic salt formation; including  $CaCO_3$  Scale inhibition mechanism is based on the prevention of nucleation and salt crystal growth in the solution (Abdel-Aal et al., 2015; Azizollah et al., 2017). There are different types of scale inhibitors for preventing different kinds of inorganic salt formation, including  $CaCO_3$  (Azizollah et al., 2017). Several existing techniques are followed to reduce scale, such as mechanical means, chemical dissolution and scale inhibitors (Johal, 2012; Azizollah et al., 2017).





Figure 6: Formation of scale in the pipe (McLay, 2015).

### **2.2.6 Corrosion**

Pipeline corrosion is one of the main causes of subsea pipeline failure. It is necessary to monitor and analyse pipeline condition to effectively predict likely failure. Subsea pipeline corrosion weakens the resistance of pipelines to internal and external forces, and it becomes the leading factor that causes the integrity loss of the pipelines (Yongsheng et al., 2017).

When carbon steel pipes are used in transporting oil and multiphase flow containing a fraction of water, there is usually a high risk of corrosion. The decision to use carbon steel is usually economic – in order to minimise capital expenditure – and its use usually requires the implementation of a full internal corrosion management strategy to control corrosion levels throughout the system life.

Various mechanisms have been postulated for the corrosion process; all of these involve the formation of a carbonic acid ion or bicarbonate when  $\text{CO}_2$  is dissolved in water. This process can lead to corrosion, see figure 7, of the material at a rate that is greater than that from general acid corrosion with the same pH value. The mechanism of corrosion is dependent on the quantity of the  $\text{CO}_2$  dissolved in the water phase, and predictions of corrosion levels are currently based on the knowledge of  $\text{CO}_2$  partial pressure and the use of correlations such as De Waard Milliams (Johal, 2012; Yongsheng et al., 2017).

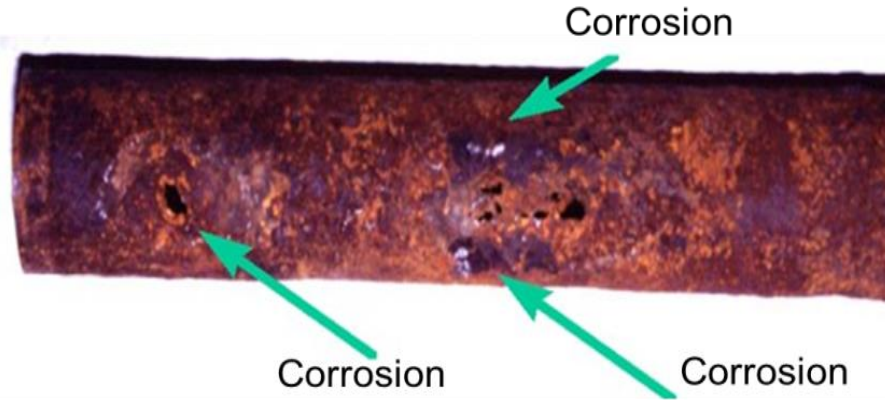


Figure 7: Corrosion formation in the pipe (Southwest Gas, 2016).

### 2.2.7 Erosion

Erosion due to solid particles is a major problem in many industrial applications, particularly in the field of oil and gas (Zamani et al., 2017). Sudden change in the flow direction in elbows leads to considerable changes in particle distribution in the flow and consequently higher erosion rate. For example Lin et al. showed that the erosion rate of 90° elbows is 50 times bigger than in straight pipes (Lin et al., 2015).

Erosion due to sand production has been considered the cause of a number of problems associated with separation efficiency, material loss and flow path blockages, see figure 8. Sand screens are generally installed in the horizontal sections of production well bores in order to minimise sand production. The erosion predictive technique should include the mechanisms of kinetic energy imparted by the sand particle velocity and size, and the angle of the impact on the material should also be included in the erosion prediction calculations in order to estimate an accurate erosion rate (Johal, 2012; Lin et al., 2015; Zamani et al., 2017).

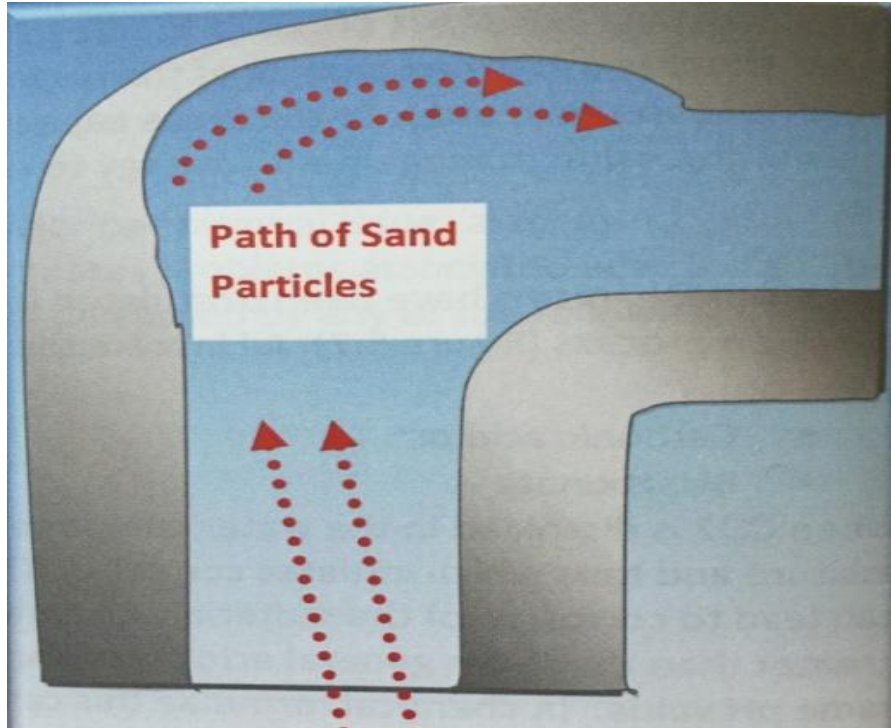


Figure 8: The effects of sand erosion at a pipe bend (Johal, 2012).

### 2.2.8 Emulsions

With a combination of low ambient sea temperature and high fluid viscosity due to inversion water cut conditions, tight emulsions can occur between the water and oil phases, see figure 9. This can impair the separation efficiency at the processing facility, and thus cause a loss in the production of the asset. In system shutdown conditions, the rheology of the fluids may change from Newtonian to non-Newtonian, exhibiting characteristics of high yield stress during low shear rate production start-up operations. In these conditions there may be a need to inject de-emulsifiers into the subsea facilities and also to ensure that sufficient pressure is available to re-start the system following an unplanned shutdown (Johal, 2012; Zhang et al., 2017).

Inappropriate handling and management of the petroleum emulsions can cause serious detrimental effects on public health and environment due to its high toxicity and high production quantity worldwide; naphthenic acids and heavy metals are the major toxic components in the petroleum emulsions, which are highly lethal for micro-organisms, aquatic algae and aquatic organisms (Zhang et al., 2017).

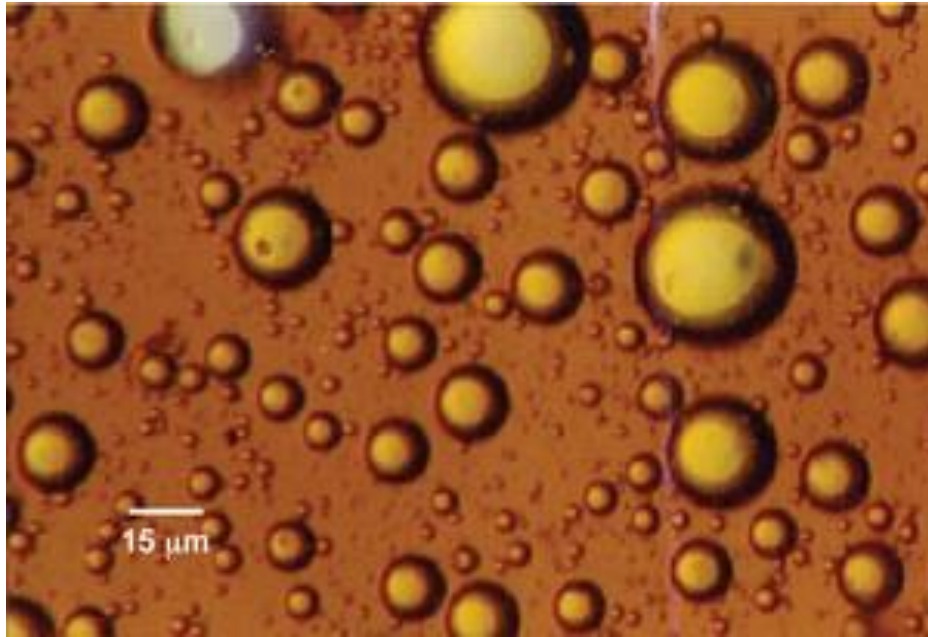


Figure 9: Photomicrograph of a water-in-oil emulsion (PetroWiki, 2015).

### 2.3 Wax Deposition

Occasionally in the literature wax deposition is referred to interchangeably with wax precipitation, but the two are in fact different concepts (Zhu et al., 2008). Wax deposition refers to the formation of a layer of separate solid phase and the eventual growth of this layer on a surface in contact with the crude oil. Wax deposits can be formed from an already precipitated solid phase (wax) through mechanisms of shear dispersion, gravity settling and Brownian motion, or from dissolved wax molecules through a molecular diffusion mechanism (Huang et al., 2015; Rosvold, 2008).

Wax deposition in the pipe can only occur when the inner pipe wall temperature is below the wax appearance temperature, also referred to as the cloud point temperature. The precipitated wax molecules near the pipe wall start to form an incipient gel at the cold surface. The incipient gel formed at the pipe wall is a 3-D network structure of wax crystals and contains a significant amount of oil trapped within it. The incipient gel grows as time progresses and there are radial thermal and mass transfer gradients as a result of heat loss to the surrounding area, as shown in figure 10 (Lee, 2008).

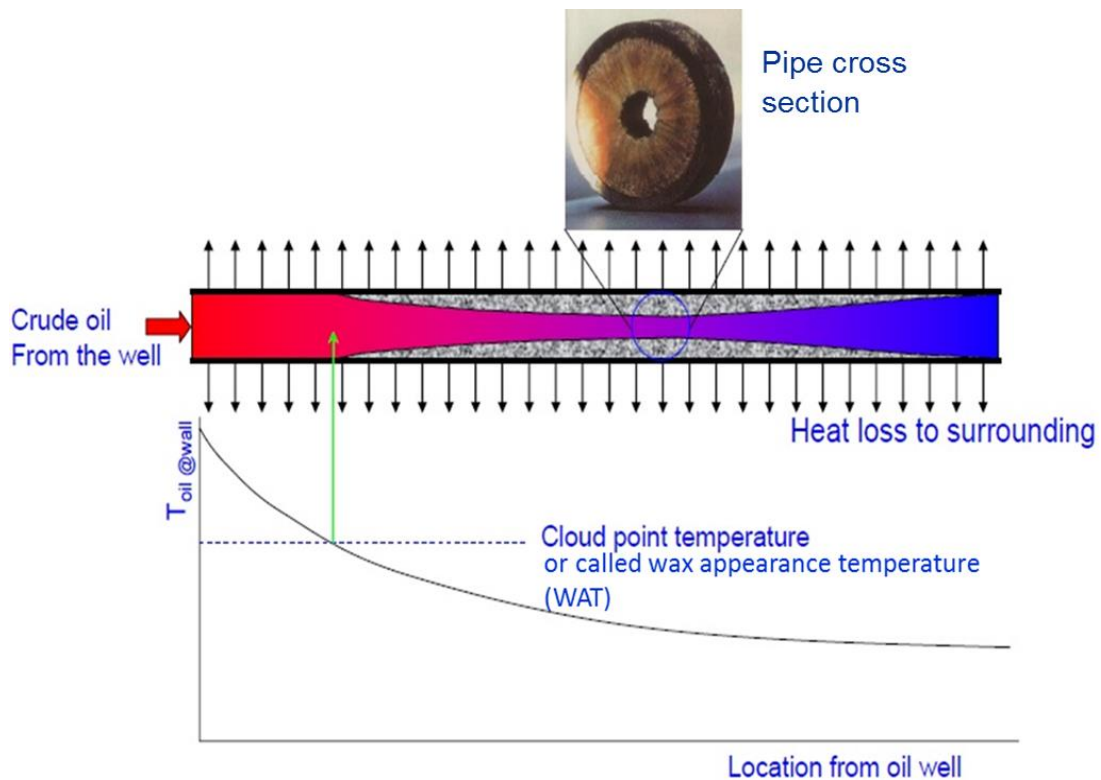


Figure 10: Wax deposition process in the hydrocarbon pipeline (Lee, 2008; Al-Yaari, 2011).

## 2.4 Wax Crystallisation

One of the important issues to be noted is that the wax deposit is not solid wax, but a gel that consists of solid wax crystals and trapped liquid. The deposit is also known to harden with time in a process termed aging (Venkatesan and Creek, 2007; Tordal, 2006). The precipitation of wax components out of the oil is responsible for changes in the waxy crude oil properties, including the gelation of oil and an increase in viscosity (Zhu et al., 2008). Wax contains a high molecular weight n-Paraffin and consists of long chain alkanes with 20 to 50 carbon atoms (Time, 2011). Wax can precipitate as a solid phase when the crude oil temperature drops below the wax appearance temperature (WAT): the temperature at which the first wax crystals start to form in the crude oil in a cooling process (Dantas Neto et al., 2009; Lee, 2008; Tordal, 2006; Botne, 2012).

Crystallisation is generally the process of separation of the solid phase from a homogenous solution; the separated solid phase appears as crystals. Paraffins (waxes) remain in solution as natural components of crude oil until the temperature gets to or below their solubility limit. The terms crystallisation and precipitation have been used interchangeably in wax deposition studies and will also be used to refer to the same process in this work. Two types of wax crystals have been distinguished: macrocrystalline wax, mainly composed of normal paraffin, and micro-crystalline wax from isoparaffins and naphthenes (Zhu et al., 2008; Kasumu, 2014).

Wax crystallisation involves two stages: nucleation and then a growth stage. As the solubility limit is approached, the kinetic energy of the paraffin molecules is reduced as a result of temperature reduction. As a consequence of this reduced kinetic energy, the motion of the wax molecules is hindered, leading to continuous reduction and closure of the space between the molecules. As this process continues, the wax molecules get tangled, forming clusters that grow larger and become stable upon reaching a certain critical size, see figure 11. Nucleation and growth occur simultaneously in the oil system, with one or other predominating (Zhu et al., 2008; Kasumu, 2014).

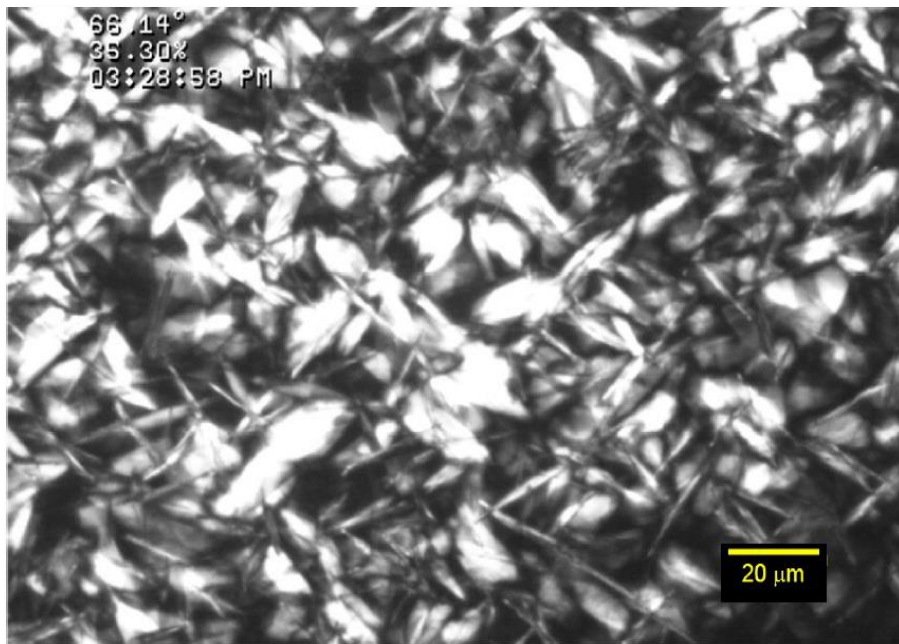


Figure 11: Polarised picture of wax crystals (Siljubergh, 2012).

## 2.5 Wax Deposition Mechanisms

Wax deposition is conceptually similar to other deposition mechanisms encountered in the engineering and medical fields, such as crystallisation fouling, frost formation and atherosclerosis. A number of mechanisms have been proposed to describe the formation of wax deposits on pipe walls. These mechanisms initially proposed by Burger et al. (1981), Singh et al. (2000) and then by Huang et al. (2015), include:

- Molecular diffusion: wax deposition due to the diffusion of the dissolved molecules of the waxy components toward the wall;
- Shear dispersion: wax deposition due to the dispersion of the precipitated particles of the waxy components toward the wall;
- Brownian diffusion: wax deposition due to the diffusion of the precipitated particles toward the wall; the diffusion of the precipitated particles is caused by Brownian motion;

- Gravity settling: wax deposition due to the settling of the precipitated particles of the waxy components toward the bottom of the pipe.

### **2.5.1 Molecular Diffusion**

For all flow conditions, oil will be in laminar flow, either throughout the pipe, or in a thin laminar sub-layer adjacent to the pipe wall. When the oil is being cooled, there is a temperature gradient across the laminar sub-layer. If the temperature is below the level where solid waxy crystals can be precipitated, then the flowing elements of oil will contain precipitated solid particles and the liquid phase will be in equilibrium with the solid phase; the liquid will be saturated with dissolved wax crystals. The temperature profile near the wall will lead to a concentration gradient of dissolved wax, and this dissolved material will be transported toward the wall by molecular diffusion. When this diffusing material reaches the solid/liquid interface, it will be precipitated out of solution (Singh et al., 2000; Lee, 2008; Han et al., 2010; Huang et al., 2015).

Singh et al. (2001) reported that there are two stages involved in wax deposition: wax gel formation and then the aging of the deposited wax gel. Petroleum wax deposits contain some entrapped crude oil, water, gums, resins, sand and asphaltenes, depending on the nature of the particular crude oil.

The trapped oil in the wax deposit causes diffusion of wax molecules into the gel deposit and counter-diffusion of oil out of the gel deposit, as shown in figure 12. A fraction of hydrocarbons with carbon numbers above a certain value (the critical carbon number) precipitate out of the oil as stable crystals to form a gel with the remaining hydrocarbons trapped in the gel network (Singh et al., 2000). In the gel deposit, the fraction of molecules with carbon numbers greater than the critical carbon number increases, while that of molecules with carbon numbers lower than the critical carbon number decreases. The diffusion and counter-diffusion, leading to hardening of the gel deposit, increases the size of the deposit, and increases the amount of wax in the gel deposit; this process is called aging, the second stage of wax deposition. Molecular diffusion is therefore critical to the aging and hardening of wax gel deposits (Singh et al., 2000; Lee, 2008).

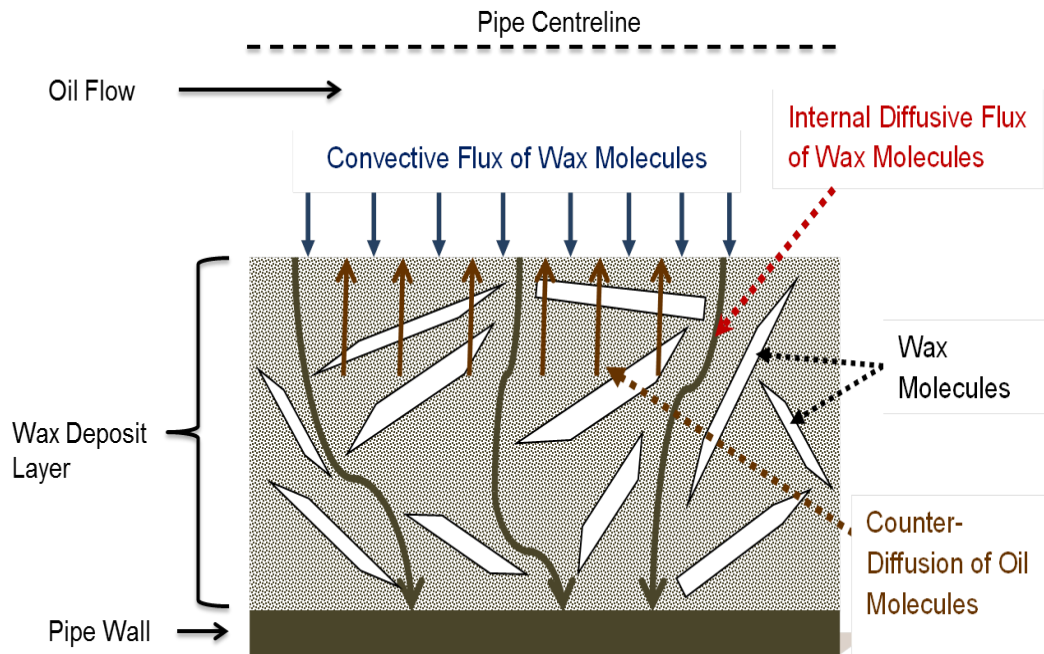


Figure 12: Illustration of how wax molecules diffuse to form the wax deposit layer (modified from Siljberg, 2012).

Huang et al. (2015) proposed four different stages in the molecular diffusion mechanisms for wax deposition, as shown in figure 13; these steps are outlined below.

**Step 1: Precipitation of dissolved wax molecules**

Once the fluid temperature decreases to below the wax appearance temperature (WAT), the dissolved waxy components start to precipitate out of the oil and form crystals. Precipitation of the waxy components can occur both in the bulk oil and on the pipe wall, as long as the temperature at that particular location is below the WAT, as shown in figure 13 (step 1). The precipitated wax crystals that form in the bulk are believed to flow with the oil and are not deposited on the pipe wall. Therefore, it is the precipitation of the waxy components at the wall that forms the incipient layer of the wax deposit (Han et al., 2010; Phillips et al., 2011).



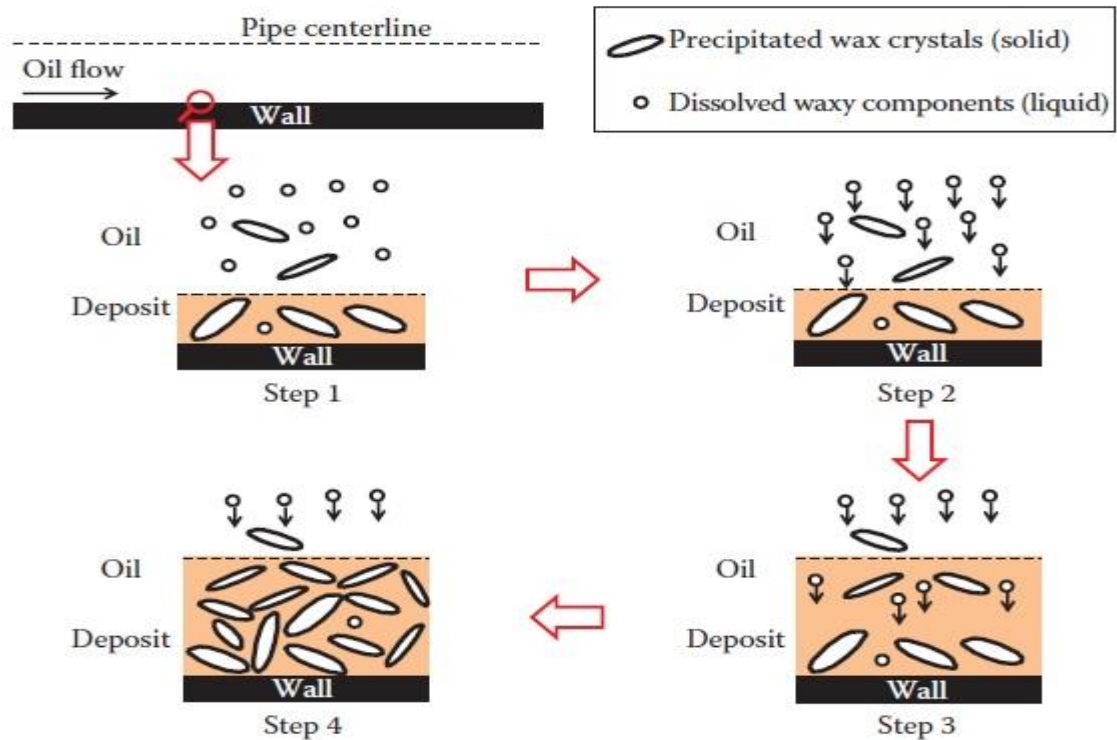


Figure 13: Schematic of molecular diffusion as the wax deposition mechanism (Huang et al., 2015).

### Step 2: Formation of radial concentration gradient of dissolved waxy components

During normal cooling conditions, the pipe inner wall usually has a lower temperature than the bulk oil. Therefore, the degree of precipitation of waxy components is generally greater on the wall than in the bulk, resulting in a greater concentration of dissolved waxy components in the bulk oil than on the pipe wall, thereby creating a radial concentration gradient of the waxy components between the bulk oil and the wall. The concentration gradient results in the diffusion of the waxy components from the bulk oil, which has a higher concentration of the dissolved waxy components, towards the wall, which has a lower concentration of the dissolved waxy components, as highlighted in figure 13 (step 2) (Green, 2008).

### Step 3: Deposition of waxy components on the surface of an existing deposit

The precipitation of waxy components on the surface of a wall contributes to the formation of the wax deposit. Once an incipient deposit layer is formed, the boundary of the oil region becomes the surface of the deposit. In this case, the precipitation of the dissolved waxy components on the deposit surface leads to further growth of the wax deposit, as shown in figure 13 (step 3). Due to the fact that the waxy crude oil continues to flow through the pipe, diffusion of dissolved waxy components towards the deposit continues

to occur, resulting in the build-up of the wax deposit (Noville & Naveira, 2012; Bai and Zhang, 2013).

#### **Step 4: Internal diffusion and precipitation of waxy components in the deposit**

Although diffusion constantly brings the molecules of waxy components to the oil-deposit interface, not all of these molecules that precipitate at the interface form a new layer of deposit. Some of these dissolved waxy components have been found to continue to diffuse into the wax deposit, resulting in an increase in the wax fraction in the wax deposit (deposit aging). Consequently, during the course of the wax deposition, most of these dissolved waxy components in the deposit are above the solubility limit and could further precipitate to form crystals, resulting in an increase in the solid fraction in the deposit (Huang et al., 2015; Solaimany Nazar et al., 2005; Hoffmann & Amundsen, 2010; Noville & Naveira, 2012; Bai and Zhang, 2013).

#### **Molecular Diffusion Equation**

As discussed, precipitation of wax occurs at contact points between the dissolved wax solution and the cool wall surface. The experiment by Burger et al. (1981) confirmed that molecular diffusion dominates as the primary mechanism at high temperature heat flux conditions typical of subsea flowline systems. They showed that Fick's law of diffusion can model molecular diffusion of solid wax in oil and gas flows. Thus, the rate of wax deposition can be described by the following equation:

$$\frac{dM_w}{dt} = \rho_w D_w A_w \frac{dC}{dr} = \rho_w D_w A_w \frac{dC}{dT} \frac{dT}{dr} \quad (2.1)$$

Where  $dM_w/dt$  is the rate of wax deposited (kg/s),  $\rho_w$  is the density of the solid wax (kg/m<sup>3</sup>),  $D_w$  is the diffusion coefficient of the wax in the oil phase (m<sup>2</sup>/s),  $A_w$  is the area of wax deposition (m<sup>2</sup>),  $dC/dr$  is the wax concentration gradient (1/m) of wax concentration over pipe radial coordinate  $r$  (m),  $dC/dT$  is the solubility coefficient of the wax crystal in the oil phase (1/°C) and  $dT/dr$  is the radial temperature gradient of the wall (°C/m).

The diffusion coefficient can be described as follows:

$$D_w = 7.4 \times 10^{-9} \frac{T_a (\xi M)^{0.5}}{\mu V^{0.6}} \quad (2.2)$$

Where  $T_a$  is the absolute temperature (K),  $M$  is the molecular weight of the oil solvent (g/mol),  $V$  is the wax molar volume (cc/gmole),  $\mu$  is the dynamic viscosity (cP) and  $\xi$  is an association parameter representing the effective molecular weight of the solvent with respect to molecular diffusion and  $V^{0.6}$  is

proportional to the absolute temperature  $T_a$ . The association parameter  $\xi$  and the molecular weight of the oil solvent  $M$  are constants in the equation. The diffusion coefficient in principle is proposed as a function of oil constant  $C_1$  and oil viscosity in many diffusion coefficient models.

$$D_w = \frac{C_1}{\mu} \quad (2.3)$$

As temperature decreases in the radial direction of the pipe, the viscosity of the oil can increase and the diffusion coefficient of the wax in oil can decrease substantially (Huang et al., 2015).

It can therefore be concluded that molecular diffusion is considered as the main mechanism for wax deposition due to the diffusion of the dissolved molecules of the waxy components toward the wall; this has also been used by many wax modelling studies (Huang et al., 2015; Solaimany Nazar et al., 2005; Venkatesan, 2004; Han et al., 2009; Singh et al., 2000).

### 2.5.2 Shear Dispersion

When small particles are suspended in a fluid that is in laminar motion, the particles tend to move at the mean speed and in the direction of the surrounding fluid. The particle speed is that of the streamline at its centre, and the particle rotates with an angular velocity that is half the fluid shear rate, as shown in figure 14 (Siljberg, 2012).

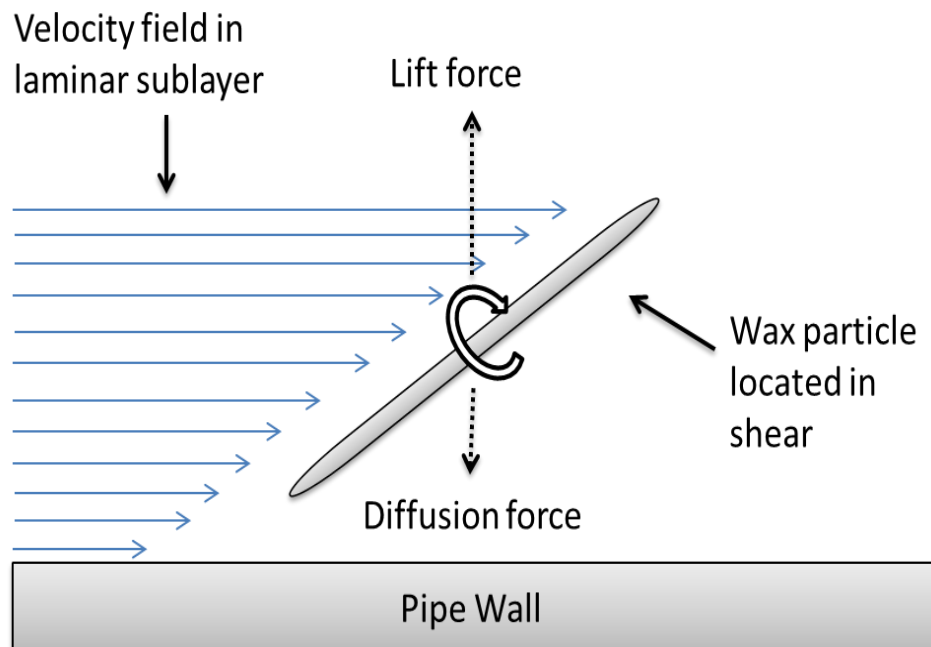


Figure 14: Long wax particle located in shear flow (modified from Siljberg, 2012).

If the particles approach a solid boundary, both linear and angular velocities will be reduced. Due to the fluid viscosity, rotating particles will impart a

circulatory motion onto a layer of fluid adjacent to the particle. This rotating fluid region exerts a drag force on neighbouring particles. In a shear field, each particle passes and interacts with nearby particles in slower or faster moving streamlines. When only two particles are present, far from a wall and at a very low Reynolds number, these passing encounters result in large temporary displacements. As the particles pass, their trajectories are such that the particles curve around one another and return to their original streamline; thus, there is no net lateral displacement. If the particle concentration is high, however, then a significant number of multi-particle interactions will occur. These multi-particle collisions result in net lateral transport and dispersion of particles (Zhu et al., 2008).

Shear dispersion can be modelled by the dispersion coefficient of Burger et al. (1981):

$$D_s = \gamma \frac{d_w^2 \phi_w}{10} \quad (2.4)$$

Where  $\gamma$  is the oil shear rate at the pipe wall (1/s),  $d_w$  is the wax particle diameter (m),  $\phi_w$  is the wax volume fraction out of the solution at the wall and  $D_s$  is the shear dispersion coefficient (m<sup>2</sup>/s).

### 2.5.3 Brownian Diffusion

When suspended in oil small waxy crystals will be continually bombarded by thermally agitated oil molecules. These collisions will lead to small random Brownian movements of the suspended particles. If there is a concentration gradient of these particles, the Brownian motion will lead to a net transport, which in nature and mathematical description is similar to diffusion (Huang et al., 2015; Zhu et al., 2008).

Agitated oil molecules bombard precipitated wax suspended in waxy-oil flows. This creates a net irregular movement of wax particles (Burger et al., 1981). If concentration gradients exist for the wax solid, a net transport of the precipitated molecules is initiated in the direction of decreasing concentration modelled by Fick's law of diffusion (Azevedo et al., 2003).

$$\frac{dM_B}{dt} = \rho_w D_B A_w \frac{dC}{dr} \quad (2.5)$$

Where  $M_B$  is the mass of deposited wax due to Brownian diffusion (kg),  $\frac{dC}{dr}$  is the concentration gradient over the pipe radial coordinate (1/m),  $A_w$  is the area of wax deposition (m<sup>2</sup>) and  $D_B$  is the Brownian diffusion coefficient

(m<sup>2</sup>/s) derived by the following equation (Burger et al., 1981; Azevedo et al., 2003; Rosvold, 2008):

$$D_B = \frac{RT_a}{6\pi\mu aN} \quad (2.6)$$

$R$  is the gas constant (J/(mol.K)),  $T_a$  is the absolute temperature (K),  $\mu$  is the oil viscosity (Ns/m<sup>2</sup>),  $a$  is the Brownian particle diameter (m) and  $N$  is Avogadro's number (1/mol).

#### 2.5.4 Gravity Settling

Precipitated waxy crystals are denser than the surrounding liquid oil phase. Hence, if particles are non-interacting, they will settle in a gravity field and can be deposited on the bottom of pipes or tanks. For an initially uniform mixture in a vessel, there will be a beginning rate of settling, followed by a diminishing rate of deposition, which will asymptotically approach zero at complete settling (Zhu et al., 2008).

In a typically active system, as found in oil and gas pipelines, gravity settling has been found to be negligible as the suggested shear dispersion mechanism or active fluid forces create dispersion of precipitated wax particles, thereby eliminating gravity settling (Burger et al., 1981; Azevedo et al., 2003). However, in low flow rates, at typical shut-in conditions or in storage tanks, the gravity effect is expected to contribute to significant wax deposition particularly observed for low viscous fluids. The settling velocity  $U$  (m/s) is given by the modified Stokes' law of settling crystals in a pseudoplastic fluid as follows (Ajayi, 2013):

$$U = \left[ \frac{g\Delta P a^{(1+n)}}{18K_p} \right]^{1/n} \quad (2.7)$$

Where  $\Delta P$  is the density difference (kg/m<sup>3</sup>) between the settling wax and the oil,  $a$  is the particle diameter (m),  $n$  the power-law index,  $g$  the acceleration due to gravity (m/s<sup>2</sup>) and  $K_p$  is the power-law consistency index.

The shear rate and shear stress relationship of a power law fluid implied in the correlation is given to be:  $\tau = K_p \gamma^n$ , where  $\tau$  is the shear stress (N/m<sup>2</sup>) and  $\gamma$  is the shear rate of the fluid (1/s) (Burger et al., 1981).

The other three mechanisms – Brownian diffusion, gravity settling and shear dispersion – are considered, according to the work of researchers (Huang et al., 2015; Solaimany Nazar et al., 2005; Venkatesan, 2004; Han et al., 2009; Singh et al., 2000; Burger et al., 1981; Hsu and Brubaker, 1994), as secondary mechanisms that can contribute to the wax deposition and identifying which mechanism plays the primary role in wax deposition.

Singh et al. (2000) and Burger et al. (1981) stated that the Brownian diffusion of wax particles is not likely to be valid because the wall temperature is lower than the oil bulk temperature, resulting in more precipitated wax particles at the wall than in the bulk oil. Consequently, the impact of Brownian diffusion is to transport these precipitated particles from the wall toward the bulk oil, instead of moving them toward the wall and deposit (Solaimany Nazar et al., 2005). Burger et al. (1981) and Hsu and Brubaker (1994) noted that gravity settling is also believed to be insignificant as there has not been a study claiming that wax deposits are generally thicker at the bottom than the top of the pipe wall in single-phase oil flow conditions. The mechanism of shear dispersion was studied by Bern et al. (1980); they found that the wax deposition rate did not increase with the increasing shear rate of the fluid, casting the first doubt on this mechanism for wax deposition.

## **2.6 Factors Affecting the Wax Deposition Process**

Several factors affect and control the wax deposition process in pipelines, such as pipe wall temperature (inlet coolant temperature), crude oil composition, crude oil temperature, ambient temperature, flow rate, thermal history, time and pressure (Kasumu, 2014; Adeyanju and Oyekunle, 2013; Dwivedi, 2012; Noville and Naveira, 2012; Semenov, 2012; Leontaritis and Geroulis, 2011; Tiwary and Mehrotra, 2009; Solaimany et al., 2005; Singh et al., 2001; Singh et al., 2000; Creek et al., 1999; Hammami and Raines, 1999; Misra et al., 1995). Lab and field data shows that some of the most dominant factors in the deposition of waxes, as mentioned in Leontaritis and Geroulis (2011), are:

- Wall-fluid temperature difference;
- Shear stress and shear rate;
- Flow rate or flow regime (Reynolds number);
- Wax bulk concentration;
- Wax crystal formation rate;
- Gravity in non-flowing systems;
- Conduit wall wettability;
- Conduit wall roughness.

### **2.6.1 Temperature Differential and Cooling Rate**

Wax deposition increases with an increase in the temperature difference between the bulk of the wax solution and the cold surface (Singh et al., 2001). Wax deposition will only occur when the surface temperature is below both the solution temperature and the solution cloud point.

The impact of pipe wall cold surface (inlet coolant temperature) on wax deposition has been studied and reported in many recently-published

papers, where it is considered as one of the main factors to affect wax deposition (Adeyanju and Oyekunle, 2013; Dwivedi, 2012; Noville and Naveira, 2012; Semenov, 2012; Al-Yaari, 2011; Leontaritis and Geroulis, 2011). The main conclusion in these works was that the inlet coolant temperature plays an important role in the wax deposition process; decreasing the inlet coolant temperature will increase the wax deposition, even when the crude oil temperature is above the wax appearance temperature.

Initially, the rate of wax deposition is high, but it slows down as more wax is deposited on the pipe surface. The thickness of the wax layer increases and this layer acts as thermal insulation and reduces the effective temperature differential. This lowers the availability of wax crystals for further deposition (Misra et al., 1995). The size and number of crystals formed are also important for wax deposition.

At a higher rate of cooling, the wax precipitates out of the oil in smaller crystals and a large number of crystals are formed because of the large number of crystallisation sites available. At a lower rate of cooling, the crystallisation process is more uniform. Thus, more uniformly packed crystals are formed that possess a relatively small surface area and free energy. The temperature differential also affects the composition of the deposited wax; if it is high, cooling is rapid and both lower and higher melting waxes crystallise simultaneously, forming a weak porous structure (owing to mal-crystallisation) with cavities full of oil (Misra et al., 1995; Kang et al., 2014).

### **2.6.2 Crude Oil Composition**

Singhal et al. (1991) stated that the crude oil composition is one of the main factors that significantly impacts wax deposition and is responsible for the pour point and viscosity reduction. The composition of crude oil comprises a mixture of molecules of different natures: there are light molecules like methane that are responsible for solid hydrate formation at high pressure and low temperature and heavy molecules such as long linear alkanes and isoparaffins that tend to change phase at low temperature in the phase of both macro and microcrystalline solids. There is also a transition towards more polar compounds due to the appearance of aromatic compounds and the presence of heteroatoms (oxygen, sulphur and nitrogen) in the fractions known as resins and asphaltenes (Merino-Garcia et al., 2013; Zerpa et al., 2011; Merino-Garcia et al., 2010).

Valinejad and Solaimany (2013) mentioned in their literature review that the amount of deposited wax is impacted by the concentration of paraffin, light ends, and nucleating or inhibiting materials in the crude oil.

### **2.6.3 Experimental Time (Lab Rigs)**

The experimental time is considered to be one of the important factors that influence wax deposition inside the pipelines (Adeyanju and Oyekunle, 2013; Dwivedi et al., 2012; Huang et al., 2011; Hoffman and Amundsen, 2010; Rosvold, 2008; Venkatesan, 2004). Wax deposition increased regularly during the first two hours of running the experiments in the lab rig because most of the dissolved paraffin in the crude oil was deposited on the pipe wall, but despite the reduction in the paraffin content in the crude oil, the wax deposit increased slightly with increasing experimental time. In the oil fields the wax deposition increases regularly due to more and more paraffin being deposited from the fresh crude oil on the hydrocarbon pipeline, providing a greater opportunity for deposition upon the cold surface (Abdel-Waly, 1999).

Lab rig studies have shown that a thermal pseudo-steady state is attained in less than 30 minutes during deposition from wax solvent mixtures under laminar and turbulent conditions (Kasumu and Mehrotra, 2013; Tiwary and Mehrotra, 2009). Laboratory studies have also shown a negligible increase in the mass of the deposit after 4 hours (Kasumu, 2014) due to most of the wax molecules in the crude oil having been deposited on the pipe wall.

### **2.6.4 Flow Rate**

In laminar flow, wax deposition increases with decreasing flow rate. This can be explained by the availability of more particles for deposition at the surface. As the flow rate increases to turbulent regimes, wax deposition decreases because shear dispersion increases. Thus, wax deposition gradually decreases as turbulence and flow rate increases. Shear dispersion is predominant in turbulent flow in all stages. The flow behaviour in a flowing stream is described by the Reynolds number; above 2,000 this is often considered to be turbulent flow (Misra et al., 1995).

The nature of the wax crystals is to adhere to the pipe surface with good cohesion among themselves; therefore, increasing the flow rate leads to breaking wax crystals up into smaller particles, reducing the rate of wax deposition and preventing it by minimising wax adhesion to the pipe wall. On the other hand, the wax that deposits at higher flow rates is harder and more compact due to only those wax crystals and crystal clusters being capable of firm attachment to the surface and these will not be removed from the deposit (Misra et al., 1995; Bott and Gudmunsson, 1977).

Wax deposition is found to be problematic in low-flow-rate wells. Low flow rates generally affect wax deposition because of the longer residence time of the oil in the tubing. This increased residence time permits more heat loss and leads to a lower oil temperature, which in turn leads to wax precipitation and deposition. The minimum flow rate in the experimental rig to avoid



deposition has been proposed to be 0.56 ft/sec (Misra et al., 1995; Kang et al., 2014).

### **2.6.5 Pressure**

The pressure drops during oil production from the reservoir to the surface facilities. Lighter hydrocarbons in the reservoir tend to be the first to leave the reservoir as the pressure falls; hence, the solubility of the wax is reduced. The WAT increases with the pressure above the bubble point pressure, for a constant composition. This phenomenon implies that an increase in the pressure in the single-phase liquid region (above the bubble point pressure) will aggravate wax deposition. The situation is different below the bubble point, where the oil has a two-phase constitution. The WAT decreases with an increase in the pressure up to the bubble point pressure owing to the dissolution of light hydrocarbon back into the liquid phase. Therefore, the dissolution of light hydrocarbons caused by variations in pressure directly affects wax deposition (Kang et al., 2014).

Valinejad and Solaimany (2013) stated that pressure is not considered an important factor for wax deposition, especially for dead or stock tank oil; but despite this, it should not be neglected. The pressure helps to reduce the wax deposition due to increasing the solubility of the wax in crude oil.

### **2.6.6 Pipe Surface Properties**

It is evident that during deposition, wax crystals adhere to the pipe surface; so wax deposition can also be a function of surface properties. As the paraffin wax is deposited on a surface, it is held in place by adsorption forces. These adsorption forces are dependent on the free surface energy of both the paraffin and the surface (Misra et al., 1995). The deposits do not adhere to the metals themselves but are held in place by surface roughness (Jonathan, 2004).

There is no direct correlation between wax deposition and surface roughness. However, the adhesion bond at a surface should be proportional to the total contact area and therefore related to surface roughness (Patton and Casad, 1970; Jonathan, 2004). Wax molecules move toward via diffusion and adhere at the wall. The rate of adhesion is largely governed by the temperature difference between wall and fluid (Leontaritis and Geroulis, 2011).

Low friction internal pipe surfaces will also discourage deposition, if not precipitation, as wax crystals can only adhere to pipe walls if they have a sufficiently large coefficient of friction. The cohesive strength of sample wax deposits is of little consequence if they do not adhere well to the pipe wall. Field reports suggest that wax deposits' adhesive strength is at least equal to their cohesive strength and they cling tenaciously to the pipe wall. When casting pure macrocrystalline wax onto a steel pipe wall under laboratory

conditions, however, this is not the case. The wax adheres so poorly to the steel that a negligible force is required to cause gross fracture at the steel/wax interface. If a wax model is to be found that can provide robust testing of removal concepts, it needs to allow cohesive failure of simulated deposits. That is, it needs to stick well to the pipe wall (Leontaritis, 2007).

It can be concluded that, at the very least reduced pipe diameter and increased surface roughness creates a larger pressure drop and reduced throughput; at the worst, wax deposits can be so severe that the pipe is blocked and production ceases completely.

### **2.6.7 Lab Experiment Investigation Rigs**

Venkatesan and Creek (2007) illustrated the difference between the laboratory conditions and the field conditions. They recommended that the existing laboratory methods should be reviewed in order to simulate field conditions more closely and develop an understanding of the deposition in turbulent flow conditions, deposition over longer time periods and deposition at low heat transfer, developing methods to obtain credible field data for comparison and guiding research in the deposition area. They further mentioned that one of the important differences between the wax deposition scenario in a lab scale pipe and that in field pipelines is the heat flux. Even if the Reynolds number is matched in the two cases, the heat flux in the field pipeline will be much lower compared to typical lab experiments. This is because the temperature difference between the bulk fluid and the inside wall is very low in the field pipeline, whereas this difference is typically quite high in lab experiments. Venkatesan and Creek concluded that more serious work needs to be done to develop an understanding of deposition in turbulent flow conditions, deposition over longer time periods, deposition at low heat transfer, and devising methods to obtain credible field data for comparison and guiding research in this area.

On the other hand, Adeyanju and Oyekunle (2013) experimentally studied the key factors affecting wax deposition on high wax content oil in pipelines, such as inlet oil temperature, inlet coolant temperature, oil flow rate and the wax content, using a test flow loop consisting of a mild steel pipe of a length of 140cm with an inside diameter of 1.5cm, which was used to perform the wax deposition experiments under the single oil phase conditions. Contrary to the general theory that wax deposit volume increases with an increase in the temperature difference between the pipe wall and the bulk oil, Adeyanju and Oyekunle, (2013) observed that when the oil temperature is above its wax appearance temperature (WAT) and the pipe wall temperature below its WAT, the wax deposit volume decreases with an increase in temperature difference, while the reverse is the case when both the oil and pipe wall temperature are below the oil WAT.

Adeyanju and Oyekunle (2013) used the pressure drop method to estimate the wax thickness inside the test section of the pipe. This method depends on the pressure drops along the test section due to the deposit wax that reduces the pipe diameter (Chen et al., 1997; Huang et al., 2015).

Dwivedi et al. (2012) conducted an experimental study in a flow loop to find the effect of turbulence, shear and thermal driving force on wax deposition. The flow loop consists of three schedule-40 carbon steel pipes with normal diameters of 0.5, 1 and 1.5. All three sections are in a pipe configuration wherein glycol-water mixture flows in the annulus. The tests were conducted under different operating conditions with a wide range of Reynolds numbers from 3,700 to 20,500. They observed that the paraffin deposition is highly dependent on the thermal effective driving force, which is the temperature difference between the oil bulk and initial pipe wall. They also observed that the deposit thickness increased with deposition time, resulting in an increase in pressure drop across the test section.

Dwivedi et al. (2012) used the pressure drop method and the liquid displacement-level detection method (LD-LD) to estimate the wax thickness. The LD-LD method determines this by measuring the change in the volume of a test pipe section before and after wax deposition (Chen et al., 1997; Huang et al., 2015).

Kasumu (2014) studied the effects of adding water to the waxy crude oil, wax mixture and coolant temperatures, and flow rate in two-phase waxy mixtures flowing under turbulent flow conditions. His results indicated that the wax precipitation temperature of a waxy mixture is not a constant property as it varied with the cooling rate. Al-Yaari (2011) used an experimental petroleum production model to review the wax deposition problem in flow and during shut-in conditions, proposing important wax deposition models and mechanisms to illustrate the wax deposition, such as cold flow, crystal modifier, solvents and dispersant.

Hilbert (2010) experimentally studied the effect of different crude mixtures, emulsion and pipeline cooling properties on wax behaviours in subsea pipelines and concluded that the shear yield stress of the pipeline fluid decreases with increasing water cut. He suggested that the oil and water mixtures formed stronger wax matrices that require larger applied stresses to induce flow.

Botne (2012) used data from 21 experiments performed by others, which were digitised and evaluated; 18 of these show a good match with the logarithmic deposition-release model. This model consisted of two coefficients. Both coefficients were evaluated against wall shear stress for the varying rate experiments. He outlined those changes in temperature and

flow rate cause changes in initial deposition rate and asymptotic deposition level.

Botne (2012) used the pressure drop method to measure the wax deposition thickness as this method assumes that wax roughness is equal to pipe roughness and evenly distributes deposits. He mentioned that the pressure drop method does not consider pressure drop changes because of increased pipe roughness and uneven distribution of deposits. He observed that both of these effects will increase the pressure drop, and found that neglecting these will cause overestimation of the calculated thickness. Due to the overestimation of thickness, it was difficult to get an accurate match with models.

The experimental work of previous researchers provides a broader understanding of the main factors that affect the wax deposition process and presents various mitigation methods to reduce or prevent wax deposition in the pipe. This understanding forms the basis of the experimental work in this research, designing the flow loop system to carry out experiments and to examine the mitigation methods on the wax deposition process.

## **2.7 Wax Mitigation Methods**

Wax deposition in crude oil production systems can be reduced or prevented by one or a combination of: chemical, mechanical and thermal remediation methods (Woo et al., 1984; Al-Yaari, 2011).

- **Thermal Methods**

The thermal methods include heat retention, active heating and use of suitable exothermic chemical reactions. Thermal insulations, bottom hole heaters, hot oil circulation, steam circulation and on demand 'intervention' heating are appropriate for deep waters.

- **Mechanical Removal**

The mechanical removal method includes running scrappers in the borehole and pigging in pipelines at an intervention frequency. For deep waters, frequent intervention is not possible due to the long distance of the flow pipeline.

With the advent of extremely deep production, offshore drilling and ocean floor completions, the use of the mechanical and thermal remediation methods has become economically prohibitive, as a result, the use of chemical additives as wax deposition inhibitors is becoming more prevalent (Adeyanju and Oyekunle, 2014, Al-Yaari, 2011) due to the long distances covered by hydrocarbon flowlines; therefore, the chemical additives are the best solution for wax deposition in pipelines.

- **Chemical Treatment**

Chemical inhibitors have been used to reduce or prevent wax deposition in crude oil production. These inhibitors can be divided into four types: pour point depressants (PPD), crystal modifiers, dispersants and solvents.

This study focuses on the chemical and mechanical mitigation methods of reducing wax deposition in the pipe wall. A literature review of some of the relevant researches that relate to chemical inhibitors and spiral flow is outlined below.

### **2.7.1 Chemical Inhibitors**

As mentioned above, chemical inhibitors are considered the best solution for deepwater hydrocarbon production. Therefore, the four groups of chemical inhibitors that are discussed above will be presented in this work in more detail. Pour point depressants hinder the formation and growth of wax crystals by modifying the crystal structure (by merging with the edge of a growing wax crystal). Although this reduces the viscosity, yield stress and pour point of the oil, it cannot reduce the wax deposition rate (Kang et al., 2014; Adeyanju and Oyekunle, 2014; Jennings and Newberry, 2008).

A crystal modifier has a similar molecular structure to wax. It co-precipitates or co-crystallises with a wax crystal by replacing wax molecules on the crystal lattices. It imposes steric hindrance on paraffin crystals, which interferes with the proper alignment of the new incoming paraffin molecules to the degree that growth terminates. Although this can reduce the wax deposition rate and prevent wax deposition on the pipe wall, it cannot prevent wax precipitation (Dobbs, 1999; Kang et al., 2014). A crystal modifier may also adsorb onto the paraffin crystal, thereby preventing agglomeration or deposition. Commercially, the crystal modifiers are referred to as pour point depressants (Woo et al., 1984).

Typical crystal modifiers are polyethylene, copolymer esters, ethylene/vinyl acetate copolymers, olefin/ester copolymers, ester/vinyl acetate copolymers, polyacrylates, polymethacrylates and alkyl phenol resins (Dobbs, 1999; Kang et al., 2014).

Dispersants are similar to surfactants in their molecular structure. One end of the molecule is attracted to the paraffin, but the other end is soluble in either oil or water, depending on the phase in which the paraffin is dispersed. Dispersants break wax crystals up into much smaller particles and reduce the rate of wax deposition, preventing it by minimising wax adhesion to the pipe wall (Dobbs, 1999; Kang et al., 2014). Alkylaryl sulfonate is an example of a dispersant.

Solvents increase the solubility of wax in oil and dissolve already deposited wax. The solvents most commonly used today include xylene, toluene, benzene, carbon tetrachloride, trichloroethylene, perchloroethylene, carbon disulfide, white or unleaded gasoline and pine-derived terpenes (Kang et al., 2014).

Chlorinated hydrocarbons of various types are efficient solvents because they are relatively inexpensive and have a high specific gravity. High specific

gravity is an important factor that will help solvents penetrate and dissolve the paraffin deposits typically at the bottom of the flow section. The use of some of the solvents mentioned above is problematic, however: chlorinated hydrocarbons cause poisoning of the downstream process, aromatic solvents have low specific gravities and it is difficult to use them on the well bottoms, they also have low flash points and handling becomes difficult, while carbon disulphide is highly effective but also highly flammable with toxic fumes (Woo et al., 1984; Al-Yaari, 2011).

The advantage of the wax inhibitor in addition to the crude oil sample compared to the pigging method is that deposition can be mitigated without stopping production. Even though many wax inhibitors have been developed, there is currently no universal type that can be used for all types of crude oils due to the varying properties of the crude oils (Ridzuan et al., 2014; Kang et al., 2014; Adeyanju and Oyekunle, 2014; Halim et al., 2011).

Hoffmann and Amundsen (2013) found that about 60%-90% of wax thickness is reduced by applying different inhibitor concentrations during experimental work investigation. The presence of a small concentration of inhibitors, such as poly ethylene-co-vinyl acetate (EVA) and poly maleic anhydride-alt-1-octadecene (MA), can coalesce with wax crystals and interfere with their growth (Jafari Ansaroudi et al., 2013; Wu et al., 2012).

Molecular simulation methods have developed a better understanding of the interaction mechanism of polymers; for example, the inhibition of wax formation and growth has been examined using poly octadecyl acrylate, where it interacts with the wax molecules and prevents long chain wax formation (Duffy and Rodger, 2002; Ridzuan et al., 2014).

Polymers have been successfully used as crystal modifiers in some areas and their use should be expanded as more effective polymers are developed. The polymer's molecular weight also has an influence on the pour point depression. Short or lower molecular weight polymers may cause little disruption to the wax crystal agglomeration and growth, while very long and high molecular weight polymers can interact with the molecule itself instead of with the wax structures. This interaction reduces the rate of wax formation, leading to the formation of softer wax that is easy to transport (Adeyanju and Oyekunle, 2014; Jang et al., 2007; Al-Sabagh et al., 2009; Han et al., 2009).

### **2.7.2 The Spiral Flow**

After going through the literature accessed, it was noticed that wax deposition is affected by increasing the shear rate, which increases the shear dispersion and reduces the wax deposition. Based on this, the author focused on researches that study the effect of shear rate to decrease the wax deposition. Increasing the shear rate leads to a high concentration of

sediment transport; this kind of transport can be found, for example, in the turbulence flow and spiral flow, as was noticed in this research.

A few types of research mentioned the spiral flow in different study areas; however, to the best of the author's knowledge, they did not mention using spiral flow to reduce or mitigate wax deposition.

Xie (2013) defined spiral flow as a common flow form in nature; tsunamis, cyclones and sudden changes of flow rate due to tide and ebb are all considered to be spiral flows. Spiral flows have a wide range of applications in various engineering areas, such as chemical and mechanical mixing and separation devices, chemical reactors, combustion chambers, turbo machinery, rocketry, fusion reactors and pollution control devices. Studying the mechanism of spiral flow is useful for promoting industrial and economic development because the spiral flow contains more energy, which plays an important role in the flow (Betül and Tulin, 2007).

Spiral flow has been used to transport sediment, particularly implemented in the vortex tube. Such aspects were studied as diversion ratio and sand interception conditions (Xie, 2013). Li et al. (2011) studied spiral flow in a local generator key device to maintain the spiral system, using a combination of theoretical analysis and model experiments. They found that the generator guide vanes have a significant influence on flow rate and vorticity. Velocity gradients vary greatly near the guide vanes.

Zhang et al. (2001) and Zhang et al. (2005) studied the characteristics of sediment transportation in the spiral flow. Zhang et al. (2005) mentioned that the velocity distribution of flow in the spiral pipes is different from that of usual pipes; a target with a high concentration and long-distance sediment transportation can be achieved if the specific property of spiral flow is used in a pipe.

Spiral flow velocity distribution is unique; its tangential velocity of almost linear distribution, which forms a tangential velocity, is conducive to the pipeline sediment 'spin float', thereby forming a high concentration of transport.

Zhang et al. (2002) studied rotary actuator structure, resistance loss and rotation efficiency. According to the hydraulic character of the spiral flow and the movement status of sediments with different size in the decay spiral flow produced by the local pipe, starting a cyclone, the hydraulic requirements of changing bed load to spiral load are obtained. They compared the cyclone section (cyclone intensity decay segment) and the direct current section, in a certain amount of sediment conditions tangential swirl segment differentials, often do not occur siltation, and the direct current segment is silt larger

portion. Spiral flow can significantly reduce energy consumption and achieve the purpose of low-energy slope transportation.

The spiral flow in the 90° elbow was simulated using the finite volume method; 6 kinds of spiral flows were studied which were formed by various angles of tangential inlet velocity. The formation, development and attenuation of spiral flows in the elbow were investigated and the results show that tangential velocity becomes largest when the angle of the inlet is 60°, which is good for removing the impurities deposited in a pipeline (Xie, 2013).

Liu et al. (2012) carried out an experimental study to investigate the structure parameters and pressure drop characteristics of a spiral flow generator in a horizontal liquid-solid circulation fluidised bed. They used water and small plastic particles as the liquid and solid phase respectively in the experiments. The geometry of the spiral flow generators consisted of a core and circumferentially attached vanes around this core. The spiral flow generators were made up of stainless steel. The number of vanes amounted to three and the vanes of thickness 0.3 mm and length of 14 mm were attached about the core with different angles covering 10°, 15°, 20° and 25° normal to the axial flow direction.

Liu et al. (2012) found that the local pressure loss with the spiral flow generator is clearly higher than that without the spiral flow generator because of the higher surface area. The spiral flow generator with a vane angle of 25° represented the highest pressure drop values, while those of 15° represented the minimum ones. The pressure drop values increase with increasing the mass flow rate. This results mainly from the dissipation of the dynamic pressure of the fluid (i.e. particle and liquid) due to very high viscous losses near the pipe wall and the extra force exerted by rotation.

Liu et al. (2012) investigated the suggestion that spiral flow enhances heat transfer due to the increased velocity in the swirl tube and the circulation of the fluid by centrifugal convection because the low density of the warmer fluid at the pipe wall is displaced into the cooler stream in the central region by centripetal force. This kind of transport mechanism decreases the wax deposition in the pipe wall due to increasing the shear dispersion that makes the wax molecules rotate.

The previous researches provide the author with an understanding of the spiral flow mechanism and its influence on the sediments. Therefore, the spiral flow is considered as an important factor to remove the sediment inside the pipes and it was used in this study as a mitigation method to remove or prevent wax deposition.



## 2.8 Wax Deposition Simulation

Wax deposition, as explained in previous sections, is a very complicated phenomenon and it is a major unsolved issue for subsea oil production systems with regard to flow assurance. Therefore, modelling wax deposition in pipelines is required for the crude oil composition, experimental rig details and the operational parameters. To control the wax deposition, the amount of deposited wax and wax deposition rates in the pipeline must be accurately predicted through numerical simulation. OLGA is a dynamic multiphase simulator employed for transient and steady state simulations. OLGA is used for networks of wells, flowlines and pipelines and process equipment, covering the production system from the bottom hole to the production system. OLGA is a multiphase flow simulator that has been widely used for several decades in the flow assurance industry (Huang et al., 2015).

OLGA is structured into modules and some of these modules include the slugging and wax deposition module that is commercially used for wax precipitation and slugging prediction and calculations in the oil and gas industry.

The simulation of multiphase fluid flow involves conservation equations such as mass, momentum and energy; it also requires a numerical simulator to solve these equations.

Many numerical simulation studies on wax deposition have been conducted and the study results published; most have focused on how soon wax starts forming deposits in the pipeline. This information is useful for the design stages of pigging in the pipeline for wax removal (Akabarzadeh et al., 2010; Labes-Carrier et al., 2002; Noville and Naveira, 2012; Pan et al., 2009).

Ajayi (2013) investigated a modelling concept for controlling wax deposition and wax loosening that is applicable to subsea flowlines in oil and gas production systems. An annulus active cooling model and an annulus heating model are developed to simulate thermal methods and prevent and control the wax deposition.

Jung et al. (2014) used a sensitivity analysis to investigate how various parameters affect wax deposition in single-phase and two-phase flow numerical models of a subsea oil production system. Their results showed that the molecular diffusion parameter and oil fraction in wax has a significant effect on wax accumulation. The wax roughness and pipe roughness did not have much impact on the wax deposition on the inner walls of pipelines; however, they affected the flow pressure behaviour in the pipeline and this agrees very well with the observation of Labes-Carrier et al. (2002) and Noville and Naveira (2012). The numerical simulations of the single-phase and two-phase flow models showed similar wax deposition

behaviour, but the two models showed large differences in the wax deposition thickness. This may be because the wax deposition is further accelerated by the light hydrocarbon component associated with gas, which is only represented in the two-phase flow model.

Gonçalves et al. (2011) conducted eight paraffin deposition tests for different liquid flow rates and shear stresses at different oil and coolant temperatures. The measured data were compared with computational simulations using both OLGA and WAXPRO software. This software was tuned using the flow loop data, thereby lowering the uncertainty in predictions and increasing the project reliability.

The simulation results of Gonçalves et al. (2011) were compared with the measured data of the paraffin deposition tests. Some model parameters were adjusted in the simulations so that the calculated values were closer to those of the measured data. In the case of OLGA, two versions – 5.3 and 6.2.6 – were used to predict deposition while keeping all the files and input data the same for simulations.

### **2.8.1 Wax Deposition Models Contained in OLGA**

The wax module consists of three implemented models for wax prediction and deposition calculation. These are the RRR (Rygg, Rydahl and Rønningsen) model, the Matzain and Heat Analogy models (Huang et al., 2015).

- **RRR Model**

The RRR wax model is a multi-phase wax model used for predicting wax deposition properties in pipelines and oil and gas systems. The RRR model implements a molecular diffusion and shear dispersion effect as the mechanisms responsible for wax deposition. It performs a continuous estimate of the wax build-up along the pipeline over integrations of time for a multicomponent mixture. It is considered a steady state model because the wax deposition time is much longer as compared with the active flow process and system disturbance time in a typical oil and gas pipeline.

The effect of wax deposition on pressure and temperature is calculated by integration in time. The wax deposition is estimated based on the diffusion of wax from the bulk towards the surface of the pipeline due to temperature gradients and shear dispersion effect. The inner pipe wall friction is varied based on the wax deposition rate (Rosvold, 2008; Ajayi, 2013).

The RRR model functions as an integrator of sub models that account for the pressure drop and regime changes, viscosity of the fluid mixture, heat and energy balances, wax thermodynamic properties and the wax transport mechanism itself. This is a fully compositional model as it accounts for an individual representation of the property of components in the sub-model while keeping track of each compositional behaviour using heat, mass and

energy balances on discretised sections of the pipeline (Rosvold, 2008; Ajayi, 2013).

Deposition in the RRR model is based on molecular diffusion and shear dispersion, both of which mechanisms enhance the wax deposition. The volume rate  $Vol_{wax}^{diff}$  of wax deposition by molecular diffusion for a wax forming composition  $i$  is found from the following equation (Rosvold, 2008):

$$Vol_{wax}^{diff} = \sum_{i=1}^{N_w} \frac{D_i(\Delta C_i)S_f M_i}{\delta \rho_w} 2\pi rL \quad (2.8)$$

Where  $N_w$  is the number of wax components,  $D_i$  is the diffusion coefficient ( $m^2/s$ ),  $\Delta C_i$  is the concentration difference between the bulk phase and the wax phase for component  $i$ ,  $S_f$  is the fraction of the wetted perimeter by wax,  $M_i$  is the molecular weight (g/mol),  $L$  is the length of the pipe (m),  $r$  is the effective inner pipeline radius to account for wax deposition (m),  $\rho_w$  is the density of the wax component  $i$  ( $kg/m^3$ ) and  $\delta$  is the thickness of the laminar sub-layer (m) (Rosvold, 2008; Ajayi, 2013).

The volume rate of wax deposited from shear dispersion can be estimated from the following correlation:

$$Vol_{wax}^{shear} = \frac{K\gamma A\phi_w}{\rho_w} \quad (2.9)$$

Where  $K$  is the shear deposition constant,  $\phi_w$  is the volume fraction of deposited wax in the bulk fluid,  $\gamma$  is the shear rate in the oil (1/s),  $\rho_w$  is the average density of wax precipitated in the bulk fluid ( $kg/m^3$ ) and  $A$  is the surface area available for deposition ( $m^2$ ) (Rosvold, 2008; Ajayi, 2013).

The total volume rate of deposited wax given as  $l_{wax}$  is calculated as a sum of two contributing mechanisms for molecular diffusion and shear dispersion, as calculated by the equation below:

$$x = \frac{\sum_{i=1}^n x_i}{n} \quad (2.10)$$

$\phi$  is the wax deposit porosity. The porosity is usually assumed to be in the range of 0.6-0.9. Burger et al. (1981) determined the wax porosity to range from 0.83-0.86, while Rygg et al. (1998) used 0.85 as the value for wax porosity for oil with less than 0.5% water, and 0.6 wax porosity was assumed for an oil-gas turbulent field.

Wax layer porosity is an adjustable parameter in the model. The RRR model has been applied to several single and multiphase pipeline systems. An

assumption made for this model is that the precipitation rate at the wall is not a limiting factor, and that all wax transported to the wall will stick to the surface as long as the temperature is below the WAT. It should be noted that no removal mechanisms are discussed in this model. Therefore, the main drawback concerning the RRR model is the lack of shear incorporated into the model. Additionally, this model may give reasonable predictions at the time when wax starts to grow at a clean pipe, but after some time the results become less reliable due to there being no release mechanism included in the model (Rosvold, 2008).

- **Matzain Model**

The Matzain model incorporates shear stripping alongside molecular diffusion and shear dispersion as potential wax deposition models. The shear stripping model serves as a wax reducing mechanism in the Matzain implemented model. The deposition tests performed by the Matzain model for two-phase flow showed that wax deposition depends on flow pattern. At low mixture velocities, the trend for deposition build-up is similar to observations in laminar single-phase flow tests. The build-up trend at high mixture velocities is similar to observations for turbulent single-phase flow. This semi-empirical kinetic model predicts the wax thickness. The accuracy is acceptable, especially at high flow rates (Rosvold, 2008).

The Matzain model is, as with the RRR model, based on mechanisms such as molecular diffusion and shear dispersion, but shear dispersion is found to be of minor importance (Rosvold, 2008; Ajayi, 2013). Matzain et al. (2001) proposed that the rate may be influenced by other mechanisms as well. Shear stripping will result in a reduced deposition rate, and rate enhancement occurs due to entrapment of oil and other mechanisms. Since Fick's mass diffusion theory does not account for such influences of the rate, Matzain et al. tried to account for this by empirically modifying Fick's law. Based on experiment, two empirical correction terms are added.

$$\frac{d\delta}{dt} = \frac{\Pi_1}{1+\Pi_2} D_w \left[ \frac{dC_w}{dT} \frac{dT}{dr} \right] \quad (2.11)$$

Where  $\frac{d\delta}{dt}$  is the change in wax thickness deposited on the wall layers with time (m/s),  $\Pi_1$  is the empirical relation for the rate enhancement due to oil being trapped in the deposited wax layer,  $\Pi_2$  is the empirical relation for the rate reduction due to shear stripping,  $d\delta$  is the change in wax thickness deposited on the wall layers with time (m/s),  $D_w$  is the diffusion coefficient,  $C_w$  is the concentration of wax in solution (weight %),  $r$  is the pipe radial distance (m) and  $T$  is the bulk fluid temperature ( $^{\circ}\text{C}$ ) (Rosvold, 2008; Ajayi, 2013).

$$\Pi_1 = \frac{100C_1}{1-C_L} \quad (2.12)$$

The porosity effect coefficient  $C_L$  is defined as the amount of oil trapped in the wax layer. A regime dependent Reynolds number in a multiphase flow system calculates for flow regime changes.  $C_1 = 15$  is the Matzain constant.

$$C_L = 100 \left( 1 - \frac{N_{Re}^{0.15}}{8} \right) \quad (2.13)$$

$N_{Re}$  is the Reynolds number calculated from the equation  $N_{Re} = \frac{\rho v d}{\mu}$  where

$\rho$  is the oil density (kg/m<sup>3</sup>),  $v$  the oil velocity (m/s),  $d$  the pipe diameter (m) and  $\mu$  the viscosity of the oil (kg/m.s) (Ajayi, 2013).

$$\Pi_2 = 1 + C_2 N_{SR}^{C_3} \quad (2.14)$$

$N_{SR}^{C_3}$  is the flow regime dependent Reynolds number. It is observed that the Matzain constants  $C_1$ ,  $C_2$  and  $C_3$  have been supplied as flow parameters accounting for single-phase and two-phase flow behaviour in this correlation,  $C_2 = 0.055$  and  $C_3 = 1.4$  (Rosvold, 2008; Ajayi, 2013).

The implemented flow regime Reynolds number in the Matzain model is given by the following equations:

$$\text{Single-phase and stratified wavy flows: } N_{SR} = \frac{\rho v \delta}{\mu} \quad (2.15)$$

$$\text{Bubble and slug flow: } N_{SR} = \frac{\rho_m v \delta}{\mu} \quad (2.16)$$

$$\text{Annular flow: } N_{SR} = \frac{\sqrt{\rho \cdot \rho_m} v \delta}{\mu} \quad (2.17)$$

Where  $v$  is the oil velocity (m/s),  $\delta$  is the thickness of the wax layer (m) and  $\rho_m$  is the average density of the gas-oil mixture (kg/m<sup>3</sup>).

The thermal gradient of the laminar sub-layer for the deposition is found by the following equation:

$$\frac{dT}{dr} = \frac{(T_b - T_{wall})}{k_L} h_{wall} \quad (2.18)$$

Where  $k_L$  is thermal conductivity of the oil (W/mK),  $h_{wall}$  the inner wall heat transfer coefficient (W/m<sup>2</sup> K),  $T_b$  is the bulk fluid temperature (K) and  $T_{wall}$  the inner wall surface temperature (K) (Rosvold, 2008; Ajayi, 2013). The weakness with the Matzain model is that it does not include much physics and there are several constants. Another concern is the experiments that the model is based on (Rosvold, 2008).

- **Heat Analogy Model**

The principle of the Heat Analogy is assumed to be similar to the Singh et al. (2000) wax deposition principles to employ the heat and mass balances coupled with energy balances for its wax precipitation and deposition predictions. Singh et al. (2000) opined that a non-uniform diffusion occurs in wax deposits as a result of a concentration gradient existing in the sub-layer of wax deposits. This considers an internal diffusion mechanism for waxy gel layers inducing physical gelation on the wall. The initial formation of wax at the wall serves as the beginning of the deposition process, while trapped oil between successive wax layers provides an opportunity for further internal diffusion and continued wax deposition (Ajayi, 2013).

After going through the wax deposition models contained in OLGA, it can be concluded that the RRR model is preferred to the other two models, the Matzain and Heat Analogy models, due to the RRR model implementing the molecular diffusion and shear dispersion as the main mechanisms responsible for wax deposition, thereby producing a reasonable prediction of the experimental outputs.

## **2.9 Original Contribution to Knowledge**

After going through the previous literature accessed, it was noticed that several methods have been used in the past to prevent wax deposition by one or a combination of chemical, mechanical and thermal remediation methods, but the problem of wax deposition remains a challenge. It was also mentioned that such mitigation methods become significant due to the oil industry continuing to expand the operations to greater depths and distances in the offshore and onshore oilfields in the cold environments, which poses a major challenge.

Nowadays, chemical additives are preferred in analysing the economics of waxy crude oil production in cold environments and considered as the best available solution to reduce wax deposition in pipelines due to the chemical inhibitor can be mitigated wax without stopping production, but the cost of using the chemical inhibitors is higher and looking for another solution to reduce wax deposition in low cost.

Some researchers are stating that even though many wax inhibitors have been developed, there is currently no universal type of inhibitor that can be used for all kinds of crude oil due to the varying properties of crude oils (Ridzuan et al., 2014; Kang et al., 2014; Adeyanju and Oyekunle, 2014; Halim et al., 2011). This is an investigation to understand the wax deposition problem, because of the universal inhibitor may solve the wax deposition problem and create more problems such as (corrosions, erosions, emulsions, scales) due to varying properties of crude oils and the different climate of the oil fields.

A universal solution would be a both convenient and cost effective response to the current demand. Presently, most of the companies have their personalised technique to tackle the wax deposition. This is not very practical as oil viscosity changes depending on the geology and geographical location. If spiral flow technique is adopted universally in the correct way, it will help to reduce the amount of investment as well as man power to achieve better results.

After going through the previous researches, it was noted that needs to develop a fundamental understanding of wax deposition phenomena and a comprehensive wax deposition model based on this fundamental understanding is strongly necessitated in order to overcome the challenges in production and transportation of pipelines in the cold environment. Develop an understanding of wax deposition in turbulent flow conditions can be done by increasing the shear rate and changing the path way of the crude oil as a spiral flow that works to mitigate wax deposition inside the hydrocarbon pipelines. Also, develop an understanding of increasing the synergy of the mixtures of chemical inhibitors and study it effects on wax deposition.

This study presents the chemical and mechanical methods and a combination of the two as a solution to the wax deposition problem. The author came up and designed this research, and designed and structures the new rig from a crash in the lab of this study aiming to reduce or prevent wax deposition. and to study and investigate the influence of some factors that control and affect the wax deposition process, such as pipe wall temperature (inlet coolant temperature), flow rate, pressure drop, oil temperature, shear stress, recirculation time of crude oil and viscosity, by using the chemical (polyacrylate polymer (C16-C22)) and mechanical (spiral flow) methods as mitigation techniques for wax deposition. The author included a condenser in the rig structure to help to condense the light components that evaporated during heating the crude oil; where the light components works as an inhibitor to dissolve wax crystals inside the crude oil.

It was noticed from the literature review above that the wax deposition process being affected by increasing the shear rate leads to increasing the shear dispersion and reducing the wax deposition. Increasing the shear rate and shear dispersion leads to a high concentration of sediment transport; this kind of transport can be found in the spiral flow, as was noticed during this research. In this study, the spiral flow was implemented and created in the wax deposition experiments by inserting a thin twisted aluminum plate inside the test section of the pipe.

The technique of using spiral flow as a mitigation method has not been used before in the oil fields to reduce or prevent wax deposition inside

hydrocarbon pipelines may due to increase the cost in times of pressure drop; so during this study spiral flow was used for the first time as a mitigation method for wax deposition. The effect of combining spiral flow with the chemical inhibitor has also not been used before; it was used for the first time in this study to prevent wax deposition.

To evaluate the economic cost of this project, experiments are carried out at flow rate 2.7 L/min and inlet coolant temperature 14°C using only crude oil, using the inhibitor W802 with the crude oil at concentration 1000, using the effect of spiral flow, and using the combination of spiral flow with W802 at concentrations 1000ppm. The economic cost evaluated depending to the consumed electricity in each part of the rig parts. According to the average charges of electricity in 2016 for UK regions, the average variable unit price used in this evaluation is (£0.14/kWh), and the cost of the inhibitor W802 is £0.015 for each 1 ml.

During run the experiments for 2 hours, it was noticed that the total cost of the electricity consumed in the experiment using just crude oil is £0.38. The total cost of carrying out the experiments using the inhibitor W802 is £0.347, using the spiral flow is £0.52, and using the spiral flow with the inhibitor W802 together is £0.46.

It can be seen that the highest cost is by run the experiment using spiral flow, and the lowest cost is by run the experiment using the inhibitor W802. At the same time, when compares the wax volume produced from each experiment, it can be noticed that the wax volume produce from the experiment using spiral flow is 40 ml, and that produced from experiments using inhibitor W802 is 70 ml. That's mean; reduce the wax volume leads to increase the production even if the cost increased little bit.

The cost of running the experiment using the effect of blending spiral flow with the inhibitor W802 is £0.46 and the wax volume produced is 30 ml, and the cost of running the experiment using just crude oil is £0.38 and wax volume is 120 ml. Comparing these two experiments are shown that the lowest operation cost produced a higher value of wax that's mean higher reduction in crude oil production, while increasing the operational cost of blending the spiral flow with the inhibitor to %17 leads to decrease the wax volume to %75 and this reduction in wax deposition results in high increase in crude oil production.

This analysis cost is according to the lab conditions, but in the real conditions of the oil field the cost will be different. In the real conditions, the crude oil will be under high pressure and high temperature that are responsible to keep the wax crystals in solution in the crude oil due to exits the high concentration of the light ends (light components) in the crude oil.



Inserting the twisted plate inside the test section of the rig to create spiral flow leads to increase the pressure drop. Therefore, its recommended for the real oil field to use spiral flow should change the flow geometry to increase the shear rate that influence on wax deposition. Also, recommended to use the benefit of combined flow geometry with the light components (light end) on wax deposition.

The literature available lacked a comparison of the experimental study parameters (flow rate, pressure drop, density, pipe length and diameter, oil temperature, and viscosity) using the pigging method, pressure drop method, heat transfer method and liquid displacement-level detection (LD-LD) method and aiming at simulation using OLGA software to compare the results.

The experimental rig of this study was modelled to transport the oil from the oil source (oil inlet) in the first node of pipe-1 into the flow line to predict the behaviour of the wax deposition. The crude oil properties and wax properties are converted to tab file (pvt file) through PIPEsim then imported to OLGA software to run the simulation. The oil enters the flow line at 44.5°C at a mass flow rate 0.04 kg/s or 0.08 kg/s depending on the desired flow rate. The oil flows out of the flow line at 5 bars and 42°C through a pressure node called the oil outlet. Other details such as geometry of pipeline, diameter, pipeline material, pipeline thermal conductivity, pipeline roughness, density, viscosity, are entered as an input data in the simulator to run the simulation.

In the wax deposition simulation, the wax deposition option is turned ON and the input parameter, including wax deposition model RRR, is as follows: wax diffusion coefficient multiplier equal to 1, wax roughness value zero, porosity of wax 0.6 (automatic default value), seabed temperature 6°C, and the simulation end time 2, 3, 4, 5 and 6 hours and for the study of the effect of a long time on wax deposition, the simulation end time is 12 and 24 hours. After run the simulation, the resulting wax thickness versus time was plotted using Excel in order to compare results from the experiments with the simulation results.

There are some differences between the components of the crude oil in this study and that of Jha et al. (2014) that used to run the simulation such as SARA, specific gravity and API. So, to avoid these differences between the experimental results and the predicted results, a tuning of OLGA parameters for improved predictions was undertaken. Three scenarios were created to match the experimental wax thickness, including studying the effect of change wax porosity in OLGA, changing the crude oil components and the influence of simulation time on wax deposition. After apply the three scenarios, the predicted results using OLGA software are show agreement with the experimental results.

## Chapter 3: Experimental Methodology

### 3.1 Chapter Three Overview

This chapter reviews the methodology used in this research. It outlines the details of the flow loop system used in this work to study the influence of some of the factors that control the wax deposition process. The chapter presents the different chemicals used as inhibitors to mitigate wax deposition and spiral flow as a mechanical method used in this study to reduce wax deposition in the crude oil pipeline. This chapter further presents the multiphase flow simulator OLGA to implement the wax models using the experimental data from this study as a base case to predict the behaviour of the wax deposition.

### 3.2 Crude Oil under Study

The crude oil used in this study is from one of the oil field reservoirs that experience waxing problems in the Arunachal Pradesh state in the extreme north-eastern part of India; this sample of crude oil was obtained from Roemex Limited Company. The crude oil characterisation was carried out in the lab using experimental methods and standard analytical techniques. The physical and chemical properties of the crude oil are classified in this work and presented in chapter 4.

#### 3.2.1 Specific Gravity and API

Specific gravity was calculated using the ratio of the density of crude oil  $\rho_{oil}$  to the density of water  $\rho_{water}$ . Specific gravity is a dimensionless quantity.

$$SG = \frac{\rho_{oil}}{\rho_{water}} = \frac{850}{1000} = 0.85 \quad (3.1)$$

API gravity is a measure of how heavy or light the petroleum liquid is compared to water. The formula used to calculate API gravity from specific gravity (SG) is:

$$API = \frac{141.5}{SG} - 131.5 = \frac{141.5}{0.85} - 131.5 = 35 \quad (3.2)$$

#### 3.2.2 Rheological Behaviour

A Bohlin Gemini II Rheometer was used to measure the rheological behaviour of the crude oil during this study. The principle of the rheometer work is to placing the crude oil sample between a lower horizontal plate and an upper rotating plate to measure the crude oil viscosity, WAT and pour point at different shear rates, temperatures and shear stresses see figure 15. The measurements begin by cooling down the crude oil sample at a range from 55°C to 0°C at a rate of 5°C/min and shear rates of 10, 60, 120 and 180 1/s. The intersection between the viscosity lines at different shear rates represents the wax appearance temperature.

The effect of the inhibitors on crude oil viscosity was evaluated at temperature of 4°C, as illustrated in chapter 4.



Figure 15: A Bohlin Gemini II Rheometer used to measure WAT (LSBU).

The pour point was determined from the elbow point in the viscosity curve of the crude oil, at which the liquid is converted from a non-Newtonian to a Newtonian liquid. Figure 16 shows the wax appearance temperature and the pour point of the crude oil.

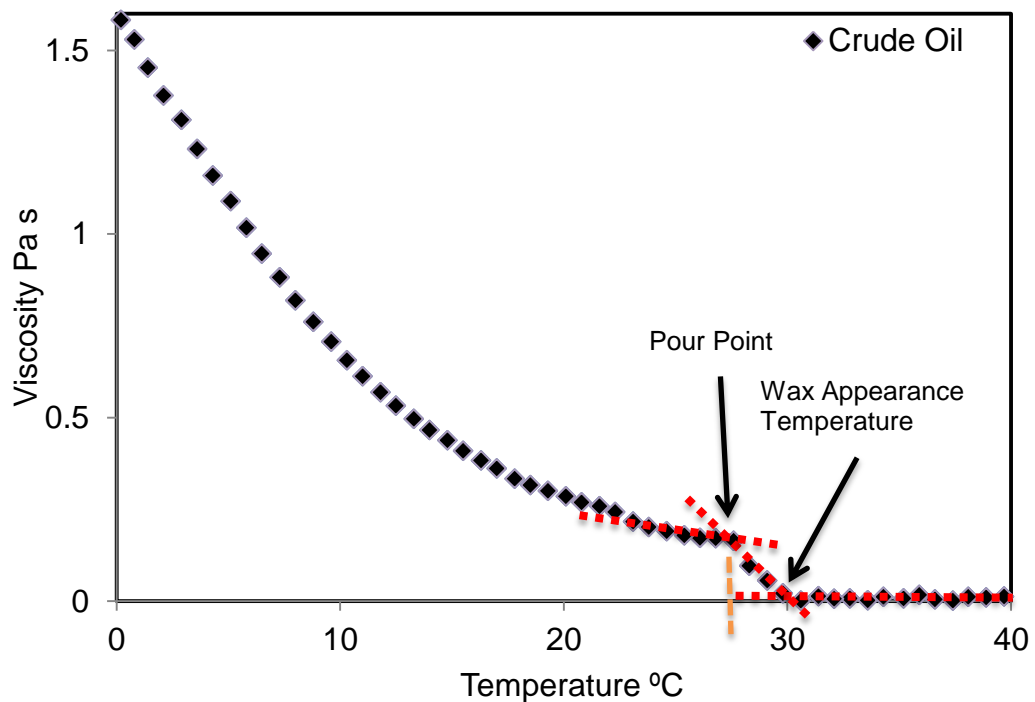


Figure 16: Variation of viscosity of Arunachal crude oil with temperature, indicating the WAT and pour point using the rheometer.

### **3.2.3 Wax Content**

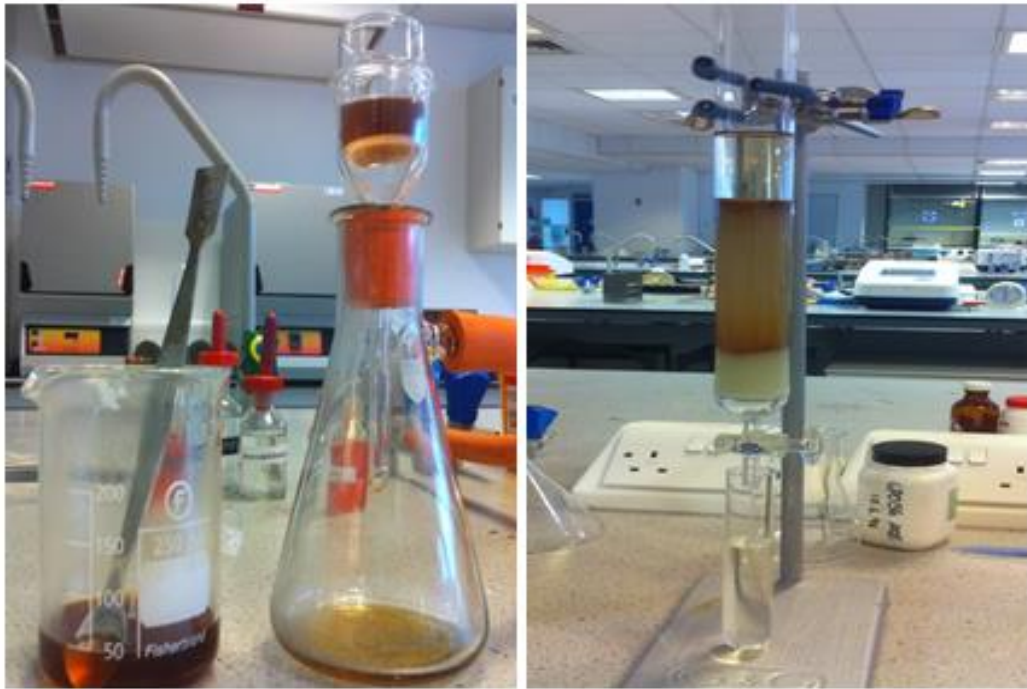
Wax content was determined by using the precipitation method (Coto et al., 2008). 2 ml of crude oil is diluted in 4 ml of n-pentane and stirred for 30 minutes. Acetone (acetone/n-pentane ratio 3:1) is added to the mixture and cooled down to -20.15°C for 24 hours. The solid phase present in the oil is separated by filtration in a Buchner funnel using a glass microfibre Whatman filter N° 934. The solid phase is re-dissolved in n-hexane in order to remove asphaltenes. After solvent removal, the final product is weighed.

### **3.2.4 SARA Analysis**

SARA analysis was used to separate the crude oil into four major classes of compounds – saturates, aromatics, resins, and asphaltenes (SARA) – using a chromatographic column (Jha et al., 2014), as shown in figure 17. The purpose of this analysis is to understand what the crude oil contains, which helps in easily dealing with the wax deposition problem.

This method was carried out on a de-asphaltene 10 gram of crude oil with n-heptane; the asphaltene content measured from the weight of the precipitate. The maltene (filtrate) was freed from the solvent to the greatest possible extent, then weighed, and 2 gm of it was added to the chromatographic column with activated silica (100°C) saturated with n-heptane and eluted sequentially with 100 ml of n-heptane (elution of saturates); 100 ml of toluene (elution of aromatics); 100 ml of toluene-methanol solution (50:50) (elution of polars/resins); 100 ml of methanol-chloroform solution (50:50) (elution of polars/resins); 100 ml of chloroform (elution of polars/resins); and 100 ml of acetonitrile (elution of polars/resins) (Jha et al., 2014).

Elutes were initially collected in separate containers and those from the last four elution sequences were subsequently mixed, stripped of their respective solvents under vacuum and weighed. The saturate, aromatic and resin contents were calculated from the weight percent of the residue in the whole crude (Jha et al., 2014).



(a)

(b)

Figure 17: (a) Filtration equipment used to separate asphaltene, and (b) chromatographic column used to separate saturate, aromatic and resin during this study.

### 3.3 Study of the Effect of the Inhibitors on Crude Oil Rheology

In the experiments, the crude oil was heated to 60°C to dissolve all wax crystals present in the oil then the crude oil was brought temperature to study the effect of several chemical inhibitors on crude oil rheology, using a rheometer.

The synergy of using a mixture of inhibitors was investigated in this study by mixing the inhibitors that reduced wax deposition more efficiently.

Three mixtures were prepared in the lab for this work, coded Mix01, by mixing 33% of each of W802, W804 and W805. Those inhibitors are mixture of copolymers and acrylated monomers (see table 1). The second mixture, coded Mix02, involved mixing 33% of each of W802, W302 and W510; these inhibitors include alkylated phenol, copolymer and polyacrylate polymer. Finally, the third inhibitor was Mix03, produced by mixing 50% of W802 and 50% of brine (H<sub>2</sub>O+NaCl). The idea of mixing brine with the inhibitor comes from the fact that most of the crude oils contain a percentage of brine.

**Table 1: The chemistry of wax inhibitors used during this study.**

Inhibitor Code	Inhibitor Chemistry
W302	Alkylated phenol in Heavy Aromatic Naptha (HAN).
W802	Polyacrylate based polymer (C16-C22).
W804	Copolymer + acrylated monomers.
W805	Copolymer + acrylated monomers.
W510	Co-polymer dissolved in solvent naphtha.
W705	Ethylvinyl Acetate (EVA) copolymer chemistry.
Mix01 (New)	Polyacrylate based polymer (C16-C22) + copolymer + acrylated monomers.
Mix02 (New)	Polyacrylate based polymer (C16-C22) + Alkylated phenol in Heavy Aromatic Naptha (HAN) + Co-polymer dissolved in solvent naphtha.
Mix03 (New)	Polyacrylate based polymer (C16-C22) + Brine (H <sub>2</sub> O + NaCl).

### **3.4 Wax Deposition Experimental Rig Design**

The author was designed and manufactured the wax deposition experimental rig of this study for the first time in the lab of London South Bank University from scratch to study the variation of wax deposition thickness under the single-phase transport. This rig was modified based on the apparatus of the published research of Adeyanju and Oyekunle (2013), the differences between the rig design in this study and that of Adeyanju and Oyekunle (2013) are that the flow loop in this study is made of a copper pipe, 150 cm in length with an inside diameter of 1.35 cm, while Adeyanju and Oyekunle (2013) used a mild steel pipe, 140 cm in length with an inside diameter of 1.5cm. This study included a condenser in the rig design, which was used to condense the remaining light components that evaporated from the heating crude oil; a condenser was not used in the study of Adeyanju and Oyekunle (2013).

This developed rig facilitated a study of the influence of some of the factors that affect and control the wax deposition process, such as inlet coolant temperature, flow rate, pressure drop, oil temperature, shear stress, time, oil viscosity, chemical inhibitors, and spiral flow.

The real conditions of the oil field differ from the lab conditions; this difference represents the changes in the length of the pipeline, the diameter, the pipe material, the pressure, temperature, flow rate, crude oil composition, and ambient temperature. Where, in the real conditions the pipe should be strong enough to bear the high pressure and high temperature of the crude oil, the flow rate will be high enough that able to remove wax more than the flow rate in the lab condition.

Also, the crude oil composition in the real oil field will be different from the crude oil composition in the lab. This can be illustrated as, in the real conditions the crude oil will be under high pressure and high temperature that are responsible to keep the wax crystals in solution in the crude oil due to exists the high concentration of the light ends (light components) in the crude oil.

Furthermore, the ambient temperature in the real world conditions will be different and changed from time to time depend to the environmental change, while, the ambient temperature conditions in the lab will be constant and can be controlled by the researcher.

Despite of the above differences between the real and lab conditions, the lab conditions can reflect the real conditions. Where, the lab conditions can mimic the environmental conditions essential for wax deposition in the hydrocarbon pipeline. Such as, provide the ambient temperature required to decrease the pipe wall temperature essential for wax deposition process. Despite of the laboratory conditions are reflecting the real one, the laboratory test results are not able to accurately reflect the real life.

The test flow loop of this study consists of test section, copper pipe jacket, pump, crude oil reservoir, hot bath water, Churchill Conair chillier, manometer pressure gauge, thermocouples, condenser, and Pico-Meter, as shown in figures 18 and 19.

### **3.4.1 Test Section**

The place where paraffin deposition investigation takes place is called the pipe test section. The test section is consist of a copper pipe 150 cm in length with an inside diameter of 1.35 cm and the pipe wall thickness is 0.09 cm. The copper pipe material properties are 385 J/kg.°C heat capacity, 401 W/m.k thermal conductivity, 8960 kg/m<sup>3</sup> density and 0.00009 m pipe wall roughness. The high thermal conductivity of copper pipe facilitates heat transfer between the crude oil and the environment leading to form wax crystals and precipitates on the pipe wall. This type of pipe material is suitable for the lab studies and not suitable for the oil fields in the cold environment.

### **3.4.2 Copper Pipe Jacket**

The crude oil pipe (test section) is jacketed with a copper pipe jacket in which cold glycol-water mixture is pumped from the chillier to maintain a pipe wall temperature lower than the wax appearance temperature. The jacket pipe length is equal to the test section pipe with an inside diameter of 2.54 cm and the pipe wall thickness is 0.12 cm. The copper pipe material properties are 385 J/kg.°C heat capacity, 401 W/m.k thermal conductivity, 8960 kg/m<sup>3</sup> density and 0.00009 m pipe wall roughness.

### **3.4.3 Pump**

A Charles Austin pump C25C used to recycling crude oil through the test section and go back to the oil reservoir, connected with a valve to control the desired flow rate. The pump flow rate had  $\pm 0.05$  L accuracy in the flow range of 0-4.8 L/min. The pump was calibrated to give a specific flow rate; this is achieved by measuring the amount of crude oil at a given time at various flow rates 2.7 and 4.8 L/min, until the specified rate is reached.

### **3.4.4 Crude Oil Reservoir**

A three-neck glass boiling flask, round bottom glass, 2000ml, made from borosilicate glass 3.3, weight 0.8kg, and range of operating temperature between  $-80^{\circ}\text{C}$  to  $200^{\circ}\text{C}$ , was used as a reservoir for crude oil. One of these necks allows entry of the crude oil into the flask after recycling in the test section; the second neck allows exit of the crude oil to the pump; and the third neck is for the condenser. This flask is fixed in a controlled heating bath. The crude oil reservoir volume was calibrated by measuring its volume with 2000ml of crude oil.

### **3.4.5 Hot Bath Water**

A water bath is laboratory equipment made from a container stainless steel, length 0.5m, width 0.4m, and height 0.4m, filled with heated water was used to incubate the crude oil reservoir in water at a constant temperature over a long period of time. The water bath has a manual control to set the desired temperature for the experiment. Water bath is a preferred heat source for heating flammable chemicals instead of an open flame to prevent ignition, its temperature range can be used up to  $100^{\circ}\text{C}$ . A thermometer was used for verification of the temperature of the hot bath.

### **3.4.6 Churchill Conair Chiller**

The type of the chiller used during this study was Churchill Conair; the cooling liquid used inside the chiller is glycol-water mixture and the temperature range of the chiller is between  $-60$  to  $+60^{\circ}\text{C}$ . The chillier model number is 02 CTCV, serial number 8341695, length 0.6m, width 0.4m, and height 0.5m.

The chiller has dual rules in the experiments, where it was used to maintain the pipe wall temperature of the test section at the desired temperature, also used to melt the wax deposit on the pipe wall after each experiment, by heating the recycling glycol-water mixture that works to increase the pipe wall temperature and melt the deposit wax.

### **3.4.7 Manometer Pressure Gauge**

Two manometers Pressure/Vacuum Gauges type Fisher Scientific™ Traceable™ were used to measure the inlet pressure and outlet pressure of the test section pipe.



The pressure gauge is portable unit measure and display differential pressure/vacuum in 11 different units (psi, mbar etc). The pressure range is between 0 -  $\pm 100$  Psia, the accuracy  $\pm 0.3\%$  according to the company record, dimensions (L x W x H) (18.1 x 7 x 2.9cm), and display type LCD.

#### **3.4.8 Thermocouples**

Four types of self-adhesive patch thermocouples were used to measure the temperature in different positions. These types of thermocouples are suitable for attaching to flat or curved surfaces, these self-adhesive patch thermocouples are rated for operation temperature between  $-50^{\circ}\text{C}$  and  $+250^{\circ}\text{C}$ . The self-adhesive patch thermocouple was pre-calibrated for temperature from Thermosense Direct Company. They are made from PFA insulated thermocouple cable which is attached to a high temperature rated patch of PTFE impregnated adhesive fibreglass tape.

The patch size is 25mm x 20mm, 0.2mm diameter solid PFA insulated twisted pair leads, and the lead length is 2 metres.

Two thermocouples used to measure temperatures of crude oil at the inlet and outlet of the pipe. Two thermocouples used to measure the recycling cooling and the inner pipe wall surface temperatures. A thermometer was used for verification.

#### **3.4.9 Condenser**

A condenser is a device or unit used to condense a substance from its gaseous to its liquid state, by cooling it. In this study, it was used to condense the remaining light components that evaporated when heating the crude oil.

The condenser is made from Pyrex borosilicate glass with quickfit ground glass joints for easy assembly. The total length of the condenser is 32.5cm, body length 20cm, bottom diameter 15mm, upper diameter 25mm, and joints both are 24/29.

#### **3.4.10 Pico-Meter**

Pico is a full-featured Multimeter that accurately measures AC/DC voltage, AC/DC current, resistance and ambient temperature. The four types of self-adhesive patch thermocouples was connected to the Pico Meter for data accumulation to a PC via Pico Logger software using intervals of one minute to achieve the best resolution of the results.

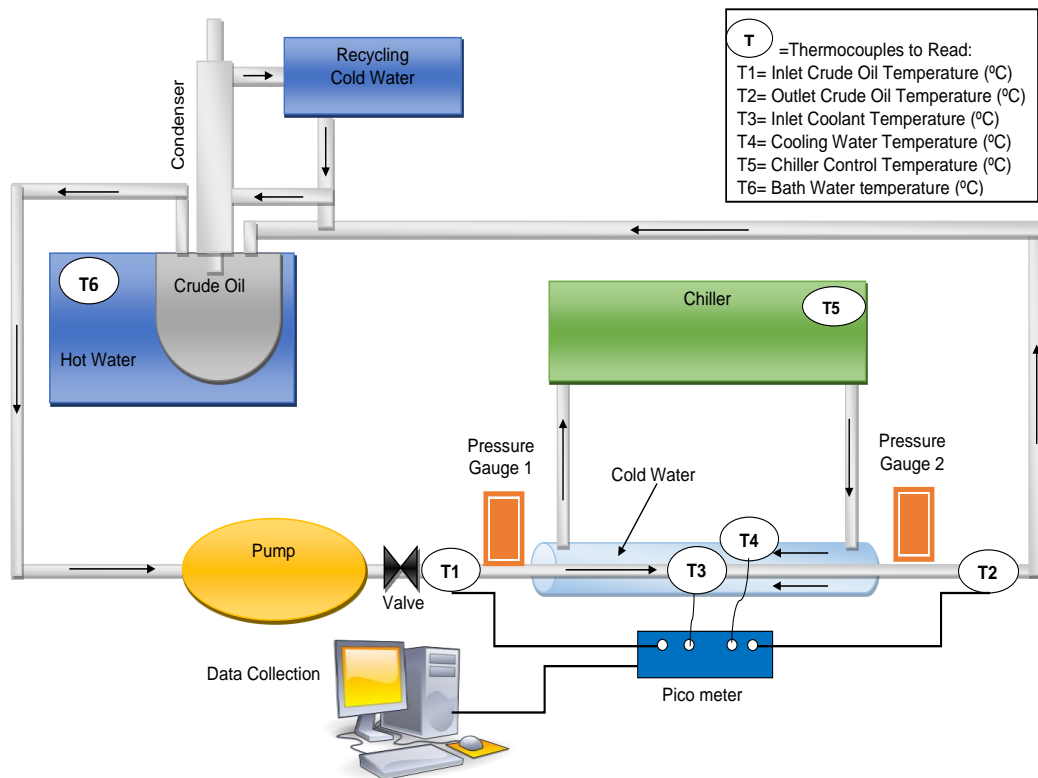


Figure 18: Schematic of wax deposition test flow loop in this study.

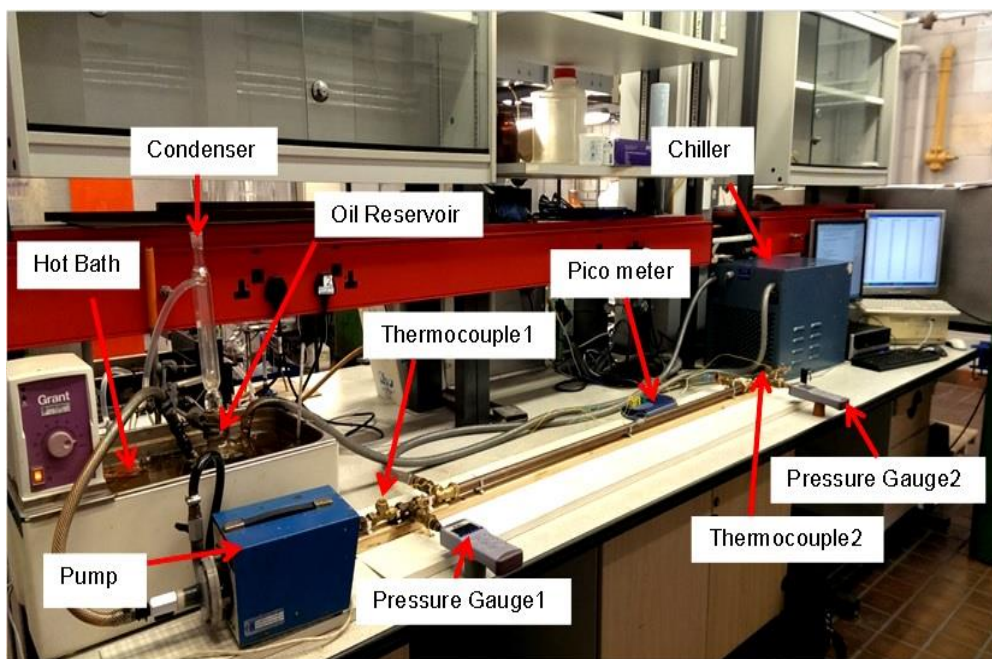


Figure 19: Apparatus of wax deposition in the lab for this study.

### 3.5 Study of the Effect of the Spiral Flow on Wax Deposition

In this study, a new technique was used to create a spiral flow inside the pipe in order to increase the shear rate and shear dispersion and mitigate wax deposition. This flow was created by inserting an in-house made twisted aluminum stripe into a test section of the pipe with 1.5m long and 1cm width

with angle of  $80.5^\circ$ , as shown in figure 20. The length of the twisted plate was equal to the pipe length.

The spiral flow was generated and examined in the test section of the rig to study its effect on wax deposition at different flow rates.

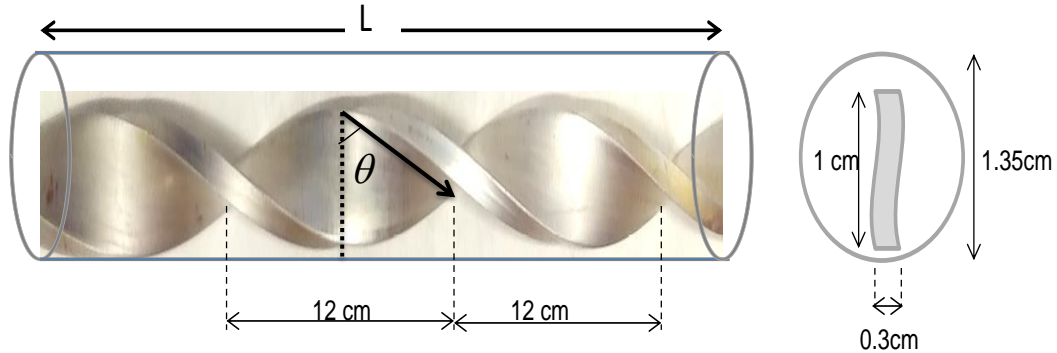


Figure 20: Illustration of the twisted aluminium plate inside the test section pipe to create spiral flow.

### 3.6 Process of Experiments

The most important point before starting any wax deposition experiment is to make sure that the pipe section is clean of any wax deposits remaining from previous experiments. For this, oil is flowing through the test section, which will be used for the following experiment at a temperature well above the wax appearance temperature for about half an hour.

After this step, the oil temperature is set at the desired operating conditions ( $44.5^\circ\text{C}$ ). At the same time, to prevent wax deposition in the desired test section for the following test, the glycol-water mixture that recycle through the chiller is kept flowing in this section at a temperature close to the wax appearance temperature of the oil ( $39^\circ\text{C}$ ) to avoid any possible thermal gradient in the radial direction. The purpose is to ensure that no wax will deposit on the test section wall before the experiment starts.

After the oil temperature reaches the desired value, the glycol-water mixture temperature should be cooled down to the set value to start the experiment. The experiments for wax deposition in the pipe were carried out by pumping the waxy oil through the inner pipe at a relatively higher temperature ( $44.5^\circ\text{C}$ ) than the inlet coolant temperature (pipe wall temperature) 14, 24, and  $33^\circ\text{C}$  desired for each experiment, to create the appropriate environment for the deposition inside the test section. The pressure drop of the fluid across the test section and consequently the paraffin build-up along the test section of the pipe was then monitored using two manometers pressure gauges.

A change in the temperatures in different positions along the test section of the pipe was monitored using four types of self-adhesive patch

thermocouples. Two thermocouples used to measure temperatures of crude oil at the inlet and outlet of the pipe. Also, two thermocouples used to measure another temperatures, one of them used to measure the temperature of the recycling cooling (glycol-water mixture) and the other one to measure the inner pipe wall temperature (inlet coolant temperature). The collected data of the different types of temperatures was accumulation to the PC via the Pico Meter through Pico Logger software.

Eight different sets of experiments were carried out during this work to study the effects of experimental parameters on wax deposition; the experiments were run for crude oil and crude oil with inhibitor at different concentration(500, 1000 and 2000ppm). The experiments were carried out at different flow rates (2.7 and 4.8 L/min), different inlet coolant temperatures (14, 24, and 33°C) and different experimental times (2, 3, 4, 5 and 6 hrs), as shown in tables 2 and 3.

These experiments were carried out at different parameters – such as inlet coolant temperature, flow rate, pressure drop, shear stress, oil viscosity, experimental time, chemical inhibitors and spiral flow – to investigate the dependence of wax deposition on these parameters.

Once an experiment is completed, the shutdown procedure for the experiment should be initiated. Before stopping the flow loop system, should make sure that all the data are monitored. The next step is to shut down the hot bath water that is responsible for heating the crude oil and then shut down the oil pump and after that shut down the chiller.

After completing the shutdown procedure, the sampling ports are opened to drain the remaining fluids in the test section. The main purpose in this step is to have a visual observation of the wax deposit and collect the wax samples to measure its volume. After this, the wax is scratched out from the pipe wall using a plastic conical and stored in a small cup to measure both of its volume and weight. After the scratched process, there is a small amounts of wax are still inside the wall of the test section, therefore, the chiller is used to melt all the remaining wax by increase the temperature of the recycled glycol-water mixture to 60°C. Then pigging the test section of the pipe from wax many times to make sure it's clean and ready for the next experiment.

Four different methods were used to measure wax deposit thickness inside the pipe including the pigging method, pressure drop method, heat transfer method and liquid displacement-level detection method (LD-LD). The details and the procedure of those four methods are illustrated in the next section (3.7 methods for estimate wax thickness).

Table 2: Experiments carried out at a flow rate of 2.7 L/min., different inlet coolant temperatures, different recirculation times and different methods.

Experiment at Flow Rate 2.7 L/min.	Inlet Coolant Temperature 14 °C					Inlet Coolant Temperature 24 °C					Inlet Coolant Temperature 33 °C				
	Experimental Time (hour)					Experimental Time (hour)					Experimental Time (hour)				
Crude Oil	2	3	4	5	6	2	3	4	5	6	2	3	4	5	6
500ppm W802	2	3	4	5	6	2	3	4	5	6	2	3	4	5	6
1000ppm W802	2	3	4	5	6	2	3	4	5	6	2	3	4	5	6
2000ppm W802	2	3	4	5	6	2	3	4	5	6	2	3	4	5	6
Oil+Spiral Flow	2	3	4	5	6	2	3	4	5	6	2	3	4	5	6
500ppm+Spiral Flow	2	3	4	5	6	2	3	4	5	6	2	3	4	5	6
1000ppm+SpiralFlow	2	3	4	5	6	2	3	4	5	6	2	3	4	5	6
2000ppm+SpiralFlow	2	3	4	5	6	2	3	4	5	6	2	3	4	5	6

Table 3: Experiments carried out at a flow rate of 4.8 L/min., different inlet coolant temperatures, different experimental times and different methods.

Experiment at Flow Rate 4.8 L/min.	Inlet Coolant Temperature 14 °C					Inlet Coolant Temperature 24 °C					Inlet Coolant Temperature 33 °C				
	Experimental Time (hour)					Experimental Time (hour)					Experimental Time (hour)				
Crude Oil	2	3	4	5	6	2	3	4	5	6	2	3	4	5	6
500ppm W802	2	3	4	5	6	2	3	4	5	6	2	3	4	5	6
1000ppm W802	2	3	4	5	6	2	3	4	5	6	2	3	4	5	6
2000ppm W802	2	3	4	5	6	2	3	4	5	6	2	3	4	5	6
Oil+Spiral Flow	2	3	4	5	6	2	3	4	5	6	2	3	4	5	6
500ppm+Spiral Flow	2	3	4	5	6	2	3	4	5	6	2	3	4	5	6
1000ppm+SpiralFlow	2	3	4	5	6	2	3	4	5	6	2	3	4	5	6
2000ppm+SpiralFlow	2	3	4	5	6	2	3	4	5	6	2	3	4	5	6

Several strategies were followed to achieve the objectives of this study, including:

- Investigation of the dependence of wax deposition on inlet coolant temperatures by carrying out the experiments at the same flow rate 2.7 L/min and the same oil temperature 44.5°C, but at different inlet coolant temperatures 14, 24, and 33°C.
- Examination of the dependence of wax deposition on inlet coolant temperatures by carrying out the experiments at the same flow rate 4.8 L/min and the same oil temperature 44.5°C, but at different inlet coolant temperatures 14, 24, and 33°C.

- Evaluation of the dependence of wax deposition on the flow rate by running the experiments at the same inlet coolant temperature 14°C and the same oil temperature 44.5°C, but at different flow rates 2.7 and 4.8 L/min.
- Assessment of the dependence of wax deposition on the flow rate by running the experiments at the same inlet coolant temperature 24°C and the same oil temperature 44.5°C, but at different flow rates 2.7 and 4.8 L/min.
- Examine of the dependence of wax deposition on the flow rate by running the experiments at the same inlet coolant temperature 33°C and the same oil temperature 44.5°C, but at different flow rates 2.7 and 4.8 L/min.
- Studying the dependence of wax deposition on the inhibitor W802 at different concentrations 500, 1000 and 2000ppm and the dependence on the spiral flow.
- Studying the dependence of wax deposition on the effect of merging the spiral flow with the inhibitor W802 at different flow rates 2.7 and 4.8 L/min and different inlet coolant temperatures 14, 24, and 33°C at the same oil temperature 44.5°C.
- Carry out all the steps above at different experimental time 2, 3, 4, 5 and 6 hours

### **3.7 Methods for Estimate Wax Thickness**

Four different methods were used in this work to measure wax deposit thickness inside the pipe. These methods are the: pigging method, pressure drop method, heat transfer method and liquid displacement-level detection method (LD-LD).

#### **3.7.1 Direct Method (Pigging Method)**

The pigging method is a technique used for measuring wax thickness in a test section of the pipeline. This method is based on the concept of passing spheres through the test section and measuring the wax volume removed (Chen et al., 1997). In this study, a plastic conical was used instead of the sphere for pigging the wax. This method is direct and simple because it provides a visual examination of the wax deposit; it is still widely used in experimental studies of wax deposition in low pressure and single-phase flow (Chen et al., 1997). The average wax thickness of the pigging method is estimated from the developed method as will show in section 3.8 depending to the wax volume removed.

#### **3.7.2 Pressure Drop Method**

The pressure drop method is an online technique that does not require depressurisation and restart in order to obtain wax measurements (Chen et al. 1997). The pressure drop method is used in this study to calculate wax

thickness inside the pipe. One of the main techniques used to calculate wax thickness inside the pipe in this study is the pressure drop method. This method is based on the concept that wax deposition in a pipe section reduces the hydraulic diameter of the flowing fluid inside the pipe, resulting in an increase in frictional pressure drop over the pipe section (Chen et al., 1997; Huang et al., 2015). The wax thickness present in the pipe wall can be calculated accurately from equation (1) presented by Chen et al, (1997):

$$(d_i - 2\delta_w)^{5-n} = \frac{2c\rho L}{\Delta p_f} \left(\frac{\mu}{\rho}\right)^n \left(\frac{4Q}{\pi}\right)^{2-n} \quad (3.3)$$

Where  $\Delta p_f$  is the pressure drop, L is the length of pipe section,  $d_i$  is the hydraulic diameter or effective inside diameter,  $\delta_w$  is the wax deposit thickness, Q is the volumetric flow rate,  $\rho$  is the fluid density and  $\mu$  is the apparent viscosity of the crude oil.  $c = 16$ ,  $n = 1$  for laminar flow and  $c = 0.046$ ,  $n = 0.2$  for turbulent flow. Laminar flow exists when  $NRe < 2000$ .

### 3.7.3 Heat Transfer Method

After the wax deposition layer is formed on the pipe wall, a convective heat transfer will apply between the flowing fluids and the deposited wax layer. A thermal resistance term due to heat conduction through the wax layer is added to the total resistance to heat transfer from the flowing fluid to the environment. The average wax thickness can be estimated from the heat transfer equation (Chen et al., 1997).

$$\frac{T_f - T_o}{q_o} = \frac{1}{h_w} \frac{r_o}{r_i - \delta_w} + \frac{r_o}{k_w} \ln \frac{r_i}{r_i - \delta_w} + \frac{r_o}{k_p} \ln \frac{r_o}{r_i} \quad (3.4)$$

Where  $T_f$  is the bulk fluid temperature in the pipe,  $T_o$  is the outside pipe wall temperature,  $q_o$  is the heat flux through the outside pipe wall,  $r_o$  and  $r_i$  are the outside and inside diameters of the pipe respectively,  $h_w$  is the film heat transfer coefficient from the flowing fluid to the wax layer,  $k_p$  and  $k_w$  are the thermal conductivities of the pipe wall and deposited wax respectively, and  $\delta_w$  is the thickness of the wax layer.  $r_i$ ,  $r_o$  and  $k_p$  are usually known for a given pipeline.  $k_w$  can be assumed to be equal to the thermal conductivity of waxy crude oil since wax thermal conductivity is very close to that of waxy crude oil and a significant amount of oil is usually trapped in the wax deposits.  $h_w$  can be estimated using an appropriate correlation or model. Thus, the wax thickness can be calculated from equation (2) when the bulk oil is temperature  $T_f$ , the outside pipe wall is temperature  $T_o$ , and the heat flux through the outside pipe wall  $q_o$  are measured.  $q_o$  can also be obtained from a heat balance. The heat lost from the fluids over a length of pipe must equal the heat transfer to the surroundings. Thus,

$$C_p \rho Q \Delta T_f = 2\pi r_o L q_o$$

(3.5)

where  $\Delta T_f$  is the oil temperature drop over the wax measurement pipe section and  $C_p$  is the specific heat of the waxy oil (Chen et al., 1997).

### 3.7.4 Liquid Displacement-level Detection Technique (LD-LD)

This technique allows estimating the volume of the wax deposit by measuring the change in the volume of a removable pipe section before and after wax deposition (Chen et al., 1997; Huang et al., 2015). In the current research, the test section of the pipe was displaced with water before running the experiment and after wax deposit in the pipe. The difference between the two volumes of water represents the wax volume.

The limitation of this technique is evidenced when it is used to measure the thickness of soft or thin wax deposits as the residual oil layer on top of the deposit can further increase the error of measurement (Chen et al., 1997; Huang et al., 2015).

## 3.8 Average Wax Thickness Measurement

The average wax thickness  $\delta_{wax}$  represents the difference between the diameter of the clean pipe  $d_1$  and the diameter of the pipe with wax  $d_2$  divided by 2, as shown in figure 21.

$$\frac{d_1 - d_2}{2} = \delta_{wax} \quad (3.6)$$

Wax volume  $V_{wax}$  represents the difference between the volume of the clean pipe  $V_1$  and the volume of the pipe with wax  $V_2$

$$V_{wax} = V_1 - V_2 \quad (3.7)$$

Further, wax volume can represent the difference between the area of the pipe without wax  $A_1$  and the area of the pipe with wax  $A_2$  multiplied by the pipe length  $L$

$$V_{wax} = LA_1 - LA_2 \quad (3.8)$$

$$V_{wax} = L(A_1 - A_2) \quad (3.9)$$

$$V_{wax} = 2\pi L(d_1^2 - d_2^2) \quad (3.10)$$

$$d_2^2 = d_1^2 - \frac{V_{wax}}{2\pi L} \quad (3.11)$$



$$d_2 = d_1 - \sqrt{\frac{V_{wax}}{2\pi L}} \quad (3.12)$$

$$\frac{d_1 - d_2}{2} = 0.5\sqrt{\frac{V_{wax}}{2\pi L}} \quad (3.13)$$

$$\delta_{wax} = 0.5\sqrt{\frac{V_{wax}}{2\pi L}} \quad (3.14)$$

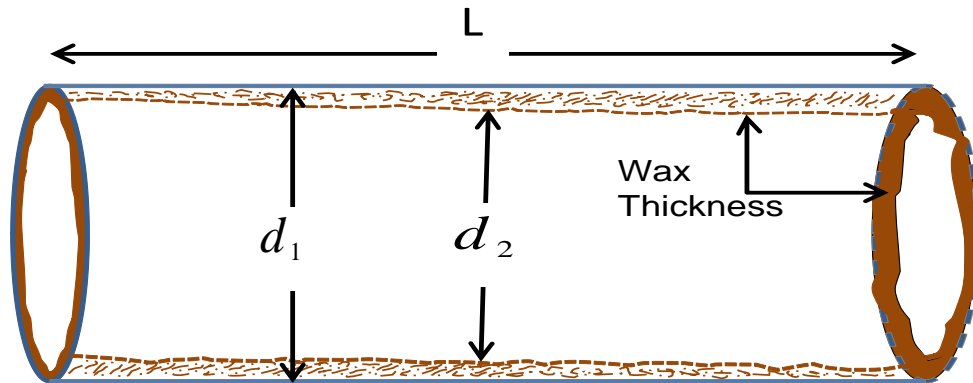


Figure 21: Average wax thickness inside the flow loop pipe for this study.

### 3.9 Benchmarking of the Rig of this Study

Benchmarking is a tool for improving performance. Benchmarking is a continuous and systematic process of comparing products, services, processes and outcomes with other organisations or exemplars (either internal or external) for the purpose of improving outcomes by identifying, adapting and implementing good practice (Edith Cowan University, 2013).

The wax deposition experimental rig was designed and manufactured during this research to study the process of wax deposition under the single-phase transport. This rig was modified based on the apparatus of the published research of Adeyanju and Oyekunle (2013), the differences between the rig design in this study and that of Adeyanju and Oyekunle (2013) are that the flow loop in this study is made of a copper pipe, 150 cm in length with an inside diameter of 1.35 cm, while Adeyanju and Oyekunle (2013) used a mild steel pipe, 140 cm in length with an inside diameter of 1.5cm. This study included a condenser in the rig design; a condenser was not used in the study of Adeyanju and Oyekunle (2013).

The crude oil used in this study is from one of the oil field reservoirs that experience waxing problems in the Arunachal Pradesh state in the extreme north-eastern part of India. While, the oil of Adeyanju and Oyekunle's (2013) study is one of the oil fields of Nigeria's Niger Delta.

The methodology of run the experiments in the two rigs (this study and the study of Adeyanju and Oyekunle, 2013) are conducted by entering the waxy

oil sample to the test section at a relatively higher temperature than the wall/coolant temperature in order to generate wax deposit in the inner section of the flow-line. Adeyanju and Oyekunle (2013) carried out their experiments at four different flow rates 1, 1.4, 1.8 and 2.2 L/min, at different inlet coolant temperatures of 40, 35 and 30°C to investigate the dependence of wax deposition on the pipe wall temperature. This study carried out the experiments at three different flow rates 1, 2.7 and 4.8 L/min, at different inlet coolant temperatures of 14, 24, 33 and 40°C.

Four different methods were used in this study rig to measure wax thickness including the pigging method, pressure drop method, heat transfer method and liquid displacement-level detection (LD-LD) method. While, Adeyanju and Oyekunle (2013) have used just a pressure drop method to measure wax thickness in their rig.

In both rigs, several common factors have been examined their effects in wax deposition process such as the effect of inlet coolant temperature, flow rate, pressure drop, oil temperature and experimental time.

The effect of the chemical inhibitor and spiral flow was examined in the rig of this study, while Adeyanju and Oyekunle (2013) did not use it.

For example, the results of Adeyanju and Oyekunle (2013) shows that at flow rate 2.2 L/min, at oil temperature of 56°C, at experimental time 4 hours, and at inlet coolant temperature of 37°C, the wax thickness was 0.98mm.

During this study, at flow rate 2.7 L/min, at oil temperature of 44.5°C, at experimental time 4 hours, and at inlet coolant temperature of 33°C, the wax thickness was 0.86mm. From the results above, it can be noticed that the wax deposit thickness of Adeyanju and Oyekunle's (2013) rig is higher than the wax deposit thickness of this study rig, despite of, their oil temperature is higher than the oil temperature of this study.

Also, the difference between the two flow rates is 0.5 L/min and the inlet coolant temperature of them is higher than the inlet coolant temperature of this study in 23°C.

Furthermore, the thermal conductivity of Copper (401 W/m.k) is higher than the thermal conductivity of mild steel (45 - 65 W/m.k). From all the above operational conditions of Adeyanju and Oyekunle's (2013) rig, it was expected to have a lower wax thickness than this study, but the results show the reverse. This can be illustrated as, this study rig contains a condenser that works to condense the remaining light components that evaporated from the heating crude oil and these light components work as a solvent to melt the wax crystals in the crude oil and reduce deposition. While the condenser is not found in the rig structure of Adeyanju and Oyekunle (2013). Also, the difference between the crude oils of the two studies has an effect on the results of wax deposition.

As a recommendation, if the pipe material of the test section of this study changed to ones has lower thermal conductivity, the results of wax deposit thickness will be lower than that of the existing one.

### 3.10 Uncertainty, Standard Deviation (SD), and Reproducibility of Experimental Data

#### Uncertainty

Experimental uncertainty analysis is a technique that analyses a derived quantity, based on the uncertainties in the experimentally measured quantities that are used in some form of mathematical relationship (model) to calculate that derived quantity (EUROLAB Technical Report 1., 2006).

The uncertainty can be estimated from the following equation:

$$\text{Uncertainty} = (\text{MaximumValue} - \text{MinimumValue}) / 2$$

.....(3.15)

#### Standard Deviation (SD)

Standard deviation is a measure that is used to quantify the amount of variation or dispersion of a set of data values. A low standard deviation indicates that the data points tend to be close to the mean (also called the expected value) of the set, while a high standard deviation indicates that the data points are spread out over a wider range of values (Bland and Altman, 1996).

The standard deviation can be calculated from the following equation:

$$s = \sqrt{\frac{\sum (x_i - \bar{x})^2}{n-1}}$$

.....(3.16)

Where,  $s$  is the standard deviation,  $x_i$  is the test result value,  $\bar{x}$  is the average value of the results, and  $n$  is the number of the test results. The average value of the test results can be calculated from the equation below (American Association for Laboratory Accreditation, 2014).

$$\bar{x} = \frac{\sum x_i}{n}$$

.....(3.17)

**For example:** To calculate the uncertainty using equation (3.15) and standard deviation using equation (3.15) and (3.17) of the experimental results of wax thicknesses (1.5, 1.61, 1.3, 1.5) using different measurement methods, can be calculated as follow:

$$\text{Uncertainty} = (1.61 - 1.3) / 2 = \pm 0.16$$

To calculate the standard deviation, should at first estimate the average value of the results.

$$\text{The average value} = \bar{x} = \frac{\sum x_i}{n} = (1.5+1.61+1.3+1.5)/4 = 1.48\text{mm}$$

Calculate  $(x_i - \bar{x})^2$  for each value

$$(1.5 - 1.48)^2 = 0.0004\text{mm}$$

$$(1.61 - 1.48)^2 = 0.0169\text{mm}$$

$$(1.3 - 1.48)^2 = 0.0324\text{mm}$$

$$(1.5 - 1.48)^2 = 0.0004\text{mm}$$

$$\sum (x_i - \bar{x})^2 = 0.0004 + 0.0169 + 0.0324 + 0.0004 = 0.0501\text{mm}$$

$$\text{The standard deviation} = s = \sqrt{\frac{\sum (x_i - \bar{x})^2}{n-1}}$$

$$s = \sqrt{\frac{0.0501}{4-1}} = 0.129\text{mm}$$

### **Reproducibility**

Reproducibility is the ability of an entire analysis of an experiment or study to be duplicated, either by the same researcher or by someone else working independently, whereas reproducing an experiment is called replicating it. Reproducibility and replicability together are among the main principles of the scientific method (Leek et al, 2015).

The results of wax thicknesses demonstrates a high degree of reproducibility of the test data for the different measurement methods conducted under the same operating conditions.

### **3.11 OLGA Wax Module**

In order to construct an OLGA model, it was necessary to gather data (e.g. pvt file and wax file), to build the model and define the simulation case, and to run simulations and view results in the form of graphs. Wax deposition simulations performed in this work are done using the OLGA 2014 version. OLGA receives the crude oil propriety input values (for example, weight percentage of carbon numbers, density, compressibility, viscosities, surface tension, enthalpies, heat capacities and thermal conductivity) in pressure and temperature values. These properties enter the OLGA simulator as a tab file created from tab, generating a PVT package such as the PIPEsim (OLGA, 2014, User Manual).

The wax deposition module in OLGA further requires details about the wax component, structure, porosity, etc., converted to a wax file in a tab format generated from the PIPEsim wax interface. The wax file provides information about the wax fraction as a function of the wax forming components, temperature and pressure, and wax mixture. Results and prediction of the OLGA simulator are largely influenced by the accuracy of table values generated from PIPEsim (OLGA, 2014, User Manual). The OLGA simulator process steps are shown in figure 22.

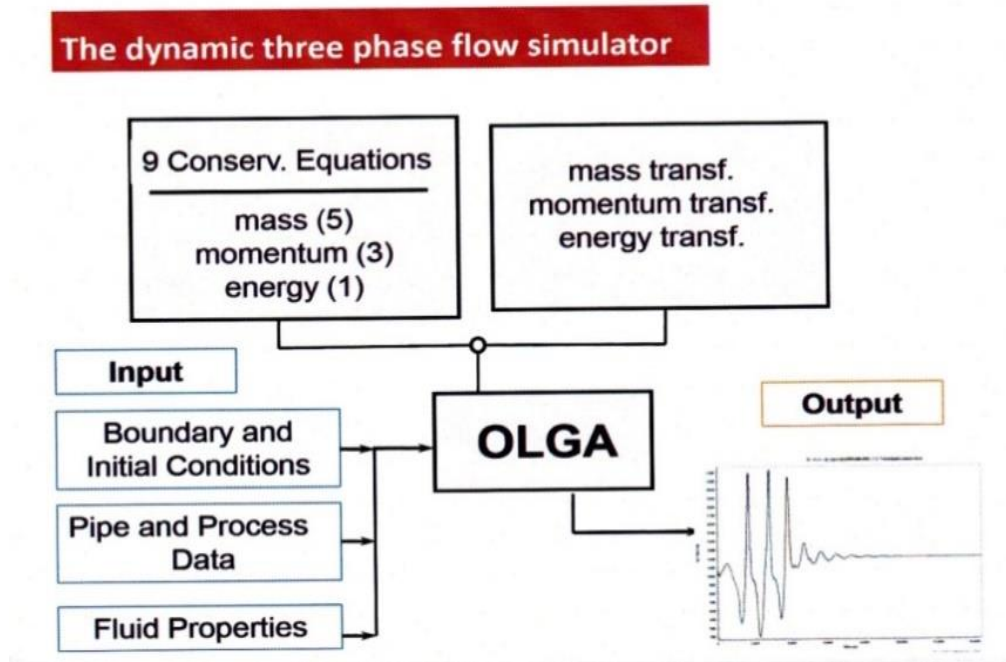


Figure 22: Steps of the OLGA simulation process (OLGA 7, SPT Group).

1. Input – input boundary and initial conditions, fluid data and pipe and process data.
  - Add and define the pipeline materials and pipe.
  - Add network component, i.e. nodes and flow path.
  - Define the properties for flow path; connect the flow path to the nodes.
  - Create flow path geometry for the pipeline using case study information.
  - Add boundary and initial conditions for pipeline length.
2. Output – define variables to be reported in the output file.
  - The following trends and profile variables are to be saved for viewing after the simulation has been run: trend variables – PT (pressure), TM (temperature), QLT (liquid flow rate), QG (gas flow rate), USG (superficial gas velocity), USLT (superficial liquid velocity), ACCLIQ (accumulated liquid flow), SURGELIQ (surge volume); and profile variables – DXWX (thickness of wax layer deposited at wall), MWXDIS (mass of wax dissolved in oil), HOL (liquid holdup fraction),

PT, TM, VISHLTAB (oil viscosity from fluid tables) and ID (flow regime identification).

3. Process – calculations of variables along the pipeline.
  - Specify the start and end time of the simulation.
  - Verify simulation case for possible error before running.
  - Run the simulation.
  - Results can be viewed in the output window.

### 3.11.1 Crude Oil Properties used in PIPEsim to Create PVT File

It was mentioned above in this chapter that the crude oil used in this study is from one of the oil field reservoirs in India and during characterisation the crude oil was found to be close to the crude oil of the Upper Assam oil field, India, which was used in the study of Jha et al. (2014), as shown in table 4.

In order to run the simulation using OLGA software, two types of data were borrowed from the study of Jha et al. (2014), see tables 5 and 6, the data of carbon number distribution in the crude oil, and the data of distribution the normal and non-normal paraffin in wax of crude oil. Those data should be entered in PIPEsim 2013 software to convert it to a pvt tab file and wax file, respectively, in order to use it to run the OLGA simulation. Other necessary data was used from the crude oil of this study such as the percentage of saturates, aromatics resins, asphaltene, specific gravity, API, density, WAT and wax content.

A sensitivity study was done on crude oil composition, using OLGA software, to reduce the difference between the crude oils for this study and that of Jha et al. (2014).

Table 4: Characterisation of crude oil for this study and Jha et al.'s (2014) study.

Property	Value of this study	Value of Jha et al., (2014) study
Density g/cm <sup>3</sup> (15°C)	0.85	0.82
Specific Gravity (60/60 °F)	0.85	0.82
API Gravity (60 °F)	35	40.51
Saturates Content (wt%)	74.91	66.46
Aromatics Content (wt%)	20.44	22.86
Resins Content (wt%)	4.26	10.34
Asphaltene Content (wt%)	0.39	0.34

Table 5: Carbon number distribution in the crude oil (Jha et al., 2014).

Carbon Number	Weight%	Carbon Number	Weight%
C6	28.5	C21	0.31
C7	14.85	C22	0.29
C8	13.62	C23	0.27
C9	9.16	C24	0.24
C10	7.6	C25	0.24
C11	7.28	C26	0.19
C12	8.05	C27	0.19
C13	2.09	C28	0.15
C14	2.15	C29	0.14
C15	0.61	C30	0.08
C16	1.97	C31	0.08
C17	0.35	C32	0.03
C18	0.4	C33	0.01
C19	0.42	C34	0
C20	0.74	C35	0

Table 6: Distribution of normal + non-normal paraffin in wax of crude oil (Jha et al., 2014).

Carbon Number	Normal %
C19	7.81
C20	6.12
C21	14.75
C22	23.84
C23	30.6
C24	11.66
C25	5.22

### 3.11.2 Methodology of Wax Deposition Simulation

The tab file of crude oil properties and wax file is imported from PIPEsim to OLGA as a pvt file to run the simulation. The experimental rig of this study was modelled to transport the oil from the oil source (oil inlet) in the first node of pipe-1 into the flow line, as shown in figure 23. The oil enters the flow line at 44.5°C at a mass flow rate 0.04 kg/s or 0.08 kg/s depending on the desired flow rate. The oil flows out of the flow line at 5 bars and 42°C through a pressure node called the oil outlet.

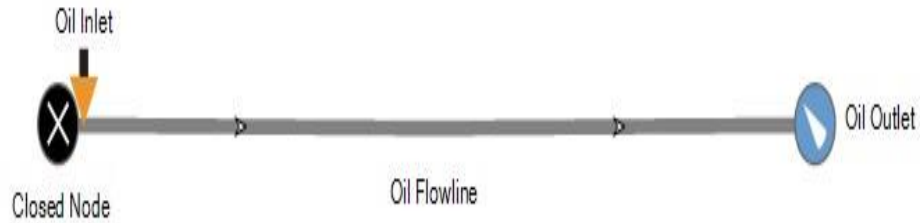


Figure 23: Schematic flow line diagram in the OLGA software for this study.

The test section of the rig is a horizontal pipe consisting of one section, so in order to simulate it using the OLGA software, the flow line geometry in the model is assumed to consist of 15 equal pipelines and each section to equal 10 cm; the minimum sections of pipe required to run the simulation using OLGA should be 3. Increasing the number of pipeline sections will not affect the accuracy of the simulation due to the pipeline being horizontal and the deviation angle zero.

The copper pipeline material properties used in the OLGA simulation model are 385 J/kg.°C heat capacity, 401 W/m.k thermal conductivity, 8960 kg/m<sup>3</sup> density and 0.0009 m pipe wall thickness.

In the wax deposition simulation, the wax deposition option is turned ON and the input parameter, including wax deposition model RRR, is as follows: wax diffusion coefficient multiplier equal to 1, wax roughness value zero, porosity of wax 0.6 (automatic default value), seabed temperature 6°C, and the simulation end time 2, 4 and 6 hours and for the study of the effect of a long time on wax deposition, the simulation end time is 12 and 24 hours.

### 3.11.3 Methodology of Tuning OLGA Parameters for Improved Predictions

There are some differences between the components of the crude oil in this study and that of Jha et al. (2014) such as SARA, specific gravity and API. So, to avoid these differences between the experimental results and the predicted results, a tuning of OLGA parameters for improved predictions was undertaken.

Three scenarios were created to match the experimental wax thickness, including studying the effect of change wax porosity in OLGA, changing the crude oil components and the influence of simulation time on wax deposition.

A sensitivity study was carried out in OLGA simulation to study the effect of changing the wax porosity to 0.2, 0.4, 0.6 and 0.8 and its impact on the predicted wax thickness to match the experimental wax thickness.

A sensitivity study was undertaken to achieve the experimental thickness using OLGA software at an inlet coolant temperature of 14°C and wax porosity 0.6 and changing the weight percentage of carbon numbers distributed in the crude oil.



Hexane or C6 in the crude oil in high percentage leads to a reduction in the wax formation in the crude oil. Therefore, the procedure involved reducing 10, 20 and 30% respectively of C6 weight percentage and distributing the removed percentage to the remaining carbon numbers in the crude oil. Increasing the simulation time from 2 to 4, 6, 12 and 24 hours was also done to study its effects on wax deposition.

## Chapter 4: Results and Discussion: Rheological Evaluation – Inhibitor Effects

### 4.1 Chapter Four Overview

This chapter presents the results of investigations into the wax inhibition process using different types of chemical inhibitors, and the results of the synergy of using mixtures of such chemical inhibitors on the rheological properties of the crude oil. The chapter outlines the effects of the inhibitors on wax appearance temperature, pour point, viscosity and density of the crude oil. It also presents the results of the crude oil that have been characterised in this work.

### 4.2 Characterisation of Crude Oil

All the crude oil characterisation was carried out in the lab for this work, through the experimental methods and the standard analytical techniques, as shown in table 7.

Table 7: Crude oil characteristics.

Property	Unit	Value	Experimental Method
Density	kg/m <sup>3</sup> (15°C)	850	mass/volume
Sp. Gravity	60/60 °F	0.85	Calculated
API Gravity	60 °F	34.97	API Method
WAT at shear rate 10 1/s	°C	39	Rheometer
WAT at shear rate 120 1/s	°C	30	Rheometer
Pour Point	°C	27.6	Rheometer
Wax Content	wt%	20.15	Precipitation Method
Saturates Content	wt%	74.91	SARA
Aromatics Content	wt%	20.44	SARA
Resins Content	wt%	4.26	SARA
Asphaltene Content	wt%	0.39	SARA

### 4.3 Effect of Inhibitors on Crude Oil Rheology

The effect of several of the chemical inhibitors, at a concentration of 1000 and 2000ppm, on the crude oil rheology was evaluated, as shown in figure 24. The rheological analysis of the crude oil shows that the inhibitors W802, W804 and W805 at a concentration of 2000ppm produced a high reduction in the value of crude oil viscosity, wax appearance temperature and pour point compared with the rest of the inhibitors. This can be illustrated as follows: the inhibitor W802 polyacrylate polymer (C16-C22) has a high molecular weight, thereby preventing agglomeration of wax crystals due to the interference of the inhibitor molecules with wax crystal growth. Increasing the concentration of W802 from 1000 to 2000ppm leads to increasing the inhibitor molecules that work to increase wax crystal prevention.

The inhibitors W804 and W805 consist both of copolymers and acrylated monomers, which prevent wax formation by the inhibitor interfering with the wax crystal growth; by increasing the inhibitor concentration, the wax prevention process increases due to increased structures of copolymers and acrylated monomers.

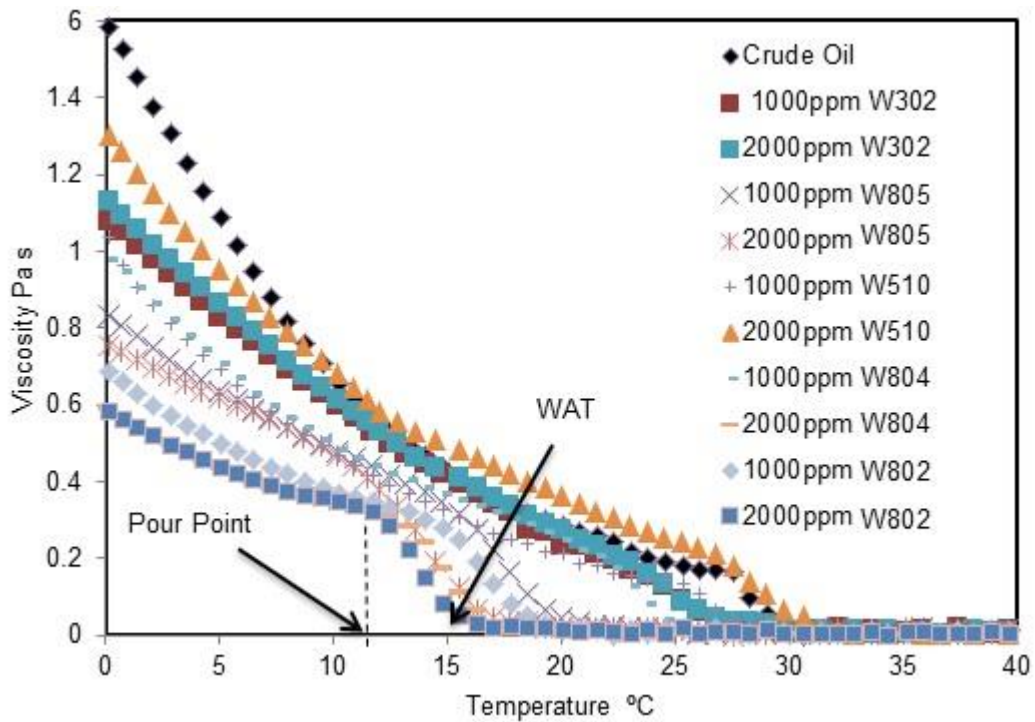


Figure 24: The rheological behaviour of the crude oil with the chemical inhibitors at a concentration of 1000 and 2000ppm and different range of temperatures, and shear rate 120 1/s.

The rheological analysis of the crude oil with the inhibitors shows that the inhibitor polyacrylate polymer (W802) presents the best results in reducing wax deposition compared with the other inhibitors. Therefore, W802 was used during this study to examine its effects on wax deposition through the experimental flow loop at different concentrations.

#### 4.3.1 Effect of Inhibitors on Viscosity

The analysis of change in the crude oil viscosity behaviour with regard to the inhibitors shows that the mixtures of inhibitors Mix01 and Mix02 present the greatest reduction in viscosity at a concentration of 2000ppm, compared with its original components at the same concentration, due to an increase in the numbers of monomers and thus an increase in the ability to prevent wax formation.

The first mixture of inhibitors Mix01 at 2000ppm reduced the crude oil viscosity from 1.16 to 0.39 Pa.s, at a seabed temperature of 4°C, see figure 25. The crude oil viscosity is a proportional to the inhibitor concentration 500,

1000, and 2000ppm. This can be explained as follows: increasing the concentration of the inhibitor mixtures leads to increasing the molecules of the polyacrylate polymer, acrylated monomers and the copolymers that might potentially interact between them and creating different structure of mixtures of inhibitors that work to prevent the wax aggregation and this helps to reduce the crude oil viscosity. Increasing the reaction temperature leads to reduce the crude oil viscosity at the same shear rate and as a result this will increase the shear stress the resistance force to wax deposition. In the same time, increasing the shear rate leads to reduce the viscosity of the crude oil at the same concentration of the inhibitor. At lower concentrations of the inhibitor mixtures, the interfere of the mixture molecules between the wax molecules will be not enough to reduce the crude oil viscosity comparing with high concentration of the inhibitor.

The second mixture of inhibitors, Mix02 at a 2000ppm concentration, reduced the viscosity from 1.16 to 0.41 Pa.s, at a seabed temperature of 4°C, see figure 26. The molecule mechanisms of the inhibitor mixtures become more efficient compared with their original components due to increasing the percentage of the inhibitors that prevent the wax formation, or those inhibitors which might react with each other producing a new structure of inhibitor, thereby improving the wax inhibition. At lower concentrations of Mix02, the oil viscosity reduced from 1.16 to 0.49 Pa.s. This lower reduction in viscosity was due to the volume percentage of the inhibitors that prevent the wax formation is lower than the percentage of the crude oil volume.

Finally, the third mixture of inhibitors, Mix03 at a 1000ppm concentration, has reduced the viscosity from 1.16 to 0.54 Pa.s, at a seabed temperature of 4°C, see figure 27. At lowest concentration, the reduction in crude oil viscosity is less. This can be illustrated as follows: adding brine to the polyacrylate polymers leads to forming a sodium polyacrylate polymer that has a high absorption capacity due to its having a divalent cation, an ion with a positive charge characteristically moving toward the negative charge (Conway and Williams, 2000). This mixture of inhibitors works more efficiently by increasing the shear rate due to it prevents the aggregation and form a long chain between the wax structures. At 500ppm of Mix03, the viscosity of the crude oil reduced from 1.16 to 0.6 Pa.s due to the percentage of the created sodium polyacrylate polymer will be less, therefore, the reduction in crude oil viscosity will be less.

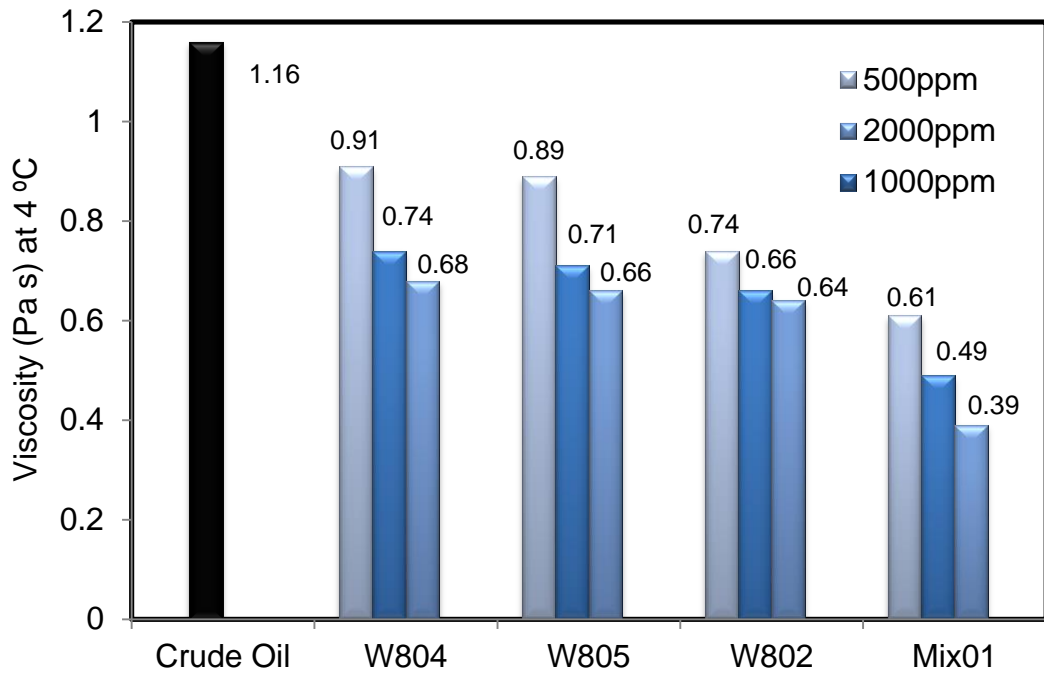


Figure 25: The effect of inhibitors mixture Mix01 and its components on crude oil viscosity at 4°C, at 500ppm, 1000ppm and 2000ppm.

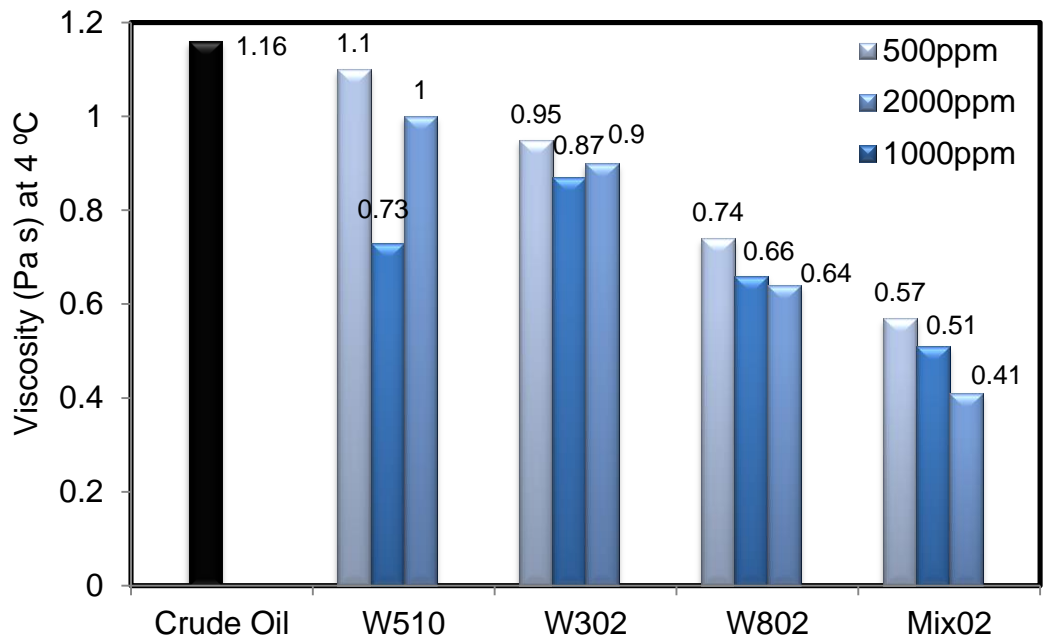


Figure 26: The effect of inhibitors mixture Mix02 and its components on crude oil viscosity at 4°C, at 500ppm, 1000ppm and 2000ppm.

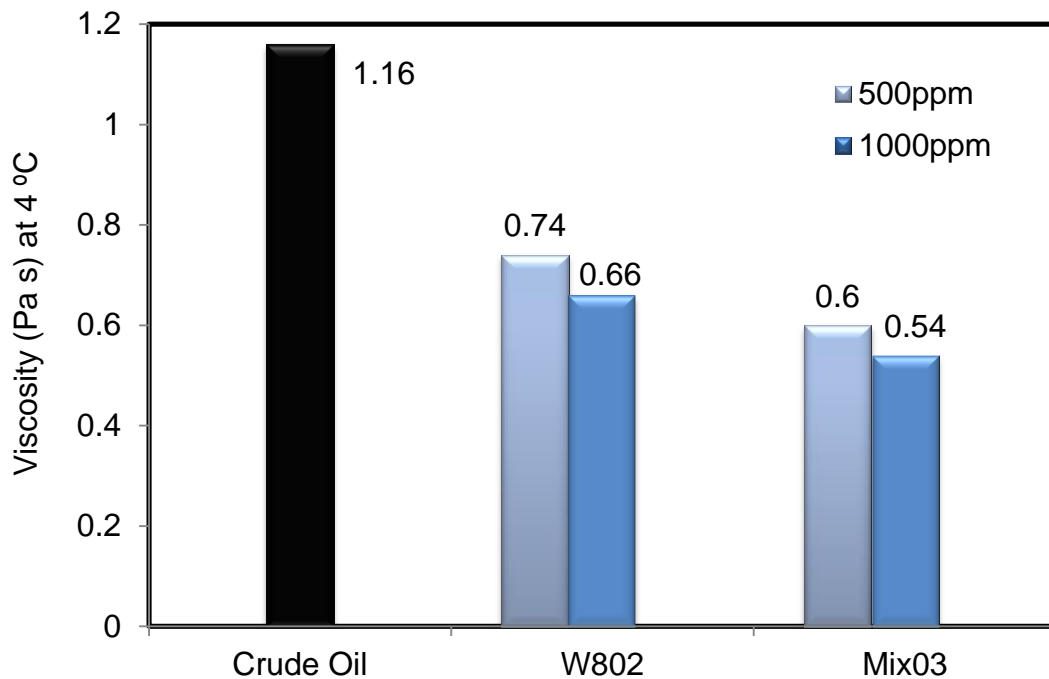


Figure 27: The effect of inhibitors mixture Mix03 and its components on crude oil viscosity at 4°C and a concentration of 500ppm and 1000ppm.

#### 4.3.2 Effect of Inhibitors on Pour Point

The pour point is the temperature at which the crude oil becomes semi-solid and loses its flow characteristics. During examine the effect of the chemical inhibitors on the crude oil rheology, it was noticed, that the chemical inhibitors affects on the pour point temperature. The first inhibitor mixture Mix01 reduced the pour point of the waxy crude oil from 27.6°C to 10.5°C, at a concentration of 2000ppm, while at lower concentration the pour point reduced to 13.7 °C as shown in figure 28.

The second inhibitor, Mix02 at a 2000ppm concentration, produced a better result compared with its components; it decreased the pour point of the crude oil from 27.6°C to 11°C, while at lower concentration 500ppm the pour point reduced to 15.2 °C as shown in figure 29. Finally, the third inhibitor, Mix03 at a 1000ppm concentration, reduced the pour point of the oil from 27.6°C to 13°C and at 500ppm, he pour point reduced to 15.1°C, see figure 30.

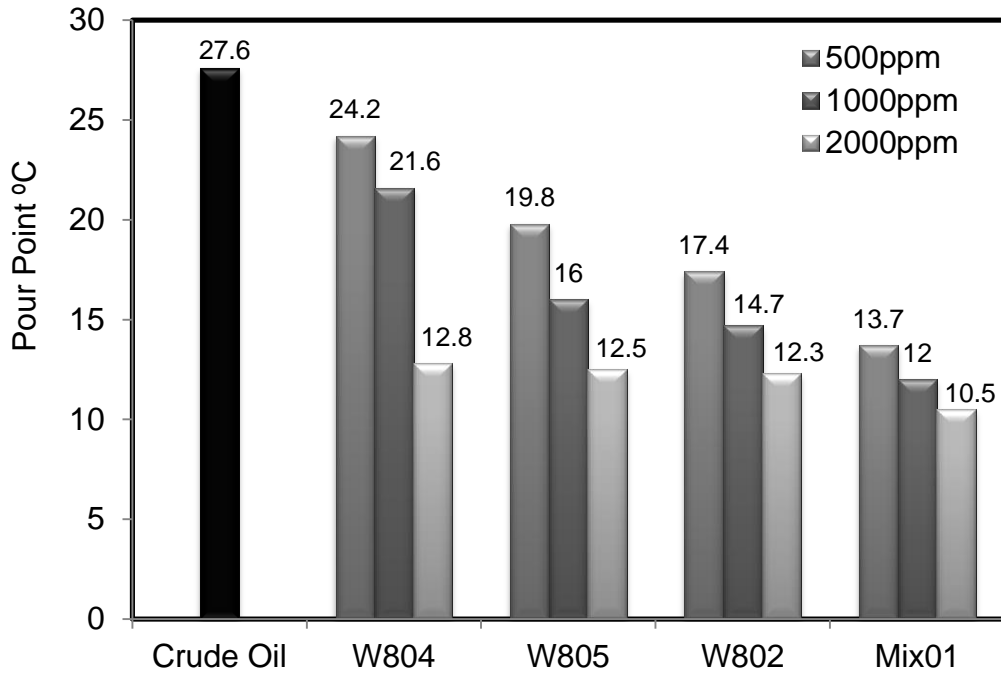


Figure 28: The effect of inhibitors mixture Mix01 and its components on pour point temperature at 500ppm, 1000ppm and 2000ppm.

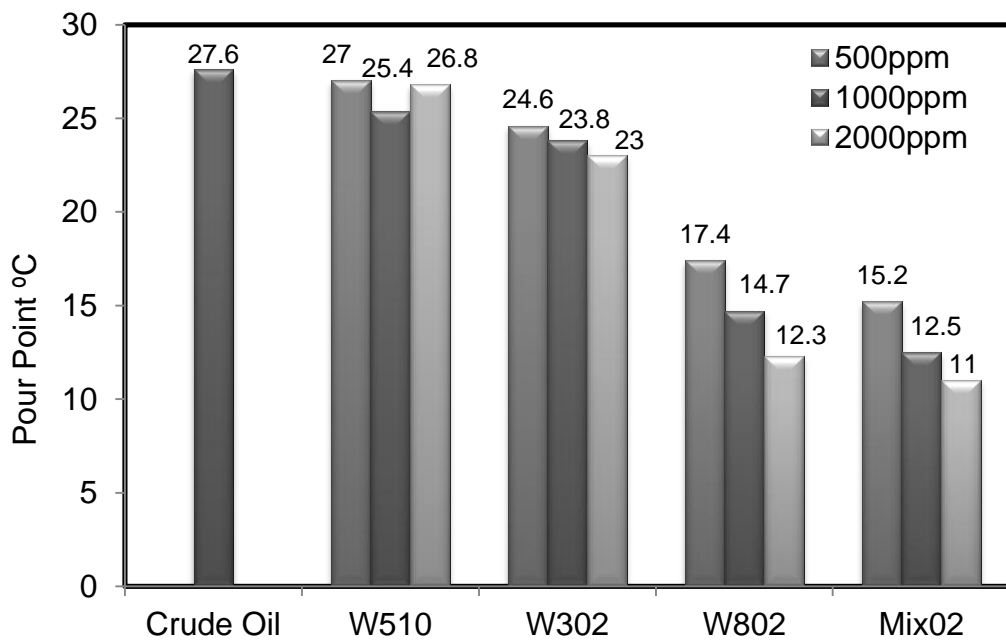


Figure 29: The effect of inhibitors mixture Mix02 and its components on pour point temperature at 500ppm, 1000ppm and 2000ppm.

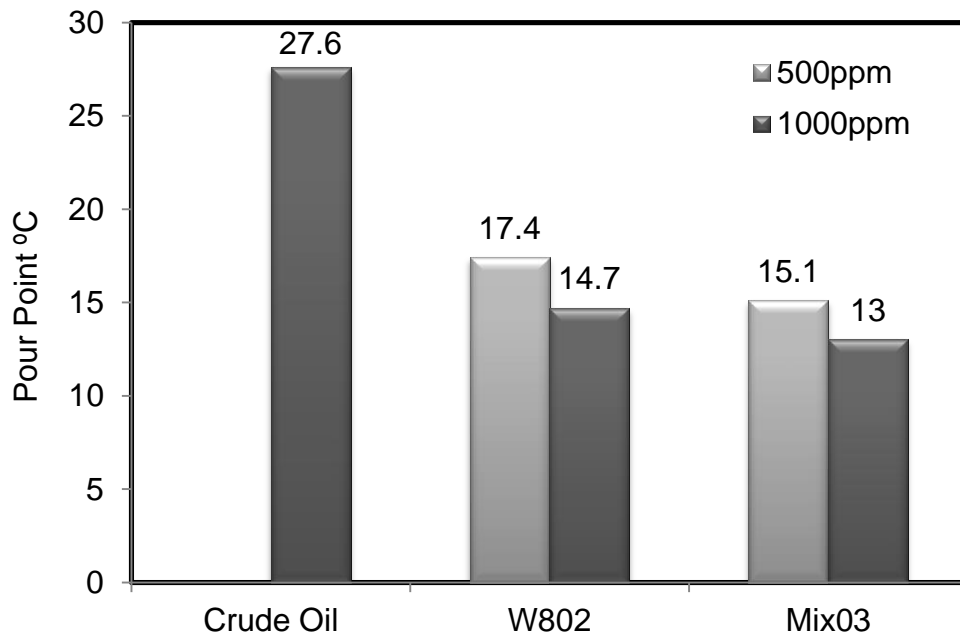


Figure 30: The effect of inhibitors mixture Mix03 and its components on pour point temperature at a concentration of 1000ppm.

#### 4.3.3 Effect of Inhibitors on Wax Appearance Temperature

The wax appearance temperature of the crude oil has been reduced by adding the mixture of inhibitors for this study; it decreased up to 52% after adding Mix01 and up to 48.3% after adding Mix02 at a concentration of 2000ppm; it decreased up to 41% after adding the inhibitor Mix03 at a concentration of 1000ppm. At concentrations 500ppm, the reduction in wax appearance temperature was 38.9% after adding Mix01 and up to 40.1% after adding Mix02 at a concentration of 2000ppm respectively as shown in Figures 31, 32 and 33. While, the reduction in WAT was 35.6% after adding the inhibitor Mix03 at a concentration of 500ppm.

This can be interpreted as follows: by increasing the concentration of Mix01 from 500ppm to 1000ppm then to 2000ppm, the quantity of the polyacrylate polymer and the acrylate monomers will be increased, providing more structures to interfere and merge with the edge of the growing wax crystals, leading to a reduced wax appearance temperature.

The reduction in WAT due to adding Mix02 can be explained as follows: by increasing the concentration of polyacrylate polymer, alkylated phenol and copolymer dissolved in naphtha, the wax crystals size will be reduced due to an increase in the molecules that prevent wax crystal formation and preserve it as smaller particles. The third Mix03 contains a mixing polyacrylate polymer and brine ( $H_2O + NaCl$ ), and this will lead to producing sodium polyacrylate, which will absorb and merge with the wax crystals and prevent them from growing together.



The effectiveness of the mixture of inhibitors is affected by other factors besides the molecular interaction between the inhibitors and wax in the crude oil. These other factors include shear rate, shear stress, temperature, and pressure. As mentioned before, the temperature had an effect on crude oil viscosity where increasing the temperature leads to decrease crude oil viscosity due melt the wax crystals in the crude oil. The effect of shear rate was obvious on the effectiveness of the mixture of inhibitors, where, increasing the shear rate leads to reduce the wax appearance temperature due to increasing the force of shear stress at the same time.

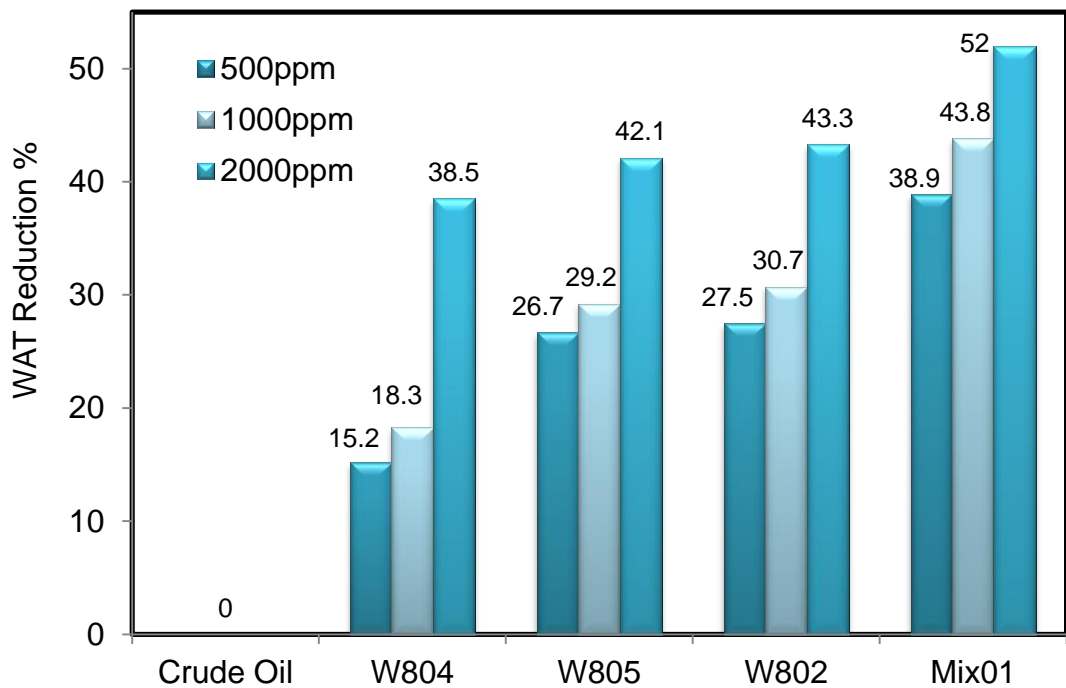


Figure 31: The effect of inhibitors mixture Mix01 and its components on WAT at 500ppm, 1000ppm and 2000ppm.

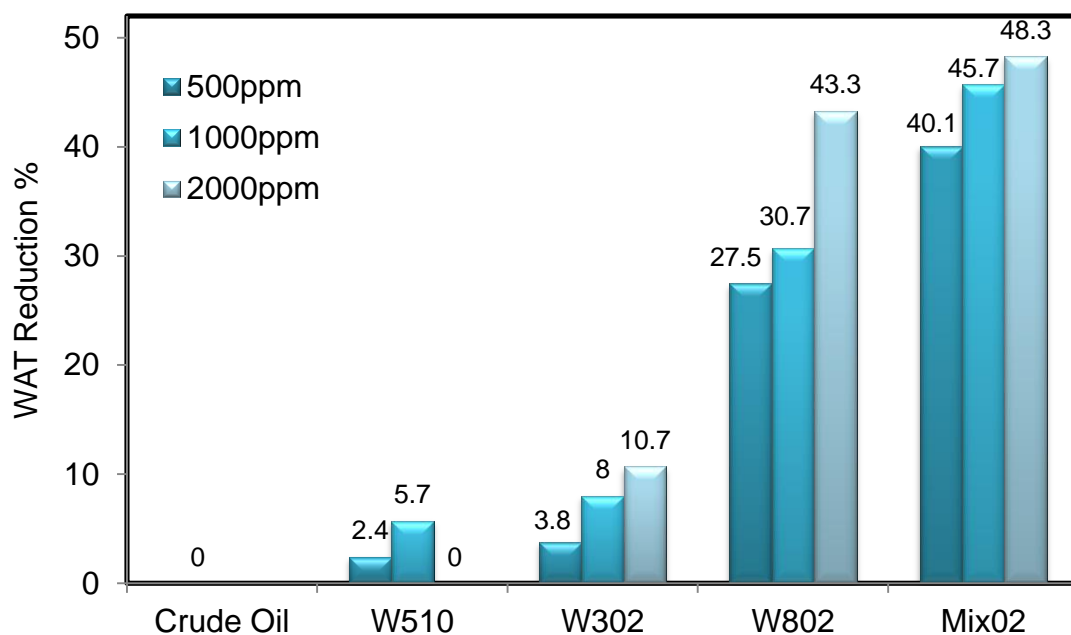


Figure 32: The effect of inhibitors mixture Mix02 and its components on WAT at 500ppm, 1000ppm and 2000ppm.

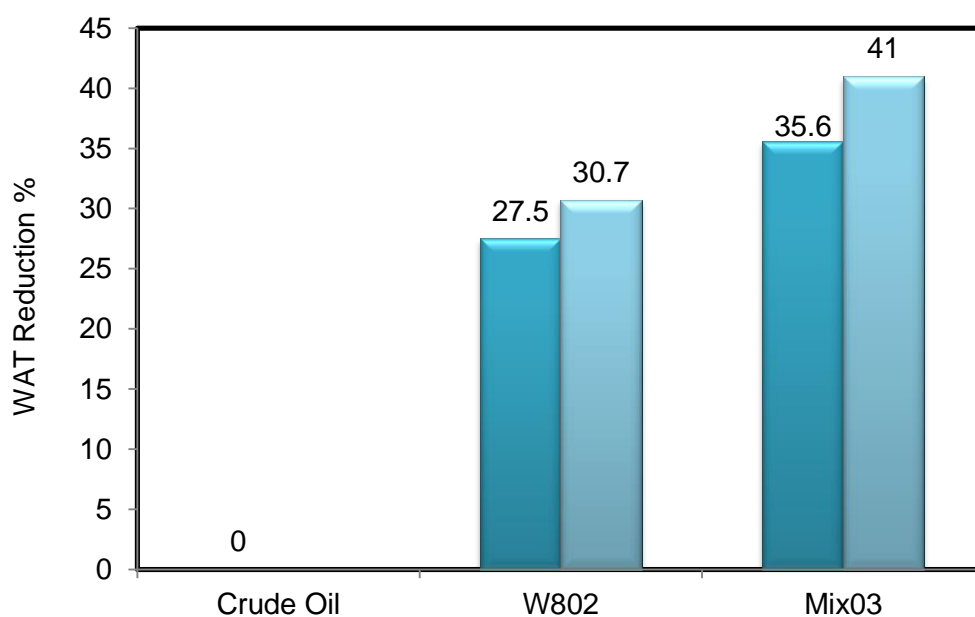


Figure 33: The effect of inhibitors mixture Mix03 and its components on WAT at 500ppm and 1000ppm.

#### 4.3.4 Study of the Effect of Inhibitor Mixtures on Oil Rheology

From figure 34, it was noticed that at a concentration of 1000ppm, Mix02 produced better results, compared with Mix01 and Mix03, in the reduction of pour point and wax appearance temperature 12.5 and 16.3°C, respectively. At 2000ppm Mix01 produced the best results compared with the prepared mixtures and the original inhibitors, where it had a pour point and wax appearance temperature of 11 and 14.5°C, respectively.

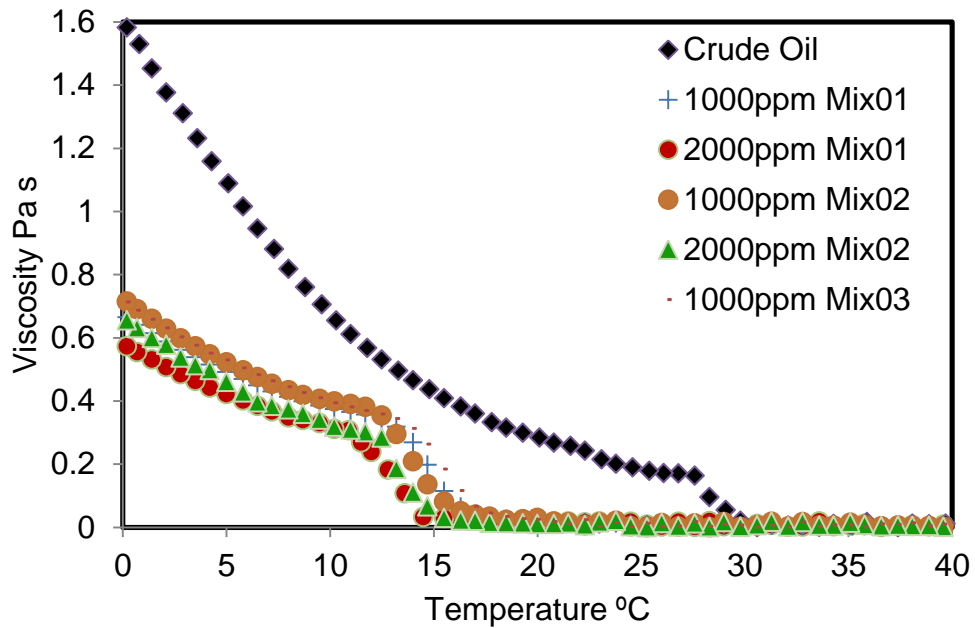


Figure 34: The effect of the inhibitors, Mix01 and Mix02 at 1000ppm and 2000ppm, and Mix03 at 1000ppm, on crude oil rheology (WAT, pour point and viscosity) at different temperatures.

These inhibitor mixtures at a concentration of 500ppm, 1000ppm and 2000ppm improved the reduction in wax crystal formation by interfering with wax crystallisation and preventing the growth process. However, this interfering mechanism has not yet been fully understood (Jennings and Newberry, 2008). The major theory stated the possibility of wax inhibitor polymers containing a similar structure to the wax structure, such as the polyacrylate polymer, thereby allowing the inhibitor crystal to be incorporated into the wax crystal growth. Sometimes the structural part of the polymer covers the wax site, thereby preventing further wax crystal growth and promoting the formation of smaller wax aggregates (Jennings and Newberry, 2008; Adeyanju and Oyekunle, 2014).

Most of the components of the new mixtures of inhibitors come from the polymer family and as a result of mixing them, they might interact and cooperate, thereby creating a long structure of inhibitor and producing a combined effect greater than the sum of their separate effects on wax deposition.

The rate of shearing and shear force depends largely on the flow rate, viscosity, and temperature. The viscosity is significantly decreased when inhibitor was added leading to increase the shear rate. This increase in the shear rate causes an increase in the shear stress on wax molecules and formed wax crystals which acts to diminish the wax deposition rate.

#### **4.4 Effect of Shear Rate on Oil Viscosity at Different Concentrations of Inhibitor**

Adding wax inhibitor significantly changed the fluid's rheological characteristics, the fluid became much less viscous when the inhibitor was added. Also the viscosity became much less shear-dependent. A possible explanation is that the inhibitor affects the sizes of the formed wax crystals.

Additional measurements at different shear rates and constant temperature showed also that the viscosity depends on the shear rate decreased significantly when inhibitor was added, in other words the fluid became more Newtonian.

From figure 35, it can be seen that increasing the shear rate leads to decrease the viscosity of the crude oil at temperature 4°C. At the same shear rate 10 1/s, adding the mixtures of the inhibitors Mix01, Mix02, and Mix03 at a concentration 500ppm result in decreasing the oil viscosity, where Mix01 shows more reduction in the viscosity than the other two mixtures of inhibitors. The reduction in oil viscosity means a reduction in wax formation.

Increasing the shear rate to 60 1/s results in decreasing the oil viscosity more and by increasing the concentration of the mixtures of inhibitors to 1000ppm, the reduction in the viscosity was clearly obvious, due to increase the force of the shear rate that leads to increase the shear stress and decrease the wax deposition. Also, the reduction in viscosity is due to increase the amount of the inhibitor molecules that interfere between the wax molecules and prevent them to combine together.

Increasing the shear rate value to 120, and 180 1/s, respectively, leads to reduce the oil viscosity more and more. At the same time, increasing the inhibitor concentration to 2000ppm, with increasing the shear rate works together to decrease the oil viscosity clearly. This combination of the effects leads to reduce the availability of wax formation.

From the analysis, it can notice that Mix01 works more efficiently than Mix02, and Mix03 at all concentration. Therefore, this mixture of inhibitors is suitable for the crude oil with high content of wax, and it is more active by increasing the shear.

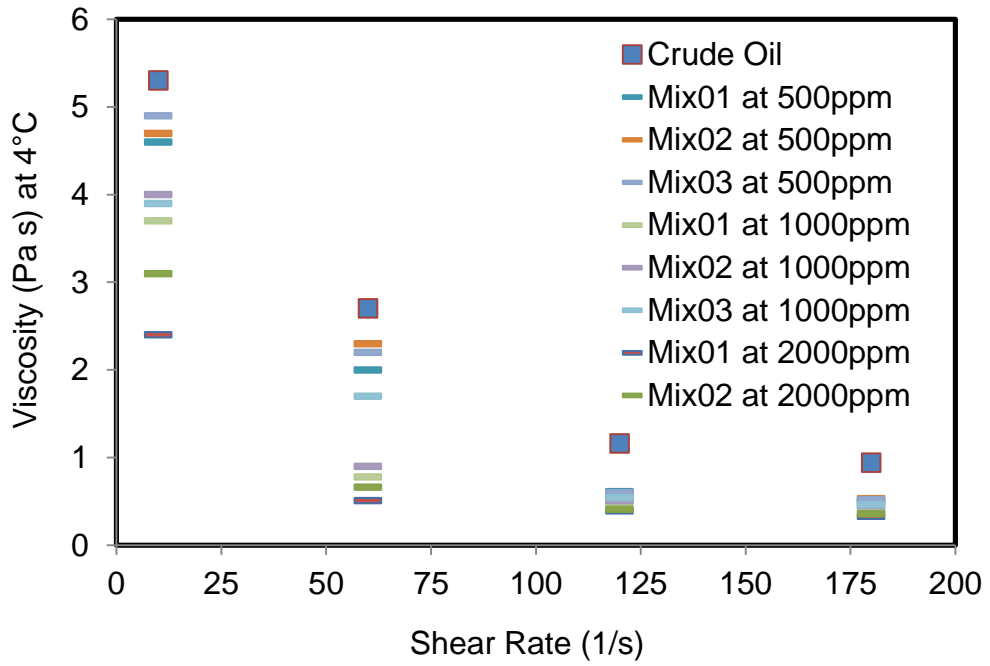


Figure 35: The effect of shear rate on crude oil viscosity at concentration 500, 1000, and 2000ppm of the mixtures of inhibitors Mix01, Mix02, and Mix03.

## **Chapter 5: Results and Discussion: Wax Formation**

### **5.1 Chapter Five Overview**

The experiments conducted throughout this section of the research were intended to develop understanding of the wax deposition process. Whilst carrying out the experiments, it was observed that the thickness of wax deposited in the test section pipe increased as the inlet coolant temperature was reduced. Other factors such as flow rate, recirculation time of crude oil, pressure drop and oil temperature had a significant impact on wax thickness. Mitigation methods to reduce wax deposition were presented, such as inhibitor W802 polyacrylate polymer, spiral flow, and bending the effect of the inhibitor and spiral flow. A comparison between the best mitigation methods to reduce wax deposition will be presented in this chapter.

### **5.2 Wax Deposition Process**

A series of experiments were carried out during this research in order to study the wax deposition process. The impact of various factors on the wax deposition process were studied, such as the inlet coolant temperature 14, 24 and 33°C, circulating time of oil at 2, 3, 4, 5 and 6 hours and the variation of flow rate from 2.7 to 4.8 L/min.

Eight different experiment sets were applied to the above conditions, as shown in tables 8, 9 and 10. Seven of these were mitigation methods, including the commercial inhibitor W802 method at a concentration of 500ppm, the commercial inhibitor W802 method at a concentration of 1000ppm, the commercial inhibitor W802 method at a concentration of 2000ppm, the new spiral flow method, the new method of bending the spiral flow with the inhibitor W802 at a concentration of 500 and 1000ppm respectively, and finally, the method of bending the spiral flow with the inhibitor W802 at a concentration of 2000ppm. These included a set of experiments carried out at different flow rates, different inlet coolant temperatures, and different aging times.

Table 8 shows the wax deposit volumes at inlet coolant temperature 14°C for each experiment set. At the flow rate of 2.7 L/min, the maximum volumes of wax were found by carrying out the experiment using just crude oil at a different experimental time, while the minimum volumes of wax were found by carrying out the experiment using the effect of bending the spiral flow with 2000ppm of the inhibitor W802 polyacrylate polymer (C16-C22).

The wax volume reduced more than 67% when using the spiral flow and it reduced by about 75% after both merging the effect of the spiral flow with the inhibitor at a concentration of 1000ppm, and using the effect of the spiral flow with the inhibitor at a concentration of 2000ppm. Increasing the flow rate to

4.8 L/min led to a reduction in general in the wax deposit volume in the pipe wall due to increasing the shear stress.

The results in table 8 show that the wax deposit volumes are very close to each other after using the inhibitor polyacrylate polymer W802 at a concentration of 1000ppm and 2000ppm.

Table 8: Wax deposit volume at inlet coolant temperature 14°C.

Experiment at 14°C	Wax Volume (ml) at Q=2.7 L/min					Wax Volume (ml) at Q=4.8 L/min				
	At 2 hrs	At 3 hrs	At 4 hrs	At 5 hrs	At 6 hrs	At 2 hrs	At 3 hrs	At 4 hrs	At 5 hrs	At 6 hrs
Crude Oil	120	122	125	124	130	85	87	90	94	100
500ppm W802	102	102	103	102	103	76	76	77	75	76
1000ppm W802	70	72	74	77	80	62	63	65	64	67
2000ppm W802	70	71	73	73	75	60	60	63	63	65
Oil+Spiral Flow	40	40	42	43	43	23	25	25	27	27
500ppm+Spiral Flow	36	37	37	36	37	21	20	22	19	20
1000ppm+Spiral Flow	30	31	33	34	35	16	18	18	17	18
2000ppm+Spiral Flow	30	30	31	32	33	14	16	16	17	17

Table 9 illustrates the effect of the eight experiment sets on wax deposit volume at an inlet coolant temperature of 24°C, at different time and flow rates.

Increasing the pipe wall temperature leads to a decrease in the wax deposit due to an increase in dissolving the wax molecules and reducing the crude oil viscosity. It could be seen that in general the wax volume reduced and this was highest with the method of using just crude oil and lowest when using the effect of bending the spiral flow with the inhibitor at 2000ppm.

Table 9: Wax deposit volume in different experiment sets, at inlet coolant temperature 24°C.

Method at 24°C	Wax Volume (ml) at Q=2.7 L/min					Wax Volume (ml) at Q=4.8 L/min				
	At 2 hrs	At 3 hrs	At 4 hrs	At 5 hrs	At 6 hrs	At 2 hrs	At 3 hrs	At 4 hrs	At 5 hrs	At 6 hrs
Crude Oil	83	83	87	89	89	70	74	75	75	77
500ppmm W802	63	63	65	64	64	50	49	52	52	51
1000ppm W802	45	47	47	46	50	30	31	32	33	33
2000ppm W802	42	43	43	42	44	28	30	30	29	31
Oil+Spiral Flow	27	27	29	28	26	14	13	15	14	15
500ppm+Spiral Flow	22	22	23	22	22	9	8	10	9	9
1000ppm+Spiral Flow	7	8	8	9	9	4	7	6	8	7
2000ppm+Spiral Flow	6.5	7	7	8	8	4	4	5	4	6

Table 10 presents the wax volume deposit on the pipe wall at an inlet coolant temperature of 33°C, at flow rate 2.7 and 4.8 L/min, and at different aging times. The wax volume was 25 ml from running the experiment using just crude oil at 2.7 L/min for 2 hours; this reduced to 18 ml at a flow rate of 4.8 L/min for the same experimental time. The reduction in the wax deposition was 100% after using the effect of the inhibitor W802 at a concentration of 1000 and 2000ppm and a flow rate 2.7 and 4.8 L/min respectively for the different experimental times. While, the reduction in wax deposition was about 20% after using the effect of the inhibitor W802 at a concentration 500ppm at flow rate 2.7 L/min, and reduced to about 23% at flow rate 4.8 L/min.

The reduction in the wax deposition was also 100% after using the effect of bending the spiral flow with the inhibitor W802 at a concentration of 1000 and 2000ppm at different time and flow rates. The reduction in wax deposition was 100% after using the effect of bending the spiral flow with the inhibitor W802 at a concentration of 500ppm at flow rate 4.8 L/min, and the reduction in wax deposition was 94% at the same concentration and flow rate 2.7 L/min.



Table 10: Wax deposit volume at inlet coolant temperature 33°C.

Method at 33°C	Wax Volume (ml) at Q=2.7 L/min					Wax Volume (ml) at Q=4.8 L/min				
	At 2 hrs	At 3 hrs	At 4 hrs	At 5 hrs	At 6 hrs	At 2 hrs	At 3 hrs	At 4 hrs	At 5 hrs	At 6 hrs
Crude Oil	25	27	28	28	30	18	17	19	18	20
500ppm W802	20	23	22	22	23	15	14	16	15	15
1000ppm W802	0	0	0	0	0	0	0	0	0	0
2000ppm W802	0	0	0	0	0	0	0	0	0	0
Oil+Spiral Flow	5	7	7	6	8	6	5	7	7	8
500ppm+Spiral Flow	1	2	2	1	2	0	0	0	0	0
1000ppm+Spiral Flow	0	0	0	0	0	0	0	0	0	0
2000ppm+Spiral Flow	0	0	0	0	0	0	0	0	0	0

From the above three tables, it can be concluded that the spiral flow method and the spiral flow with the 1000ppm W802 method are the best economical methods to reduce the wax deposit mitigation cost. Therefore, these two methods will be illustrated in detail, comparing them with the method of carrying out the experiments with just crude oil.

The reproducibility degree of each value in the three tables above was in the high level under the same operating conditions due to the uncertainty average of each value is about  $\pm 1$  ml at different sets of experiments; and the average standard deviation of each value is about 1.41ml.

### 5.2.1 Effect of Mitigation Methods on Wax Deposition

This part presents the five mitigation methods mentioned in the previous section in order to study their effect on wax deposition volumes and draw a comparison between them to choose the best methods to reduce wax deposition.

Figure 36 shows the effect of the mitigation methods on wax deposition volumes at a flow rate of 2.7 L/min and experimental time of 2 hours; it can be seen that the wax volume was 125 ml after running the experiment using just crude oil. The highest wax volume reductions were 73.6% and 75.2% from using the new method of blending the effect of the spiral flow with the inhibitor at 1000ppm and using the new method of blending the effect of the spiral flow with the inhibitor at 2000ppm respectively.

This reduction occurs due to the double effect of the spiral flow, which increases the shear stress and moves the wax molecules to the pipe centreline, and the inhibitor, which prevents the formation of a long chain of wax by enter the inhibitor molecules between the wax molecules. The

difference between the two new methods was 1.6%, so the first new inhibitor involving bending the spiral flow with 1000ppm of the inhibitor is preferred because this method reduced the cost of the inhibitor used in the mitigation method.

The new method of spiral flow represents a second best method to reduce wax. This method reduced the wax volume to 66.4% and it works efficiently even at low temperatures due to increasing the shear stress and preventing the wax molecules from connecting with each other and depositing as long chains on the pipe wall.

The other two mitigation methods include adding the inhibitor W802 to the crude oil at a concentration of 1000 and 2000ppm respectively. The reduction in those two methods was 40.8% and 41.6% respectively; therefore the difference between the two percentages was 0.8%. The method of the inhibitor W802 at 1000ppm is therefore preferred to that at 2000ppm due to the fact that it reduces the economic cost of the inhibitor. While, at a concentration 500ppm of W802 leads to reduce the wax deposition to 18%, due to this concentration of the inhibitor is not enough to prevent the wax formation and deposited on the pipe wall.

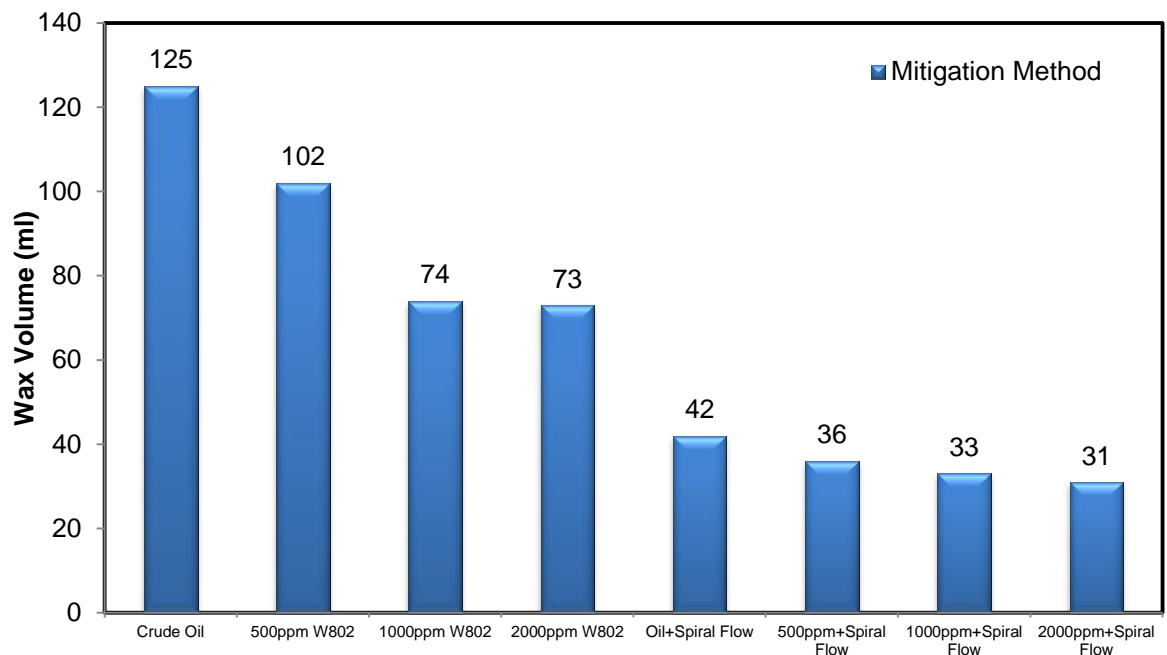


Figure 36: The effects of mitigation methods on wax deposition volume at flow rate 2.7 L/min and experimental time 2 hours.

### 5.2.2 Effect of Shear Rate on Wax Appearance Temperature

As discussed above in the methodology, the WAT of the crude oil sample was determined by using a programmable rheometer that measured the viscosity of the crude oil at different temperatures and different shear rates. The WAT of the oil sample was 39°C, as shown in figure 37. It can be seen that increasing the shear rate value leads to a decrease in the viscosity

below the WAT. This can be explained by the fact that by increasing the shear rate the viscosity of the crude oil will decrease and, as a result, the wax appearance temperature will reduce due to increasing the reverse forces on wax deposition forces inside the pipeline.

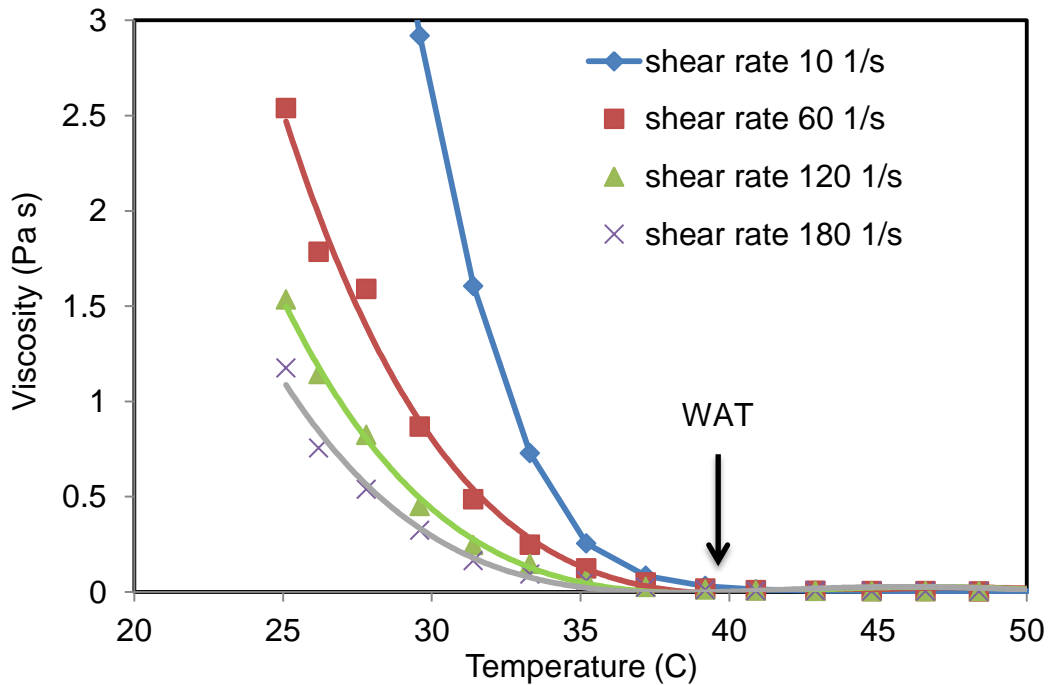


Figure 37: Viscosity profile of the oil sample at different shear rates and temperatures; shows the WAT around 39°C measured in this study.

In the present work, it was noticed that increasing the shear rate leads to a decrease in viscosity at the same temperature because viscosity is inversely proportional to the shear rate, which results in a reduction in the wax deposition, as shown in figure 38. This is evidence that increasing the flow rate reduces the wax deposit due to decreasing the oil viscosity.

This will begin to occur when the cohesive and adhesive forces of the paraffin wax molecules and the deposition surface are overcome by the rate of shear (Bott and Gudmunsson, 1977).

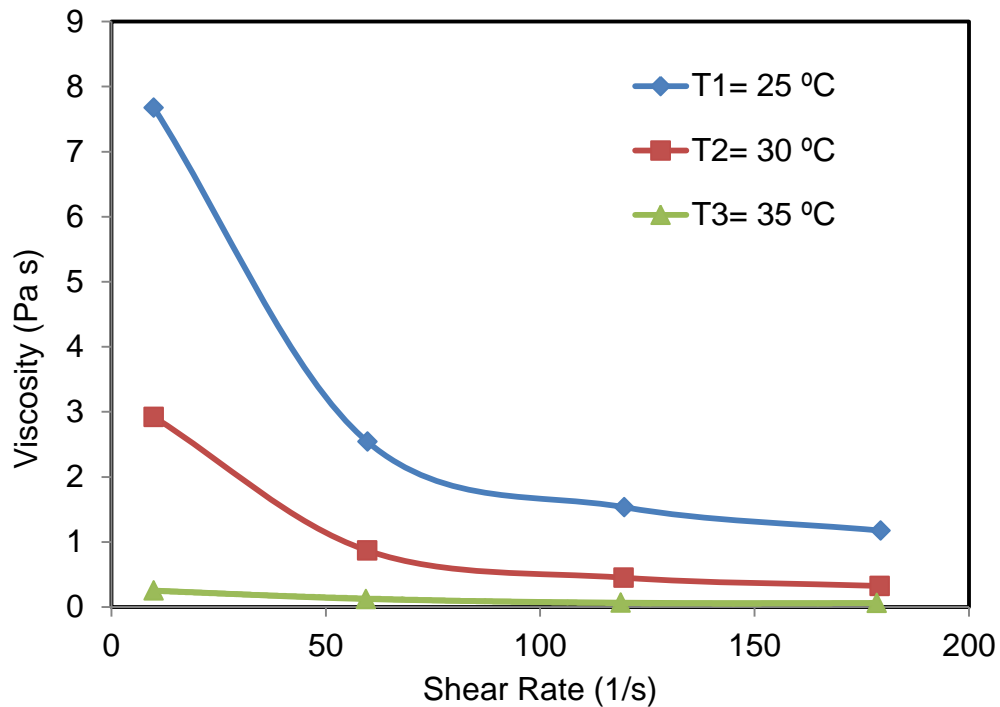


Figure 38: Effect of the shear rate on the viscosity at the same temperature.

### 5.2.3 Effect of Shear Rate and Shear Stress on Crude Oil Viscosity

Experimentally, it was noticed that an increase in the oil flow rate caused an increase in the shear stress at different temperatures. It was observed in the current research that the deposit thickness decreased with the increasing shear stress, while it increased at low shear stresses. This somewhat agrees with Dwivedi's (2012) observations; he noticed a general decreasing trend in the deposit thickness due to increasing the shear stress.

The shear stress will contribute to breaking down the microstructures that bind the crystals together; therefore, the chance of gelling reduces when the shear stress increases. The wall shear stress is proportional to the velocity squared. Therefore, an increase in velocity will cause a larger increase in the wall shear stress. An increase in wax thickness will reduce the effective diameter of a pipe, causing increasing velocity and increasing wall shear stress (White, 2008; Botne, 2012).

From figure 39, it was noticed that at the same oil temperature increasing the shear rate leads to an increase in the shear stress. Also, the value of the shear stress at lower oil temperatures is larger than at higher oil temperatures. This can be interpreted as an increase in the oil temperature leading to a decrease in the oil viscosity due to an increase in the wax solubility; therefore the wax deposition forces decrease and, as a result, the shear stress value will reduce.

At the same crude oil temperature the shear stress increased gradually due to increasing the shear rate, and suddenly converted to a nearly straight line

at the elbow point. This point represents the pour point, at which the liquid converted from a non-Newtonian to a Newtonian liquid due to decreasing the crude oil viscosity by increasing the shear rate.

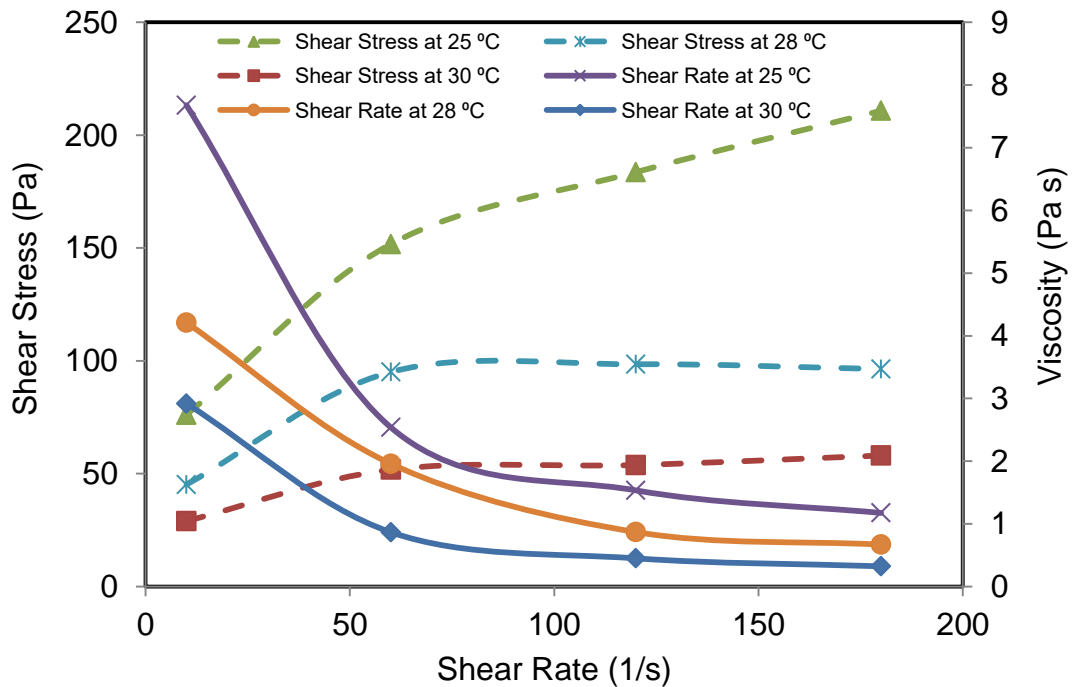


Figure 39: Shear stress and shear rate at different temperatures.

#### 5.2.4 Measuring Wax Thickness Using Different Methods

The four different methods used to evaluate the wax thickness in the test section of the pipe include: the direct pigging method, pressure drop method, heat transfer method, and liquid displacement-level detection method.

Tables 11 and 12, show a comparison between the four methods to estimate the wax thickness at different flow rates. The results show a large correspondence between the wax volumes measured during the pigging method and LD-LD method; this illustrates the validity of the experimental method to estimate the wax thickness. The pressure drop method and heat transfer method are similar in the results at the high-pressure drop and they are slightly different at the lower pressure drop at the same flow rate.

Table 11, shows that at the lower flow rate and temperature the wax thickness was the highest and as a result the pressure drop increased. Overall, the wax thickness at an inlet coolant temperature of 14 °C was about 1.83 mm which is higher than that of 24 and 33 °C, respectively, by carrying out the experiments with just crude oil at flow rate 2.7 L/min. This indicates that the inlet coolant temperature has the main effect on wax deposition process, and the four different methods to estimate the wax thickness shows agreement between them.

The uncertainty range of the results arise between (0.01 - 0.03mm) at different inlet coolant temperature (14, 24, 33, 1nd 40 °C). The standard deviation range is between (0.01 – 0.03mm). The results of wax thicknesses demonstrate a high degree of reproducibility of the test data for the four different measurement methods conducted under the same operating conditions.

Table 11: Estimating wax thickness ( $\delta_w$ ) using the different methods at flow rate 2.7 L/min.

Inlet Coolant Temperature	14°C	24°C	33°C	40°C
Pressure Drop(Pa)	1200	1000	900	600
Exp. Wax Volume(ml)	125	83	19	0
Wax Volume (ml) LD-LD	126	83	20	0
$\delta_w$ mm (Pigging Method)	1.82	1.5	0.7	0
$\delta_w$ mm (Pressure Drop)	1.83	1.61	0.69	0.04
$\delta_w$ mm (Heat Transfer)	1.83	1.3	0.71	0.06
$\delta_w$ mm (LD-LD)	1.84	1.5	0.73	0
Uncertainty mm	±0.01	±0.16	±0.02	±0.03
Standard Deviation (SD) mm	0.01	0.129	0.017	0.03

Table 12, illustrates that the effect of increasing the flow rate to 4.8 L/min was obvious on wax thickness due to increase the shear stress. Overall, the wax thickness at an inlet coolant temperature of 14 °C was the highest which is higher than that of 24 and 33 °C, respectively, by carrying out the experiments with just crude oil. The results of wax thicknesses demonstrate a high degree of reproducibility of the test data for the four different measurement methods conducted under the same operating conditions. The reproducibility degree of the four different measurement methods was in the high level under the same operating conditions due to the results uncertainty range is between (0.11 - 0.03mm) at different inlet coolant

temperature (14, 24, 33, and 40 °C); and the standard deviation range is between (0.122 – 0.03mm).

Table 12: Measuring wax thickness ( $\delta_w$ ) using different techniques at flow rate 4.8 L/min.

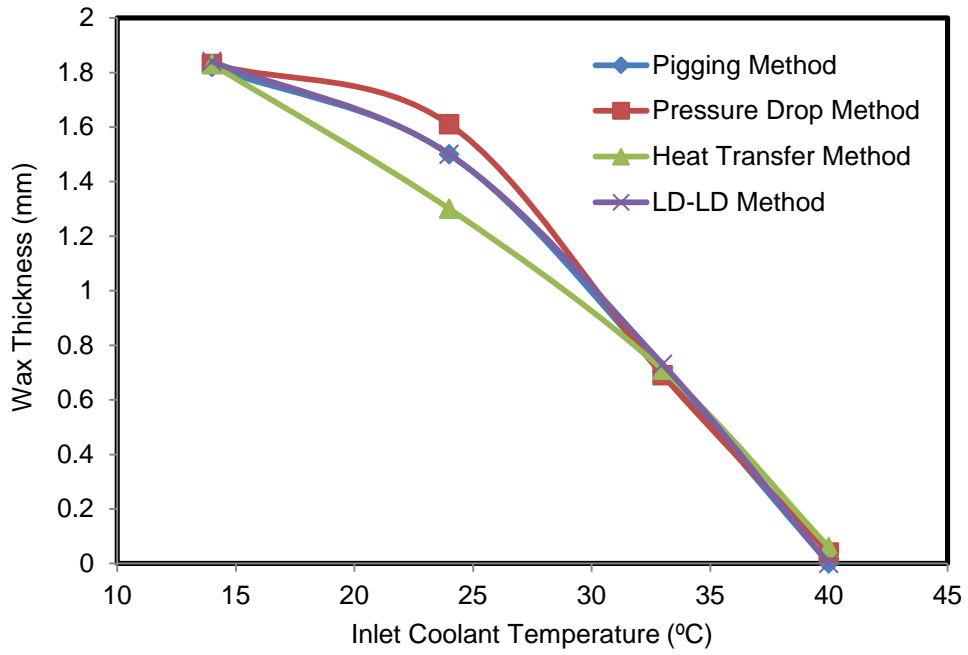
Inlet Coolant Temperature	14°C	24°C	33°C	40°C
Pressure Drop(Pa)	3000	2700	2100	1200
Exp. Wax Volume(ml)	85	70	15	0
Wax Volume (ml) LD-LD	87	70	17	0
$\delta_w$ mm (Pigging Method)	1.5	1.36	0.63	0
$\delta_w$ mm (Pressure Drop)	1.72	1.45	0.79	0.054
$\delta_w$ mm (Heat Transfer)	1.72	1.27	0.65	0
$\delta_w$ mm (LD-LD)	1.52	1.36	0.67	0
Uncertainty mm	±0.11	±0.09	±0.08	±0.03
Standard Deviation (SD) mm	0.122	0.073	0.072	0.03

### 5.2.5 Effect of Inlet Coolant Temperature

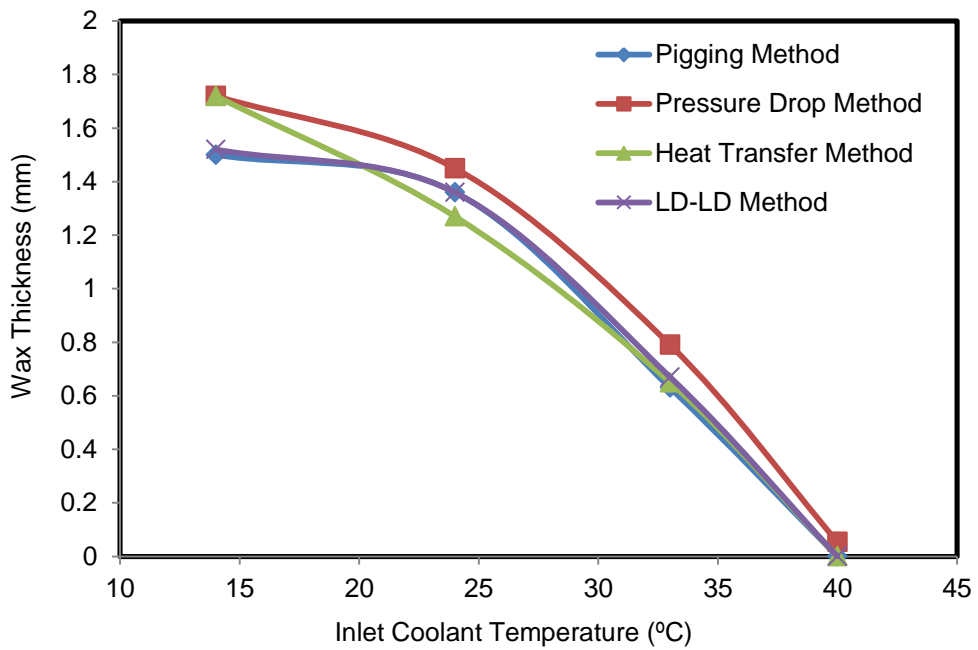
In this study, it was observed that the inlet coolant temperature affects the wax deposition inside the pipe. Whilst running the experiments, it was noted that the deposit thickness increased with decreasing the inlet coolant temperature, even when the crude oil temperature was above wax appearance temperature due to heat transfer taking place at the pipe wall. The crude oil temperature started to gradient toward the pipe wall until it reached the wax appearance temperature, forming a solid crystal able to deposit on the pipe wall.

Therefore, wax deposition depends on the inlet coolant temperature more than on the crude oil temperature gradient. Wax thickness increased to 1.83 mm at the end of the experiment when the inlet coolant temperature was equal to 14°C.

The wax thickness decreased when the inlet coolant temperature increased by 24, 33 and 40°C respectively and stopped to precipitate when the inlet coolant temperature as obvious as 39°C is WAT, as shown in figure 40, because increasing the inlet coolant temperature leads to increasing the wax crystal solubility, therefore the wax deposit reduced.



(a)



(b)

Figure 40: The effect of inlet coolant temperature on wax thickness at different flow rates, (a) 2.7 L/min, (b) 4.8 L/min, and different techniques.

### 5.2.6 Effect of Wax Deposition Recirculation Time

The wax deposit principle increases as time progresses, while there are radial thermal and mass transfer gradients as a result of heat losses to the surroundings (Al-Yaari, 2011).



The influence of the experimental time on wax deposit volume can be illustrated as a number of wax molecules increased by increasing the experimental time, which becomes approximately constant before the experimental time gradually reaches higher values. The wax deposition volume starts to be constant or drops at a longer time due to the wax deposit layer inside the pipe working as a thermal insulation between the crude oil temperature and the surrounding temperature; therefore, the heat exchange will reduce, leading to increasing the crude oil temperature and melting some of the wax molecules, then leading to a reduction in the deposited wax.

At the same flow rate, by increasing the experimental time most of the wax crystals are deposited at the first two hours of run the experiment after that the wax deposited rate increased slowly at 4 and 6 hours of run the experiment due to reduce the wax content in the crude oil and therefore the wax deposit volume reduced as shown in figure 41.

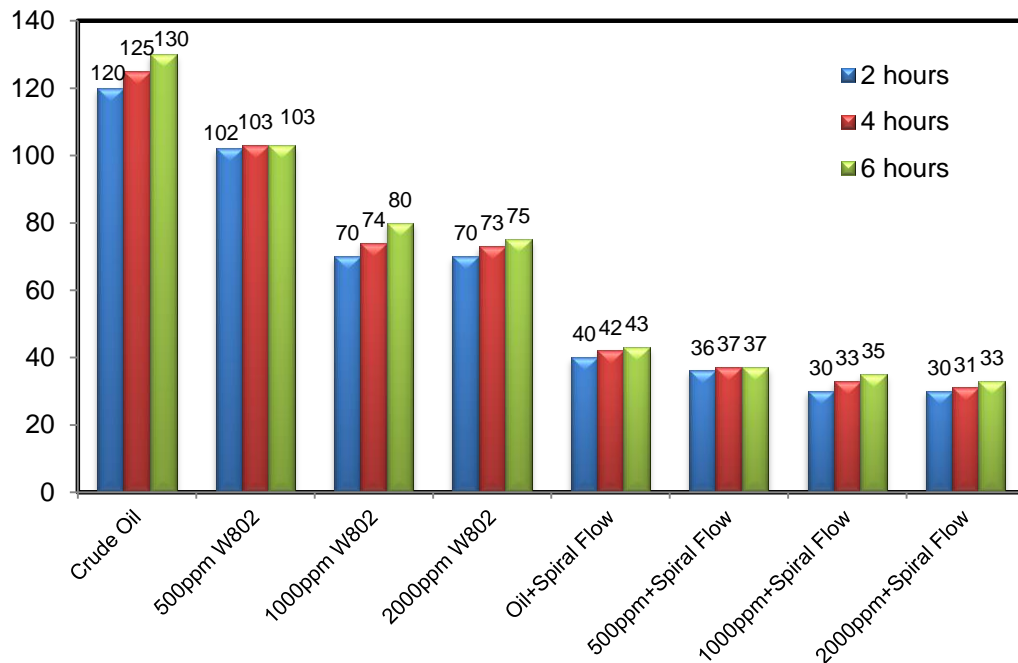


Figure 41: The effect of the experimental time on wax deposited volume at flow rate 2.7 L/min and an inlet coolant temperature of 14°C.

### 5.2.7 Effect of Flow Rate on Wax Deposit Volume

The effect of the flow rate on wax deposited is most evident in the colder tube sections. As the flow rate increases, there is a definite increase in the higher carbon number components and melting point. At the higher flow rates, the lower and softer molecular weight components are removed, leaving the higher molecular weight compounds deposited on the pipe surface. Thus, wax deposition gradually decreases with an increase in flow

rate and turbulence. The same effect of the flow rate on wax deposition was illustrated in a study by Hsu et al. (1994).

The influence of the flow rates 1, 2.7 and 4.8 L/min on wax volume was examined at an inlet coolant temperature of 14°C and experimental time of 2 hours for each flow. The reduction in wax volume was obvious from the increasing flow rate, as shown in figure 42. At a flow rate 1 L/min using crude oil only, the wax volume was 197 ml, reduced to 120 ml at flow rate 2.7 L/min, then wax volume reduced to 85 ml by increasing the flow rate to 4.8 L/min.

It was noticed during this study that the wax deposits at a higher flow rate are harder and more compact. The effect of increasing flow rate decreases the amount of wax deposited or the oil entrapped between the wax molecules in the layer of the deposit. This can be explained by the fact that increasing the fluid velocity leads to increasing the viscous drag force that tends to remove the accumulation as it exceeds the shear stress within the deposited wax (Zhu et al., 2008). Low flow rates affect the wax deposit mainly because of the longer residence time of the oil in the tubing.

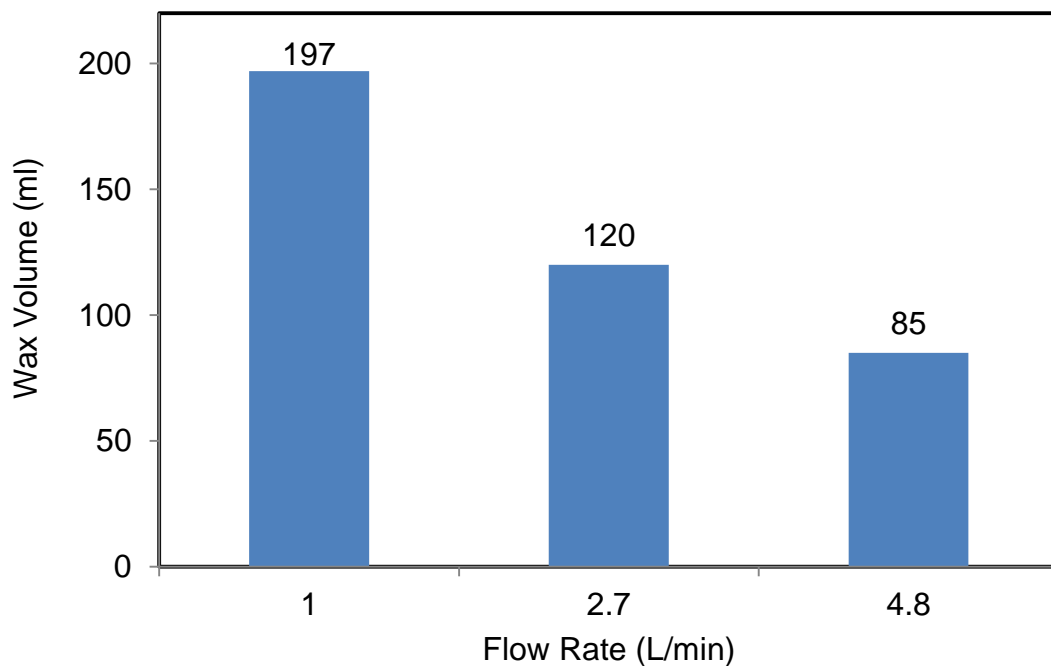


Figure 42: The effect of flow rate on wax deposition volume at inlet coolant temperature 14°C.

### 5.2.8 Effect of Inhibitor Poly Acrylate Polymer on Wax Deposition

The performance of some of the wax inhibitors was evaluated at a concentration of 1000ppm to determine their effect on the wax deposition using the Bohlin Gemini II Rheometer. The effect of the inhibitor was noticed on the wax appearance temperature and the viscosity of the crude oil.

Analysis of the crude oil with the inhibitors shows that the inhibitor W802 poly acrylate polymer (C16-C22) produced the greatest reduction in viscosity, which means a reduction in the wax appearance temperature.

Figure 43 shows that the inhibitor reduced the estimated wax thickness at a flow rate of 2.7 L/min and inlet coolant temperature of 14°C from 1.86mm to 1.42mm; this is considered a significant reduction at this low temperature. It also reduced the estimated wax thickness from 1.63 mm to 1.3 mm at a flow rate of 4.8 L/min and inlet coolant temperature of 14°C.

The inhibitors used in the current work are based on polymers that are normally used as a pour point depressant. The reduction in the pour point and the crude oil viscosity makes transportation of the crude oil easier (Pedersen and Ronningsen, 2003; Adeyanju and Oyekunle, 2014) because the reduction in the crude oil viscosity leads to an increase in the shear rate and shear stress according to the proportional equation of shear stress.

It has been proposed that the inhibitor reduces the wax deposition process by interfering with the wax crystallisation and growth process. However, this interfering mechanism has not yet been fully understood (Jennings and Newberry, 2008). The effect of the inhibitor on wax structures has been examined using Scanning Electron Microscopy (SEM); the changes in wax structure are obvious, as shown in figure 44.

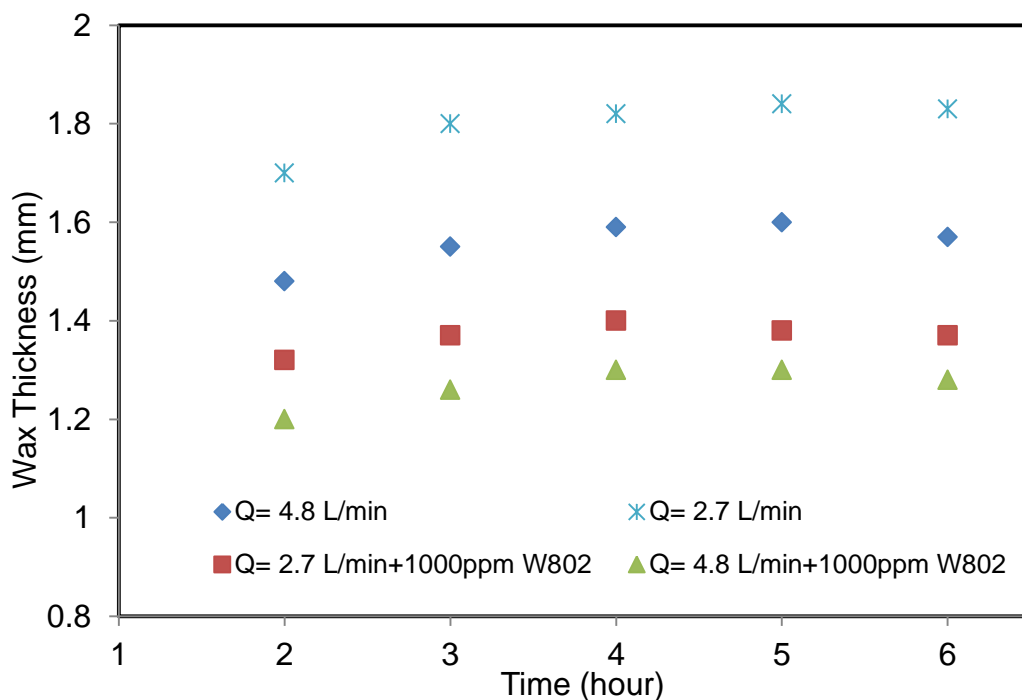


Figure 43: The effect of inhibitor W802 on wax thickness at 2.7 and 4.8 L/min, at inlet temperature 14°C.

The change in the surface of the wax deposit can be illustrated by the fact that the inhibitor contains a similar structure to the wax structure; therefore it allows the inhibitor crystal to be incorporated into the wax crystal growth. Sometimes the structural part of the polymer covers the wax site, thereby preventing further wax crystal growth and promoting the formation of smaller wax aggregates (Jennings and Newberry, 2008; Adeyanju and Oyekunle, 2014).

The structure of wax without inhibitor is different from the structure of wax with inhibitors. Where, without inhibitor the wax structure consists of long chains of normal and non-normal paraffin that connected and trapped oil between them creating the shape appear in figure 43 (a). While, with inhibitor the structure of wax is different and appear softer because of the inhibitor structure is similar to the wax structure and works to inter, between the paraffin chains and prevent it to connect between them to create the complicated wax structure.

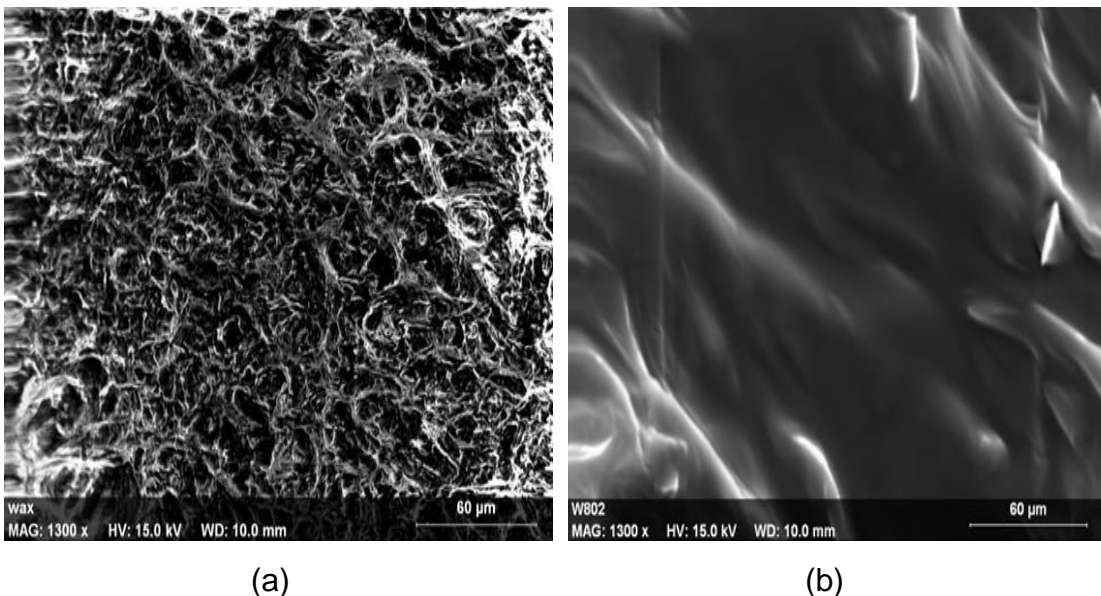


Figure 44: SEM micrographs showing the structure of wax before (a) and after (b) adding the inhibitor W802.

Experimentally, the effects of the inhibitor are clear from the wax deposit inside the pipe, as shown in figure 45(a) without the inhibitor and (b) with the inhibitor.

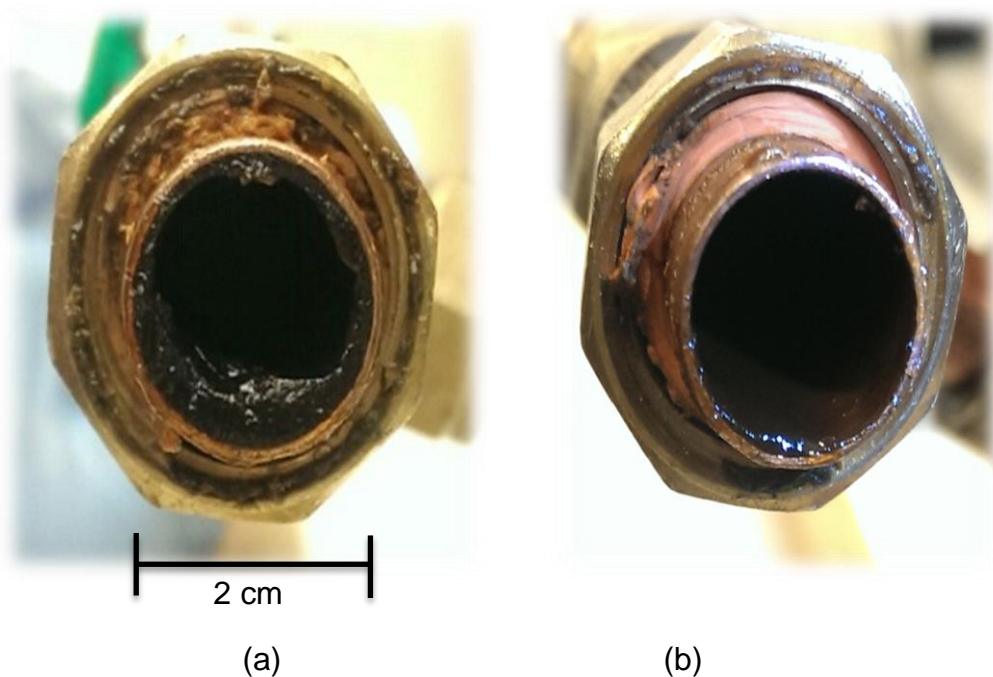


Figure 45: Wax deposition inside the pipe (a) without inhibitor and (b) with W802 inhibitor.

### 5.2.9 Effect of Spiral Flow on Wax Deposition

In this study, spiral flow was used to mitigate wax deposition inside the pipe. The concept of the spiral flow in this study comes from seeing the water flow through a bathroom cham sink, where it moves like a helical with a high velocity. This kind of flow is created by inserting a thin twisted aluminum plate inside the test section of the pipe, equal to the pipe length.

In this work, the spiral flow was created and examined in the rig, where the experiments were carried out at different flow rates, different coolant temperatures, and different times. Whilst carrying out the experiments it was noticed that the pressure drop along the pipe was increased due to the twisted plate inside the pipe. In this situation, the shear stress is high due to the increasing flow velocity, and the force of the shear stress (lift force) will be higher than the force of wax deposition (diffusion force), which prevents wax crystal growth, as shown in figure 46.

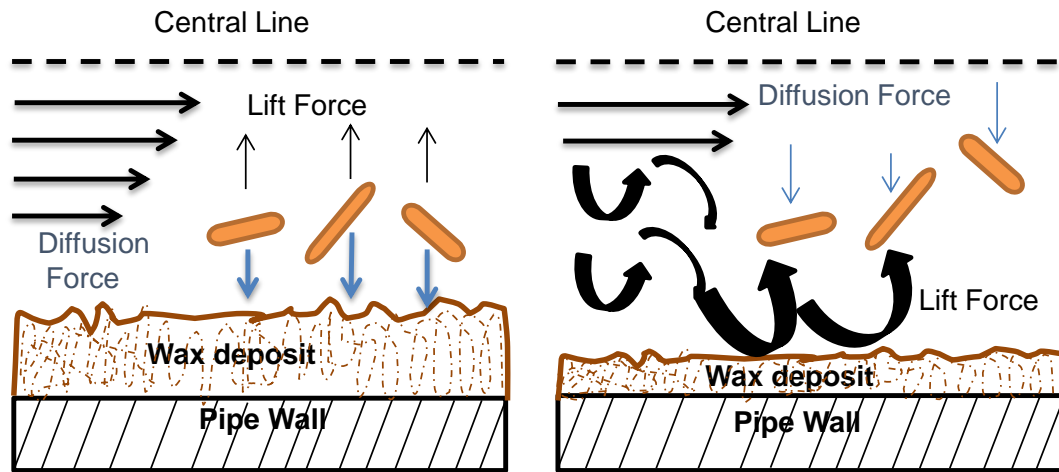


Figure 46: Mechanisms of wax deposition inside the pipes for this study, with laminar flow (left: modified from Siljuberg, 2012) and spiral flow (right: in this study).

On the other hand, it was noticed that the temperature drop of the crude oil along the test pipe was double compared with the temperature drop of the crude oil without a twisted plate. This drop in temperature occurred due to increasing the path of the crude oil flow, causing it to lose heat to the surrounding area. Despite increasing both the pressure drop and the temperature drop, the volume of the wax deposit inside the pipe was less when comparing the wax volumes of the experiments with the laminar flow because the spiral flow increased the shear stress inside the pipe.

The spiral flow reduces the wax deposition in the pipe, reducing the wax thickness from 1.86 to 1.07 mm at an inlet coolant temperature of 14°C, flow rate 2.7 L/min and 6 hour time of the experiment. The reduction in wax thickness at inlet coolant temperature 14°C, flow rate 4.8 L/min and the same experiment period was from 1.63 to 0.85mm, as shown in figure 47. This indicates that the effect of the spiral flow increased by increasing the shear rate.

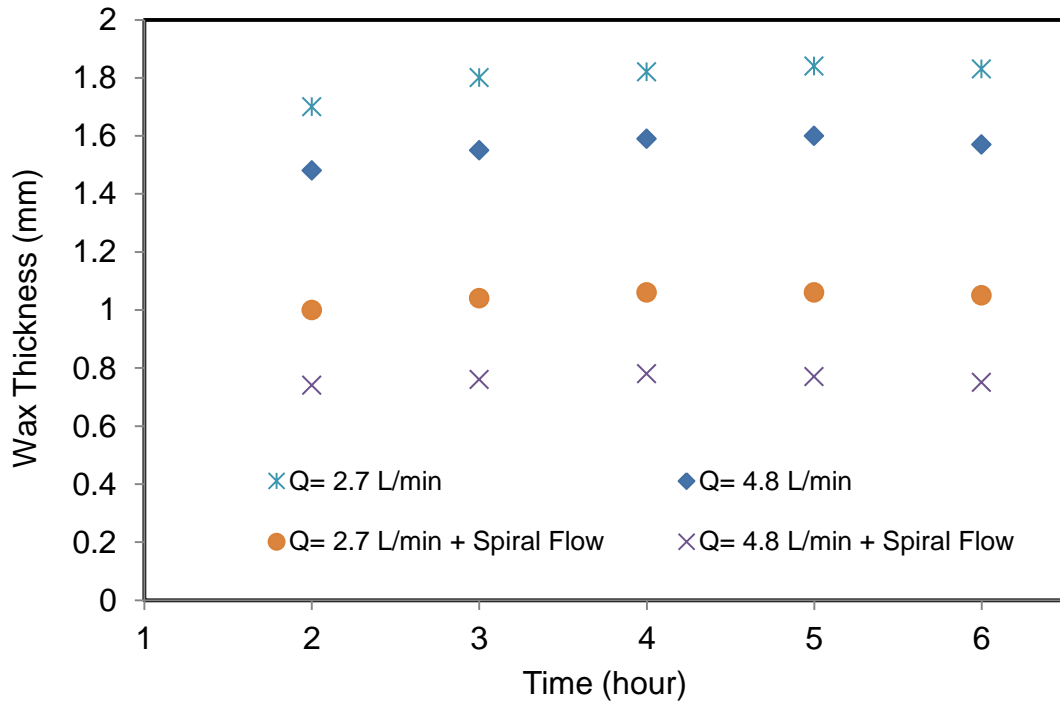


Figure 47: The effects of spiral flow on wax thickness at an inlet coolant temperature of 14°C.

### 5.2.10 Effect of Spiral Flow on Wax Deposition at Different Inlet Coolant Temperatures

The wax deposition thickness was measured by using the effect of the spiral flow at different inlet coolant temperatures 14, 24 and 33°C, different flow rates 2.7 and 4.8 L/min and different experimental times 2, 4 and 6 hours. The results were compared with the spiral flow effects in the same operational conditions.

Overall, the wax thickness at an inlet coolant temperature of 14°C was higher than that of 24 and 33°C, by carrying out the experiments with crude oil only at a flow rate of 2.7 L/min. This indicates that the inlet coolant temperature has the major effect on the wax deposition process. The lowest wax thickness was at an inlet coolant temperature of 33°C, as shown in figure 48.

The influence of the spiral flow was obvious in the wax deposit thickness, where it reduced the wax thickness from around 1.8 mm to around 1 mm at an inlet coolant temperature of 14°C. The reduction of wax deposition using the spiral flow was more important by increasing the effect of inlet coolant temperature, where it was reduced to around 0.8 and 0.4 mm at 24 and 33°C respectively. This can be explained by the fact that at the lower inlet coolant temperature the wax deposition layer will be harder than the layer of the deposited wax at the higher inlet coolant temperature, due to increasing the crude oil temperature and the pipe wall temperature that leads to dissolving

the wax crystals; therefore, the force of the spiral flow will be more impacted to remove the wax deposit and the wax thickness will reduce clearly.

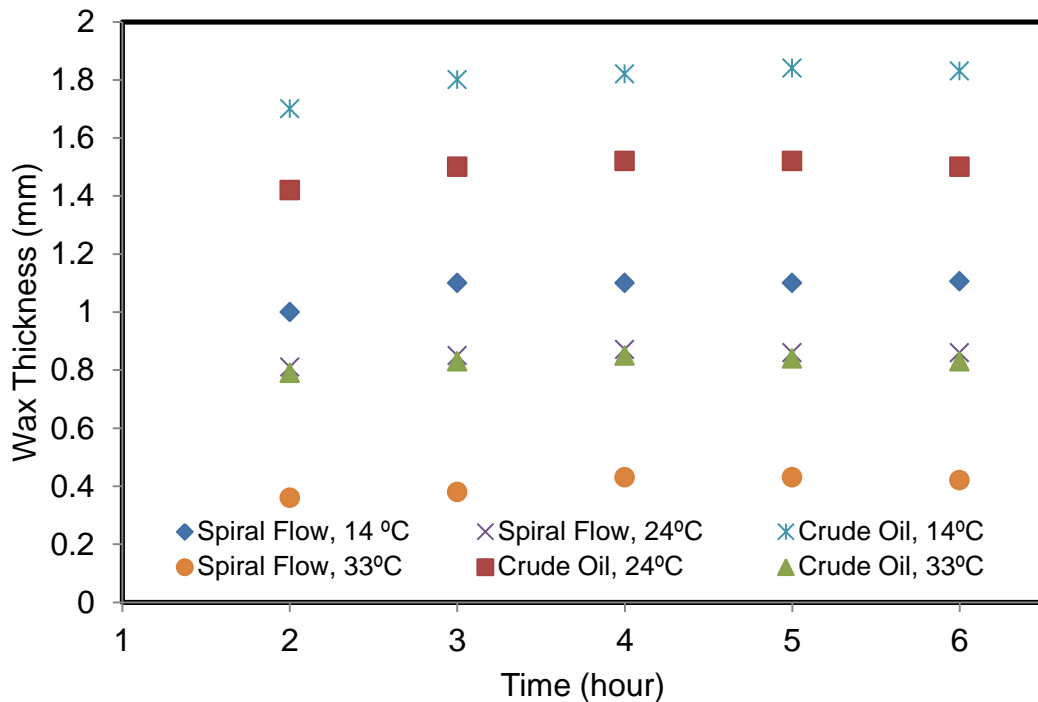


Figure 48: The effect of the spiral flow on wax thickness at different inlet coolant temperatures at flow rate 2.7 L/min.

### 5.2.11 Effect of Spiral Flow on Crude Oil Temperature

In the case of experiments carried out in the laminar flow type, the inlet crude oil temperature was about 44.5°C and due to the heat exchange between the crude oil and the cooling water through the pipe wall; the outlet crude oil temperature was around 42°C. In the case of carrying out the experiment using the spiral flow method, the difference between the inlet and outlet oil temperatures, was about 4°C, as shown in figure 49.

The difference between the inlet and outlet temperatures of the crude oil is due to the fact that the spiral flow makes the path way of the crude oil inside the pipe longer and this will increase the chance of heat exchange between the crude oil and the cooling water, causing the reduction in the outlet temperature of the crude oil. Also, the aluminium twisted material inside the pipe, which was creating the spiral flow, changes the crude oil flow from the central line of the pipe towards the pipe wall, so this flow will increase the touch surface area and lead to a loss of temperature to the surrounding area.

In the case of using spiral flow, the outlet oil temperature was less than the wax appearance temperature and this provided an indication that the wax deposit should be more due to the temperature drop; but in the real case, the wax deposit volume was less due to the effect of the high shear rate formed by the spiral flow.



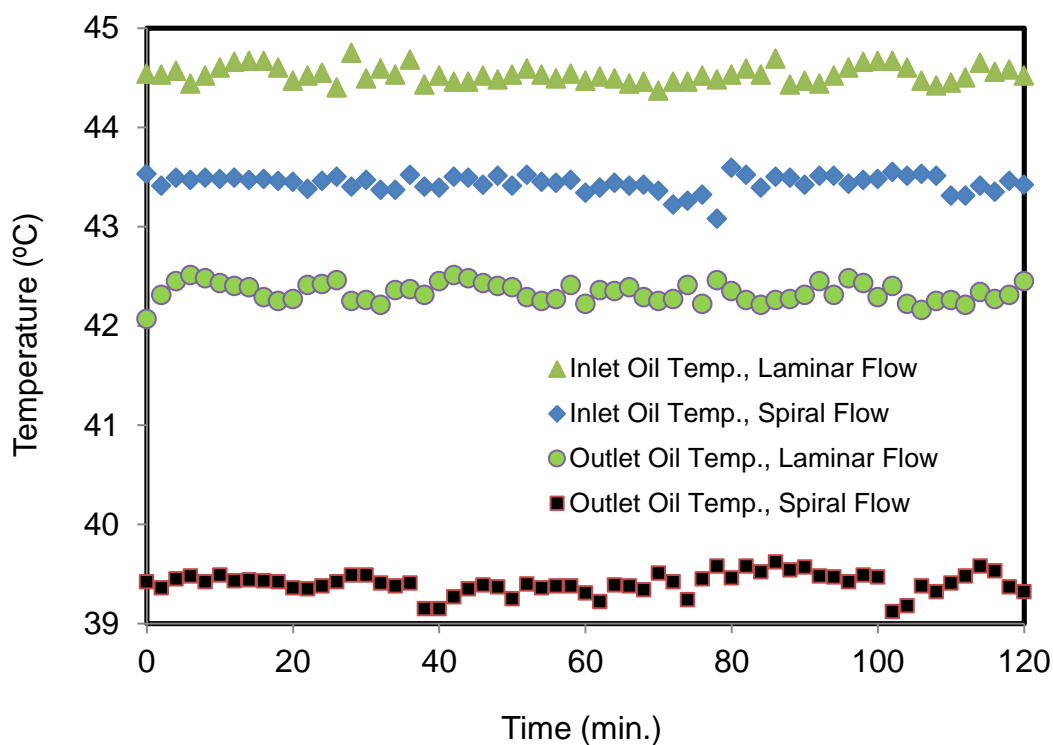


Figure 49: The impact of the spiral flow on the crude oil temperature.

### 5.2.12 Comparison of the Best Mitigation Methods

The best mitigation methods used during this study were the inhibitor W802 polyacrylate polymer (C16-C22) at a concentration of 1000ppm, spiral flow, and bending the effect of spiral flow with the inhibitor W802 at 1000ppm. The effect of these methods on wax deposition was obvious, as shown in figure 50, where at an inlet coolant temperature of 14°C, flow rate 2.7 L/min and experiment time 6 of hours, the wax thickness decreased from 1.86 mm to 1.42 mm by using the inhibitor W802, while the spiral flow at the same condition reduced the wax thickness from 1.86 mm to 1.07 mm. The effect of bending the spiral flow with the inhibitor W802 presented better results than the previous two methods, reducing the wax thickness from 1.86 to 0.9 mm due to bending the effect of increasing the shear rate and the effect of the inhibitor by entering between the wax structures.

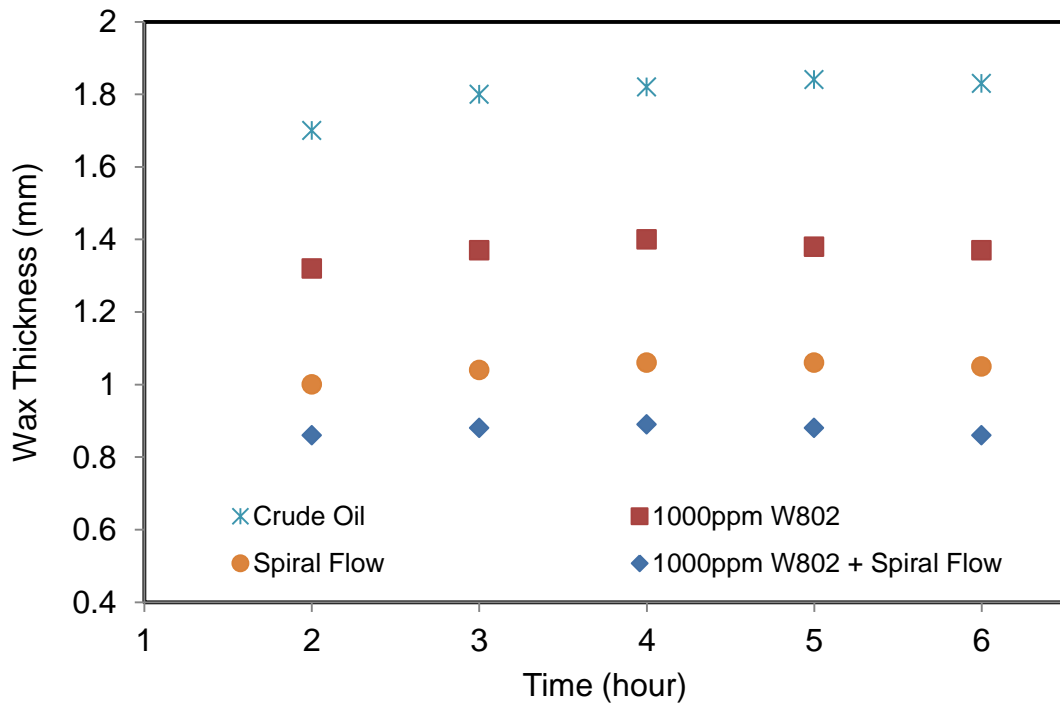


Figure 50: The effects of the inhibitor W802, spiral flow, and bending the spiral flow with the inhibitor on wax thickness at the same experimental conditions.

### 5.2.13 Analysis of Spiral Flow Mechanism

This section describes mathematically the effect of shear stress, due to the spiral flow, on wax deposition on the hydrocarbon pipe wall. It shows the forces that influence on the crude oil flow in the pipe with and without inserting the twisted plate depending to the pressure drop along the pipe.

- **Fluid Flow in a Pipe**

The concept of the spiral flow mechanism in this research is based on an elemental fluid flowing in the pipe. The initial conditions for the elemental fluid are taken in the way that; the high-pressure value is taken from the injection side and goes uniformly decreasing throughout the pipe. Shearing action is integrated from the elemental radius up to maximum flow channel radius. The forces acting in the system are quantitatively described below (Crawford, 2005; Gebrehiwot, 2014).

The driving force due to pressure ( $\text{Force} = \text{Pressure} \times \text{Area}$ ) can describe as shown in figure 51.

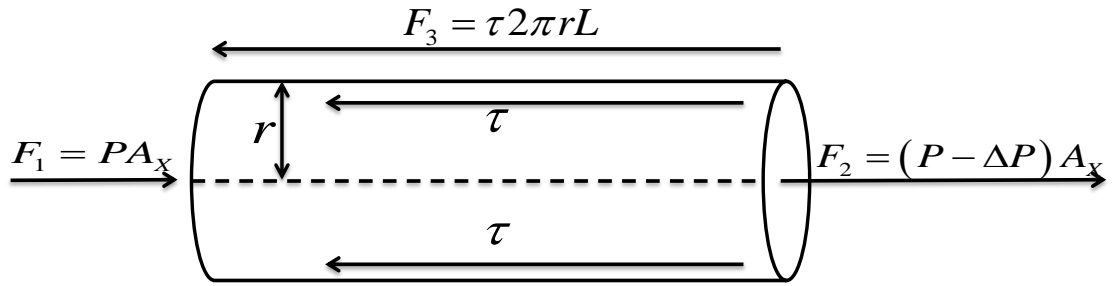


Figure 51: Forces affects on the element of fluid flow in a pipe.

Where:

Inlet force = Inlet pressure x cross-section area of the pipe ( $F_1 = PA_x$ ).

Outlet force = outlet pressure x cross-section area of the pipe ( $F_2 = (P - \Delta P) A_x$ ), Where,  $P$  is the inlet pressure (Pa),  $\Delta P$  is the pressure drop along the pipe (Pa), and  $A_x$  is the cross-section area of the pipe ( $m^2$ ).

Shear stress force = shear stress x surface area of the pipe ( $F_3 = \tau 2\pi rL$ ).

Where,  $\tau$  is the shear stress (Pa),  $r$  is the radius of the pipe (0.00675 m), and  $L$  is the length of the pipe (1.5 m).

The driving force due to pressure equals to:

$$F_3 = F_1 - F_2$$

$\tau 2\pi rL = P\pi r^2 - (P - \Delta P)\pi r^2$ , simplify the equation results to  $\tau 2\pi rL = \Delta P\pi r^2$ , then shear stress equals to:

$$\tau = \frac{\Delta P r}{2L}$$

(5.1)

For example, at flow rate 2.7 L/min and pressure drop 1200 Pa, the shear stress calculated from equation (1) results:

$$\tau = \frac{(1200 \times 0.00675)}{(2 \times 1.5)} = 2.7 Pa, \text{ and by increasing the flow rate to 4.8 L/min.},$$

shear stress at pressure drop 3000 Pa results using equation (1) to:  $\tau = 6.75 Pa$

Equation (1) represents the shear stress inside the pipe without the twisted plate.

The velocity of the fluid inside the pipe can be calculated from divide the volumetric flow rate to the cross-section area of the pipe  $Q = uA$

$$u = Q / \pi r^2 \tag{5.2}$$

Where,  $Q$  is the volumetric flow rate of the fluid ( $m^3$ ),  $u$  is the fluid velocity ( $m/s$ ).

For example to calculate the fluid velocity in the pipe at flow rate 2.7 L/min ( $4.5 \times 10^{-5} m^3 / s$ ) using equation (2) results:

$$u = 4.5 \times 10^{-5} / \pi(0.00675)^2 = 0.31 m / s$$

By increasing the flow rate to 4.8 L/min ( $8 \times 10^{-5} m^3 / s$ ), leads to  $u = 8 \times 10^{-5} / \pi(0.00675)^2 = 0.56 m / s$ . The increase in the velocity means an increase in the shear stress that reduces wax deposit on the pipe wall.

- **Fluid Flow through Spiral**

In order to develop an equation for the pipe wall shear stress plus the shear stress of the twisted plate inside the pipe, the following steps will illustrate that, see figure 52.

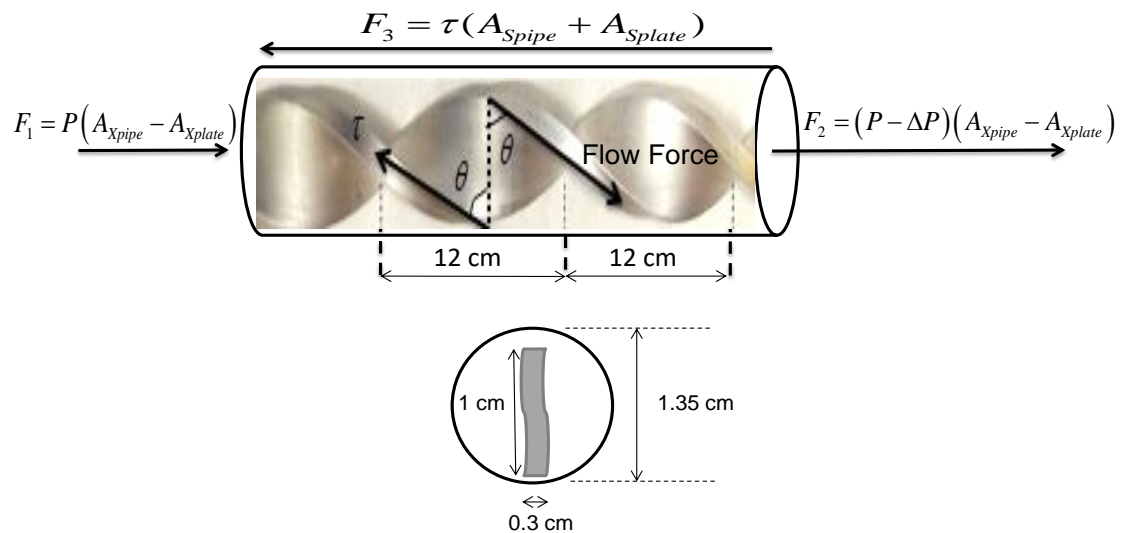


Figure 52: Forces affects on the element of fluid in a pipe with the effect of spiral flow.

Inlet force = inlet pressure x (cross-section area of the pipe - cross section area of the twisted plate).

$$F_1 = P(A_{xpipe} - A_{xplate})$$

Where,  $A_{xpipe}$  is the cross-section area of the pipe ( $m^2$ ), and  $A_{xplate}$  is the cross section area of the twisted plate ( $m^2$ ).

$$F_1 = P(\pi r^2 - 3 \times 10^{-5})$$

Outlet force = outlet pressure x (cross-section area of the pipe - cross section area of the twisted plate).

$$F_2 = (P - \Delta P)(A_{xpipe} - A_{xplate})$$

$$F_2 = (P - \Delta P)(\pi r^2 - 3 \times 10^{-5})$$

$$F_2 = P\pi r^2 - 3 \times 10^{-5} P - \Delta P\pi r^2 + 3 \times 10^{-5} \Delta P$$

Shear stress force = shear stress x (surface area of the pipe + surface area of the twisted plate inside the pipe).

In order to calculate the shear stress force, it should be taken into account the shear stress of the pipe plus the shear stress results from the twisted plate inside the pipe.

The twisted plate divided to 12.5 sections, each section equals to 12 cm and height 1 cm. Therefore, to calculate the total shear stress results from the twisted plate, it should be calculated the shear stress results from each section multiplied by 12.5.

The surface area of each section of the twisted plate equals  $3.12 \times 10^{-3} m^2$ , and the angle of each section of the twisted plate estimates to be about  $80.5^\circ$ .

$$F_3 = \tau 2\pi rL + \tau(12.5 \times \cos \theta \times 3.12 \times 10^{-3})$$

$$F_3 = \tau 2\pi rL + \tau(12.5 \times \cos 80.5 \times 3.12 \times 10^{-3})$$

$$F_3 = \tau 2\pi rL + 0.00644\tau$$

$$F_3 = \tau(2\pi rL + 0.00644)$$

In the case of the spiral flow, the driving force due to pressure equals to:

$$F_3 = F_1 - F_2$$

$$\tau(2\pi rL + 0.00644) = P(\pi r^2 - 3 \times 10^{-5}) - (P\pi r^2 - 3 \times 10^{-5} P - \Delta P\pi r^2 + 3 \times 10^{-5} \Delta P)$$

Simplify the equation,

$$\tau(2\pi rL + 0.00644) = P\pi r^2 - 3 \times 10^{-5} P - P\pi r^2 + 3 \times 10^{-5} P + \Delta P\pi r^2 - 3 \times 10^{-5} \Delta P$$

$$\tau(2\pi rL + 0.00644) = \Delta P\pi r^2 - 3 \times 10^{-5} \Delta P$$

$$\tau(2\pi rL + 0.00644) = \Delta P(\pi r^2 - 3 \times 10^{-5})$$

So, the total shear stress results from the pipe and the twisted plate can be calculated from the following equation:

$$\tau = \frac{\Delta P(\pi r^2 - 3 \times 10^{-5})}{(2\pi rL + 0.00644)} \quad (5.3)$$

The velocity of the fluid flow is increased by inserting a twisted plate inside the pipe, due to reducing the cross-section area of the pipe with the constant flow rate. In this case, the velocity can be calculated by dividing the

volumetric flow rate to the (cross-section area of the pipe minus the cross section area of the twisted plate).

For example, at flow rate 2.7 L/min and pressure drop 4000 Pa, the shear stress calculated from equation (3) results:

$$\tau = \frac{4000(\pi(0.00675)^2 - 3 \times 10^{-5})}{(2\pi \times 0.00675 \times 1.5 + 0.00644)} = 6.46 Pa , \text{ and by increasing the}$$

flow rate to 4.8 L/min., the shear stress at 8000Pa results using equation (3) to:  $\tau = 12.93 Pa$ .

$$u = \frac{Q}{(\pi r^2 - 3 \times 10^{-5})} \tag{5.4}$$

For example to calculate the fluid velocity at flow rate 2.7 L/min using equation (4) in the case of using the twisted plate inside the pipe leads to:

$$u = \frac{4.5 \times 10^{-5}}{(\pi(0.00675)^2 - 3 \times 10^{-5})} = 0.4 m / s , \text{ and at flow rate 4.8 L/min. using the}$$

same equation leads to  $u = 0.71 m / s$ .

From the above, it can be concluded that the twisted plate changed the fluid flow type from laminar or turbulent to spiral flow depending on the velocity and the angle of the fluid flow. This angle is analysed the angular flow to two forces one vertical to the wax deposit and the second force horizontal, those forces work together to reduce wax deposition on the pipe.

Tables 13, 14 and 15 shows the data of shear stress at the different wax thickness, different pressure drop, and different inlet coolant temperatures.

At the same inlet coolant temperature, it can be seen that increasing the shear stress, due to the effect of the spiral flow, leads to decrease the wax deposit thickness with increasing the pressure drop. On another hand, increasing the inlet coolant temperature leads to decrease the shear stress and wax thickness because of decreasing the value of the crude oil viscosity, see table 13.

Table 13: Estimated shear stress and wax thickness at different pressure drops and different inlet coolant temperature at flow rate 2.7 L/min with and without the spiral flow.

Type of Flow	Temperature °C	Pressure Drop (Pa)	Shear Stress (Pa) at 2.7 L/min.	Wax Thickness (mm)
not spiral	14	1200	2.7	1.82
spiral		4000	6.46	1.03
not spiral	24	1000	2.25	1.5
spiral		3400	5.5	0.85
not spiral	33	900	2.03	0.7
spiral		2500	4.04	0.36
not spiral	40	600	1.35	0
spiral		1700	2.75	0

Increasing the flow rate from 2.7 to 4.8 L/min, leads to increasing the shear stress and pressure at the same inlet coolant temperature drop due to reducing the cross-sectional area of the pipe that affects to increase the crude oil velocity. This high velocity minimises the wax deposit on the pipe wall due to converting the laminar or turbulent flow to the spiral flow (angular flow). The high temperatures of the pipe wall lead to low shear rates and low wax thickness because of increasing the solubility of wax in the crude oil, that works to reduce the crude oil viscosity, see table 14.

Table 14: Estimated shear stress and wax thickness at different pressure drops and different inlet coolant temperature at flow rate 4.8 L/min with and without the spiral flow.

Type of Flow	Temperature °C	Pressure Drop (Pa)	Shear Stress (Pa) at 4.8 L/min.	Wax Thickness (mm)
not spiral	14	3000	6.75	1.5
spiral		8000	12.93	0.78
not spiral	24	2700	6.08	1.36
spiral		7000	11.31	0.61
not spiral	33	2100	4.73	0.63
spiral		6100	9.86	0.39
not spiral	40	1200	2.7	0
spiral		4500	7.3	0

If we assumed, that the flow rate increased to 6 L/min and by following the same procedure above it can be estimate the shear stress produced at different inlet coolant temperature and with and without spiral flow as shown in table 15.

Table 15: Estimated shear stress and wax thickness at different pressure drops and different inlet coolant temperature at flow rate 6 L/min with and without the spiral flow.

Type of Flow	Temperature °C	Pressure Drop (Pa)	Shear Stress (Pa) at 6 L/min.	Wax Thickness (mm)
not spiral	14	4000	9	1
spiral		10000	16.15	0.6
not spiral	24	3000	6.75	0.8
spiral		8000	12.92	0.5
not spiral	33	2500	5.63	0.4
spiral		7000	11.3	0.3
not spiral	40	1500	3.38	0
spiral		5000	8.1	0

Figure 53, shows the effect of increasing the shear stress on wax deposit thickness, where at the same flow rate 2.7 L/min it can be seen that increasing the shear stress leads to reduce wax deposit thickness from 1.8 to 1 mm at inlet coolant temperature 14 °C. Increasing the flow rate to 4.8 L/min leads to increase the shear stress that works to reduce wax deposit thickness from 1.5 to 0.78 mm at the same temperature. While increasing the flow rate to 6 L/min results in increasing the shear stress that reduced the wax thickness from 1 to 0.6mm.

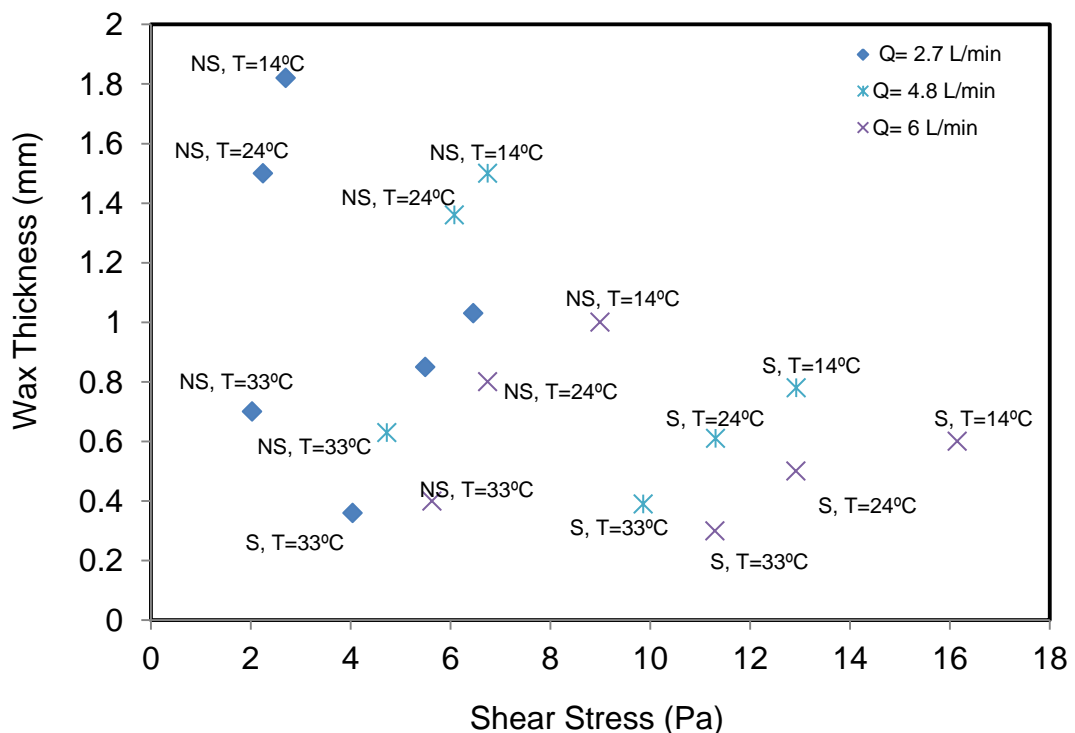


Figure 53: The effect of shear stress with spiral flow (S) and non-spiral flow (NS) on wax deposit thickness at different pressures and different inlet coolant temperatures.



### 5.3 Comparison between Real Field Data and Laboratory Data

The real field data is a research conducted in the real world or a natural setting. It tends to observe, analyse, and describe what exists rather than manipulating a factor under study. The research settings resemble the situations encountered in daily living, preserving the naturalness of the setting. On the other hand, controlled laboratory research is a research conducted in a setting specifically designed for research. Laboratory research is often described as a tightly controlled investigation in which the researcher manipulates the particular factor under study to determine if such manipulation generates a change in the subjects.

The real field data of Ekofisk-Teesside pipeline was used during this research to compare it with the experimental rig data of this study. Ekofisk-Teesside pipeline is used to transport crude oil from the greater Ekofisk area (and for third parties operating) in the Norwegian sector of the North Sea to Phillips' refinery at Teesside in UK (Hamouda and Ravneøy, 1992).

The different properties used during this comparison include pipeline length, diameter, flow rate, ambient temperature, wax appearance temperature, pipeline material and as a result show the wax volume deposited in the real pipeline and the experimental pipe, as shown in table 16.

Table 16: Comparison between the real field data of Ekofisk-Teesside pipeline and the data of the experimental rig pipeline of this study.

Properties	Ekofisk-Teesside Pipeline (Hamouda and Ravneøy, 1992)	Experimental Rig Pipeline
Length	354000 m	1.5 m
Diameter	0.84 m	0.0135 m
Flow Rate	47033 L/min	4.8 L/min
Wax Appearance Temperature	20°C	30°C
Ambient Temperature	6°C	4°C
Wax Deposit Volume	330 m <sup>3</sup> (330000000 ml) for three months	85 ml for two hours
Pipeline Material	Carbon Steel (thermal conductivity: 54 W/m.k)	Copper (thermal conductivity: 401 W/m.k)

The following steps show an illustration of the validity of the experimental rig comparing with the real field data.

The experimental wax deposit volume after two hours of carry out the experiment equals to 85 ml at flow rate 4.8 L/min. To calculate the wax deposited volume in the real pipeline, at first, should find the ratio between

the real oil field flow rate to the experimental flow rate then multiply this ratio by the experimental volume of wax.

Ekofisk-Teesside pipeline flow rate / experimental flow rate = (47033 L/min) / (4.8 L/min) = 9798.5

Therefore, the expected volume of wax deposited in the Ekofisk-Teesside pipeline at the same experimental conditions = 9798.5 x 85 ml = 832872.5 ml

The real wax deposit volume after three months equals to 330 m<sup>3</sup> (330000000 ml)/90 days = 3666666.67 ml/day.

3666666.67 day/24 hours= 152777.8 ml/hour

The real wax volume for two hours equals to 152777.8 x 2 = 305555.6 ml.

It can be seen that for two hours, the expected volume of wax deposited in the Ekofisk-Teesside pipeline is 832872.5 ml and the real wax volume of Ekofisk-Teesside pipeline is 305555.6 ml.

The difference between the two values 832872.5 ml - 305555.6 ml = 527316.9 ml

This difference in wax deposit volume can be illustrated as, the material of Ekofisk-Teesside pipeline is carbon steel and the thermal conductivity of this material equals to 54 W/k.m, while the material of the experimental pipeline is copper and the thermal conductivity of this material is 401 W/k.m.

The high thermal conductivity of copper pipe facilitates heat transfer between the crude oil and the environment leading to loss of heat to the surrounding and forms more wax crystals that precipitate on the pipe wall. While the low thermal conductivity of carbon steel pipeline leads to low heat transfer between the crude oil and the ambient temperature, therefore, the wax deposit volume will be less.

Also, the ambient temperature of the experiment (4°C) is lower than the ambient temperature (6°C) of the real field and this will lead to more wax deposit. On the other hand, the wax appearance temperature of the experimental crude oil is 30°C, while in the real field it is 20°C. This indicates that the types of the crude oil of the real field and the experimental are different, therefore, there was a difference in the wax deposit volumes between the real and the experimental data.

#### **5.4 Economical Evaluation of Research**

The notion behind this research project is to present a convenient, attainable and cost-effective process for mitigating the wax deposition in the test section of the small flow loop system in the lab of London South Bank University.

Currently, almost all the technologies for on-demand to mitigate wax deposition are expensive. As discussed, in the literature review that this

research would be used spiral flow, and blending spiral flow with the inhibitor W802 at different concentrations for the first time in this study as a main methods to reduce or mitigate wax deposition in the hydrocarbon pipeline.

During run the experiments and use spiral flow to mitigate wax deposition it was noticed that spiral flow was challenged such as it is very energy intensive and expensive. The literature review discusses using spiral flow in different areas, but did not mention about using spiral flow to mitigate wax deposition.

To evaluate the economic cost of this project, a set of experiments will take as an example of this analysis. The analysis includes the experiments are carried out at flow rate 2.7 L/min and inlet coolant temperature 14°C by using only crude oil, using the inhibitor W802 with the crude oil at concentration 1000, using spiral flow, and using spiral flow with the inhibitor at concentrations 1000 and 2000ppm. According to the obtained results, there is no much difference between the methods of blending spiral flow with 1000 and 2000ppm of W802. Therefore, 1000ppm of the inhibitor W802 preferred in this study because it will reduce the cost of using inhibitor and gives the same results. According to the average charges of electricity in 2016 for UK regions, the average variable unit price used in this evaluation is (£0.14/kWh), and the cost of the inhibitor W802 is £0.015 for each 1 ml.

During run the experiment using just crude oil for 2 hours, it was noticed that pump used 0.82 kW of electricity to recycle the crude oil, the chillier used 1 kW to keep the crude oil temperature over the wax appearance temperature, while the chillier used 0.634 kW of electricity to maintain the required temperature of the pipe wall, and the condenser used 0.24 kWh of electricity to condense the evaporated light components from the crude oil. The total cost of the electricity consumed in the above experiment is £0.38.

By following the same procedure in the above experiment, it can calculate the cost of carrying out the experiments using the inhibitor W802 (£0.347), using the spiral flow (£0.52), and using the spiral flow with the inhibitor W802 together (£0.46), as shown in table 17.

Table 17: Illustrate the electricity consumed and the total cost of each experiment.

	Run Experiment with just Crude Oil	Run Experiment using W802	Run Experiment using Spiral Flow	Run Experiment using W802+Spiral
Electricity Consumed in the Pump (kW/2hr)	0.82	0.25	1.86	0.7
Electricity Consumed in the Chillier (kW/2hr)	0.634	0.634	0.634	0.634
Electricity Consumed in the Hot Bath (kW/2hr)	1	1	1	1
Electricity Consumed in the Condenser (kW/2hr)	0.24	0.24	0.24	0.24
Total Cost (£)	0.38	0.347	0.52	0.46
Wax Volume Produced (ml)	120	70	40	30

It can be seen from the table 17 that the highest cost is £0.52 by run the experiment using spiral flow, and the lowest cost is £0.347 by run the experiment using the inhibitor W802. At the same time, when compares the wax volume produced from each experiment, it can be noticed that the wax volume produce from the experiment using spiral flow is 40 ml, and that produced from experiments using inhibitor W802 is 70 ml. That's mean; reduce the wax volume leads to increase the production even if the cost increased little bit.

The cost of running the experiment using the effect of blending spiral flow with the inhibitor W802 is £0.46 and the wax volume produced is 30 ml, and the cost of running the experiment using just crude oil is £0.38 and wax volume is 120 ml. Comparing these two experiments are shown that the lowest operation cost produced a higher value of wax that's mean higher reduction in crude oil production, while increasing the operational cost of blending the spiral flow with the inhibitor to %17 leads to decrease the wax volume to %75 and this reduction in wax deposition results in high increase in crude oil production.

## Chapter 6: Multiphase Flow Simulation

### 6.1 Chapter Six Overview

This chapter describes the underlining wax models implemented in OLGA, using the experimental data from this study to predict the behaviour of the wax deposition. The chapter presents a comparison of the results of the experimental wax deposition and the predicted wax deposition, as well as the mitigation methods in OLGA software, such as the chemical inhibitors, and the insulator material propylene.

### 6.2 Distribution of the Single Carbon Number and the n-Paraffin in Crude Oil

Figure 54 shows a comparison of the experimental results and PIPEsim calculations of the single carbon number (SCN) distribution in the crude oil and n-Paraffin distribution in the wax of the crude oil. The comparison shows that the calculated single carbon number completely matches with the experimental results. The calculated n-Paraffin agrees with the experimental n-Paraffin in some points and differs in others.

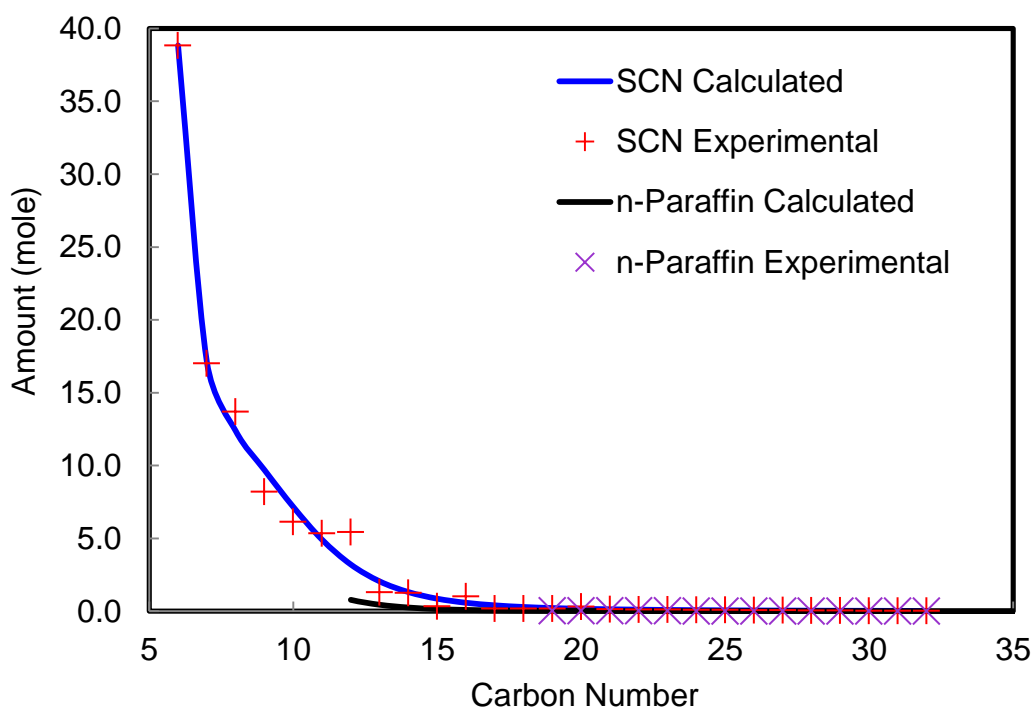


Figure 54: Distribution of the single carbon number (SCN) in the crude oil and the n-Paraffin using PIPEsim.

The phase envelope of the crude oil shown in figure 55 was obtained using PIPEsim 2014; this reveals a critical point of 470.56°C at 40.46 bars. Liquid fractions are present in the hydrocarbon mixture at all temperature conditions below this critical temperature. This suggests the presence of heavy fractions and the stable properties of the liquid phase at high temperatures.

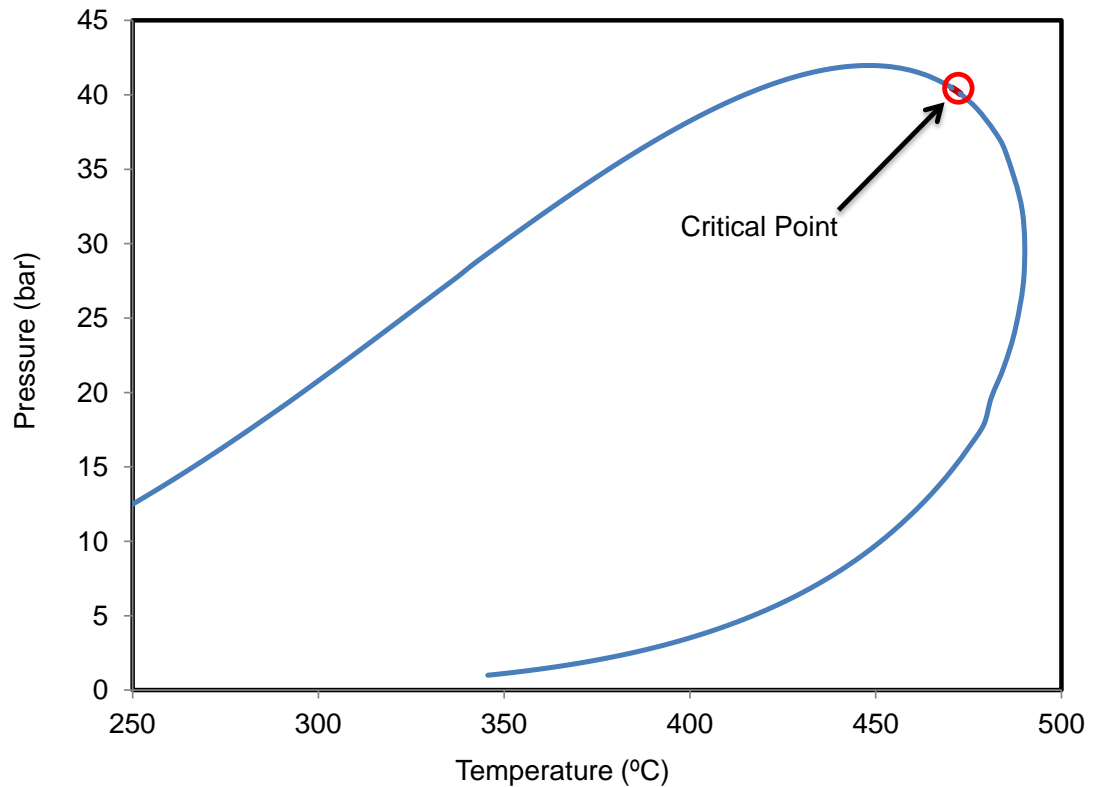


Figure 55: Phase envelope of the crude oil used for wax simulations using PIPEsim.

### 6.3 Comparison between the Wax Simulation Models

The wax deposition simulation for this study shows that the wax thickness predicted using the RRR model is closer to the experimental wax thickness than the other two models – Matzain and Heat Analogy.

Therefore, during this study the RRR wax model was preferred to the Matzain and Heat Analogy models, as shown in figure 56, because it produces a consistent increase in the continuous estimate of the wax build-up over the integration of time for multicomponent mixtures (Ajayi, 2013). The RRR model predicts a conservative result as compared to the Matzain and Heat Analogy models due to the ability of the RRR model to initiate a dissolution possibility, coupled with the consistency of its prediction, which influenced its selection. There are no dissolution possibilities in the Matzain and Heat Analogy models in the wax modules of OLGA (Ajayi, 2013).

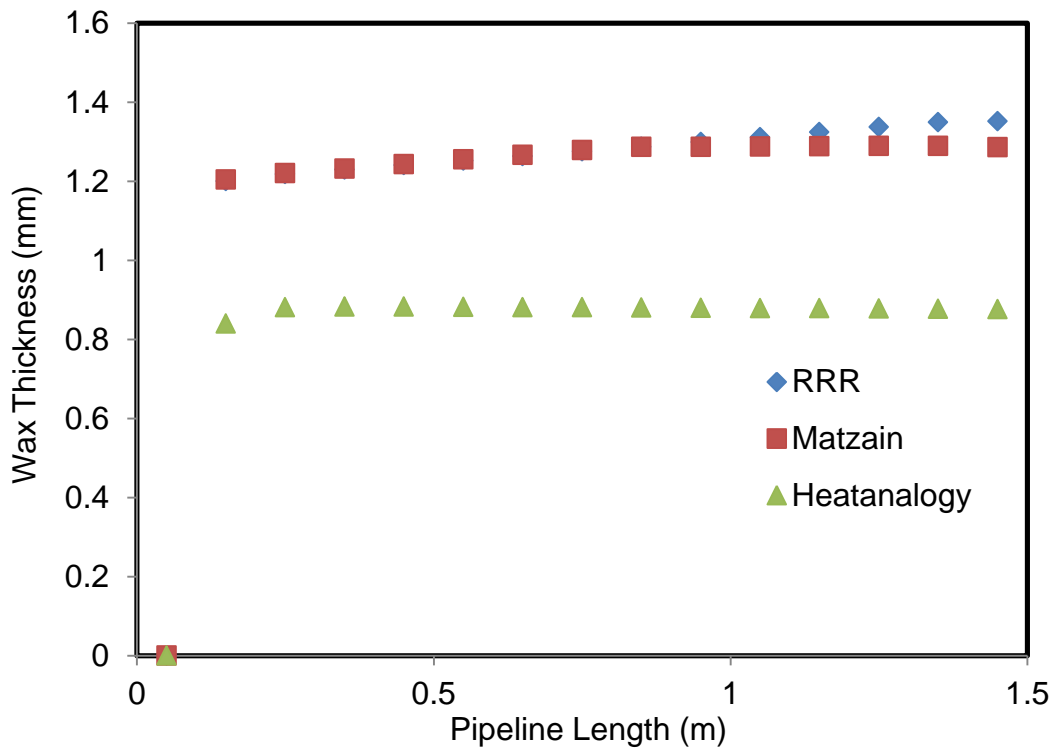


Figure 56: Comparison of the three models in the OLGA software: RRR, Matzain and Heat Analogy.

#### 6.4 Results and Discussion of the Wax Simulation

Efforts were made to simulate the rig of this study, but this was difficult due to the complicated system of the rig. Therefore, the simulation was undertaken, including the test section of the pipe where the wax deposition process occurs.

After circulating the crude oil through the pipe, the oil flows back into the oil reservoir. It should be noted that by recirculating the oil, the amount of dissolved wax is reduced as there are more wax deposits on the wall. In order to be certain that the available amount of wax that can deposit on the wall is not limited or influencing the deposition rate, the total amount of dissolved wax is large compared to the amount of wax deposited on the wall.

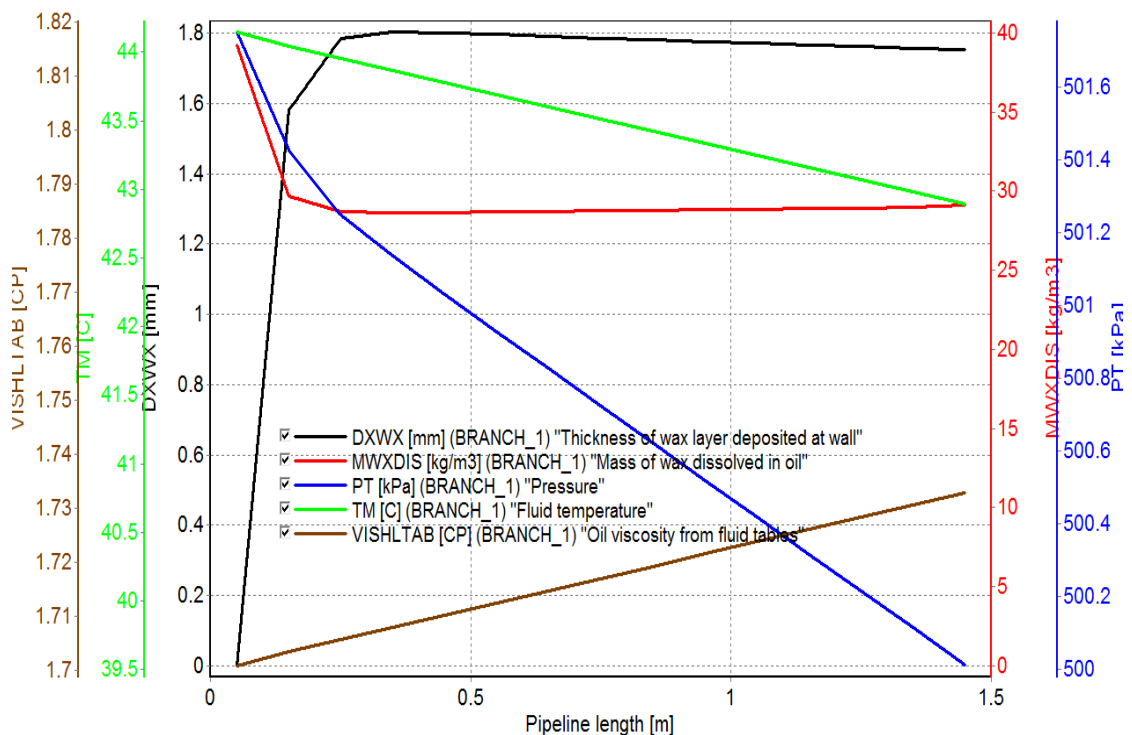
##### 6.4.1 The Base Case of Wax Deposition Simulation

Profiles in figures 57 and 58 at flow rate 2.7 and 4.8 L/min respectively present the thickness of the wax layer deposited on the pipe wall, the mass of wax dissolved in oil, pressure, crude oil temperature and oil viscosity along the tube length. After running the simulation and at an inner pipe wall temperature less than the wax appearance temperature, a sharp growth in the amount of wax precipitated is observed resulting in a reduction of mass of wax dissolved in oil. The reason for this sharp growth in wax thickness is the high thermal conductivity of the pipe material.

The crude oil temperature reduced gradually along the pipeline due to heat loss to the surrounding area and the pressure drop increased in the system

due to the wax precipitated in the pipe wall. The oil viscosity was increased gradually due to the decrease in the crude oil temperature and the loss of heat to the surrounding area through the pipe wall; this loss in the heat leads to the wax crystals forming, and therefore the oil viscosity increases and tends to transform from Newtonian to non-Newtonian behaviour. The wax deposition leads to increasing wall roughness and a reduction in the effective flow diameter of the pipe. This principle of wax deposition, as a consequence of a necessary temperature gradient between the bulk fluid and a surrounding ambient fluid, is simulated in the test section as an important flow assurance concept for handling wax deposition in subsea flow lines.

OLGAF



File: WaxDepositionNew.ppt

Figure 57: Simulation output of wax deposition profile along the test section pipe of the experimental rig for this study, at a flow rate of 2.7 L/min.



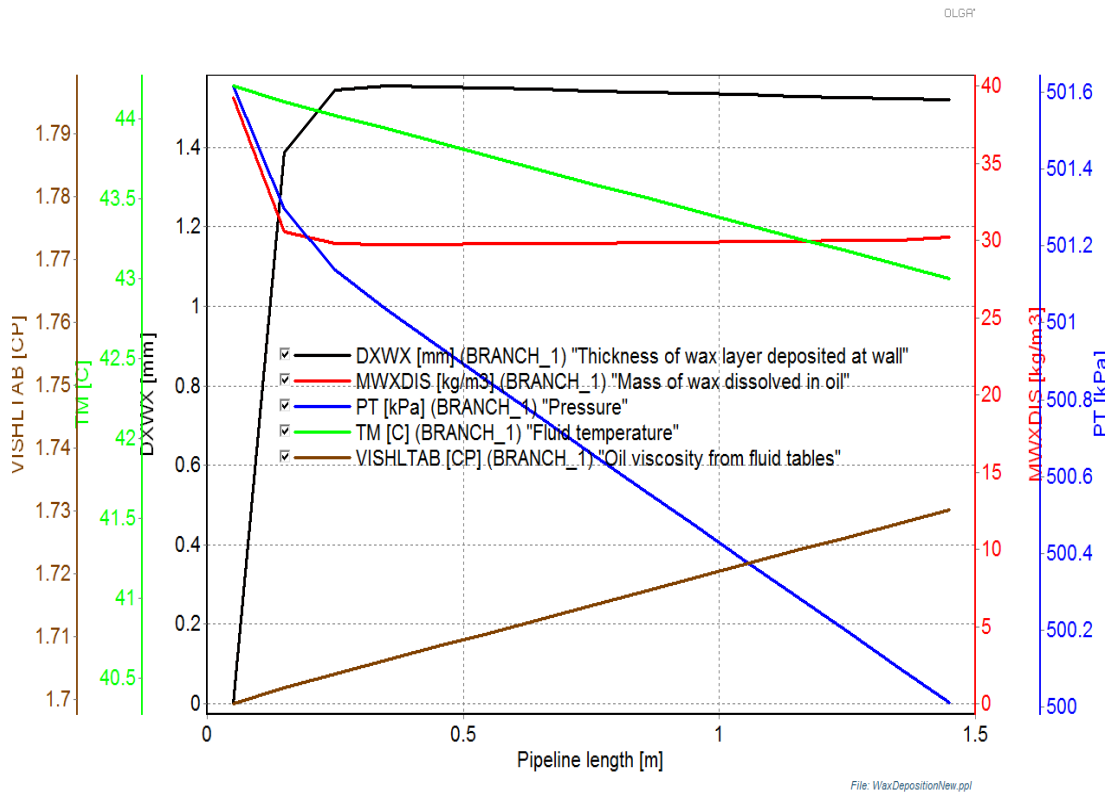


Figure 58: Simulation output of wax deposition profile along the test section pipe of the experimental rig for this study, at a flow rate of 4.8 L/min.

The difference between the two figures presented by the predicted wax thickness at the flow rate 2.7 L/min is higher than the predicted thickness at 4.8 L/min because increasing the flow rate leads to an increase in the shear stress and removal of the small molecules of wax to the crude oil. It can also be seen that the mass of wax dissolved in oil is higher at the high flow rate and lower at the low flow rate.

The simulation results show agreement and somewhat less accuracy than the experimental results due to using the crude oil composition of Jha et al. (2014). In order to reduce this gap between the simulated and experimental results, a sensitivity study has been undertaken as part of this work, as will be outlined below.

#### 6.4.2 Tuning of OLGA Parameters for Improved Predictions

Since simulations based on the default wax parameters did not achieve a complete match with experiments, as will be shown in the scenarios below, it was important to find out to what extent tuning of wax parameters was necessary. Three scenarios were created to match the experimental wax thickness, including studying the effect of changing wax porosity in OLGA, changing the crude oil components and the influence of simulation time on wax deposition.

### **Scenario A: The Effect of Changing Wax Porosity**

A sensitivity study was carried out in OLGA simulation to study the effect of changing the wax porosity from 0.2, to 0.4, 0.6, 0.8 and 0.9 and their impact on the predicted wax thickness to match the experimental wax thickness. The predicted wax thickness was lower than the experimental thickness at a flow rate of 2.7 L/min by using the value 0.6 as default wax porosity in OLGA. It was observed from the simulation results that increased wax porosity leads to an increase in wax deposition thickness.

Figure 59 shows the results and, as expected, the predicted wax thickness increased after increasing the wax porosity from 0.6 to 0.9 and reduced after reducing the wax porosity to 0.4 and 0.2 respectively. This gives an indication that wax porosity is one of the tuning parameters that has major effects on wax deposition thickness; a small adjustment in the wax porosity from 0.6 to 0.8 leads to the better prediction of the experimental wax thickness.

The wax porosity value 0.9 leads to over predicted of the experimental wax thickness, therefore, it was neglected, due to increase the volume of the trapped oil between wax structures in the deposit layer leading to the soft layer of deposit and can easily remove by the crude oil flow; so, this value of porosity will not give an accurate prediction of wax deposit thickness. Therefore, in this research, the wax porosity of 0.8 depends on OLGA calculations to simulate the wax deposition thickness at different inlet coolant temperatures, so the wax porosity values using the RRR model should be in the range of 0.6–0.9 (Coto et al., 2011; Rosvold, 2008). This increase in wax thickness can be explained by the fact that as the wax porosity and the trapped oil increase, this will lead to an increase in the wax deposit thickness.

The wax thickness is still somewhat underpredictable, even at a wax porosity of 0.8 and a flow rate of 2.7 L/min; therefore, OLGA simulation requires additional tuning parameters, such as a change in the crude oil components, in order to match the experiment properly.

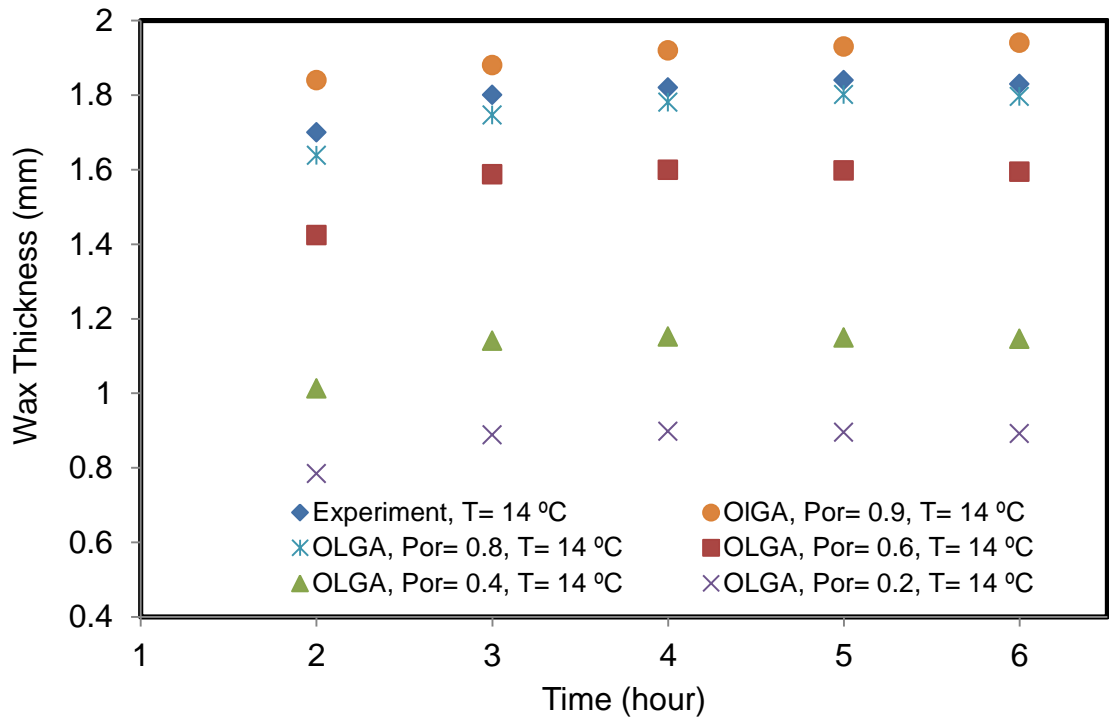


Figure 59: The effect of wax porosity on predicted wax thickness at flow rate 2.7 L/min and an inlet coolant temperature of 14°C.

As the flow rate increases to 4.8 L/min, lower wax porosity is expected. Figure 60 shows the results: the wax thickness is under-predicted at wax porosity 0.2, 0.4 and 0.8, but the prediction of wax thickness was over the experimental thickness at wax porosity 0.6 and 0.9.

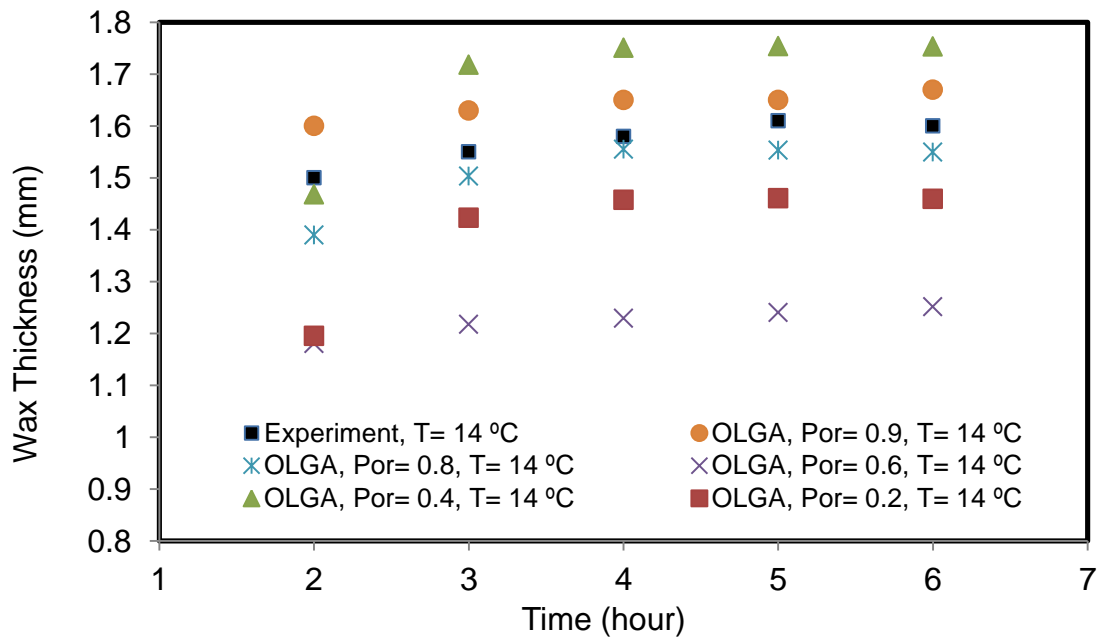


Figure 60: The effect of changes in wax porosity in OLGA simulation on predicted wax thickness at flow rate 4.8 L/min and an inlet coolant temperature of 14°C.

It can be seen that at a flow rate of 4.8 L/min, the value of wax porosity 0.8 provides better prediction in wax deposition using OLGA so, this value of wax porosity dependent in OLGA calculations. OLGA simulation at a flow rate of 4.8 L/min still needs some additional tuning parameters such as changes in the crude oil components in order to match the experiment properly.

### **Scenario B: The Effect of Changing Crude Oil Components**

A sensitivity study was undertaken to achieve the experimental thickness using OLGA software at an inlet coolant temperature of 14°C and wax porosity of 0.6 and by changing the weight percentage of carbon numbers distributed in the crude oil.

Hexane or C6 in the crude oil in high percentage reduces the wax formation due to C6 working as a solvent, helping to dissolve the wax molecules in the crude oil. Therefore, the procedure was done by reducing 10, 20 and 30% of C6 weight percentage and distributing the removed percentage to the remaining carbon numbers in the crude oil.

This sensitivity study also included adding 10% to C6 and removing the equal percentage from the other components, as shown in table 18.

Figure 61 shows the C6 sensitivity analysis; the lower solid line represents the predicted wax thickness using the original crude oil components (Jha et al., 2014) and the difference between this and the experimental wax thickness of the upper solid line is about 0.3 mm. The predicted wax thickness increased by about 0.1 mm from the lower solid line after removing 10% of C6. Removing 20% of C6 leads to improving the predicted wax thickness and nearly reaching the experimental wax thickness; by increasing the removal percentage to 30%, the predicted thickness exceeds the experimental wax thickness in the upper solid line. On the other hand, adding 10% of C6 leads to reducing the predicted thickness to lower than the predicted thickness of the original components due to the high amount of C6 melting the wax in the crude oil.

From this study it can be concluded that reducing the C6 content by 20% presents a better predicted wax thickness but this thickness is still not reaching the desired value; therefore, it will depend on the next simulations with a wax porosity of 0.8 to achieve the experimental wax thickness.

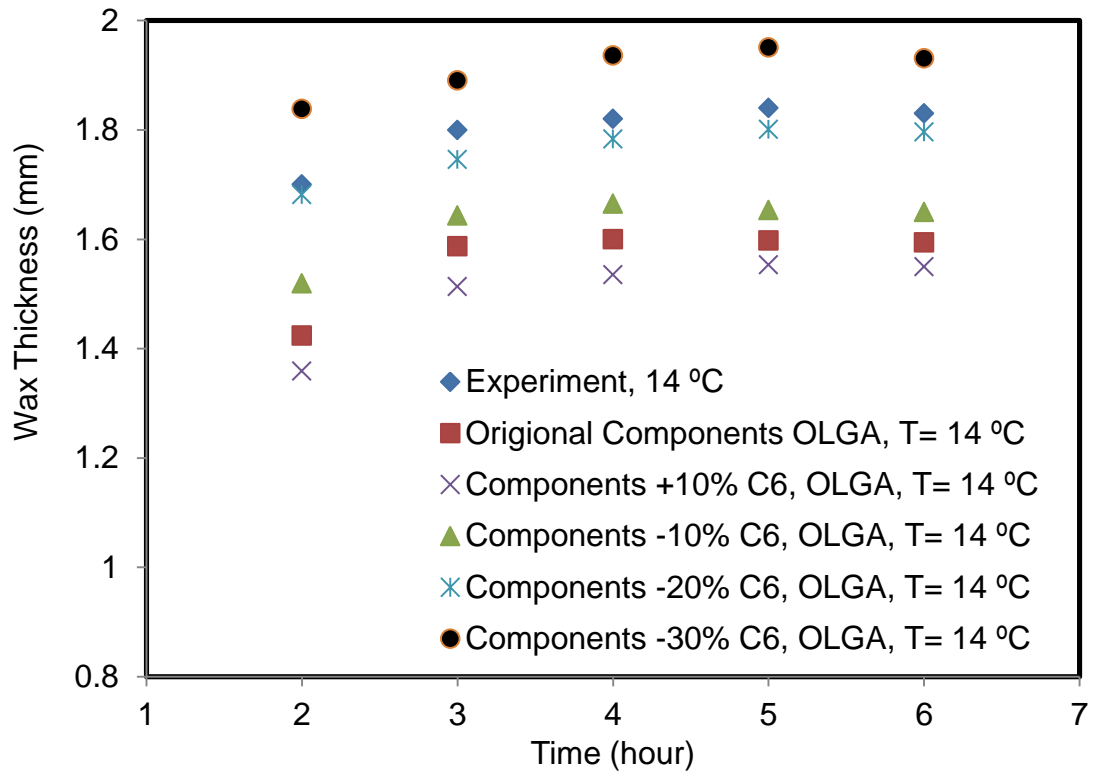


Figure 61: The effect on the predicted wax thickness of changing crude oil components, using OLGA at a flow rate of 2.7 L/min and an inlet coolant temperature of 14°C.

Table 18: Weight percentage of carbon number distributed in the crude oil used in the simulation with the new weight percentage after removing 10, 20 and 30% from C6 and distributing that percentage of each case to the rest of the carbon numbers.

Carbon Number	Weight% Original (Jha, 2014)	Weight% (- 10 % C6)	Weight% (- 20 % C6)	Weight% (- 30 % C6)	Weight% (+ 10 % C6)
C6	28.5	25.65	22.8	19.95	31.35
C7	14.85	15.27	15.7	16.12	14.43
C8	13.62	14.01	14.4	14.8	13.24
C9	9.16	9.42	9.7	9.94	8.90
C10	7.6	7.82	8.03	8.25	7.38
C11	7.28	7.49	7.7	8	7.10
C12	8.05	8.28	8.51	8.84	7.82
C13	2.09	2.15	2.21	2.4	2.03
C14	2.15	2.21	2.27	2.43	2.09
C15	0.61	0.63	0.74	0.76	0.59
C16	1.97	2.03	2.18	2.24	1.91
C17	0.35	0.36	0.47	0.48	0.34
C18	0.4	0.41	0.52	0.53	0.39
C19	0.42	0.422	0.54	0.56	0.41
C20	0.74	0.76	0.88	0.9	0.72
C21	0.31	0.42	0.43	0.48	0.30
C22	0.29	0.4	0.41	0.46	0.28
C23	0.27	0.38	0.39	0.39	0.26
C24	0.24	0.35	0.35	0.36	0.23
C25	0.24	0.35	0.35	0.36	0.23
C26	0.19	0.295	0.3	0.31	0.18
C27	0.19	0.295	0.3	0.31	0.18
C28	0.15	0.2015	0.26	0.26	0.146
C29	0.14	0.1915	0.25	0.25	0.136
C30	0.08	0.082	0.13	0.19	0.078
C31	0.08	0.082	0.13	0.19	0.078
C32	0.03	0.031	0.032	0.13	0.029
C33	0.01	0.01	0.018	0.11	0.009

### Scenario C: The Impact of Simulation Time on Wax Thickness

From figure 62 it can be seen that at 0.6, the default wax porosity in OLGA, the wax thickness is still increasing by increasing the simulation time from 6 to 12 and 24 hours. This is illustrated due to the fact that the simulation considered the crude oil passing through the pipe to be fresh, so the wax content in the crude oil was constant and not reduced due to reducing the mass of wax dissolved in the oil, as in the case of recirculating crude oil in the rig.

Increasing the simulation time leads to an increase in the wax deposit thickness due to an increase in the wax deposit on the pipe wall. The simulation results show that the increase in the wax thickness was slight and it looks like a constant line. This can be explained by the high thermal conductivity of copper pipe as the increasing wax deposited on the pipe wall forms a layer of wax; this layer works as an insulator preventing the heat exchange through the copper pipe between the crude oil and the surrounding temperatures. Therefore, the crude oil temperature inside the pipe will be constant and the wax deposition rate will be in a balance with the removal wax rate or the deposition rate, somewhat higher than the removal wax deposition due to increasing the crude oil velocity by reducing the pipe diameter because of the deposit wax.

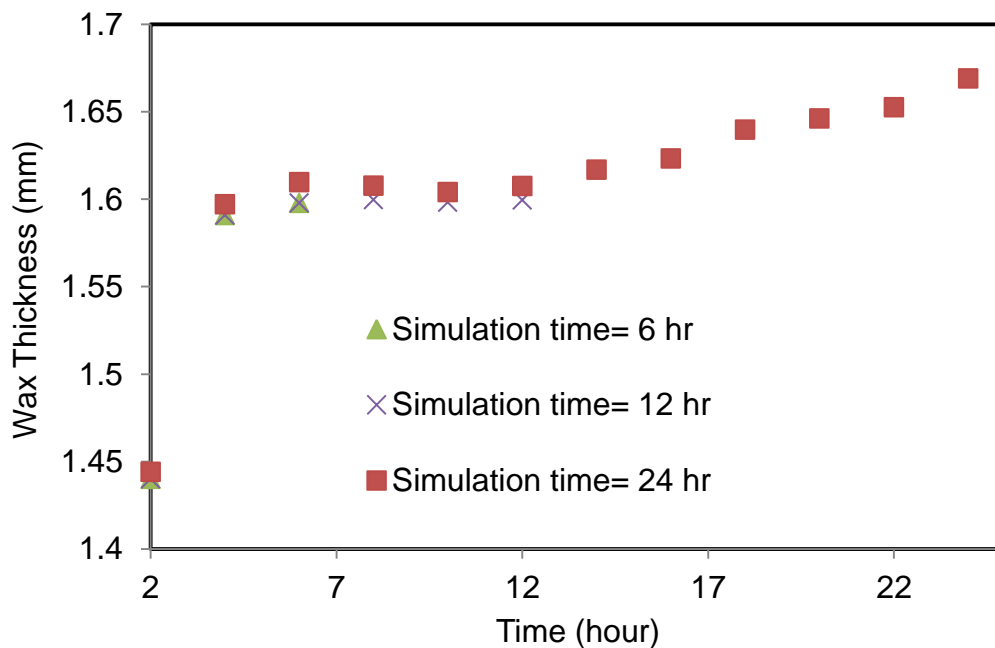


Figure 62: The effect of simulation time on the wax thickness at 2.7 L/min, an inlet coolant temperature of 14°C and a wax porosity of 0.6.

It can be concluded from the results of the sensitivity study of the three previous scenarios that the suitable OLGA parameters improve and match the experimental wax thickness by considering the wax porosity 0.8 and running the simulations using the effects of changed crude oil components by reducing C6 to 20%. This is due to the results of these parameters presenting agreement with the experimental results of wax deposition.

#### 6.4.3 Comparison of Wax Simulations with Experimental Data

All simulations run in OLGA are based on the experimental conditions of this study. The resulting wax thickness versus time was plotted using Excel in order to compare results from the experiments with the simulation results. Figure 63 illustrates a comparison between the experiments and the simulation models, showing the influence of inlet coolant temperature

variation and the experimental time (2, 3, 4, 5 and 6 hours) on wax thickness at a flow rate of 2.7 L/min.

Overall, the wax thicknesses of the experimental results are somewhat higher than the simulation results in the same process conditions. Whilst at an inlet coolant temperature of 14°C, the different experimental time was about 1.8 mm; it was about 1.78 mm by using the simulation mode. At an inlet coolant temperature of 24°C, the wax thickness decreased to about 2 mm in the experiments, while it was decreased to 1.8 mm using the model. Increasing the temperature of the pipe wall to 33°C leads to reducing the wax thickness from 0.85 mm in the experiment to 0.84 mm in the model.

Experimentally, it was proved that the wax thickness decreased by increasing the flow rate from 2.7 to 4.8 L/min. This is the same using the simulation model, as shown in figure 64. The wax thickness decreased experimentally from 1.6 to 1.4, then 0.7 mm at inlet coolant temperatures 14, 24 and 33°C respectively.

The predicting model shows the reduction in wax thickness from 1.55 to 1.4 and 0.7 mm at inlet coolant temperatures 14, 24 and 33°C respectively.

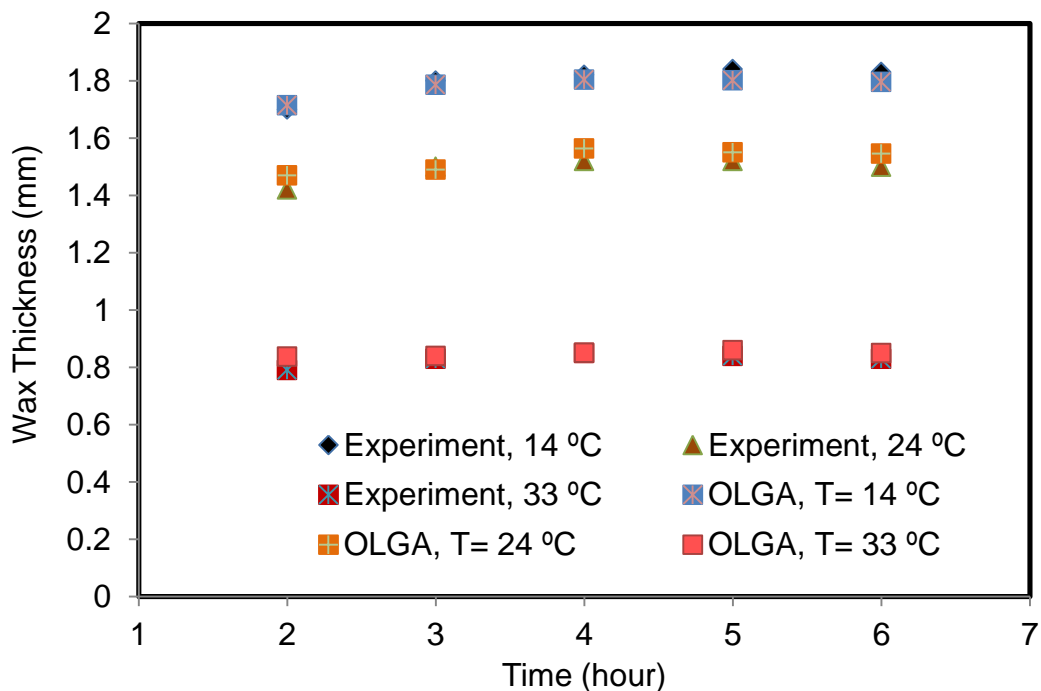


Figure 63: Comparison between the experimental results and the simulation results at flow rate 2.7 L/min.

The comparison indicates that the model results are slightly lower than the experimental results. These differences can be explained by the fact that there are unknowns and assumptions in the experiments; for example, the wax roughness and wax porosity is unknown, which leads to additional uncertainty in the wax simulations. Comparing simulation results to the experiments provides information on the reliability of a wax deposition model.



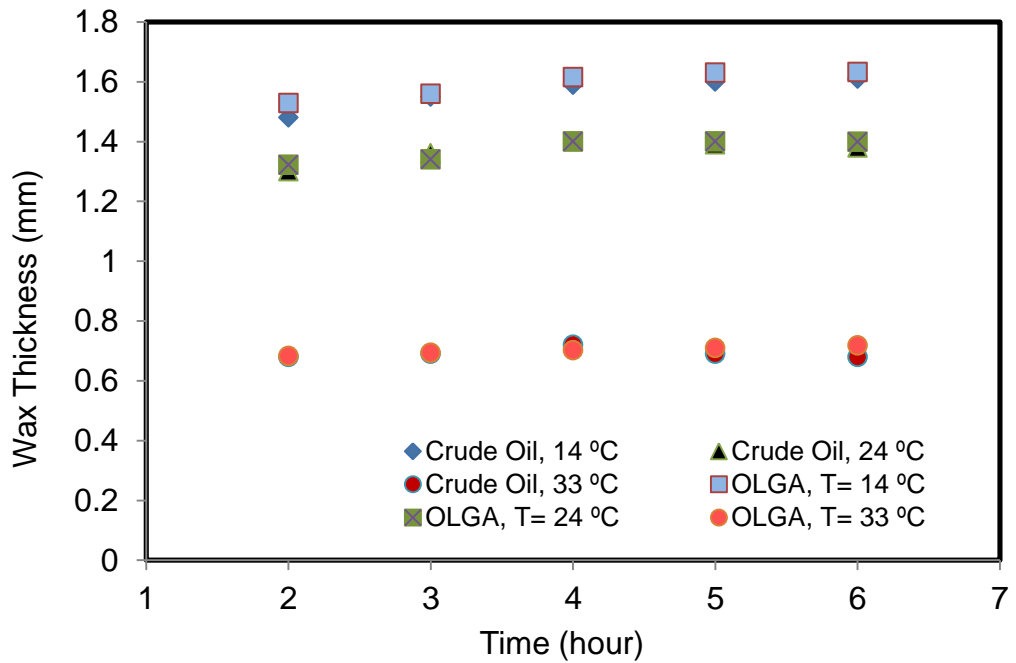


Figure 64: Comparison between the experimental results and the simulation results at a flow rate of 4.8 L/min.

#### 6.4.4 Wax Mitigation Methods

OLGA software contains many mitigation methods such as an inhibitor, insulation materials, thermal insulation and pigging. During the simulation for this study, these methods were used to prevent wax deposition.

##### A. Wax Mitigation using Inhibitor

Experimentally, the polyacrylate polymer was used to reduce wax deposition inside the test section of the pipe, as shown in figure 65. During the simulation, methanol was used as an inhibitor to mitigate wax deposition due to OLGA software containing methanol, but not polyacrylate polymer.

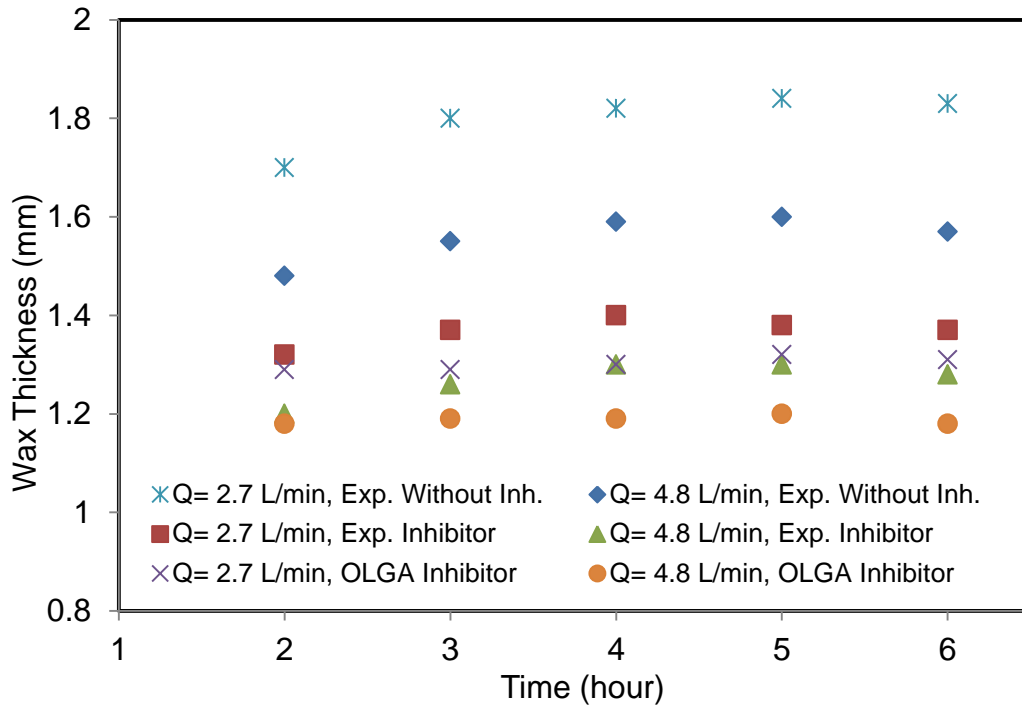


Figure 65: Simulating the effect of the inhibitor on wax thickness using OLGA and comparing this with the experimental results with and without the inhibitor.

### B. Polypropylene Insulation Material

In the past years, thermal insulation of subsea flow lines and risers has become increasingly important. With the advent of multi-phase flow in flow lines and risers from subsea completions, possibilities for wax and hydrate formation have prevailed. Thermal insulation is used to prevent hydrate and wax formation during shutdowns and to maintain the fluid temperature inside the flow lines for easier fluid separation topside or onshore (Boye Hansen and Rydin, 2002). Polypropylene is a high thermal insulation for high temperature and deepwater applications; therefore, it has been used in this simulation to prevent wax deposition formation. Polypropylene material has suitable properties for insulation; for example, the thermal conductivity is 0.12 W/ (m. °C), the heat capacity is 1675 J/ (kg. °C) and the density is 960 kg/m<sup>3</sup>. During the simulation, it was noticed that the suitable thickness of the insulation material to coat the pipe is 1 mm in order to prevent wax formation in the pipe at a flow rate of 2.7 L/min and inlet coolant temperature of 14°C, as shown in figure 66. The thickness of the insulation layer was decreased to 0.8 mm at a flow rate of 4.8 L/min and inlet coolant temperature of 14°C, as shown in figure 67.

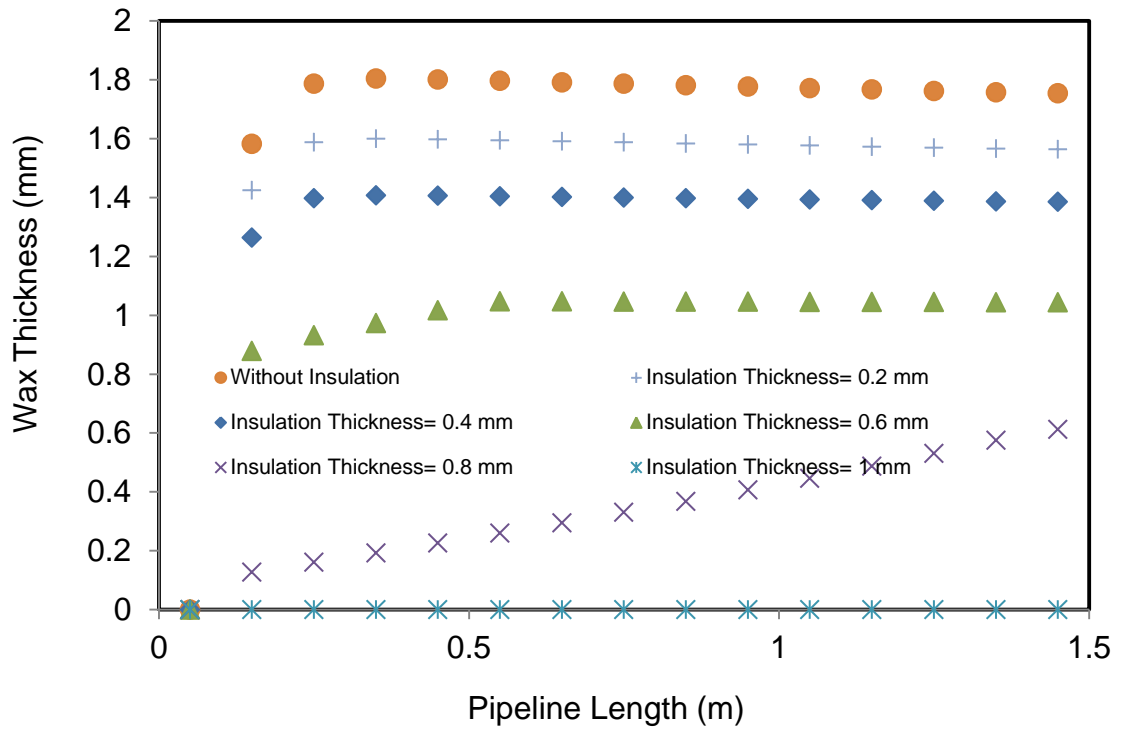


Figure 66: The effect of the insulation layer thickness on the wax formation at a flow rate of 2.7 L/min and coolant temperature of 14°C.

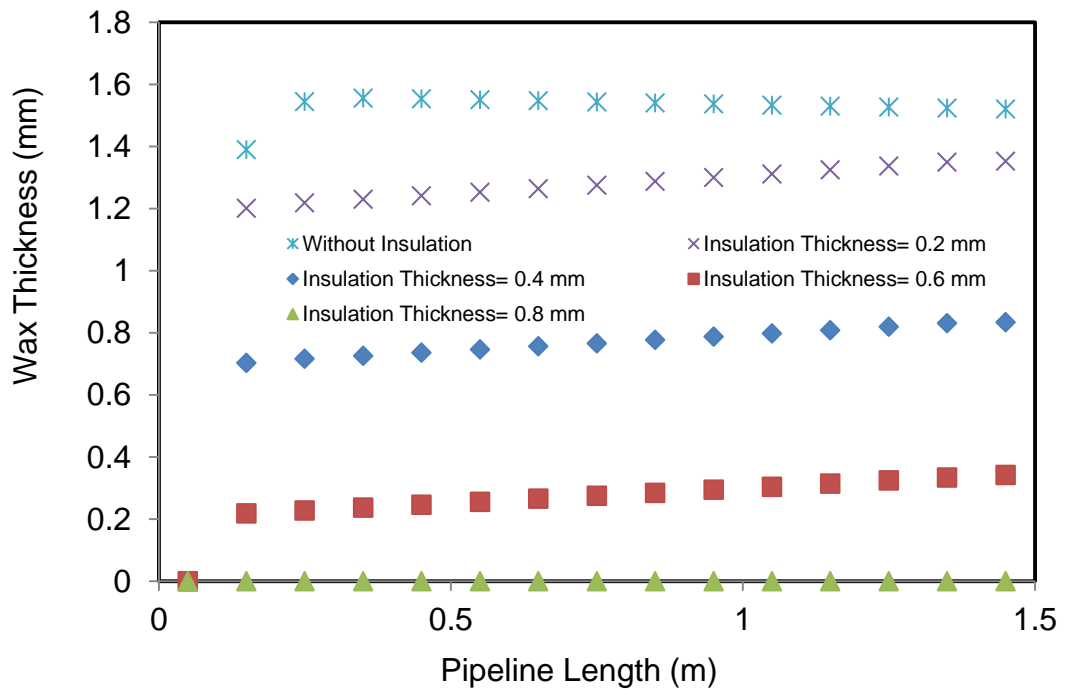


Figure 67: The effect of the insulation layer thickness on the wax formation at a flow rate of 4.8 L/min and coolant temperature of 14°C.

## Chapter 7: Conclusions and Future Work

### 7.1 Conclusions

The current work studied one of the main flow assurance problems in the oil industry: wax deposition. A specialised rig platform was designed and constructed at the university laboratory to study and understand the effects of factors such as inlet coolant temperature, flow rate, pressure drop, oil temperature, shear stress, experimental time and oil viscosity, on the wax deposition process.

A series of experiments were carried out at different flow rates 2.7 and 4.8 L/min to study wax deposition process. Three different techniques were employed to reduce wax formation in the hydrocarbon pipeline. These techniques involved using a chemical, a mechanical separately and in the end using them in combination. The chemical method used a particular inhibitor (W802 polyacrylate polymer C16-C22), and the mechanical method include creating spiral flow inside the test section by inserting an in-house made twisted plate 1.5m long and 1cm width with angle of 80.5°. Four different mathematical modelling techniques have been used to evaluate the wax thickness in the test section include pigging, pressure drop, heat transfer and liquid displacement-level detection technique. The methodology was very robust and delivered exceptional results parallel to the mathematical modelling equations.

It was observed that wax deposit increases with decreasing the inlet coolant temperature (pipe wall temperature). Visa versa, when the temperature was increased it reduced wax build up and completely disappearing above wax appearance temperature. On the other hand, an increase in flow rate results in a decrease in the wax deposition due to increasing the shear stress. The experimental time effect on wax deposition was studied and the wax volume increased by increasing the cycle of crude oil from the rig to the reservoir, placed in a water bath.

The results present a high reduction in wax deposition by using spiral flow and using combination of spiral flow with the inhibitor W802 polyacrylate polymer (C16-C22), compared with commercial mitigation methods. The best results were attained when they were used in combination making this research the first to use this approach. It was also seen when these techniques were used separately still did better than commercial mitigation methods.

In another chemical study, commercially available inhibitors were selected having unique set polymers from each other. In a novel approach, they were mixed to create an in-house inhibitor containing most of them the features of polymers in one. When this was tested against the conventional inhibitors it did exceed their resistance against wax deposition. As well as, a significant reduction in pour point temperatures and crude oil viscosity was observed.

The findings of the numerical simulation, using OLGA simulator to reproduce the experimental results by tuning analogical properties (assumptions), show agreement with the experimental results. Some mitigation methods were used in OLGA software to predict its influence on wax deposition such as the chemical inhibitors, and propylene material.

It can be concluded that this study has achieved all the intended objectives and presents the spiral flow method and combination of spiral flow with the inhibitor method as a new mitigation methods to prevent or reduce wax deposition in the hydrocarbon pipelines.

## **7.2 Recommendations for Future Work**

- Carry out the experiments with more different flow rates.
- Analyse the cost of spiral flow in the real oil field (flow geometry).
- Study the effect of flow geometry and consider it as one of the factors that affecting on wax deposition process.
- Use the software model to simulate flow regime.
- Study the effect of flow geometry on wax deposition under single phase flow.
- Study the effect of flow geometry on wax deposition under multiphase flow.
- Carry out the experiments to study the effect of combined flow geometry with the light components (light end) on wax deposition.
- Study the effect of wax inhibitors on wax deposition at different flow geometry and different flow regime.
- Study the impact of pipe wall roughness on wax deposition process at different flow rates and different flow geometry.

## References

- American Association for Laboratory Accreditation, (2014), G104 – Guide for Estimation of Measurement Uncertainty in Testing.
- Abdel-Waly, A. A. (1999) The factors affecting paraffin deposition in oil wells. *Journal of Engineering and Applied Science*, 46, 381-386.
- Adeyanju, O. A., and Oyekunle, L. O. (2013) Experimental Study of Wax Deposition in a Single Phase Sub-cooled Oil Pipelines, in: The Nigeria Annual International Conference and Exhibition, University of Lagos, Nigeria, 30 July - 1 August, pp. 1-18. Available from: <https://0-www.onepetro.org/lispac.lsbu.ac.uk/download/conference-paper/SPE-167515-MS?id=conference-paper%2FSPE-167515-MS> [Accessed 27 August 2016].
- Aiyejina, A., Chakrabarti, D. P., Pilgrim, A. and Sastry, M. K. S. (2011) Wax formation in oil pipelines: A critical review, *International Journal of Multiphase Flow*, 37 (7), pp. 671-694.
- Abdel-Aal, E.A., Abdel-Ghafar, H.M., El Anadouli, B.E. (2015) New findings about nucleation and crystal growth of reverse osmosis desalination scales with and without inhibitor. *Cryst. Growth Des.* 15 (10), 5133–5137. <http://dx.doi.org/10.1021/acs.cgd.5b01091>.
- Azizollah Khormali, Dmitry G. Petrakov, Rasoul Nazari Moghaddam (2017) Study of adsorption/desorption properties of a new scale inhibitor package to prevent calcium carbonate formation during water injection in oil reservoirs, *Journal of Petroleum Science and Engineering*, (153), 257-267. <https://doi.org/10.1016/j.petrol.2017.04.008>.
- Alberta Innovates Technology Futures. 2016. Near Infrared Asphaltene Analyzer. [ONLINE] Available from: <http://www.albertatechfutures.ca/OurTeams/AppliedSpectroscopy/SensorforMiningandBitumenExtraction/NearInfraRedAsphalteneAnalyzer.aspx>. [Accessed 15 June 2016].
- Akbarzadeh, K., Ratulowski, J., Eskin, D., and Davies, T. (2010) The Importance of Wax-Deposition Measurements in the Simulation and Design of Subsea Pipelines. *SPE Projects, Facilities & Construction*, 5 (2), pp. 49-57.
- Azevedo, L.F.A. and Teixeira, A.M., (2003) A Critical Review of the Modeling of Wax Deposition Mechanisms. *Petroleum Science and Technology*, 21(3-4), pp. 393-408.

- Akpabio Moses Gideon (2013) Cold Flow in Long-Distance Subsea Pipelines. MSc Thesis, Norwegian University of Science and Technology.
- Adeyanju, O. A., & Oyekunle, L. O. (2014) Influence of Long Chain Acrylate Ester Polymers as Wax Inhibitors in Crude Oil Pipelines, *Society of Petroleum Engineers*, doi:10.2118/172844-MS.
- Al-Sabagh, A.M., Noor-EI-Din, M.R., Morsi, R.E. and Elsabee, M.Z. (2009) Styrene-Maleic Anhydride Copolymer Ester as Flow Improvers of Waxy Crude Oils. *Journal of Petroleum Science and Engineering*, 65 (3-4), pp. 139-146.
- Ajayi, O.E., (2013) Modelling of controlled wax deposition and loosening in oil and gas production systems. MSc Thesis, Norwegian University of Science and Technology NTNU.
- Bai, C., and Zhang, J. (2013), Effect of carbon number distribution of wax on the yield stress of waxy oil gels, *Industrial and Engineering Chemistry Research*, 52, 2732–2739.
- Betül, A.S., Tulin, B., (2007) An Experimental Study on Heat Transfer and Pressure Drop Characteristics of Decaying Swirl Flow through a Circular Pipe with a Vortex Generator, *Experimental Thermal and Fluid Science*, (32), pp. 158–165.
- Baudilio Coto, Carmen Martos, José L. Peña, Juan J. Espada, María D. Robustillo, (2008) A New Method for the Determination of Wax Precipitation from Non-Diluted Crude Oils by Fractional Precipitation, *Fuel Journal* (87), pp. 2090–2094.
- Barreto, C. V., Pimenta, A., Karami, H., Pereyra, E., & Sarica, C. (2017), Experimental Investigation of Severe Slugging Control by Surfactant Injection, *Offshore Technology Conference*. doi:10.4043/27681-MS
- Burger, E.D., Perkins, T.K., and Striegler, J.H., (1981) Studies of Wax Deposition in the Trans Alaska Pipeline. *SPE Journal of Petroleum Technology*, 33(6), pp. 1075-1086.
- Boye Hansen, A., Rydin, C., (2002) Development and Qualification of Novel Thermal Insulation Systems for Deepwater Flowlines and Risers based on Polypropylene, in: *Offshore Technology Conference*, Texas, USA, 6 – 9 May, pp. 1-8. Available from: <https://0-www.onepetro.org/lispac.lsbu.ac.uk/download/conference-paper/OTC-14121-MS?id=conference-paper%2FOTC-14121-MS> [Accessed 7 October 2012].

- Beggs, H. D., and Brill, J.P. (1973) A Study of Two-Phase Flow in Inclined Pipes, *Society Petroleum Engineers Journal*, pp. 607-617.
- Botne, K. K. (2012) Modelling wax thickness in single-phase turbulent flow. MSc thesis, Norwegian University of Science and Technology, Department of Petroleum Engineering and Applied Geophysics. Available from:  
<http://daim.idi.ntnu.no/masteroppgaver/007/7848/masteroppgave.pdf>  
[Accessed 8 January 2013].
- Bern, P.A., Withers, V.R. and Cairns, J.R., (1981) Wax deposition in crude oil pipelines, in: Proc European Offshore Petroleum Conference and Exhibition, London, England, October 21-24. Available from:  
<https://0-www.onepetro.org.lispac.lsbu.ac.uk/download/conference-paper/SPE-206-1980-MS?id=conference-paper%2FSPE-206-1980-MS>  
[Accessed 19 February 2013].
- Bott, T. R., and Gudmunsson, J. S., (1977) Deposition of Paraffin Wax from Kerosene in Cooled Heat Exchanger Tubes, *Canadian Journal of Chemical Engineering*, 55 (4), pp. 381-385.
- Bland, J.M.; Altman, D.G. (1996), Statistics notes: measurement error, *BMJ*. 312 (7047): 1654. doi:10.1136/bmj.312.7047.1654
- Creek, J.L., Lund, H.J., Brill, J.P., and Volk, M. (1999) Wax deposition in single phase flow. *Fluid Phase Equilibria Journal*, (158–160), pp. 801–811.
- Craddock, H.A., Mutch, K., Sowerby, K., McGregor, S., Cook, J., and Stranchan, C. (2007). A Case Study in the Removal of Deposited Wax From a Major Subsea Flowline System in the Gannet Field, SPE 105048 presented at SPE International Symp in Oilfield Chemistry, Houston.
- Coto, B., et al., (2011) A New DSC-Based Method to Determine the Wax Porosity of Mixtures Precipitated from Crude Oils. *Energy & Fuels*, 25(4), pp. 1707-1713.
- Conway, M.E., and Williams, K.R. (2000) Polyacrylate gel for horticultural use. EP1027402 A1. Available from:  
<https://www.google.com/patents/EP1027402A1?cl=en> [Accessed 13 July 2016].
- Crawford, R.J., (2005) *Plastics Engineering*. 3rd. Ed. Burlington: Elsevier Butterworth-Heinemann.
- Chen, X.T., Volk, B. M., Bwith Stuck Pig, and rill, J.P. (1997) Techniques for Measuring Wax Thickness during Single and Multiphase Flow, in: SPE Annual Technical Conference and Exhibition, San Antonio, Texas, USA., 5-8 October, pp. 249-256. Available from:  
<https://0-www.onepetro.org.lispac.lsbu.ac.uk/download/conference-paper/SPE-38773-MS?id=conference-paper%2FSPE-38773-MS>  
[Accessed 9 June 2014].



- Dantas Neto, A. A., Gomes, E. A. S., Barros Neto, E. L., Dantas, T. N. C., and Moura, C. P. A. M. (2009) Determination of Wax Appearance Temperature (WAT) in Paraffin/Solvent Systems by Photoelectric Signal and Viscosimetry. *Brazilian Journal of Petroleum and Gas*, 3(4), pp. 149-157.
- Duffy, D.M., and Rodger, P.M. (2002) Modeling the activity of Wax Inhibitors: A Case Study of Poly (octadecyl acrylate). *The Journal of Physical Chemistry B*, 106 (43), pp. 11210-11217.
- Dwivedi, P., Sarica, C. and Chang, W. (2012) Experimental Study of Wax deposition Characteristics of a Waxy Crude oil under Single Phase Turbulent Flow Conditions. *Society of Petroleum Engineers Journal*, 61-73. Available from: <https://0-www.onepetro.org.lispac.lsbu.ac.uk/download/journal-paper/SPE-163076-PA?id=journal-paper%2FSPE-163076-PA> [Accessed 21 May 2013].
- Euro-Argo. 2013. An Argo tour of the ocean. [ONLINE] Available at: [http://www.euroargo-edu.org/argoeu\\_4.php](http://www.euroargo-edu.org/argoeu_4.php). [Accessed 29 February 2016].

EUROLAB Technical Report 1 (2006), Guide to the Evaluation of Measurement Uncertainty for Quantitative Test Results.

- Gonçalves, M. A. L., Pinho, S. P. G., Montesanti, J. R. T., Shang, W., & Sarica, C. (2011). A Case Study of Scale-Up of Wax Deposition Model Predictions Using Flow Loop Wax Deposition Data for Pipeline Design. BHR Group. Available from: <https://0-www.onepetro.org.lispac.lsbu.ac.uk/download/conference-paper/BHR-2011-B1?id=conference-paper%2FBHR-2011-B1> [Accessed 2 March 2013].
- Goodman, N.T., and Joshi, N. (2013). A Tale of Two Flowlines-Paraffin Plugging and Remediation, SPE 166196 presented at SPE Annual, Tech Conf and Exh, New Orleans.
- Gebrehiwot, Silas Zewdie , (2014) Manufacturing and Rheological Analysis of Spiral Flow Test Piece, *Plastics Technology*, Arcada University of Applied Sciences.
- Guo, B., Song, S., Chacko, J., and Ghalambor, A., (2005), *Offshore Pipelines*, 5th ed. Oxford: Elsevier publication.
- Green, D. W. (2008). *Perry's chemical engineers' handbook* (8th edition). New York: McGraw-Hill.
- Hamouda, A. A., and Ravneøy, J. M. (1992), *Prediction of Wax Deposition in Pipelines and Field Experience on the Influence of Wax on*

Drag-Reducer Performance, 24th Annual Offshore Technology Conference, Houston, Texas, 4-7 May. doi:10.4043/7060-MS

- Halim, N., Ali, S., Nadeem, M. N., Abdul Hamid, P., and Tan, I. M. (2011) Synthesis of Wax Inhibitor and Assessment of Squeeze Technique Application for Malaysian Waxy Crude, *Society of Petroleum Engineers*, doi:10.2118/142288-MS
- Hammami, A., and Raines, M.A. (1999) Paraffin deposition from crude oils: comparison of laboratory results with field data. *Society of Petroleum Engineers Journal*, 4, pp. 9-18.
- Han, S., Song, Y. and Ren, T. (2009) Impact of Alkyl Methacrylate-Maleic Anhydride Copolymers as Pour Point Depressant on Crystallization Behaviour of Diesel Fuel. *Energy and Fuel*, 23 (5), pp. 2576-2580.
- Han, S., Huang, Z., Senra, M., Hoffmann, R., & Fogler, H. S. (2010), Method to determine the wax solubility curve in crude oil from centrifugation and high temperature gas chromatography measurements, *Energy & Fuels*, 24, 1753–1761.
- Hilbert, J., (2010), Flow Assurance: Wax Deposition and Gelling in Subsea Oil Pipelines, in: SPE Annual Technical Conference and Exhibition, Brisbane, Queensland, Australia, pp. 1-9. Available from: <https://0-www.onepetro.org/lispac.lsbu.ac.uk/download/conference-paper/SPE-133948-MS?id=conference-paper%2FSPE-133948-MS> [Accessed 17 May 2013].
- Hsu, J. J. C., Santamaria, M. M., Brubaker, J. P., & Hawker, P., (1994) Wax Deposition And Gel Strength Of Waxy Live Crudes, in: Offshore Technology Conference, Texas, USA, 2-5 May, pp. 555-562, doi:10.4043/7573-MS.
- Hoffman R. and Amundsen L. (2010), Single-Phase Wax Deposition Experiments. *Energy & Fuels*, 24, pp. 1069-1080.
- Heriot-Watt University. 2014. Heriot-Watt Institute of Petroleum Engineering. [ONLINE] Available from: [http://www.pet.hw.ac.uk/research/hydrate/hydrates\\_why.cfm](http://www.pet.hw.ac.uk/research/hydrate/hydrates_why.cfm). [Accessed 17 June 2016].
- Huang Z., Lee H.S., Senra M., and Fogler H.S. (2011) A Fundamental Model of Wax Deposition in Subsea Oil Pipelines. *AIChE Journal*, 57 (11).
- Huang, Z., Zheng, S., Fogler, H.S. (2015) Wax Deposition: Experimental Characterizations, Theoretical Modeling, and Field Practices. USA: Taylor

& Francis Group. LLC, Version Date: 20150408, ISBN-13: 978-1-4665-6767-2.

- Irmann-Jacobsen Tine Bauck (2013) Flow Assurance – A System Perspective, MEK4450-FMC Subsea technologies, Available from: [http://www.uio.no/studier/emner/matnat/math/MEK4450/h11/undervisning/smateriale/modul-5/MEK4450\\_FlowAssurance\\_pensum-2.pdf](http://www.uio.no/studier/emner/matnat/math/MEK4450/h11/undervisning/smateriale/modul-5/MEK4450_FlowAssurance_pensum-2.pdf) [Accessed 1 January 2014].
- Johal, K.S. (2012) Flow Assurance for Oil-Gas Fields Production Transport. First Edition. London: Fluids in Motion Limited.
- Jha, N. K., Jamal, M. S., Singh, D., & Prasad, U. S. (2014) Characterization of Crude Oil of Upper Assam Field for Flow Assurance. *Society of Petroleum Engineers Journal*. doi:10.2118/172226-MS.
- Jang, Y.H., Blanco, M., Creek, J., Tang, Y. and Goddard, W.A. (2007) Wax Inhibition by Comb-like Polymers: Support of the Incorporation-Perturbation Mechanism from Molecular Dynamics Simulations. *Journal of Physical Chemistry*, 111(46), pp. 13173-13179.
- Jafari Ansaroudi, H.R., Vafaie-Sefti, M., Masoudi, S., Behbahani, T.J., and Jafari, H. (2013) Study of the Morphology of Wax Crystals in the presence of Ethylene-co-vinyl Acetate Copolymer, *Pet. Sci. Technol.*, vol 31, no. 6, pp. 643-651.
- Jennings, D.W., and Newberry, M.E. (2008) Paraffin Inhibitor Applications in deepwater Offshore Development, in: The International Petroleum Technology Conference, Kuala Lumpur, Malaysia, 3-5 December. Available from:  
<https://0-www.onepetro.org.lispac.lsbu.ac.uk/download/conference-paper/IPTC-12127-MS?id=conference-paper%2FIPTC-12127-MS>  
[Accessed 24 January 2013].
- Jonathan, Southgate (2004) Wax removal using pipeline pigs, Durham theses, Durham University. Available at Durham E-Theses Online: <http://etheses.dur.ac.uk/2995/>
- Jung, S.-Y., Lee, D.-G., and Lim, J.-S. (2014) A Simulation Study of Wax Deposition in Subsea Oil Production System. International Society of Offshore and Polar Engineers Conference, Busan, Korea, June 15-20, pp. 25-30. Available from:  
<https://0-www.onepetro.org.lispac.lsbu.ac.uk/download/conference-paper/ISOPE-I-14-283?id=conference-paper%2FISOPE-I-14-283>  
[Accessed 8 July 2016].

- Joshi, N. B., Muhammad, M., Creek, J., McFadden, J. (2003) Flow assurance: A challenging path to well completions and productivity. In: Offshore Technology Conference. Houston, Texas, pp. 1-5. Available from: <https://0-www.onepetro.org.lispac.lsbu.ac.uk/download/conference-paper/OTC-15185-MS?id=conference-paper%2FOTC-15185-MS> [Accessed 8 December 2012].
- Jorda, R.M., 1966, Paraffin Deposition and Prevention in Oil Wells, *Journal Petroleum Technology*, 1605; Trans., AIME,237.
- Junior, J., Borges, L. J., Carmelino, C., Hango, P., Milliken, J. D., & Asomaning, S. (2013) Calcium Naphthenate Mitigation at Sonangols Gimboa Field. Society of Petroleum Engineers. doi:10.2118/164069-MS
- Kasumu, A.S. (2014) An Investigation of Solids Deposition from Two-Phase Wax–Solvent–Water Mixtures. PhD Thesis, Galgary University, April.
- Kasumu, A. S., and Mehrotra, A. K. (2013) Solids deposition from two-phase wax–solvent–water “waxy” mixtures under turbulent flow, *Energy & Fuels*, 27, pp. 1914-1925.
- Kjøraas (2012) Modelling of Wax Deposition in Subsea Pipelines, Norwegian University of Science and Technology, Department of Petroleum Engineering and Applied Geophysics.
- Kelechukwu, E.M., Al-Salim, H.S., and Yassin, A.A.M., (2010) Influencing factors governing paraffin wax deposition during crude production. *International Journal of the Physical Sciences*, 5(15), pp. 2351-2362.
- Kang, P.-S., Lee, D.-G., & Lim, J.-S. (2014) Status of Wax Mitigation Technologies in Offshore Oil Production, in: International Society of Offshore and Polar Engineers Conference, Busan, Korea, June 15-20, pp. 31-38. Available from:  
  
<https://0-www.onepetro.org.lispac.lsbu.ac.uk/download/conference-paper/ISOPE-I-14-285?id=conference-paper%2FISOPE-I-14-285>  
[Accessed 11 August 2015].
- Kok, M. V., & Saracoglu, O. (2000) Mathematical Modelling of Wax Deposition in Crude Oil Pipeline Systems, Society of Petroleum Engineers. doi:10.2118/64514-MS
- Labes-Carrier, C, Rønningsen, HP, Kolnes, J, Leporcher, E (2002) Wax Deposition in North Sea Gas Condensate and Oil Systems: Comparison between Operational Experience and Model Prediction, SPE 77573 presented at SPE Annual Tech Conf and Exh, San Antonio.

- Lee, H. S. (2008) Computational and Rheological Study of Wax Deposition and Gelation in Subsea Pipelines. PhD Thesis, University of Michigan.
- Larsen, R., Lund, A., Argo, C. (2003) Cold flow - a practical solution. In: 11th International Conference on Multiphase Flow. San Remo, Italy, pp. 313–331.
- Leek, J.T., Peng, R.D. (2015), Reproducible research can still be wrong: Adopting a prevention approach, Proceedings of the National Academy of Sciences of the United States of America. 112 (6): 1645–1646. doi:10.1073/pnas.1421412111.
- Leontaritis K.J., and Geroulis E., 2011, Wax Deposition Correlation-Application in Multiphase Wax Deposition Models, Asph Wax, Inc., Offshore Technology Conference, Texas, USA, 2-5 May 2011.
- Leontaritis, K. J. (2007), Wax Flow Assurance Issues in Gas Condensate Multiphase Flowlines, Offshore Technology Conference, Houston, Texas, U.S.A., 30 April–3 May. doi:10.4043/18790-MS
- Li Y. Sun X., Yan Q. 2011, Experimental study on the characteristics of spiral flow in a local generator. Journal of Hydroelectric Engineering. 30 (2): 72-77.
- Lu, Y., Huang, Z., Hoffmann, R., Amundsen, L., Fogler, H. S., & Sheng, Z. (2012), Counterintuitive effects of the oil flow rate on wax deposition, Energy & Fuels, 26, 4091–4097.
- Lin Nan, Huiqing Lan, Yugong Xu, Shaohua Dong, Gary Barber (2015), Effect of the gas-solid two-phase flow velocity on elbow erosion, *Journal of Natural Gas Science and Engineering* (26), 581-586. <https://doi.org/10.1016/j.jngse.2015.06.054>
- Matzain, A., Apte, M.S., Zhang, H., Volk, M., Redus, C.L., Brill, J.P. and Creek, J.L., (2001), Multiphase flow wax deposition modeling, ETCE, Houston, USA, February.
- Mohamed, A. S., Alian, S. S., Singh, J., Singh, R., Goyal, A., & Munainni, G. (2016), Remediation of Well Impaired by Complex Organic Deposits Embedded with Naphthenate and Contaminated with Inorganics, Offshore Technology Conference. doi:10.4043/26524-MS
- Malekzadeh, R. (2012) Severe slugging in gas-liquid two-phase pipe flow, Master of Science in Applied Earth Sciences Geboren te Ghaemshahr, Sieca Repro, ISBN 978-94-6186-059-0.

- Matthew, M. (2016), Offshore oil production in deepwater and ultra-deepwater is increasing, [ONLINE] Available at: <https://www.eia.gov/todayinenergy/detail.php?id=28552#>. [Accessed 21 May 2017].
- Merino-Garcia, D., Duenas-Diez, M., Gomez, S., and Pena, J.L., 2013 Risk Assessment Methodology for Flow Assurance Challenges: The Sooner You Look at It, the Better, Offshore Technology Conference Paper 22404.
- Merino-Garcia, D., Shaw, J., Carrier, H., Yarranton, H., Goual, L., 2010 Petrophase 2009 Panel Discussion on Standardization of Petroleum Fractions, Energy and Fuels, 24 (4), 2175-2177.
- Mirazizi, H.K., Shang, W., and Sarica, C. (2012) Paraffin Deposition Analysis for Crude Oils under Turbulent Flow, SPT Annual Technical Conference and Exhibition, San Antonio, Texas, USA, 8-10 October.
- McLay. 2015. Water Softeners and Filters. [ONLINE] Available at: <http://mclayservices.com/plumbing/water-softeners-and-filters/>. [Accessed 15 June 2016].
- Misra S., Baruah S., and Singh K., 1995, Paraffin Problems in Crude Oil Production And Transportation: A Review, SPE, Oil & Natural Gas Corp, Ltd.
- Nguyen, D. A., (2004) Ph.D. Thesis, University of Michigan.
- Noville, I, and Naveira, L (2012). "Comparison between Real Field Data and the Results of Wax Deposition Simulation," SPE 152575 presented at SPE Latin American and Caribbean Petroleum Eng Conf, Mexico.
- Ove Bratland, (2010; 2013), Pipe Flow 2: Multi-phase Flow Assurance, ISBN 978-616-335-926-1.
- OLGA 2014, User manual, Dynamic Multiphase Flow Simulator, SPT Group, Schlumberger.
- Patton, C.C. and Casad, B.M., 1970, Paraffin Deposition From Refined Wax Solvent System, SPEJ: 17.
- Pedersen, K.S. and Ronningsen, H.P. (2003) Influence of Wax Inhibitors on Wax Appearance Temperature, Pour Point, and Viscosity of Waxy Crude Oils, Energy, and Fuels, 17 (2), 321-328.
- Perez P., Boden E., Chichak K., Gurnon AK, Hu L., Lee J., McDermottJ, Osaheni J., Peng W., Richards W., Xie X., (2015) Evaluation of Paraffin

Wax Inhibitors: An Experimental Comparison of Bench-Top Test Results and Small-Scale Deposition Rigs for Model Waxy Oils, in: Offshore Technology Conference, Houston, Texas, USA.

- PetroWiki. 2015. Oil emulsions. [ONLINE] Available at: [http://petrowiki.org/Oil\\_emulsions](http://petrowiki.org/Oil_emulsions). [Accessed 18 June 2016].
- Pan, S, Zhu, J, Zhang, D, Razouki, A, and Talbot, M (2009) Case Studies on Simulation of Wax Deposition in Pipelines, International Petroleum Technology Conference, Doha, IPTC.
- Phillips, D. A., Forsdyke, I. N., McCracken, I. R., & Ravenscroft, P. D. (2011), Novel approaches to waxy crude restart: Part 2: An investigation of flow events following shut down, *J. Pet. Sci. Eng.*, 77, 286–304.
- Ridzuan, N., Adam, F., & Yaacob, Z. (2014). Molecular Recognition of Wax Inhibitor through Pour Point Depressant Type Inhibitor. International Petroleum Technology Conference. doi:10.2523/17883-MS.
- Rosvold, K. (2008) Wax Deposition Models, M.Sc. Thesis, Department of Petroleum Engineering and Applied Geophysics, Norwegian University of Science and Technology, Trondheim.
- Rygg, O.B., Rydahl, A.K. and Rønningsen, H.P., (1998), Wax deposition in offshore pipeline systems, Proc. 1st North American Conference on Multiphase technology, Banff, Canada, June.
- Southwest Gas. 2016. Controlling Corrosion in Natural Gas Pipelines in Your Facility. [ONLINE] Available at: <http://members.questline.com/Article.aspx?articleID=1859&accountID=60&nl=14330>. [Accessed 17 June 2016].
- Salam, K. K., Arinkoola, A. O., Oke, E. O., Adeleye, J. O. (2014) Optimization of Operating Parameters using Response Surface Methodology for Paraffin-Wax Deposition in Pipeline, *Petroleum & Coal*, 56 (1), 19-28.
- Singhal, H.K., Sahai, G.C., Pundeer, G.S., and Chandra, K. (1991) Designing and Selecting Wax Crystal Modifier for Optimum Field Performance Based on Crude Oil Composition, 66th Annual Technical Conference and Exhibition, Dallas, Texas, USA, October 6-9.
- Siljoberg, M. K. (2012) Modelling of Paraffin Wax in Oil Pipelines, NTNU-Trondheim, July 2012.
- Singh, A., Lee, H., Singh, P., Sarica, C. (2011) SS: Flow Assurance: Validation of Wax Deposition Models Using Field Data from a Subsea

Pipeline. Paper Presented at the Offshore Technology Conference, Houston, Texas, USA, 2–5 May.

- Singh, P., Venkatesan, R., Fogler, H.S., and Nagarajan, N. (2000) Formation and aging of incipient thin film wax–oil gels. *AIChE*, 46 (5), pp.1059–74.
- Singh, P., Venkatesan, R., Fogler, H.S., and Nagarajan, N. (2001) Morphological evolution of thick wax deposits during aging, *AIChE*, 47, pp. 6–18.
- Solaimany Nazar, A.R., Dabir, B., Islam, M.R. (2005) Experimental and mathematical modeling of wax deposition and propagation in pipes transporting crude oil, *Energy Sour*, 27, pp.185–207.
- Struchkov, I.A., Rogachev, M.K., Kalinin, E.S., Pavlov, P.V., & Roschin, P.V. (2017). Laboratory Investigation of Organic-Scale Prevention in a Russian Oil Field. Society of Petroleum Engineers. doi:10.2118/185961-PA
- Tarek Ahmed, (2007) Equations of State and PVT Analysis, Applications for Improved Reservoir Modeling. Houston, Texas, USA: Gulf Publishing Company.
- Time, R. W. (2011) Flow Assurance and Multiphase Flow (Part II). The university of Stavanger, Department of Petroleum Engineering, Seminar Presented at Aker Solutions, Stavanger.
- Tiwary, R., and Mehrotra, A.K. (2009) Deposition from wax-solvent mixtures under turbulent flow: effects of shear rate and time on deposit properties, *Energy Fuels*, 23, pp. 1299–310.
- Trina, S., and Johansen, T. (2015) An Integrated Horizontal- and Vertical-Flow Simulation With Application to Wax Precipitation. Society of Petroleum Engineers. doi:10.2118/156555-PA
- Tordal, A. (2006) Pigging Of Pipelines with High Wax Content. Publication of Pigging Products and Services Association, Statoil ASA, Stavanger, Norway. Available from:  
<http://www.ppsaonline.com/papers/2006-Aberdeen-1-Tordal.pdf>  
[Accessed 14 January 2014].
- Valinejad, R. and Solaimany Nazar, A. R. (2013) An experimental design approach for investigating the effects of operating factors on the wax deposition in pipelines, *Fuel Journal*, 106, pp. 843-850.



- Venkatesan, R. (2004) The Deposition and Rheology of Organic Gels, Doctoral Thesis in Chemical Engineering, the University of Michigan, pp. 225.
- Venkatesan, R. and Creek, J.L. (2007) Wax Deposition During Production Operations: SOTA, SPE, Chevron Energy Technology Co., Offshore Technology Conference, Texas, U.S.A., 30 April–3 May.
- White, F.M. (2008) Fluid Mechanics. Sixth Edition. Amazon: McGraw-Hill.
- Woo, G. T., Garbis, S. J., and Gray, T. C (1984) Long-Term Control of Paraffin Deposition, SPE Annual Technical Conference and Exhibition, Houston, September 16-19.
- Wu, Y., Ni, G., Yang, F., Li, C., and Dong, G. (2012) Modified Maleic Anhydride Co-polymers as Pour-Point Depressants and Their Effects on Waxy Crude Oil Rheology, *Energy and Fuels*, 26 (2), pp. 995-1001.
- Xie L., (ed.) (2013) Hydraulic Engineering. London: Taylor and Francis Group, ISBN 978-1-138-00043-8.
- Yongsheng Yang, Faisal Khan, Premkumar Thodi, Rouzbeh Abbassi (2017) Corrosion induced failure analysis of subsea pipelines, *Reliability Engineering & System Safety*, (159), 214-222, <https://doi.org/10.1016/j.ress.2016.11.014>.
- Zerpa, L.E., Sloan, E.D., Koh, C.A., Sum, A.K., 2011 Hydrate Risk Assessment and Restart Procedure Optimization Offshore Using a Transient Hydrate Prediction Model, Offshore Technology Conference Paper 22406.
- Zhang Long , Chen Jiaqing, Xiaolei Cai, Songtao Huang, Yipeng Ji (2017) Research on electrostatic coalescence of water-in-crude-oil emulsions under high frequency/high voltage AC electric field based on electro-rheological method, *Colloids and Surfaces A: Physicochemical and Engineering Aspects*, (520), 246-256, <https://doi.org/10.1016/j.colsurfa.2017.01.051>.
- Zamani, M., Sadegh Seddighi, Hamid Reza Nazif (2017), Erosion of natural gas elbows due to rotating particles in turbulent gas-solid flow, *Journal of Natural Gas Science and Engineering*, (40), 91-113, <https://doi.org/10.1016/j.jngse.2017.01.034>.
- Zhu, T., Walker, J. A., and Liang, J. (2008) Evaluation of Wax Deposition and Its Control during Production of Alaska North Slope Oils. Final Report, University of Alaska Fairbanks, ConocoPhillips Alaska, Inc., University of Kansas, United States Department of Energy National Energy Technology Laboratory, Oil & Natural Gas Technology, DOE Award No.: DE-FC26-01NT41248.

- Zhang, X.E., Sun, X.H., Huo, D.M., 2001. The Numerical Simulation of Spiral Flow Field with Continuous Guiding Vane. *Journal of Taiyuan University of Technology*. 32, 252-254.
- Zhang, Y., Peng L., Li, Z. 2002, Rotation-starting of Sediments in Spiral Flow in the Horizontal Pipe. *Journal of Sediment Research*, 2, 71-75.
- Zhang, Y., Zhang, X.E., Peng, L.S. 2005, Experimental Study on Sediment Transportation of Spiral Flow in Pipe. *Journal of Sediment Research*, 2, 34-38.

## Appendix A: Published Papers

*International Journal of Smart Grid and Clean Energy*

### Experimental Study of Wax Deposition in Pipeline – Effect of Inhibitor and Spiral Flow

Muhammad Ali Theyab<sup>a</sup>, Pedro Diaz<sup>b</sup> \*

<sup>a,b</sup> *London South Bank University, 103 Borough Rd, London SE1 0AA, UK*

---

#### Abstract

Wax deposition is one of the main flow assurance problems in the oil industry. It can result in the restriction of crude oil flow in the pipeline, creating pressure abnormalities and causing an artificial blockage leading to a reduction or interruption in the production. Wax can precipitate as a solid phase on the pipe wall when its temperature (inlet coolant temperature) drops below the Wax Appearance Temperature (WAT). An experimental flow loop system was built in the lab to study the variation of wax deposition thickness under the single phase transport. A series of experiments were carried out at different flow rates (2.7 and 4.8 L/min) to study wax deposition and measure the wax thickness using four different techniques including direct technique pigging, pressure drop, heat transfer and liquid displacement-level detection (LD-LD). The effect of factors on wax formation such as inlet coolant temperature, inhibitor and spiral flow has been examined. The results shows the wax inhibition percentage (WI) % of inhibitor W802 (polyacrylate polymer (C16-C22)) and spiral flow at flow rate 2.7 L/min, inlet coolant temperature 14 °C, was 40% with the inhibitor while was 65% with the spiral flow. At flow rate 4.8 L/min, inlet coolant temperature 14 °C and 1000ppm W802, the wax inhibition percentage was 45% while with the spiral flow was 73%. This percentage of inhibition will increased rapidly by increasing the inlet coolant temperature.

*Keywords: Wax inhibitor, spiral flow, wax inhibition, wax measuring techniques*

---

#### Introduction

Wax deposition is one of the main flow assurance problems in the oil industry. Wax deposition can result in the restriction of crude oil flow in the pipeline, creating pressure abnormalities and causing an artificial blockage leading to a reduction or interruption in the production. However, in an extreme case, this can cause a pipeline or production facility to be abandoned [1]. Wax can precipitate and arises when paraffin components in crude oil precipitate and deposit on the cold pipeline wall when the inner wall temperature (inlet coolant temperature) drops below the wax appearance temperature [2], [3], [4]. Wax appearance temperature (WAT) is the temperature at which paraffin wax start to precipitate [5].

Time (2011) [6] mentioned that the solid phase of wax begins to precipitate characteristically around 30 to 40 °C, but may possibly be as high as 50 to 55 °C [6]. The main factor that affects the wax deposition process is the low temperature, which means that subsea pipelines are especially vulnerable. Therefore, wax deposition prevention becomes very important in deep- water oil production.

Wax deposition in crude oil production systems can be reduced or prevented by one or combination of chemical, mechanical, and thermal remediation methods. However, with the advent of extremely deep production, offshore drilling and ocean floor completions, the use mechanical and thermal remediation methods becomes prohibitive economically, as a result, use of chemical additives as wax deposition inhibitors is becoming more prevalent [7]. Selected chemical inhibitor was tested in the current work to study its effect on wax deposition. Wax deposition experiments are carried out at different flow rates 2.7 and 4.8 L/min., to study the influence of factors that affect the formation of wax deposits such as inlet

\*Manuscript received March 11, 2016; revised July 30, 2016. Corresponding author. Tel.: +447833846288; E-mail address: theyabm@lsbu.ac.uk doi: 10.12720/sgce.5.3.174-181



## Experimental Study on the Effect of Inhibitors on Wax Deposition

Muhammad Ali Theyab\* and Pedro Diaz

London South Bank University, 103 Borough Road, SE1 0AA, London, UK

### Abstract

A challenge facing offshore oil production is wax deposition. It leads to increases in operational and remedial costs while suppressing oil production. Wax inhibitors are one of the mitigation technologies that had been examined its influence on crude oil viscosity, pour point and wax appearance temperature (WAT).

The performance of some of wax inhibitors was evaluated to determine their effects on the pour point, wax appearance temperature and the viscosity of the crude oil using the programmable Rheometer rig at gradient temperatures (55°C) and shear rate 120 1/s before and after adding 1000 ppm and 2000 ppm of inhibitors to the crude oil. Three different inhibitors which were not tested before were prepared in the lab of this study. These inhibitors works well compared with its original components.

The first inhibitor was coded Mix01 by mixing polyacrylate polymer (C16-C22), and copolymer + acrylated monomers. The reduction of pour point of the waxy crude oil was up to a 16.6°C at 2000 ppm concentration and this reduces the crude oil viscosity to about 61.9% at a seabed temperature of 4°C.

The second inhibitor was coded Mix02, by mixing polyacrylate polymer (C16-C22), alkylated phenol in heavy aromatic naphtha, and copolymer dissolved in solvent naphtha. At 2000 ppm, the reduction of pour point of the crude oil up to a 15.9°C and decreases the viscosity to 57% at a seabed temperature of 4°C. Finally, the third inhibitor was Mix03, by mixing polyacrylate polymer (C16-C22), and brine (H<sub>2</sub>O + NaCl). At 1000 ppm concentration, the reduction of pour point of the oil was up to a 14.4°C and reduced the viscosity to 52.5% at a seabed temperature of 4°C.

This unique blend of the inhibitory properties and significant reduction in pour point temperatures and crude oil viscosity is providing an original development in wax mitigation technology.

**Keywords:** Inhibitors; Wax; Oil; Phenol; Viscosity; Crystallization

### Introduction

Paraffin wax deposition is a phenomenon that plagues the oil industry. It can choke the production lines thereby reducing the oil production to uneconomic levels. Wax inhibitor, alternatively known as pour point depressant/ wax crystal modifier, can reduce the growth of the wax crystal and form smaller crystals allowing large free space of the liquid fraction of the crude oil to flow freely [1].

The chemical addition is one of the inhibitors that have been used to reduce or prevent wax deposition in crude oil production. These inhibitors can be divided into four types: pour point depressants (PPD), crystal modifiers, dispersants, and solvents. PPD hinders the formation and growth of wax crystals by modifying the crystal structure (by merging with the edge of a growing wax crystal). Although it reduces the viscosity, yield stress, and pour point of oil, it cannot reduce the wax deposition rate [1].

The crystal modifier has a similar molecular structure to wax. It co-precipitates or co-crystallizes with a wax crystal by replacing wax molecules on the crystal lattices. It imposes steric hindrance on paraffin crystals that interfere with the proper alignment of the new incoming paraffin molecules such that growth terminates. Typical crystal modifiers are polyethylene, copolymer esters, ethylene/vinyl acetate copolymers, olefin/ester copolymers, ester/vinyl acetate copolymers, polyacrylates, polymethacrylates, and alkyl phenol resins. Dispersants are similar to surfactants in their molecular structure. Dispersants are breaking wax crystals up into much smaller particles and reduce the rate of wax deposition and prevent it by minimizing wax adhesion to the pipe wall [1,2].

Solvents increase the solubility of wax in oil and so dissolve already deposited wax. The solvents most commonly used today include

aromatic compounds (toluene, and xylene), white or unleaded gasoline, and pine-derived terpenes [1].

The advantage of the wax inhibitor addition to the crude oil sample is the deposition can be mitigated without stopping production. Even though many wax inhibitors have been developed, there is currently no universal type can be used for all types of crude oils due to the varying properties of the crude oils [1,3].

Hoffmann and Amundsen [4] found that about 60% to 90% of wax thickness was reduced by applying different inhibitor concentration during experimental work investigation. The presence of the small amount of inhibitor concentration such as poly (ethylene-co-vinyl acetate (EVA)) and poly (maleic anhydride-alt-1-octadecene (MA)), can coalesce with wax crystals and interfere the crystal growth of the crystals [5].

Polymers have been used successfully as crystal modifiers in some areas; their use should expand as more effective polymers are developed. The polymers molecular weight also has influence on the pour point depression. Short or lower molecular weight polymers may

\*Corresponding author: Muhammad Ali Theyab, London South Bank University, 103 Borough Road, SE1 0AA, London, UK; Tel: +447833846288; E-mail: theyabm@lsbu.ac.uk

Received November 01, 2016; Accepted November 20, 2016; Published November 28, 2016

Citation: Theyab MA, Diaz P (2016) Experimental Study on the Effect of Inhibitors on Wax Deposition. J Pet Environ Biotechnol 7: 310. doi: 10.4172/2157-7463.1000310

Copyright: © 2016 Theyab MA, et al. This is an open-access article distributed under the terms of the Creative Commons Attribution License, which permits unrestricted use, distribution, and reproduction in any medium, provided the original author and source are credited.



Society of Petroleum Engineers

**SPE-181954-MS**

## **Experimental Study on the Effect of Spiral Flow on Wax Deposition Thickness**

Muhammad Ali Theyab, Pedro Diaz, London South Bank University

Copyright 2016, Society of Petroleum Engineers

This paper was prepared for presentation at SPE Russian Petroleum Technology Conference and Exhibition held in Moscow, Russia, 24–26 October 2016.

This paper was selected for presentation by an SPE program committee following review of information contained in an abstract submitted by the author(s). Contents of the paper have not been reviewed by the Society of Petroleum Engineers and are subject to correction by the author(s). The material does not necessarily reflect any position of the Society of Petroleum Engineers, its officers, or members. Electronic reproduction, distribution, or storage of any part of this paper without the written consent of the Society of Petroleum Engineers is prohibited. Permission to reproduce in print is restricted to an abstract of not more than 300 words; illustrations may not be copied. The abstract must contain conspicuous acknowledgment of SPE copyright.

### **Abstract**

Wax precipitation is one of the most important flow assurance problems, and a significant economic issue in the petroleum industry. Wax leading to increase fluid viscosity causing the blockage of filters, valves and even pipelines, increasing pumping costs, and reducing or even stopping oil production or transport. Wax can precipitate as a solid phase on the pipe wall when its temperature drops below the Wax Appearance Temperature (WAT).

The objective of this study is using spiral flow to mitigate wax deposition. An experimental flow loop system was built in the lab to study the variation of wax deposition thickness under the single phase transport. A series of experiments were carried out at different flow rates (2.7 and 4.8 L/min) to study wax deposition process and measure the wax thickness. The effects of factors on wax formation, such as spiral flow, inlet coolant temperature, temperature drop, flow rates and experimental time have been examined.

The spiral flow created inside the pipe by inserting a twisted metal along the pipe, which will create high shear stress affecting to wax deposition. The results show that the wax inhibition (reduction) percentage (WI) % by using the spiral flow at flow rate 2.7 L/min, inlet coolant temperature 14 °C, was 65%. At flow rate 4.8 L/min, inlet coolant temperature 14 °C the wax inhibition percentage was 73%. Experimentally, it was found that the spiral flow more efficient than the chemical inhibitors. This percentage of reduction will increase rapidly by increasing the inlet coolant temperature and decreased by reducing the inlet coolant temperature.

This technique of creating spiral flow inside the test section of the pipe will provide a step forward in flow assurance technology to mitigate the deposition of wax.

### **Introduction**

Wax deposition is a critical operational challenge to the oil and gas industry. As early as 1928, wax deposition was reported as an issue that presents many difficult problems while being produced, transported, and stored (Huang et al., 2015). Wax contains high molecular weight n-paraffin and asphaltenes components of the crude. They consist of long-chain alkanes with 20 to 50 carbon atoms, but also enclose minor quantities of branched and cyclic hydrocarbons. Wax deposition arises when paraffin

**SPE-182936-MS**

## **Experimental Study on the Effect of Spiral Flow on Wax Deposition Volume**

Muhammad Ali Theyab, Pedro Antonio Diaz, London South Bank University

Copyright 2016, Society of Petroleum Engineers

This paper was prepared for presentation at the Abu Dhabi International Petroleum Exhibition and Conference held in Abu Dhabi, UAE, 7–10 November 2016.

This paper was selected for presentation by an SPE program committee following review of information contained in an abstract submitted by the author(s). Contents of the paper have not been reviewed by the Society of Petroleum Engineers and are subject to correction by the author(s). The material does not necessarily reflect any position of the Society of Petroleum Engineers, its officers, or members. Electronic reproduction, distribution, or storage of any part of this paper without the written consent of the Society of Petroleum Engineers is prohibited. Permission to reproduce in print is restricted to an abstract of not more than 300 words; illustrations may not be copied. The abstract must contain conspicuous acknowledgment of SPE copyright.

### **Abstract**

One of the main flow assurance challenges in the oil industry is wax deposition. It can result in the restriction of crude oil flow in the pipeline, creating pressure abnormalities and causing an artificial blockage leading to a reduction in the production. Wax can precipitate as a solid phase on the pipe wall when its temperature drops below the Wax Appearance Temperature. The objective of this study is using spiral flow to mitigate wax deposition.

An experimental flow loop system was built in the lab to study the variation of wax deposition thickness under the single phase transport. A series of experiments were carried out at different flow rates (2.7 and 4.8 L/min) to study wax deposition and measure the wax thickness. The effect of factors on wax formation such as spiral flow, inlet coolant temperature, pressure drop, temperature drop, flow rates, time and shear stress have been examined.

The spiral flow created inside the pipe by inserting a twisted metal along the pipe, which will create high shear stress affecting to wax deposition. The results show that the wax inhibition percentage WI % by using the spiral flow at flow rate 2.7 L/min, inlet coolant temperature 14 °C, was 65%. At flow rate 4.8 L/min, inlet coolant temperature 14 °C the wax inhibition percentage was 73%. Experimentally, it was found the spiral flow more efficient than the chemical inhibitors. The WI % increased, by merging the effect of the spiral flow and the inhibitor at flow rate 2.7 L/min, to 75, 92.2 and 100 % at inlet coolant temperatures 14, 24 and 33 °C, respectively. The WI % was increased by combining the influence of the spiral flow and the inhibitor to 4.8 L/min, to 83.5% at inlet coolant temperature 14 °C, 94.3% at 24 °C and to 100% at temperature 33 °C.

This percentage of inhibition will increased rapidly by increasing the inlet coolant temperature and decreased by reducing the inlet coolant temperature.

This technique of creating spiral flow inside the test section of the pipe will provide a step forward in flow assurance technology to mitigate the deposition of wax.

### **Introduction**

The formation of wax in the pipe during the hydrocarbon production from the bottom hole of the well to the surface may restrict the flow of crude oil, creating pressure abnormalities and causing an artificial blockage leading to reduction or the cessation of production (Burke and Kashou, 1995; Bern et.al., 1981;



Society of Petroleum Engineers

## SPE-181954-RU

### Экспериментальное исследование влияния спирального потока на толщину осаждения парафина

Мухаммад Али Тхейб, Пэдро Диаз, Университет Лондона Саут Бенк

Авторское право 2016 г., Общество инженеров нефтегазовой промышленности

Этот доклад был подготовлен для презентации на Российской нефтегазовой технической конференции и выставке SPE, 24-26 октября, 2016, Москва, Россия.

Данный доклад был выбран для проведения презентации Программным комитетом SPE по результатам экспертизы информации, содержащейся в представленном авторами реферате. Экспертиза содержания доклада Обществом инженеров нефтегазовой промышленности не выполнялась, и внесение исправлений и изменений является обязанностью авторов. Материал в том виде, в котором он представлен, не обязательно отражает точку зрения SPE, его должностных лиц или участников. Электронное копирование, распространение или хранение любой части данного доклада без предварительного письменного согласия SPE запрещается. Разрешение на воспроизведение в печатном виде распространяется только на реферат объемом не более 300 слов; при этом копировать иллюстрации не разрешается. Реферат должен содержать явно выраженную ссылку на авторское право SPE.

#### Резюме

Осаждение парафина является одной из наиболее важных проблем обеспечения потока и значительной экономической проблемой в нефтяной промышленности. Парафин приводит к увеличению вязкости жидкости, вызывая закупорку фильтров, клапанов и даже трубопроводов, увеличивая расходы на помпаж, а также снижает или даже останавливает добычу нефти или ее транспортировку. Парафин может выпадать в осадок в виде твердого материала на стенку трубы, когда его температура падает ниже температуры образовавшегося парафина (WAT).

Целью данного исследования является использование спирального потока для уменьшения оседания парафина. Экспериментальная система петлевого потока была построена в лаборатории с целью исследования изменений толщины осаждения парафина при однофазной транспортировке. Серии экспериментов были проведены при разных скоростях потока (2,7 и 4,8 л/мин) для изучения процесса осаждения парафина и измерения толщины осадка парафина. Было исследовано влияние факторов на формирование парафина, таких как спиральный поток, температура охлаждающей жидкости на входе, перепад температуры, скорости потока и время эксперимента.

Спиральный поток создается внутри трубы путем вставки витой металлической пластины вдоль трубы, которая будет создавать высокие напряжения сдвига, влияющее на осаждение парафина. Результаты показывают, что ингибирование парафина (уменьшение) в процентах (WI)% при использовании спирального потока при скорости потока 2,7 л/мин и температуре подающейся охлаждающей жидкости 14°C, составило 65%. При скорости потока 4,8 л/мин и температуре подающейся охлаждающей жидкости 14°C процент ингибирования парафина составил 73%. Экспериментальным путем было установлено, что спиральный поток является более эффективным, чем химические ингибиторы. Этот процент снижения быстро увеличивается за счет увеличения температуры подающейся охлаждающей жидкости и уменьшается за счет снижения температуры подающейся охлаждающей жидкости.

Метод создания спирального потока внутри испытательной секции трубы обеспечит шаг вперед в технологии обеспечения стабильности потока с целью минимизировать осаждение парафина.

## Experimental Study on the Effect of Polyacrylate Polymer (C16-C22) on Wax Deposition

Muhammad Ali Theyab, Pedro Diaz

*Wax can precipitate as a solid phase on the pipe wall during hydrocarbon production when its temperature (inlet coolant temperature) drops below the Wax Appearance Temperature (WAT) causing an artificial blockage leading to a reduction or interruption in the production. An experimental flow loop system was built in the lab to study the variation of wax deposition thickness under the single phase transport. The Bohlin Gemini II Rheometer has been used to analysis the effect of the inhibitor W802 (polyacrylate polymer (C16-C22)), at different concentration (250, 500, 750, 1000 and 2000 ppm), on the crude oil viscosity and WAT. The results show that 1000ppm of W802 produced the greatest reduction in viscosity compared with other concentrations, which means reduction in the wax deposition; and it was selected to examine with the crude oil at different flow rates (2.7 and 4.8 L/min) using the flow rig. A series of experiments were carried out to study wax deposition and measure the wax thickness using four different techniques including pigging, pressure drop, heat transfer, liquid displacement-level detection (LD-LD). The effect of factors on wax formation such as inlet coolant temperature, pressure drop, flow rates, time, and inhibitor has been examined. The results show the wax inhibition percentage (WI) % of inhibitor W802 (polyacrylate polymer (C16-C22)) at flow rate 4.8 L/min increased at different inlet coolant temperatures from 40% at 14 °C, to 57% at 24 °C and 100% at 33 °C. This percentage of inhibition will increased rapidly by increasing the inlet coolant temperature.*

**Index Terms**—Waxy crude oil, inhibitor, WAT, Viscosity.

### INTRODUCTION

Wax deposition is one of the main flow assurance problems in the oil industry. Wax deposition can result in the restriction of crude oil flow in the pipeline, creating pressure abnormalities and causing an artificial blockage leading to a reduction or interruption in the production. However, in an extreme case, this can cause a pipeline or production facility to be abandoned [1]. Wax can precipitate and arises when paraffin components in crude oil precipitate and deposit on the cold pipeline wall when the inner wall temperature (inlet coolant temperature) drops below the wax appearance temperature [2]-[4].

Pedro Diaz is with the School of Engineering, London South Bank University, UK

(e-mail: [diazp2@lsbu.ac.uk](mailto:diazp2@lsbu.ac.uk)). doi: 10.18178/ijcea.2017.8.1.624

Wax appearance temperature (WAT) is the temperature at which paraffin wax start to precipitate [5].

The main factor that affects the wax deposition process is the low temperature, which means that subsea pipelines are especially vulnerable. Therefore, wax deposition prevention becomes very important in deep- water oil production.

Wax deposition in crude oil production systems can be reduced or prevented by one or combination of chemical, mechanical, and thermal remediation methods.

However, with the advent of extremely deep production, offshore drilling and ocean floor completions, the use mechanical and thermal remediation methods becomes prohibitive economically, as a result, use of chemical additives as wax deposition inhibitors is becoming more prevalent [6]. Selected chemical inhibitor was tested in the current work to study its effect on wax deposition.

In the current research, to study the influence of factors that affect the formation of wax deposits such as inlet coolant temperature, flow rate (2.7 and 4.8 L/min), pressure drop, deposit time, and 1000ppm of the inhibitor W802 polyacrylate polymer (C16-C22), wax deposition experiments are carried out. Four different techniques were followed to measure wax thickness including pigging, pressure drop, heat transfer and liquid displacement-level detection (LD-LD).

The results show a good inhibition percentage at flow rate 4.8 L/min and different coolant temperature reach to 100% at inlet coolant temperature 33 °C. This percentage of inhibition will increased rapidly by increasing the inlet coolant temperature.

### Experimental Methodology

#### Characterization of Crude Oil

The crude oil that has been used in this study is one of the oil fields reservoirs with waxing problems of Arunachal Pradesh state in the extreme north eastern part of India.